

https://dspace.org/

On the adsorption of Cu2+ and Zn2+ from wastewater using water hyacinth: the mathematical modelling approach

Eltahhan, Nashwa Tarek

2024

https://hdl.handle.net/10539/37373

Downloaded from a DSpace repository. https://dspace.org/

On the adsorption of Cu^{2+} and Zn^{2+} from wastewater using water hyacinth: The mathematical modelling approach

Nashwa Tarek Eltahhan (1970229)

A thesis submitted in fulfillment of the requirements for the degree

of

Doctor of Philosophy (Chemical Engineering)

Submitted to

School of Chemical and Metallurgical Engineering, Faculty of Engineering and the Built Environment, University of Witwatersrand, Johannesburg, South Africa.

Johannesburg,

DECLARATION

I declare that this thesis is my own unaided work. It is being submitted for the degree of Doctor of Philosophy in Chemical Engineering to the University of the Witwatersrand, Johannesburg. It has not been submitted before for any other degree or examination in any other University.

Nashwa Eltahhan

ABSTRACT

Several industries utilize heavy metals in their industrial processes, eventually discharging them in their wastewater. Water contamination by heavy metals is a major environmental problem due to their acute toxicity and their accumulation in food chains. Therefore, intensive research has been carried out lately on the feasibility of water hyacinth as low cost adsorbent for the removal of heavy metals from wastewater.

One of the present research objectives was to examine the potential of raw South African water hyacinth for the removal of Cu^{2+} and Zn^{2+} from a synthetic wastewater. The research work is divided into three core phases. In Phase I, batch equilibrium experiments were carried out to compare the performance of water hyacinth from the different countries, Egypt and South Africa, in the removal of copper and zinc from water solutions. The effect of several operating parameters on the uptake of Cu^{2+} and Zn^{2+} was tested. The tested parameters were the pH of the solution, contact time, water hyacinth dose and initial Cu^{2+} and Zn^{2+} concentration.

The percent removal of Cu^{2+} and Zn^{2+} was found to increase with increasing the pH, contact time, and water hyacinth dose up to the point of equilibrium. However, it decreased with the increase in the initial concentration of Cu^{2+} and Zn^{2+}. Langmuir and Freundlich isotherm models were used for the evaluation of the equilibrium experimental data. The correlation coefficients for Langmuir isotherm were 0.84 and 0.82 for copper and zinc adsorbed by Egyptian water hyacinth, respectively, and 0.98 for both copper and zinc adsorbed by South African water hyacinth. The correlation coefficients for Freundlich isotherm were 0.99 and 0.98 for copper and zinc adsorbed by Egyptian water hyacinth, respectively, and 0.94 and 0.98 for copper and zinc adsorbed by South African water hyacinth, respectively.

Phase II was carried out to investigate the optimum operating conditions using Response Surface Methodology (RSM) design and General Algebraic Modeling System (GAMS). Here, optimization of an adsorption case study with conflicting optimal solutions based on single-objective Response Surface Methodology (RSM) design was facilitated with the implementation of BARON solver based on General Algebraic Modeling System (GAMS) with identical variables, levels, and model equations. RSM suggested optimum settings of which the validation is quite expensive and onerous, whereas GAMS suggested a single optimum setting which makes it more economically viable, especially for large scale systems.

Phase III was the final stage of the experimental part. It was conducted using fixed-bed column tests (continuous flow). The more promising water hyacinth which is the South African water hyacinth was used at that phase to define the impact of a number of parameters, namely the influent heavy metal concentration, bed depth, and the flowrate. The service time of the columns to breakthrough and to exhaustion was found to increase with the increase in the bed depth of the packed water hyacinth. However, it decreased with the increase in the initial Cu^{2+} and Zn^{2+} concentrations and the flowrate of the solution.

Generic equations were used to describe the adsorption mechanism of the water hyacinth used to remove Cu^{2+} and Zn^{2+} from wastewater and validate the proposed generic model against experimental data. The results indicate the suitability of the generic models for copper and zinc removal using water hyacinth. The data obtained was used to scale up the adsorption column, and the economic feasibility was then demonstrated. Assuming 80% efficiency, the scale up column for copper can run for one day and requires 19.44 hr to treat 3.69 m^3 of contaminated water using 22 kg of water hyacinth as adsorbent. On the other hand, the scale up column for zinc can run for one day and requires 19.44 hr to treat 3.44 m^3 of contaminated water using 22 kg of water hyacinth as adsorbent. The production cost of the adsorption column was estimated at US$36,434.

LISTS OF PUBLICATIONS

JOURNAL PUBLICATIONS

Nashwa Eltahhan, Thokozani Majozi, Mamdouh Gadalla, 2019. Removal of Zn (II) and Cu (II) from Aqueous Solution Using Dried Water Hyacinth as Adsorbent: Optimization of Process Parameters Using RSM and GAMS. Journal of Functional Materials and Chemical Engineering, (1)1.

CONFERENCE

2021 International Conference on Cleaner Production and Sustainability Manila, Philippines **Hosted by De La Salle University**

Oral presentation of: Implementation of generic equations to develop a mathematical model which describes the adsorption of Cu (II) and Zn (II) from wastewater using water hyacinth

2021 South African Chemical Engineering Congress Johannesburg, South Africa

Oral presentation of: Removal of zinc and copper ions from industrial wastewater using bio-waste: a case study on water hyacinth

2019 International Conference of Functional Materials & Chemical Engineering Bangkok, Thailand

Oral presentation of: Removal of Zn (II) and Cu (II) from Aqueous Solution Using Dried Water Hyacinth as Adsorbent: Optimization of Process Parameters Using RSM and GAMS

DEDICATION

This thesis is dedicated to ALLA Almighty, you are the source and the help of my life and l will forever be grateful to you. To my loving and ever caring husband, Kareem Saleh and my lovely daughters, Malak and Farah (you are mummy's friends), thank you for your support, encouragement and for believing in me. You are the best I ever have, and I will forever love you.

ACKNOWLEDGEMENTS

I wish to express my special gratitude to my supervisors Prof. T. Majozi and Prof. M. Gadalla for their endless help in removing any obstacle that could have hindered my progress and for their continuous patience, support and guidance that helped me complete this research. I would like to sincerely thank the National Research Foundation (NRF) of South Africa for funding this project.

My special love goes to my parent, Mr. and Mrs. Eltahhan for their full support you will live to eat the fruit of your labor.

To my friend Doctor Natsayi Chiwaye who helped me reviewing my thesis.

To all my colleagues in Sustainable Process Engineering research group, for the teamwork and for making the environment conducive throughout the research period.

Lastly, to all my friends and family members, thank you for being there for me in one way or the other, l love you all.

Table of Contents

Declaration……... ….……ii
Abstract…….…….iii
Lists of Publications…….……...v
Dedication…….…….vi
Acknowledgements…….……..vii
Table of Contents…….viii
Lists of Figures……....xiii
Lists of Tables……...xviii
1. Introduction…….……1
1.1 Background……..1
1.2 Motivation……7
1.3 Research Objective……...……..….9
1.4 Thesis Layout……...….9
References……...……..…11
2. Literature Review……...……..……16
2.1. Water: A finite but Sustainable Resource……..……..16
2.2. Industrial Wastewater……...……16
2.2.1 Wastewater Treatment Data……..……17
2.2.2 Industrial Wastewater in Africa ……...…….18
2.3. Heavy Metal in Industrial Wastewater……..……...19
2.4. Heavy Metal Removal Technologies…….…….…..24
2.4.1 Chemical Precipitation…….…….24
2.4.2 Ion Exchange……...…….……24
2.4.3 Membrane Filtration……...…….…25
2.4.4 Solvent Extraction……...…….25
2.4.5 Electrochemical…….....26
2.4.6 Adsorption…….....26
2.4.6.1 Adsorption Isotherms……...…….……...28
2.4.6.2 Factors Influencing Adsorption Capacity……..……..…….29
2.4.6.3 Batch Adsorption Process……...…….…..…30

2.4.6.4 Fixed-Bed Adsorption Process……..…….……...….31
2.5 Agriculture Wastes as Adsorbents……...……...….33
2.5.1 Water Hyacinth……...…33
2.5.1.1 Negative Impact of Water Hyacinth……..……..34
2.5.1.2 Water Hyacinth in South Africa……...……...35
2.6 Process Optimization…...……...…36
2.6.1 Response Surface Methodology……..36
2.6.2 General Algebraic Modelling System…….38
2.7 Mathematical Models of Adsorption in Packed Beds…….…….……..38
2.7.1 Liquid Phase Mass Transfer……..……..……39
2.7.2 Film Diffusion……...……..39
2.7.3 Adsorption Isotherm……....40
2.8 Process Simulation……...…….….40
2.9 Existing Researches on Using Water Hyacinth as Adsorbent……...…….……41
References ……..……46

3. Experimental Material and Methods……58
3.1 Overview……58
3.2 Experimental Setup……...58
3.3 Preparation of Water Hyacinth……..……...…….59
3.4 Characterization……..…..……..60
3.4.1 Fourier Transform Infrared Spectroscopy…….……60
3.4.2 X-Ray Fluorescence (XRF)……..…….61
3.5 Preparation of Stock Solution……...…….……61
3.6 Phase I- Batch Equilibrium Experiments……...……...……61
3.6.1 Effect of Contact Time……..…….…62
3.6.2 Effect of Adsorbent Dose……..…….…62
3.6.3 Effect of pH……63
3.6.4 Effect of Initial Metal Ion Concentration……...……...…….63
3.6.5 Removal Efficiency……...……...…….63
3.6.6 Adsorption Capacity……...……...…….64
3.7 Adsorption Isotherms……...……..64

3.7.1 Langmuir Isotherm…….……64
3.7.2 Freundlich Isotherm……..……65
3.8 Kinetic Study……...…….…....65
3.8.1 Pseudo-First Order Rate Law, K1……..…65
3.8.2 Pseudo-Second Order Rate Law, K2…….…66
3.9 Phase II – Response Surface Methodology and General Algebraic Modelling System....66
3.9.1 Response Surface Methodology……..……...…66
3.9.1.1 Box–Behnken Experimental Design……...…..…….66
3.9.1.2 Optimization of Adsorption Variables using BBD Method…….……..….67
3.9.1.3 Prediction and Verification of Model Equation……..…….....73
3.9.2 General Algebraic Modelling System……....74
3.10 Phase III –Continuous Fixed-bed Column Experiments…..……...……..…75
3.10.1 Experimental Procedure…….75
3.10.2 Effect of Initial Cu^{2+} and Zn^{2+} Concentration…...……...…..…77
3.10.3 Effect of Bed Depth……..……...….77
3.10.4 Effect of Flowrate (Q)……...……...…77
3.11 Sampling and Sample Analysis……..…….....78
3.11.1 pH Analysis…..…….……78
3.11.2 Cu^{+2} and Zn^{+2} Ions Analysis……...……...…79
3.12 Mathematical Modelling and Simulation…..…….……80
3.12.1 Calculation of Model Parameters……..…….82
3.12.2 Simulation……..84
3.12.3 Model Validation…...……84
3.13 Comparison of Model and Experimental Results…….……...…..84
3.14 Packed Column Design……..……..……..85
3.14.1 Scale-up Procedure for the Adsorption Column…..…….……85
3.14.2 Scaling up……...……87
3.15 Economic Feasibility for the Scaled up Adsorption Column…….……89

References……..91

4. Results and Discussions ……..94

4.1 Characterisation of Water Hyacinth ……..…...……...…..……94
4.1.1 X-Ray Fluorescence (XRF)……..…..…94
4.1.2 Fourier Transform Infrared Spectroscopy (FTIR)…….....…97
4.2 Phase I- Batch Equilibrium Experiments.....…….……..……...103
4.2.1 Effect of Contact Time ……..……..……..……104
4.2.2 Effect of Adsorbent Dose ……..…..……..……107
4.2.3 Effect of pH on the Removal of Cu^{2+} and Zn^{2+}……...……..…….109
4.2.4 Effect of Initial Cu^{2+} and Zn^{2+} Concentrations……...……...…109
4.3 Adsorption Isotherm Models ……..……112
4.3.1 Langmuir Isotherm Model……..…112
4.3.2 Freundlich Isotherm Model……115
4.4 Kinetic Model…….118
4.5 Phase II- Design of Experimental Combinations……..…….……124
4.6 Heavy Metals Response…..……..129
4.6.1 Model Fitting and Adequacy Checking…….……..129
4.6.1.1 RSM Prediction for Removal of Copper…….…….…..…131
4.6.1.2 RSM Predication for Removal of Zinc……..……131
4.6.2 Statistical Analysis…...……132
4.7 General Algebraic Modelling System (GAMS)……...……134
4.7.1 GAMS Prediction for Removal of Copper……..……..134
4.7.2 GAMS Predication for Removal of Zinc…….…….134
4.8 Phase III- Fixed-Bed Column Experiments……..…135
4.8.1 Effect of Initial Metal Ion Concentration……..……..138
4.8.2 Effect of Bed Depth…….140
4.8.3 Effect of Flowrate (Q)…….....……143
4.9 Mathematical Modelling and Simulation……...……..146
4.9.1 Model Development……...…….146
4.9.2 Model Validation……...……...…146
4.9.2.1 Model Breakthrough Curve Vs Experimental Breakthrough Curve Result…….147

4.10 Model Validation (Comparison of Model and Experimental Results)…….159
4.11 Scale up Procedure for Packed Bed Adsorption Column…….……..…..161
4.12 Economic Feasibility for the Scaled up Adsorption Column…….……..…163
4.12.1 Cost Estimation…….…..163
References …….……168
5. Conclusion and Recommendations ……...……174
5.1 Conclusion……176
5.2 Recommendations for Future Work…….....……...…179

LIST OF FIGURES

Figure 1.1. Sources and sinks of heavy metals……...…3

Figure 2.1. Countries with all, some or no information of wastewater generation, treatment and/or use……...…19

Figure 2.2. Percentage of treated and untreated wastewater by income level of countries…..….19

Figure 2.3. Heavy metal source pathway and human exposure……21

Figure 2.4 Classifications of ion exchange resins……..……25

Figure 2.5 Schematic diagram of fixed-bed adsorption column……31

Figure 2.6 Breakthrough curve for the sorption process in fixed beds…….….32

Figure 2.7 Global spread of water hyacinth ……..….33

Figure 2.8 Water hyacinth whole plant……..……34

Figure 2.9 Water hyacinth mat over river……..34

Figure 2.10 Distribution of water hyacinth in South Africa (red points), with black points indicating the water bodies that were sampled……..35

Figure 3.1: Experimental plan flow chart……..59

Figure 3.2 Dried water hyacinth ready for use…….……60

Figure 3.3. Experimental setup of a fixed-bed column experiment…….…...…76

Figure 3.4. Schematic diagram of the column experimental setup……77

Figure 3.5. pH meter- METTLER TOLEDO……..……79

Figure 3.6: Atomic Absorption Spectrometer (A.A.S)……..……80

Figure 4.1: FTIR spectrum of raw Egyptian water hyacinth before adsorption of Cu^{2+}…….....….98

Figure 4.2: FTIR spectrum of raw Egyptian water hyacinth after adsorption of Cu^{2+}……..…98

Figure 4.3: FTIR spectrum of raw South African water hyacinth before adsorption of Cu^{2+}…....101

Figure 4.4: FTIR spectrum of raw South African water hyacinth after adsorption of Cu^{2+}…...…101

Figure 4.5: Impact of contact time on % removal of 20 mg/l Cu^{2+} by water hyacinth from Egypt and South Africa (1 g) at pH 6……...……..……105

Figure 4.6: Impact of contact time on % Removal of 20 mg/l Zn^{2+} by water hyacinth from Egypt and South Africa (1 g) at pH 6…….....…106

Figure 4.7: Impact of water hyacinth dose on the uptake of Cu^{2+}…….……...…108

Figure 4.8: Impact of water hyacinth dose on the uptake of Zn^{2+}…….……..108

Figure 4.9: Impact of pH on the percentage of removal of water hyacinth for the removal of Cu^{2+}……..110

Figure 4.10: Impact of pH on the percentage of removal of water hyacinth for the removal of Zn^{2+}……..110

Figure 4.11: Impact of Initial Cu^{2+} Concentration on % Removal of Cu^{2+} by water hyacinth…111

Figure 4.12: Impact of Initial Zn^{2+} Concentration on % Removal of Zn^{2+} by water hyacinth....112

Figure 4.13: Langmuir isotherm for adsorption of Cu^{2+} using Egyptian water hyacinth sample……..113

Figure 4.14: Langmuir isotherm for adsorption of Zn^{2+} using Egyptian water hyacinth sample.....113

Figure 4.15: Langmuir isotherm for adsorption of Cu^{2+} using SA- water hyacinth sample…….....114

Figure 4.16: Langmuir isotherm for adsorption of Zn^{2+}using SA- water hyacinth sample…….114

Figure 4.17: Freundlich isotherm for adsorption of Cu^{2+} using Egyptian water hyacinth sample.…….……..……..116

Figure 4.18: Freundlich isotherm for adsorption of Zn^{2+} using Egyptian water hyacinth sample……..116

Figure 4.19: Freundlich isotherm for adsorption of Cu^{2+} using SA-water hyacinth sample…...117

Figure 4.20: Freundlich isotherm for adsorption of Zn^{2+} using SA-water hyacinth sample…...118

Figure 4.21: Pseudo first order adsorption kinetics of Cu^{2+} adsorbed on Egyptian water hyacinth, initial concentration 20 mg/L, wt. of adsorbent 1g,T=25±2°C……119

Figure 4.22: Pseudo second order adsorption kinetics Cu^{2+} adsorbed on Egyptian water hyacinth, Initial concentration 20 mg/L, wt. of adsorbent 1g, T= 25±2°C……..…….…..120

Figure 4.23: Pseudo first order adsorption kinetics of Zn^{2+} adsorbed on Egyptian water hyacinth, initial concentration 20 mg/L, wt. of adsorbent 1g, T=25±2°C……...……120

Figure 4.24: Pseudo second order adsorption kinetics of Zn^{2+} adsorbed on Egyptian water hyacinth, initial concentration 20 mg/L, wt. of adsorbent 1g, T=25±2°C……...……121

Figure 4.25: Pseudo first order adsorption kinetics of Cu^{2+} adsorbed on SA-water hyacinth, initial concentration 20 mg/L, wt. of adsorbent 1g, T=25±2°C……...…….122

Figure 4.26: Pseudo first order adsorption kinetics of Zn^{2+} adsorbed on SA-water hyacinth, initial concentration 20 mg/L, wt. of adsorbent 1g, T=25±2°C…….…….……..….122

Figure 4.27: Pseudo second order adsorption kinetics of Cu^{2+} adsorbed on SA-water hyacinth, initial concentration 20 mg/L, wt. of adsorbent 1g, T=25±2°C……...……..……..123

Figure 4.28: Pseudo second order adsorption Kinetics of Zn^{2+} adsorbed on SA-water hyacinth, initial concentration 20 mg/L, wt. of adsorbent 1g, T=25±2°C……..…123

Figure 4.29: Breakthrough curves of Cu^{2+} adsorption by water hyacinth at various initial Cu^{2+} concentrations (bed depth 2cm; flowrate 5mL/min; pH 6)……...……...139

Figure 4.30: Breakthrough curves of Zn^{2+} adsorption by water hyacinth at various initial Zn^{2+} concentrations (bed depth 2cm; flowrate 5mL/min; pH 6)……...……140

Figure 4.31: Breakthrough curves of Cu^{2+} adsorption by water hyacinth at various bed depths (C_0= 20mg/L; flowrate 5mL/min; pH 6)……...….142

Figure 4.32: Breakthrough curves of Zn^{2+} adsorption by water hyacinth at various bed depths (C_0= 20mg/L; flowrate 5mL/min; pH 6)…….……142

Figure 4.33: Breakthrough curves of the adsorption of Cu^{2+} by untreated water hyacinth at various flowrates (C_0= 20 mg/L; bed depth=2 cm; pH 6)……..…145

Figure 4.34: Breakthrough curves of the adsorption of Zn^{2+} by untreated water hyacinth at various flowrates (C_0= 20 mg/L; bed depth=2 cm; pH 6)……145

Figure 4.35: Comparison between theoretical and experimental results obtained using proposed mathematical model for the adsorption of Cu^{2+} at various initial concentrations (Cb_0 = 20 mg/L, Q = 5 mL /min and bed height = 2 cm)……..……148

Figure 4.36: Comparison between theoretical and experimental results obtained using proposed mathematical model for the adsorption of Cu^{2+} at various initial concentrations (Cb_0 = 30 mg/L, Q = 5 mL /min and bed height = 2 cm)…….…….148

Figure 4.37: Comparison between theoretical and experimental results obtained using proposed mathematical model for the adsorption of Cu^{2+} at various initial concentrations (Cb_0 = 50 mg/L, Q = 5 mL/min and bed height = 2 cm)……..……149

Figure 4.38: Comparison between theoretical and experimental results obtained using proposed mathematical model for the adsorption of Zn^{2+} at various initial concentrations (Cb_0 = 20 mg/L, Q = 5 mL /min and bed height = 2 cm)……..……149

Figure 4.39: Comparison between theoretical and experimental results obtained using proposed mathematical model for the adsorption of Zn^{2+} at various initial concentrations (Cb_0 = 30 mg/L, Q = 5 mL /min and bed height = 2 cm)……..……150

Figure 4.40: Comparison between theoretical and experimental results obtained using proposed mathematical model for the adsorption of Zn^{2+} at various initial concentrations (Cb_0 = 50 mg/L, Q = 5 mL /min and bed height = 2 cm)……..……150

Figure 4.41: Comparison between theoretical and experimental results obtained using proposed mathematical model for the adsorption of Cu^{2+} at various flowrates (Cb_0 = 20 mg/L, Q = 5 mL /min and bed height = 2 cm)……..……152

Figure 4.42: Comparison between theoretical and experimental results obtained using proposed mathematical model for the adsorption of Cu^{2+} at various flowrates (Cb_0 = 20 mg/L, Q = 10 mL /min and bed height = 2 cm)……..…152

Figure 4.43: Comparison between theoretical and experimental results obtained using proposed mathematical model for the adsorption of Cu^{2+} at various flowrates (Cb_0 = 20 mg/L, Q = 17 mL/min and bed height = 2 cm)……153

Figure 4.44: Comparison between theoretical and experimental results obtained using proposed mathematical model for the adsorption of Zn^{2+} at various flowrates (Cb_0 = 20 mg/L, Q = 5 mL /min and bed height = 2 cm)……..…153

Figure 4.45: Comparison between theoretical and experimental results obtained using proposed mathematical model for the adsorption of Zn^{2+} at various flowrates (Cb_0 = 20 mg/L, Q = 10 mL /min and bed height = 2 cm)…….154

Figure 4.46: Comparison between theoretical and experimental results obtained using proposed mathematical model for the adsorption of Zn^{2+} at various flowrates (Cb_0 = 20 mg/L, Q = 17 ml /min and bed height = 2 cm)……..…154

Figure 4.47: Comparison between theoretical and experimental results obtained using proposed mathematical model for the adsorption of Cu^{2+} at various bed height (Cb0 = 20 mg/L, Q = 5 mL /min and bed height = 2 cm)…….156

Figure 4.48: Comparison between theoretical and experimental results obtained using proposed mathematical model for the adsorption of Cu^{2+} at various bed height (Cb_0 = 20 mg/L, Q = 5 mL /min and bed height = 4 cm)……156

Figure 4.49: Comparison between theoretical and experimental results obtained using proposed mathematical model for the adsorption of Cu^{2+} at various bed height (Cb_0 = 20 mg/l, Q = 5 mL /min and bed height = 7 cm)…….…….157

Figure 4.50: Comparison between theoretical and experimental results obtained using proposed mathematical model for the adsorption of Zn^{2+} at various bed height (Cb_0 = 20 mg/l, Q = 5 ml /min and bed height = 2 cm)……..…157

Figure 4.51: Comparison between theoretical and experimental results obtained using proposed mathematical model for the adsorption of Zn^{2+} at various bed height (Cb_0 = 20 mg/L, Q = 5 mL /min and bed height = 4 cm)…….....158

Figure 4.52: Comparison between theoretical and experimental results obtained using proposed mathematical model for the adsorption of Zn^{2+} at various bed height (Cb_0 = 20 mg/L, Q = 5 mL /min and bed height = 7 cm)……..……158

Figure 4.53: Project annual cash flow……..…169

Figure 4.54: Total cost of manufacturing……..…169

LIST OF TABLES

Table 1.1: Advantages and Disadvantages of Heavy Metals Treatment Methods……..……4

Table 2.1: Heavy Metals Produced from Various Industries…….……19

Table 2.2: South African National Water Act Waste Discharge Standard Guidelines…..……....20

Table 2.3: Metal Sources Relative to Toxicities and Human Diseases……...……..21

Table 3.1: Experimental Range and Levels of Process Variables for Cu^{2+}……..……..…67

Table 3.2: Experimental Range and Levels of Process Variables for Zn^{2+}……...……68

Table 3.3: Experimental Design and Results Layout for BBD for Cu^{2+} Adsorbed by Egyptian Water Hyacinth……..……69

Table 3.4: Experimental Design and Results Layout for BBD for Zn^{2+} Adsorbed by Egyptian Water Hyacinth……..…70

Table 3.5: Experimental Design and Results Layout for BBD for Cu^{2+} Adsorbed by SA- Water Hyacinth…….……71

Table 3.6: Experimental Design and Results Layout for BBD for Zn^{2+} Adsorbed by SA-Water Hyacinth……..……72

Table 3.7: Summary of Fixed-Bed Column Experiments using Raw Water Hyacinth of Particle Size 2mm - 3mm ……..…78

Table 4.1: Percentage of Elements (%, wt) that Found in of Raw Water Hyacinth Samples from South Africa and Egypt before Adsorption…….. 96

Table 4.2: Chemical Composition (%, wt.) of Raw Water Hyacinth Samples from South Africa and Egypt before Adsorption ……..…...…….……..……97

Table 4.3: FTIR of Egyptian Water Hyacinth Sample before Adsorption of Cu^{2+}……...…....99

Table 4.4: FTIR of Egyptian Water Hyacinth Sample after Adsorption of Cu^{2+}…….…....99

Table 4.5: Changes in Spectral Structure When Copper was Adsorbed on Egyptian Water Hyacinth Sample…….……..…….……..100

Table 4.6: FTIR of SA- Water Hyacinth Sample before Adsorption of Cu^{2+}……102

Table 4.7: FTIR of SA-Water Hyacinth Sample after Adsorption of Cu^{2+} ……101

Table 4.8: Changes in Spectral Structure when Copper was adsorbed on the SA-Water Hyacinth …….....103

Table 4.9: Parameters of Langmuir Isotherm for Adsorption of Copper and Zinc using Egyptian Water Hyacinth…….…….…….…113

Table 4.10: Parameters of Langmuir Isotherm for Adsorption of Copper and Zinc using SA- Water Hyacinth Sample …..…..……...…...……..……....114

Table 4.11: Maximum Adsorption Capacity of Water Hyacinth for Cu^{2+} and Zn^{2+} in Various Studies……..……....115

Table 4.12: Parameters of Freundlich Isotherm for Adsorption of Copper and Zinc using Egyptian Water Hyacinth Sample……117

Table 4.13: Parameters of Freundlich Isotherm for Adsorption of Copper and Zinc using SA-Water Hyacinth Sample.……...….……..118

Table 4.14: Adsorption Kinetics Parameters of Zn^{2+} and Cu^{2+} Ions on Egyptian Water Hyacinth Sample……..…….……..…….……..……..121

Table 4.15: Adsorption Kinetics Parameters of Zn^{2+} and Cu^{2+} Ions on Dried Water Hyacinth SA-Sample……..124

Table 4.16: Experimental Design and Results Layout for Box–Behnken Design Cu^{2+} Adsorbed by Egyptian Water Hyacinth……125

Table 4.17: Experimental Design and Results Layout for Box–Behnken Design Zn^{2+} Adsorbed by Egyptian Water Hyacinth…….……126

Table 4.18: Experimental Design and Results Layout for Box–Behnken Design Cu^{2+} Adsorbed by SA- Water Hyacinth…….....127

Table 4.19: Experimental Design and Results Layout for Box–Behnken Design Zn^{2+} Adsorbed by SA- Water Hyacinth…….…...128

Table 4.20: ANOVA for Quadratic Models Egypt –Water Hyacinth, SA-Water Hyacinth ……132

Table 4.21: Quadratic Regression Model of ANOVA for Removal of Cu^{2+} and Zn^{2+} using Egyptian Water Hyacinth……..…….……...…133

Table 4.22: Quadratic Regression Model of ANOVA for Removal of Cu^{2+} and Zn^{2+} Using SA-Water Hyacinth…….…….……..……133

Table 4.23: The Conflicting Region of Control Variables Egyptian Water Hyacinth...……...…….……...……..……...…135

Table 4.24: The Conflicting Region of Control Variables SA-water Hyacinth…….…….135

Table 4.25: Parameters of Fixed- Bed Column Tests at Various Cu^{2+} Concentrations (bed depth 2 cm; Q 5 mL/min; pH 6)……...……...138

Table 4.26: Parameters of Fixed- Bed Column Tests at Various Zn^{2+} Concentrations (bed depth 2 cm; Q 5 mL/min; pH 6)…….……..…..138

Table 4.27: Parameters of Fixed- Bed Column Tests for Cu^{2+} at Various Bed Depths (C_o= 20mg/l; flowrate 5 mL/min; pH 6)……..140

Table 4.28: Parameters of Fixed- Bed Column Tests for Zn^{2+} at Various Bed Depths (C_o= 20mg/l; flowrate 5 mL/min; pH 6)……..141

Table 4.29: Parameters of Fixed- Bed Column Tests for Cu^{2+} at Various Feed Solution Flowrates (C_0= 20 mg/L; bed depth=2cm; pH 6)…….…….……143

Table 4.30: Parameters of Fixed- Bed Column Tests for Zn^{2+} at Various Feed Solution Flowrates (C_0= 20 mg/L; bed depth=2cm; pH 6)……143

Table 4.31: Model Parameters Value for Simulation…….…….146

Table 4.32 Model and Experimental Breakthrough Curves Parameters at Various Cu^{2+} and Zn^{2+} Concentrations (bed depth 2 cm, Q 5 mL/min, pH 6)……...……...…..…151

Table 4.33 Model and Experimental Breakthrough Curves Parameters at Various Cu^{2+} and Zn^{2+} flowrates (bed depth 2 cm, initial conc. 20 mg/L, pH 6)…...…….155

Table 4.34: Model and Experimental Breakthrough Curves Parameters for Cu^{2+} and Zn^{2+} at Various Bed Height (flowrate 5 mL/min, initial conc. 20 mg/l, pH 6)…...……..159

Table 4.35 Results of Model and Experimental Comparison…..……160

Table 4.36. Data of Parameters of Mini Adsorption Column for Cu^{2+} Vs Scaled up Column…162

Table 4.37: Data of Parameters of Mini Adsorption Column for Zn^{2+} Vs Scaled up Column...163

CHAPTER ONE

INTRODUCTION

1.1. Background

Sustainable Development

The notion of sustainable development (SD) has developed since it was first brought up at the biosphere conference in Paris in 1968 (Kopnina, 2011). In 1987, the United Nations World Commission on Environment and Development issued a report named 'Our Common Future', commonly known as the Brundtland report, where the classic definition of sustainable development according to this report is: 'development that meets the needs of the present without compromising the ability of future generations to meet their own needs' (Bolcárová and Kološta 2015). Sustainable development integrates three complementary areas of development, which are the economic, social and environmental areas. The term 'sustainable' could be replaced by the terms 'balanced equitable'. It can also be said that the sustainable development core should be based on balancing the interests and needs of the different sectors of society within the same generation, and among the future generations, all together in the three correlated areas: economic, social and environmental (Soubbotina, 2004).

Economic growth in itself does not necessarily lead to economic sustainability. For an economic growth to be sustainable, the income of a country has to be used to provide the people with satisfying salaries, wages, good standard of hospitals, education, food, and housing that can be available for all members of the society without any kind of discrimination. Economic growth should not negatively affect the life quality, the environment, or natural resources (Munier, 2005). Social sustainability is related to social equity, which is achieved by providing every citizen with his right for housing, food, health care, and jobs (Munier, 2005). Environmental sustainability development is achieved through conservation of natural resources, prevention of environmental pollution, and compliance to environmental regulations and laws.

To minimize the damage inflicted on the world, well-known conventional eco-efficient approaches were used trying to reduce the ecological footprint. Recycling and recovery focuses on eco-effectiveness by stimulating to do the right things in order to improve our positive footprint (Toxopeus et al., 2015). Recycling is a very essential concept because creating new sources of raw material is an expensive, and a difficult task, additionally waste disposal and incineration are expensive processes, require space for land filling, and can cause contamination of soil, air, and water (El Haggar, 2007).

Solving the problem of heavy metals contamination of water has been a major preoccupation of researchers for many years due to the adverse effects that their toxicities have on aquatic lives, human beings and the environment. This is because, unlike organic pollutants, they do not biodegrade. Their presence in industrial effluents and drinking water is a public health concern (Anzeze et al., 2014).

Water is a renewable resource, it is naturally renewed within the hydrological cycle, however, once used it gets polluted and of course the extent of pollution is directly correlated to the purpose it was used for (WHO/UNEP 1997). Water of high quality is essential to human life and water of acceptable quality is essential for agriculture, industrial, domestic and commercial uses (Anzeze et al., 2014).

Freshwater availability is one of the major problems facing the world, and approximately one-third of drinking water requirement of the world is obtained from surface sources like rivers, lakes, canals and dams (Edokpayi et al., 2017). Direct pollution is caused by releasing fluids directly into the water, as shown in Figure 1.1, such as a company that dispenses of contaminated water or toxic solids mixed directly with water into the sea or river. This makes the water poisonous, every so often resulting in death, for fish and other aquatic creatures. Nevertheless, animals also drink this water, which also brings to them ill health or death. It can also affect to humans (Singh et al., 2020).

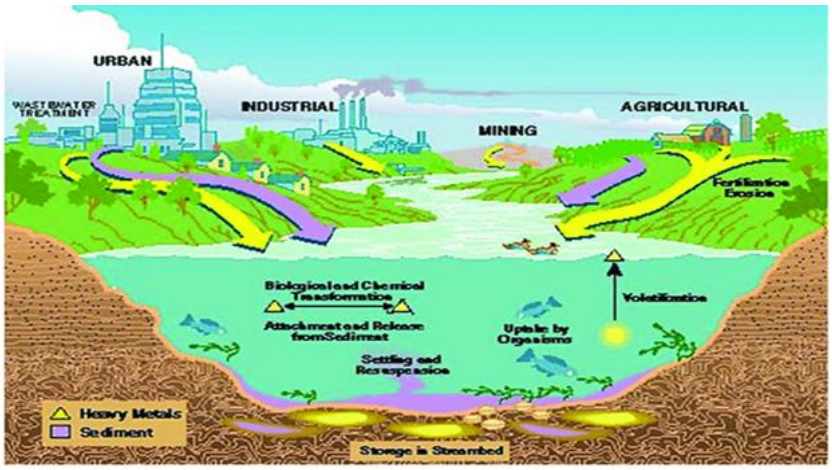


Figure 1.1. Sources and sinks of heavy metals (Garbarino et al., 1995)

Industrial Wastewater

Industrial wastewater is defined as "any wastewater generated from any manufacturing, processing, institutional, commercial, or agricultural operation, or any operation that discharges other than domestic or sanitary wastewater" (Industrial Waste Management Division 1998). Water scarcity is a problem that is facing South Africa, Egypt and many other countries all over the world and it is expected to become more serious in the future. Specifically for South Africa Harding et al. (2020) found that there were two previous Water Research Commission (WRC) projects that compiled databases and reports examining water use and wastewater generation by sector in South Africa. One study reported a total wastewater volume of 962 000 kL/day, which is approximately 350 Mm^3 /year, while the other study report 69 Mm^3 /year.

Wastewater treatment technologies, whether domestic or industrial, are very vital, therefore, more efforts and finance ought to be assigned for research work in that field. High quality water should not be used for purposes that can bear lower water quality (WHO/UNEP 1997). Treating and reusing wastewater will eventually allow conserving freshwater for potable and domestic use. Lower quality and treated wastewater, on the other hand, could be dedicated to uses that do not require high quality of water, such as, landscaping and industrial reuse. Industrial wastewater that does not comply with the permissible law limits is the main source of pollution as it consists of organic and inorganic pollutants, as well as heavy metals, varying according to the industry. Therefore, treating industrial wastewater to be suitable for reuse or to comply with the permissible limits for discharge in waterways achieves the sustainable development concept in terms of reusing

wastewater in various purposes, which is an application of the cradle to cradle concept, conserving and sustainably managing the available water resources, and protecting surface water bodies and aquatic life from potential contamination, thus, protecting human health from exposure to heavy metals.

Heavy Metals in Industrial Wastewater

Heavy metals are defined as metallic elements that have a relatively high density compared to water (Kinuthia et al., 2020). Water contamination by heavy metals is a major environmental problem. Rapid industrial development has increased the release of heavy metals in water bodies. Heavy metals endanger human health and accumulate in food chains (Sarma et al., 2015). Most heavy metals are toxic even at lower concentrations (Mendoza et al., 2023). Metal toxicity depends upon the route of exposure, absorbed dose, and duration of exposure, i.e. acute or chronic (Mitra et al., 2022). Heavy metal pollutants most common in the environment are Cr, Mn, Ni, Cu, Zn, Cd, and Pb (Ali et al., 2019). Although pollution due to heavy metals is a global concern, levels of contamination vary from place to place (Yuan and Wang, 2023). Discharge of municipal, industrial and agricultural wastewaters and sewage into rivers has been identified as a significant route of heavy metals into aquatic resources (Agoro et al., 2020). Once heavy metals enter the water body, they cause certain toxicity to aquatic organisms. Heavy metals are absorbed through the animal subcutaneous layers and then enter the bodies of the organisms through osmotic exchanges between the heavy metals and the impacted body surfaces of the aquatic organisms (Hong et al., 2020).

This study focuses on two heavy metals, copper and zinc. Copper (Cu), as a heavy metal, has been used by man for centuries, however, it is regarded as a longstanding environmental contaminant. Several industries, like mining, printing, painting, dyeing, battery manufacture and others, discharge effluent containing Cu^{2+} to waterways.

Zinc (Zn), as a heavy metal, is an essential and beneficial element for humans and plants. Complete exclusion of Zn is not possible due to its dual roles, as an essential microelement on one hand and a toxic environmental factor on the other. Zinc is a well-known toxic metal ion and can threaten human life by bio-accumulating in the food chain. Zinc can cause phytotoxic anaemia, lack of muscular coordination, abdominal pain, nonfatal fume fever and pneumonitis (Zhang et al., 2017). Although zinc is an essential requirement for a healthy body, excess zinc can be harmful and cause

zinc toxicity. Zinc is a common metal ion found in effluents of a large number of industries (Chyad et al., 2023).

Heavy Metals Treatment Methods

The removal of zinc and copper from wastewater is extremely important before its discharge into the aquatic system. Conventional treatment technologies that have been developed to remove heavy metals from wastewater are chemical precipitation (Badmus et al., 2007), ion exchange (Bai and Bartkiewicz, 2009), membrane separation (Khulbe and Matsuura, 2018), electrocoagulation (Al-Shannaga et al., 2014), dialysis/electrodialysis (Moura et al., 2012) and adsorption/filtration (Dehghani et al., 2016). Some of these current methods have some drawbacks, including inefficient metal removal, especially in treatment of wastewater contaminated with trace concentrations of heavy metals in the range of 1-100 mg/L (Sarma et al., 2015), high energy consumption and production of a secondary waste product, i.e. toxic sludge, that would require further special handling, requiring large quantities of chemical reagents, and complicated operation and maintenance (Vidu et al., 2020). By comparison, the adsorption technique is a highly effective method because it is a simple and cost-effective method for recovering and eliminating heavy metal ions from dilute solutions (Dehghani et al., 2016). Adsorption processes are attractive approaches for wastewater treatment because there are a lot of cheap adsorbents that can be used which don't require a pre-treatment step before their application. Adsorption using activated carbon, it is very expensive in large scale applications (Wang and Chen, 2009). Therefore, most of these treatment methods cannot be considered as sustainable treatment technologies. Table 1.1 presents the advantages and disadvantages of an array of treatment methods and technologies of heavy metals in wastewater

Table 1.1: Advantages and Disadvantages of Heavy Metals Treatment Methods (Ariffin et al., 2017)

Methods	Advantages	Disadvantages
Oxidation	Rapid process for toxic pollutants removal	High energy costs and formation of byproducts
Ion exchange	Good removal of a wide range of heavy metals	Adsorbents requires regeneration or disposal
Membrane filtration technologies	Good removal of heavy metals	Concentrated sludge production and expensive
Adsorption	Flexibility and simplicity of design, ease of operation and insensitivity to toxic pollutants	Adsorbents require regeneration
Coagulation/flocculation	Economically feasible	High sludge production and formation of large particles
Electrochemical treatment	Rapid process and effective for certain metal ions	High energy costs and formation of large particles
Ozonation	Applied in gaseous state; alteration of volume	Short half life
Photochemical	No sludge production	Formation of by-product
Irradiation	Effective at lab scale	Require a lot of dissolved O_2
Electrokinetic coagulation	Economically feasible	High sludge production
Fentons reagents	Effective and capable of treating variety of wastes and no energy input necessary to activate hydrogen peroxide	Sludge generation
Biological treatment	Feasible in removing some metals	Technology yet to be established and commercialized

Adsorption

Adsorption is a process that takes place when a gas or liquid solute accumulates on the surface of a solid or a liquid (adsorbent), forming a molecular or atomic film (the adsorbate). Depending on the types of phases in contact, the process can be considered in the following systems: liquid–gas, liquid–liquid, solid–liquid and solid–gas (Amosa, 2015a). Adsorption is one of the most efficient wastewater treatment technologies because of its low cost. Compared to the other technologies highlighted in Table 1.2, it does not produce a large amount of sludge and it is a simple operation (Grassi et al., 2012). Adsorbents can be classified into two main groups, which are:

- **Conventional Adsorbents**. These are commercial adsorbents and some of them are commonly used, such as activated carbon, which is the most common adsorbent used in wastewater treatment due to its inherent properties (e.g., high surface area, microporous structure, high porosity, and high adsorption capacity (Philippou, 2021). Activated carbon can be made of different materials, such as coal, coconut shells, lignite, wood, and others. Clay minerals are also categorized as conventional adsorbents, the clay adsorption property is due to its negatively charged surface that allows clay to adsorb positively charged ions (Grassi et al., 2012). Lastly, natural minerals such as zeolite and goethite are categorized as conventional adsorbents (Nwafulugo et al., 2014).
- **Unconventional Adsorbents**, which are mainly composed of cheap agricultural, and industrial wastes, naturally existing materials and other organic materials such as, bacteria, algae, fungi, or other naturally occurring materials such as water hyacinth. Natural materials are recently used as adsorbents and are eco-friendly in nature.
- **Water Hyacinth**

Water hyacinth was selected as an unconventional low-cost, naturally occurring, adsorbent to study the removal efficiency of copper and zinc from wastewater. Water hyacinth (Eichhornia Crassipes) is a floating macrophyte whose appetite for nutrients and explosive growth rate has been put to use in cleaning up municipal and agriculture wastewater. Water hyacinth is highly effective in removing Cd^{2+}, Cu^{2+}, Ni^{2+}, Zn^{2+}, Pb^{2+} and Cr^{3+} (Kumar and Roy, 2013, Mahamadi, 2011).

1.2. Motivation

The first motivation behind this work is that the situation of water scarcity in South Africa is very serious because the country is among the 30 driest countries in the world, with less than 450 mm of rainwater per year (Bwapwa, 2019), so treating industrial wastewater to be suitable for reuse or to be complying with the permissible limits for discharge in waterways is needed to prevent a crisis that can affect lives of millions of people and the economy.

Most industrial effluents contain high concentrations of heavy metal ions. Unlike organic pollutants, the majority of which are subject to biological degradation, heavy metals do not degrade into harmless end-products, and therefore it is necessary to remove these metal ions from wastewater to be within the permissible limits before they are drained to the environment.

The second motivation is that water hyacinth is considered one of the worst aquatic weed in the world (Oyinloye et al., 2018). Its rapid growth and sporadic dispersal has destroyed many ecologically and economically important water bodies and productive wetlands as it is difficult to manage once established (Honlah et al., 2019). The threat of water hyacinth is reaching alarming proportions in many parts of the world, especially in tropical water bodies (Honlah et al., 2019). South Africa is one of the countries affected by this threat, where water hyacinth has been classified as a category 1b weed according to the National Environmental Management Act, 2018. Category 1b means that this plant must be immediately removed. However, instead of removing ~~it~~ and destroying it, there are ways in can be used beneficially as an effective, economic, and eco-friendly adsorbent.

Another motivation behind the study is that the experimental work usually performed during an adsorption process does not give an optimum purification efficiency, so a better technique is needed to combine all the parameters and get the optimum operating conditions. This is particularly true since experimental determination of the adsorption performance under diverse conditions is usually of necessity.

Several studies have investigated the use of water hyacinth for the removal of heavy metals from water. However, most of these studies involve a pre-treatment step before use. Hemalatha et al. (2020), used water hyacinth to remove zinc and chromium from wastewater in a batch process. In their study they divided the plant into leaves, petiole and root and converted each part into powder and tested each part separately. Neris et al. (2019) used modified water hyacinth fibres in removal of lead, nickel and zinc using batch process. Nyamunda et al. (2019) used magnetic biochar derived from water hyacinth to remove zinc and copper from wastewater using batch process.

The aim of this study, therefore, is to observe the removal efficiency of water hyacinth to remove Cu^{2+} and Zn^{2+} without chemical or thermal pre-treatment (only minor physical treatment) in batch and continuous processes. Several parameters influence the effective removal of heavy metals by adsorption. The adsorption capacity of water hyacinth is determined with respect to various parameters. Optimisation of the adsorption process results in optimal solutions. This conclusion is based on a single objective response surface methodology (RSM) design together with the application of the branch-and-reduce optimisation navigator (BARON) solver based on the general

algebraic modelling system (GAMS) with similar variables, model equations and levels. Optimum parameters according to RSM and GAMS will be obtained.

The implementation of generic equations assists in developing a mathematical model which describes the adsorption of Cu^{2+} and Zn^{2+} from wastewater using water hyacinths. The results of a fixed bed column will be used to verify this model.

1.3. Research Objectives

The objectives of this study can be summarized as follows.

- To investigate the effectiveness of using water hyacinth, a less-expensive adsorbent to adsorb copper and zinc ions (without treatment) from synthetic wastewater in batch and continuous processes.
- To explore the effect of the location of water hyacinth on its adsorption capacity for the removal of Cu^{2+} and Zn^{2+} from wastewater, specially that both samples almost grow in similar growth conditions regarding temperature, pH value and salinity.
- To involve the use of RSM and GAMS to optimize process conditions for maximal biosorption of Cu^{2+} and Zn^{2+} from aqueous solutions.
- To determine the generic equations that best describe the adsorption mechanism of the hyacinth to remove Cu^{2+} and Zn^{2+} from wastewater and validate the proposed generic model against experimental data. The breakthrough curves provide us with the information needed for design of adsorption column.

1.4. Thesis Layout

This thesis consists of five chapters including this chapter (Chapter 1) that provides the background, motivation for the research, and the overall objective of this study. The layout is schematically represented in Figure 1.2.

Chapter 2 is the literature review, which includes the general overview on water hyacinth as an adsorbent and the nature of industrial wastewater and the toxicity of heavy metals, followed by an outline of the removal of heavy metals from wastewater using adsorption and conventional methods of removal. A broad and comprehensive review of removal of heavy metals using water hyacinth as a low-cost adsorbent is also given. This includes the different parameters used,

different methods of preparing the adsorbent and the effect of water hyacinth in adsorbing different heavy metals. The application of RSM for removal of heavy metal ions from wastewater by adsorption is demonstrated and an introduction to GAMS is given. A brief summary is provided of basic concepts and mathematical models to be used as a basis for a design and optimization of the adsorption system.

Chapter 3 is the materials and methods, where the preparation of water hyacinth and the stock solution of Cu^{2+} and Zn^{2+} is described together with the experimental set up of batch and fixed bed column. Adsorption isotherm and kinetic study are explained in this chapter. Optimisation process using RSM and GAMS are also reported. Samples and analysis techniques for water hyacinth and Cu^{2+} and Zn^{2+} ions are shown. Mathematical modelling, simulation, calculation of model parameters, model validation and how to compare between model and experimental results are explained in this chapter. Finally the scale up procedure for adsorption column and an economic feasibility on the column is described.

Chapter 4 is results and discussion. First it contains the results of the characterization of water hyacinth, then batch equilibrium experiments, adsorption isotherm and kinetic study results. The results of optimisation using RSM and GAMS are discussed. Fixed bed column experiment results, modelling and simulation results are explained extensively. Validation of the mathematical model and its comparison between the experimental data is also discussed. Finally the result of the scaled up adsorption column and the economic feasibility on it is demonstrated.

Chapter 5 concludes the thesis with a summary of the findings and recommendations.

References to all articles used in the study are provided at the end of each chapter.

References

Agoro, M.A., Adeniji, A.O., Adefisoye ,M.A., Okoh, O.O., 2020.Heavy Metals in Wastewater and Sewage Sludge from Selected Municipal Treatment Plants in Eastern Cape Province, South Africa. Water 2020, (12) 2746.

Ali, H., Khan, E., Ilahi, I., 2019. Environmental Chemistry and Ecotoxicology of Hazardous Heavy Metals: Environmental Persistence, Toxicity, and Bioaccumulation. J. Chem. 2019, 14.

Al-Shannaga, M., Al-Qodahb, Z., Bani-Melhemc, K., Qtaishat, M., Alkasrawi, M., 2015.Heavy metal ions removal from metal plating wastewater using electrocoagulation: Kinetic study and process performance. Chemical Engineering Journal, 260: 749–756.

Amosa, M., 2015a. Hybrid adsorption-membrane process for reclamation of bio-treated palm oil mill effluent for boiler-feed reuse In: Engineering, Vol. Ph.D., International Islamic University Malaysia, Kuala Lumpur, 328.

Anzeze, D., Onyari, J., Shiundu, P., Gichuki, J., 2014. Adsorption of Pb (II) ions from aqueous solutions by water hyacinth (eichhornia crassipes): equilibrium and kinetic studies. International Journal of Environmental Pollution and Remediation (IJEPR), 2: 89–95.

Ariffin, N., Abdullah, M.M., Zainol, M.R.R.M., Murshed, M.F., Zain, H., Faris, M.A., Bayuaji, R., 2017. Review on Adsorption of Heavy Metal in Wastewater by Using Geopolymer. MATEC Web of Conferences 97, 01023.

Badmus, M., Audu, T., Anyata, B., 2007. Removal of heavy metal from industrial wastewater using hydrogen peroxide. African Journal of Biotechnology, 6(3): 238–242.

Bai, Y., Bartkiewicz, B., 2009. Removal of cadmium from wastewater using ion exchange resin amber jet 1200h columns. Polish J. of Environ. Stud., 18(6): 1191–1195.

Bwapwa, J.K., 2019. Analysis on Industrial and Domestic Wastewater in South Africa as a Water-Scarce Country. International Journal of Applied Engineering Research, 14(7): 1474-1483.

Bolcárová, P., Kološta, S., 2015. Assessment of sustainable development in the EU 27 using aggregated SD index." Ecological Indicators 48, 699-705.

Chyad,T., Al-Hamadani, R., Hammood, Z.,Ali, G., 2023. Materials Today: Proceedings. Removal of Zinc (II) ions from industrial wastewater by adsorption on to activated carbon produced from pine cone. Volume 80, Part 3, 2023, Pages 2706-2711.

Dhegihan, M., Sanaei D., Ali, I., Bhatnagar A., 2016. Removal of chromium (VI) from aqueous solution using treated waste newspaper as a low-cost adsorbent: Kinetic modelling and isotherm studies. Journal of Molecular Liquids, 215(2016): 671–679.

Edokpayi, J., Odiyo, J., Durowoju O., 2017. Impact of Wastewater on Surface Water Quality in Developing Countries: A Case Study of South Africa. Water Quality book (pp.401-416) Chapter: 18 Publisher: InTech Editors: Hlanganani Tutu.

El Haggar, S., 2007. Sustainable Industrial Design and Waste Management: Cradle-to-Cradle for Sustainable Development. Elsevier, 2007.

Garbarino, J., Hayes, H., Roth, D., Antweider R, Brinton, T., Taylor, H., 1995. Contaminants in the Mississippi river. US Geological Survey Circular, Virginia (1133).

Grassi, M., Kaykioglu, G., Belgiorno, V., Lofrano, G., 2012. Removal of Emerging Contaminants from Water and Wastewater by Adsorption Process." In Emerging Compounds Removal from Wastewater Natural and Solar Based Treatments, 15-37. Salerno: Springer.

Harding, G., Chivavava, J., Lewis, A., 2020. Challenges and shortcomings in current South African industrial wastewater quality characterisation. Water SA, 46(2) 267–277.

Hemalatha, D., Narayanan, R.M., Sanchitha, S., 2020. Removal of Zinc and Chromium from industrial wastewater using water hyacinth (E. crassipes) petiole, leaves and root powder: Equilibrium study, Materials Today: Proceedings, https://doi.org/10.1016/j.matpr.2020.10.725.

Hong, Y., J., Liao, W., Yan, Z.F., Bai, Y.C., Feng, C.L., Xu, Z. X., Xu, D.Y., 2020. Progress in the Research of the Toxicity Effect Mechanisms of Heavy Metals on Freshwater Organisms and Their Water Quality Criteria in China. Journal of chemistry. Volume 2020 |Article ID 9010348.

Honlah, E., Segbefia, A.Y., Appiah, D.O., Mensah, M., Atakora, P.O., 2019. Effects of water hyacinth invasion on the healthof the communities, and the education ofchildren along River Tano and Abby-Tano Lagoonin Ghana. Cogent Social Sciences (2019), 5: 1619652.

Industrial Waste Management Division. "Guide for Discharging Industrial Wastewater to the Sewer." Environment LA Sanitation. City of Los Angeles, Department of Public Works. 1998. http://www.lacitysan.org/business/pdf/iwmguide.pdf.

Khulbe, K., Matsuura, T., 2018. Removal of heavy metals and pollutants by membrane adsorption techniques. Applied Water Science, 8(1): 1–50.

Kinuthia, G.K., Ngure, V., Beti, D., Lugalia, R., Wangila,A., Kamau, L., 2020. Levels of heavy metals in wastewater and soil samples from open drainage channels in Nairobi, Kenya: community health implication. Scientific Reports 8434 (2020).

Kopnina, H., 2011. Revisiting Education for Sustainable Development (ESD): Examining Anthropocentric Bias through the Transition of Environmental Education to ESD. Sustainable Development, Sust. Dev.22, 73–83 (2014), published online 2 November 2011 in Wiley Online Library.

Kumar, K., Roy, S., 2013. Adsorption of hexavalent chromium from aqueous solution by water hyacinth (Eichhornia Crassipes). The Ecoscan, 3(Special Issue): 205–209.

Mahamadi, C., 2011. Water hyacinth as a biosorbent: A review. African Journal of Environmental Science and Technology, 5(13), 1137-1145.

Mendoza, L.C., Nolos, R.C., Villaflores, O.B., Apostol, E.M.D., Senoro, D.B., 2023. Detection of Heavy Metals, Their Distribution in Tilapia spp., and Health Risks Assessment. Toxics 2023, 11, 286. https:// doi.org/10.3390/toxics11030286.

Mitra, S. Mitra , Chakraborty, A., , Tareq,A., , Emran.T., Nainu,F., Khusro,A., Idris,A., Khandaker,M., Osman,H., Alhumaydhi,F., Simal-Gandara,J., 2022. Impact of heavy metals on the environment and human health: Novel therapeutic insights to counter the toxicity. Journal of King Saud University – Science 34 (2022) 101865.

Moura, R., Bertuol, D., Ferreira, C., Amado, F., 2012. Study of chromium removal by the electrodialysis of tannery and metal-finishing effluents. International Journal of Chemical Engineering, 2012:1–7.

Munier, N., 2005. Introduction to Sustainability: Road to a Better Future. Dordrecht: Springer, 2005.

Neris, J.B., Francisco, H., Luzardo, M., Santos, P.F., de Almeida, O.N., Garcia, F., 2019. Evaluation of single and tri-element adsorption of Pb^{2+}, Ni^{2+} and Zn^{2+} ions in aqueous solution on modified water hyacinth (Eichhornia crassipes) fibers. Journal of Environmental Chemical Engineering 7(1):102885.

Nwafulugo, F.U., Adefila, S.S., Olawale, A.S., Ajayi, O.A., 2014. Environmental impact and removability of selected heavy metals from petroleum wastewater using zeolite 4A- metakaolin matrices. Journal of Environmental Science and Water Resources 3(6) (2014): 132-143.

Nyamunda, B.C., Chivhanga, T., Guyo, U., Chigond, F., 2019. Removal of Zn (II) and Cu (II) Ions from Industrial Wastewaters Using Magnetic Biochar Derived from Water Hyacinth. Journal of Engineering, Volume 2019, Article ID 5656983, 11 pages.

Oyinloye, M.A., Owoeye, J.O., Ogunlade, S.O., 2018. Impact of Water Hyacinth on Resident Living in Coastal Areas of Ondo State, Nigeria: A Focus on Ilaje Local Government Area. International Journal of Environmental Monitoring and Protection. 5(3), 2018, 52-63.

Philippou, K., Anastopoulos, I., Pashalidis, I., Bandegharaei, A.H., Usman, M., Kornaros, M., M Omirou, M., Kalderis, D., Milojković, J.V., Lopičić, Z.R., Abatal, M., 2021. Chapter 6 - The application of pine-based adsorbents to remove potentially toxic elements from aqueous solutions. Sorbe Sorbents Materials for Controlling Environmental Pollution. Current State and Trends 2021, 113-133.

Sarma, P.J., Kumar, R., Pakshirajan, K., 2015. Batch and Continuous Removal of Copper and Lead from Aqueous Solution using Cheaply Available Agricultural Waste Materials. Int. J. Environ. Res. 9, no. 2 (2015): 635-648.

Soubbotina, T. P. 2004. Beyond Economic Growth: An Introduction to Sustainable Development. The World Bank. 2004. http://www.worldbank.org/depweb/english/beyond/beyondco/beg_all.pdf.

Singh, J., Yadav, P., 2020. Ashok Kumar Pal and Vishal Mishra. Water Pollutants: Origin and Status, 2020 .In book: Sensors in Water Pollutants Monitoring: Role of Material (pp.5-20).

Toxopeusa, A. M.E., Koeijera, B.L.A, Meijb, A.G.G.H., 2015. Cradle to Cradle: Effective Vision vs Efficient Practice. Procedia CIRP 29 (2015) 384 – 389.

Vidu, R., Matei, E., Predescu, A.M., Alhalaili, B., Pantilimon, C., Tarcea, C., Predescu, C., 2020. Removal of Heavy Metals from Wastewaters: A Challenge from Current Treatment Methods to Nanotechnology Applications. Toxics 2020, 8.

Wang, J., Chen, C., 2009. Biosorbents for heavy metals removal and their future. Biotechnology Advances 27 (2009): 195–226.

WHO/UNEP. "Water Pollution Control: A Guide to the Use of Water Quality Management Principles: Wastewater as a Resource." World Health Organization.1997. http://www.who.int/water_sanitation_health/resourcesquality/watpolcontrol.pdf.

Yuan, C., Wang, X., 2023. Source Apportionment and Health Risk Assessment of Heavy Metals in Soils of Old Industrial Areas—A Case Study of Shanghai, China.

Zhang, X., Hao, Y., Wang, X., Chen, Z., 2017.Rapid removal of zinc (II) from aqueous solutions using a mesoporous activated carbon prepared from agricultural waste. Materials (Basel), 10(9):1002.

CHAPTER TWO

LITERATURE REVIEW

2.1. Water: A Finite but Sustainable Resource

The most common substance on earth is water; it covers virtually three quarters of the earth's surface. Water is distributed to different areas of the planets by the rain cycle powered by the energy of the sun. In order to prevent the rise in economic development and environmental degeneration, water management has to be carried out according to the principle of sustainable development, as water is a very crucial resource for both social and economic growth. According to the United Nations Resolution 64/292: "The human right to water entitles everyone to sufficient, safe, acceptable, physically accessible and affordable water for personal and domestic uses" (Choukroune and Nedumpara, 2021).Therefore, SDG 6.1 call for full coverage of safely managed drinking water by 2030. The "Safely managed drinking water" indicator includes the three following conditions: accessible on premises, available when needed and free from contamination (United Nations, 2018). This goal is a huge challenge for all countries, not only for low- and middle-income ones .The commitment to "leave no one behind" requires a focus on rural areas, which is typically neglected. While hand hygiene is one of the first lines of defense against the spread of infectious diseases, 2.3 billion people, or 29% of the global population, lacked a basic hand washing facility with water and soap at home in 2020 (WHO, 2022). At the same time, 2.1 billion people have no safely managed drinking water supply system service. This means that 14.9% of the urban- and 45.2% of the rural residents need modified services (Nwobodo and Chukwu, 2020) .A person needs 50 to 100 liters of water per day to meet hygienic and physiological needs. As people facing a limit of 20 liters per person per day, therefore they will be subjected to a high level of health concerns. Rural inhabitants usually live in worse economic conditions than urban ones and this affects the volume of water use (Omarova et al., 2019).

2.2. Industrial Wastewater

Wastewater is defined as any squall water drainage, as well as industrial, domestic or commercial sewage or any mix thereof carried by water (Naidoo and Olaniran, 2014). Industrial waste can be solid, gas, or liquid and each type has different methods of management and disposal (Awuchi et al., 2020). The water industry is very essential to human beings, animals, plants and the economy of a nation. An estimated 1.8 billion people by 2025, will live in areas plagued by water

scarcity, with two-thirds of the world's population living in water stressed regions as a result of use, growth and climate change (Alabi et al., 2019).

Treating and reusing wastewater will eventually allow conserving fresh water for domestic and potable use, while using lower quality water, treated wastewater, for other uses that does not need high quality of water, such as landscaping, irrigation and industrial re-use. High quality water should not be used for purposes that can bear lower water quality (WHO/UNEP 1997).

Industrial wastewater treatment deals with the processes used for treating wastewater (liquid wastes) produced by industries as undesirable by-products. After treatment, the treated industrial wastewater (or now called effluent) might be reused or released to sanitary sewer or to surface water in the environment either directly or through water canal. Most industries produce large volume of wastewater continuously which after treatment (effluent) is released to the aquatic environment (Awuchi et al.,2020)

Industrial wastewater that does not comply with the permissible law limits are a main source of pollution, as they consist of organic and inorganic pollutants, as well as heavy metals, varying according to the industry

2.2.1 Wastewater Treatment Data

In literature, data on wastewater is scarce and scattered and comprehensive reviews and assessments at global level are missing, with only few and partial exceptions (Sagasta et al., 2015) Figure 2.1 illustrate that studies found that 55 countries (30%) had reliable data on all three aspects (generation, treatment and use); 69 countries (38%) had data on one or two aspects, while the other 57 countries had no data (32%) (Harding et al., 2020).

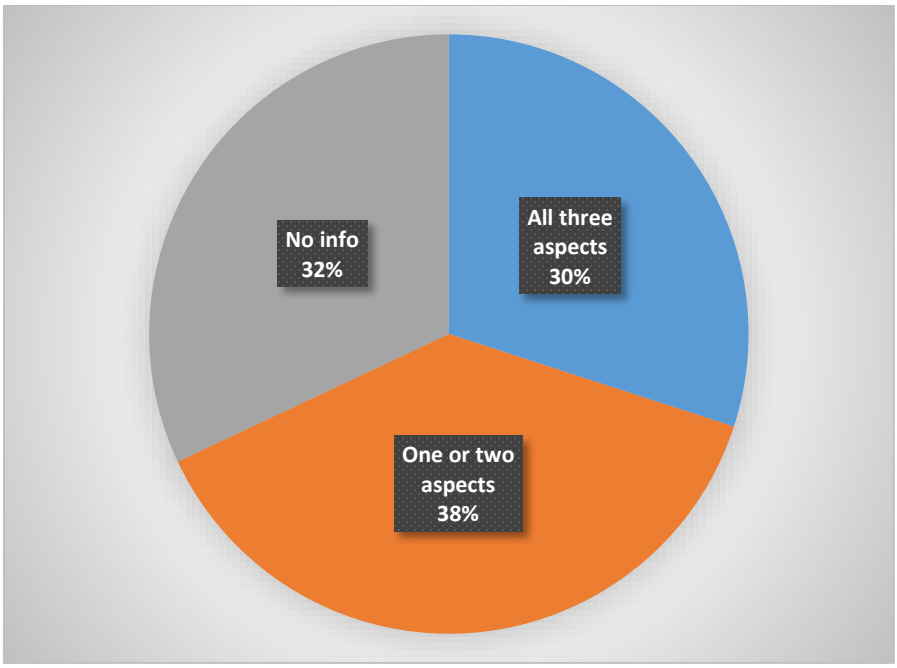


Figure 2.1. Countries with all, some or no information of wastewater generation, treatment and/or use (Harding et al., 2020)

Globally, over 80% of wastewater is released into the environment untreated (Harding et al., 2020). Figure 2.2 shows that, in high income countries 70% of wastewater is treated while 38% of wastewater is treated in upper to middle income countries, in lower to middle income countries28% of wastewater is treated and only 8% of wastewater is treated in low income countries (Harding et al., 2020).

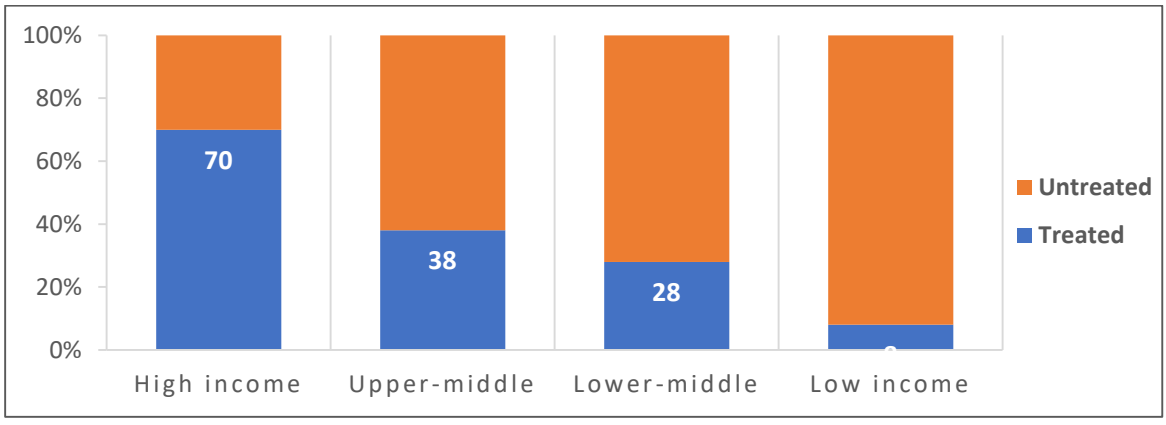


Figure 2.2. Percentage of treated and untreated wastewater by income level of countries (Harding et al., 2020)

2.2.2 Industrial Wastewater in Africa

It is noted that data on wastewater are unavailable. 32 of 48 Sub-Saharan African countries had no data available on wastewater treatment and generation (Harding et al., 2020). South Africa, Senegal and Seychelles are exceptionally have information on all three aspects of wastewater generation, use and treatment were available, however the data for South Africa was dated to 2003 and that for Seychelles was dated to 2000, so there is no updated data (Harding, 2020). Industrial wastewater pollution is a notable problem in South Africa. With just over 1200 m^3/person/year of fresh water available for a population of around 50 million, the country is currently classified as water stressed (Iloms et al., 2020). Several research studies indicate that most municipal WWTPs in South Africa rarely treat their wastewater to acceptable standards (Iloms et al., 2020).

2.3. Heavy Metal in Industrial Wastewater

Heavy metals are a group of metals and metalloids that have relatively high density and are toxic even at Part per billion (ppb) (mg/m^3) levels. Examples include Pb, As, Hg, Cd, Zn, Ag, Cu, Fe, Cr, Ni and Pd (Yadav et al., 2019). Water contamination by heavy metals is a major environmental problem. As a result of rapid industrial development is increasing the release of heavy metals in water resources. Table 2.1 demonstrates the heavy metals produced from the different industries.

Table 2.1: Heavy Metals Produced from Various Industries

Industry	Al	As	Cd	Cr	Cu	Hg	Pb	Ni	Zn
Pulp and Paper mills				X	X	X	X	X	X
Organic Chem.	X	X	X	X		X	X		X
Alkalise, Chlorine		X	X	X		X	X		X
Fertilizers	X	X	X	X	X	X	X	X	X
Petroleum refiner	X	X	X	X	X		X	X	X
Steelworks		X	X	X	X	X	X	X	X
Aircraft plating, finishing	X		X	X	X	X		X	

Heavy metals accumulate in food chains and therefore threatens human health (Sharma et al., 2015). With the rapid development of industries such as metal plating facilities, mining operations,

tanneries, fertilisers, and paper industries, heavy metals wastewaters are directly or indirectly discharged into the environment increasingly (Pohl, 2020, Atieh et. al, 2017). As a result, different heavy metal pollution sources will produced, which will have different effects on human health risk, as they cannot be broken down and are non-biodegradable and have tendency to accumulate in living beings when they are swallowed or inhaled into our bodies. Thus they are classified as dangerous. This bioaccumulation causes biological and physiological complications. Table 2.2 shows the indicators for wastewater quality management, highlighting the limit values relevant to discharge of wastewater into a receiving water body (Okeyo et al., 2018).

Table 2.2: South African National Water Act Waste Discharge Standard Guidelines

Variables and Substances	**General Standards**
Residual Chlorine (Cl)	0.25 (mg/L)
Total Cyanide (Cn)	0.02 (mg/L)
Total Arsenic (As)	0.02 (mg/L)
Total Cadmium (Cd)	0.005 (mg/L)
Total Chromium VI (Cr VI)	0.05 (mg/L)
Total Copper (Cu)	0.01 (mg/L)
Total Iron (Fe)	0.3 (mg/L)
Total Lead (Pb)	0.01 (mg/L)
Total Zinc (Zn)	0.1 (mg/L)

A pathway showing the consequences of heavy metal pollution can be seen in Figure 2.3 (Briffa et al., 2020).

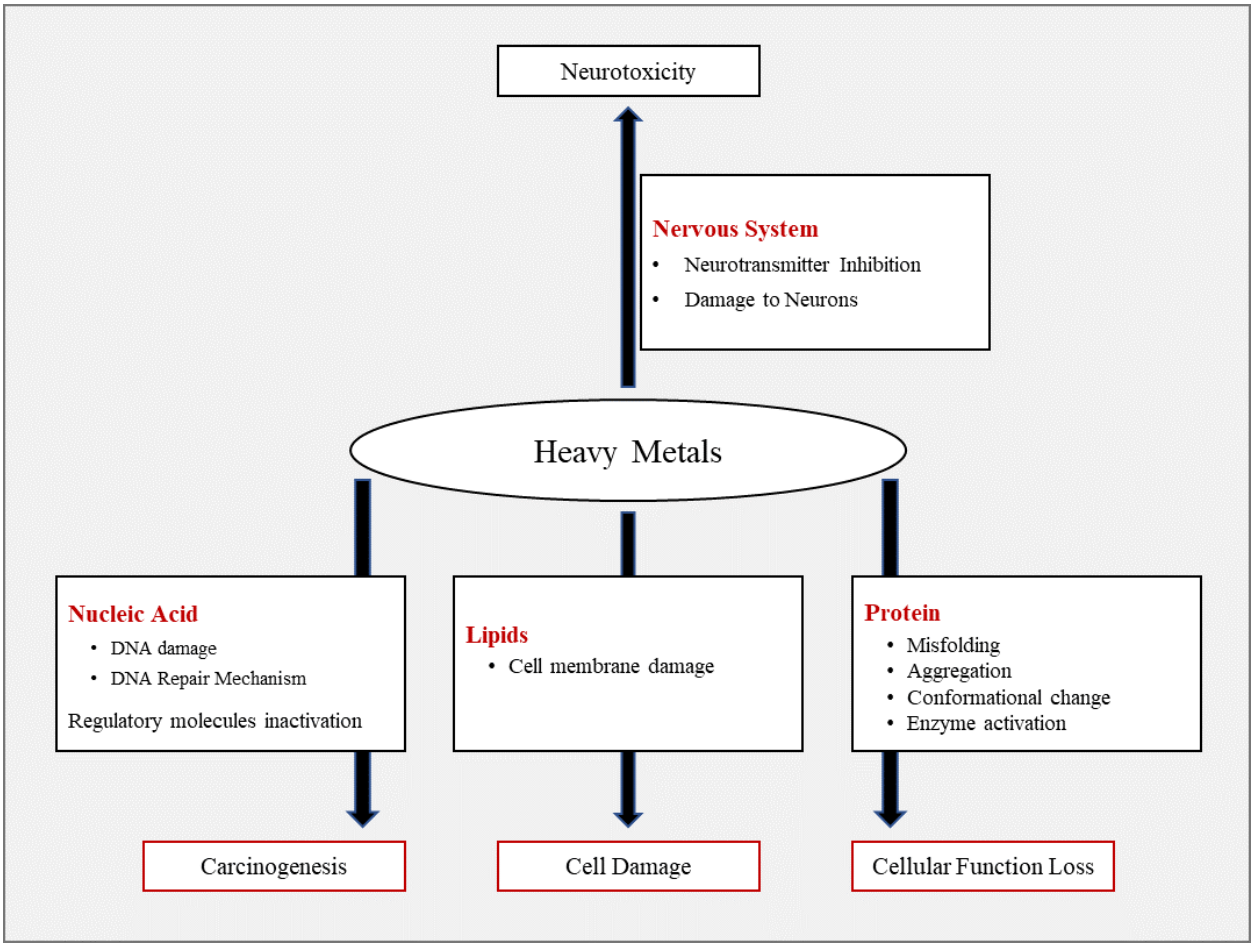


Figure 2.3. Heavy metal source pathway and human exposure (Briffa et al., 2020)

Understanding the influence of industrial production activities on human health risks is of great significance not only to control pollution at the source but also to provide a reference for optimizing industrial production (Wu et al., 2020). Table 2.1 demonstrates the heavy metals sources relative to toxicity and human disease.

Table 2.3: Metal Sources Relative to Toxicities and Human Diseases **(**Al-Musharafi, 2016)

Metal	Source	Effect in humans
Aluminium	Abundant metal in the earth's crust, found in food, water, and cosmetics	Alzheimer, Parkinson, senility, prehensile dementia,
Arsenic	Natural existence in inorganic and organic forms. Organic form commonly found in seafood, pesticides, coal combustion, metal smelters, mine leachate, wood preservative, tobacco smoke, cosmetics	Non-essential element, trivalent arsenic is more toxic than pentavalent, cumulative poison, carcinogen, abdominal pain, black foot disease, hepatoxicity, birth defects, cardiovascular mortality, gastrointestinal damage, vomiting and diarrhoea

Continued Table 2.3: Metal Sources Relative to Toxicities and Human Diseases

Chromium	Element of earth crust, soil, water, lather and tanning industries, paper and pulp manufacturing, mineral resources, mines, cosmetics	Essential element (chromium III), lung damage, hepatoxicity, carcinogen, renal tubular necrosis, skin and stomach ulceration, hematological toxicity, weakened immune system, central nervous system
Cobalt	Alloy manufacture, corrosion resistant alloys, petroleum and chemical industries, paint drying agent, medical treatment, food preservation, ceramic and porcelain production, nuclear power plants	Essential element, weakening human health, reactive oxygen species
Copper	Utensil manufacturing, pipes, bronze, electrical wires, mining, chemical industry, pesticide production, metal piping	Essential element, DNA damage and carcinogen, embryotoxic, stomach and kidney damages, diarrhea, vomiting, loss of strength
Iron	Most common metal, drinking water, cosmetics	Essential element, affecting melanin and causing grey or bronze skin color pigmentation, kdney, hepatoxicity, heart failure, joint diseases, acute toxicity to newborn babies and young children
Lead	Painted items with led paint, water pipes, children toys and some cosmetic, industrial discharges, electronic solders, sewage effluent, fossil fuels burning, roofing industry, ceramic industry, battery manufacturing, textiles	Non-essential element, DNA damage, carcinogen, embryotoxic, most frequent toxic metal, metabolic toxicity, joint disease, kidney toxicity, reproductive system, abnormal circulatory system, central nervous system and gastrointestinal tract, affects hemoglobin synthesis. neurotoxicity, osteoporosis, breaks blood-brain barrier, decrease sperm count and motility
Manganese	Drinking water, cosmetics	Essential element, hemoglobin synthesis, gastrointestinal tract, cells functions,, neurological disturbances, muscle dysfunction,
Zinc	Most abundant in earth crust, battery manufacturing, roofing building construction, paints, cosmetics, photocopier papers, wall papers, inks, rubber production, metal plating, brass manufacture, plumbing, refineries, cosmetics, textiles	Essential element, DNA damage, carcinogen, hemotoxicity, fatigue, decrease test and smell, skin sores, stomach cramps, nausea and vomiting, respiratory diseases, eye irritation, pancreatic damage, birth defects.

Copper: Copper is usually found at high concentrations in wastewater, because it is considered as the most valuable and commonly used metal in many industrial applications (Al-Saydeha et al., 2017). It is one of the most present metals in the industry due to its widest application compared to all non-ferrous metals. The copper mine plants are designed with the capacity that is more than ten times higher compared with the other heavy metals facilities. Therefore, there is a growing interest in solving the environmental issues of the copper mine industry especially because the heavy metals are non-biodegradable and tend to accumulate in living organisms causing serious diseases and disorders (Mili´cevi´ et al., 2020).

Although copper is an essential nutrient required by the body in very small amounts, it can cause diseases if it exceeds the required limits. Large concentrations of copper in the effluent stream cause serious health problems in brain, kidney and anaemia. Copper consumption at high dosages leads to serious toxicological concerns since it could be deposited in the brain, skin, liver and kidney (Al Moharbi et al., 2019)

Short periods of exposure can cause gastrointestinal disturbance, including nausea and vomiting. Use of water containing copper that exceeds the permissible level over many years could cause liver or kidney damage (Rana et al., 2014). Copper is rarely found in source water, but copper mining and smelting operations and municipal incineration may be sources of contamination (Ye et al., 2012).

Zinc: Zinc (Zn), as a heavy metal, is an essential and beneficial element for human and plants. Complete exclusion of Zn is not possible due to its dual roles, as an essential microelement on one hand and a toxic environmental factor on the other. Zinc (II) is a well-known toxic metal ion and can threaten human life by bio-accumulating in the food chain. Zn can cause nonfatal fume fever, pneumonitis, and is a potential hazard as an environmental pollutant (Zhang et al., 2017, Gautam et al., 2015, Zwain et al., 2014). Although zinc is an essential requirement for a healthy body, excess zinc can be harmful and cause zinc toxicity. Zn^{2+} is a common metal ion found in effluents of a large number of industries (Kabeer et al., 2013).

2.4. Heavy Metal Removal Technologies

Several methods have been used to remove heavy metals from contaminated water. They include chemical precipitation, ion exchange, adsorption, membrane filtration, solvent extraction, and electrochemical treatment (Wołowiec et al., 2019).

2.4.1 Chemical

Precipitation: Chemical precipitation is one of the most widely used methods for heavy metal removal from inorganic effluent in laboratory and even in industry due to its simple operation. These conventional chemical precipitation processes produce insoluble precipitates of heavy metals as hydroxide, sulfide, carbonate and phosphate (Chaemiso and Nefo, 2019). In simpler cases, the added chemicals aim just to change the pH of the stream so that the speciation of a substance is changed to an insoluble form (Anastasios et al., 2015). In the precipitation process very fine particles are generated and chemical precipitants, coagulants, and flocculation processes are used to increase their particle size to remove them as sludge. Once the metals precipitate and form solids, they can easily be removed, and low metal concentrations can be discharged. Removal percentage of metal ions in the solution may be improved to optimum by changing major parameters such as pH, temperature, initial concentration, and charge of the ions (Chaemiso and Nefo, 2019).

2.4.2 Ion Exchange: Ion exchange is a chemical reaction in which free mobile ions of a solid, the ion exchanger, are exchanged for different ions of similar charge in solution. The exchanger must have an open network structure, either organic or inorganic, which carries the ions and which allows ions to pass through it (Kumar and Jain, 2013). Figure 2.4 illustrate the classifications of ion exchange ions.

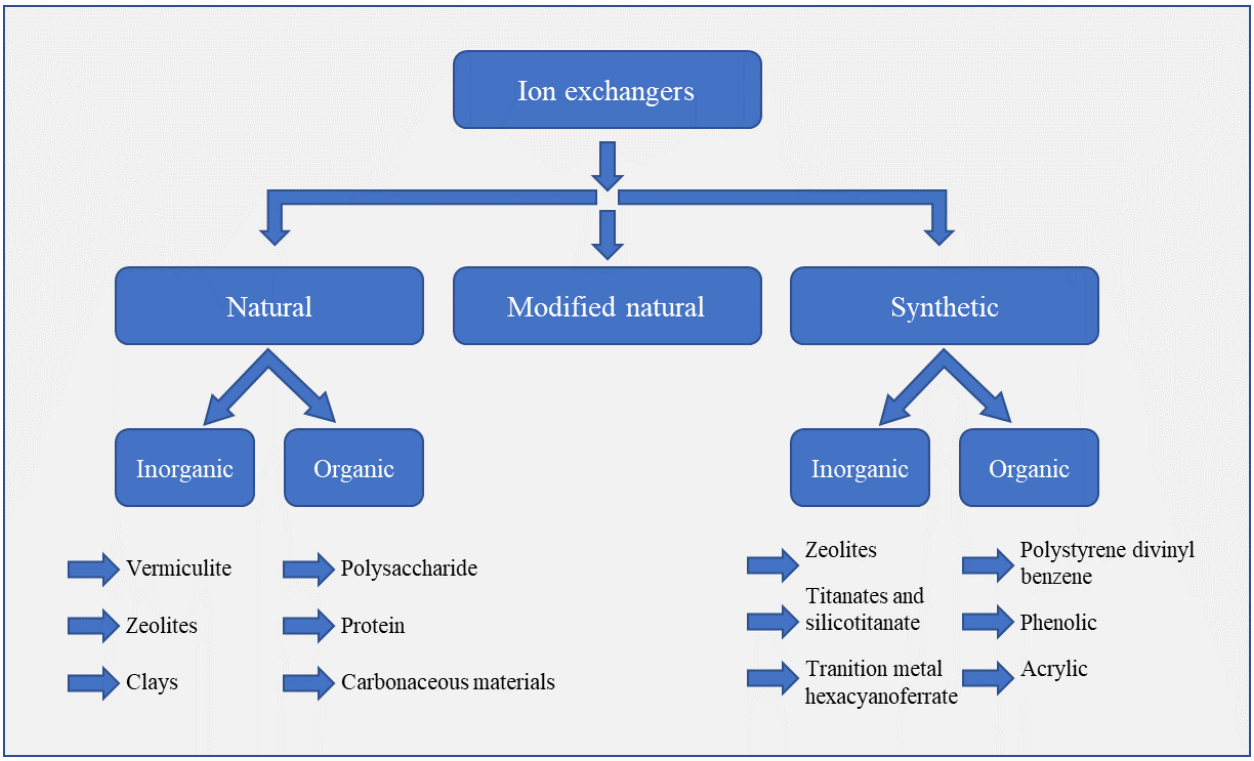


Figure 2.4 Classifications of ion exchange resins (Al-Asheh and Aidan, 2020)

2.4.3 Membrane Filtration: A membrane is a barrier which separates two phases from each other by restricting movement of components through it in a selective style. Membranes have been in existence since the 18th century. Since then, a lot of improvements have taken place to make membranes better suited for many different applications (Ezugbe and Rathilal, 2020). Membranes can offer high productivity both in terms of product recovery as well as pollutants retention and low operational cost compared to other competing technologies, since there is no water phase change and often minimal or no use of chemical additives (Hakami et al., 2020).

2.4.4 Solvent Extraction: Solvent extraction, depending upon the nature of the sample to be extracted, can fall into the sub-groups of liquid–liquid or solid–liquid extraction (Pawliszyn, 2012). Solvent ectraction can be used to separate a solute from a solution and that is by extracting it into another solvent. The two solvents must be essentially immiscible (Towler and Sinnott, 2013). Solvent extraction typical procedure can be carried out as follows:

-The frozen sample is crushed and ground to powder form

-Mix the powder obtained with anhydrous sodium sulphate, after that suspended it in a solvent such as diethyl ether, and mixed at ambient temperature for a couple of hours.

-The extract is filtered out and the insoluble part is again subjected to solvent extraction, up until the extraction is considered complete (Pawliszyn, 2012).

The main disadvantages of solvent extraction are connected to the use of organic solvents that increase environmental pollution, are hazardous to operator's health, and are expensive (Pawliszyn, 2012).

2.4.5 Electrochemical: Electrochemical is a simple and efficient process, where the production of coagulating agent is managed in situ by means of sacrificial anode. In this case, there is no need for adding chemical coagulants or flocculants to perform the treatment (Bhagawan et al., 2018).

Electrochemical treatment has the following advantages: direct or indirect oxidation flexibility; space saving; high-performance processing and can be integrated with environmentally friendly methods (Tien et al., 2017). Electrochemical processes include: electro-coagulation, electro-flocculation, electro flotation, electro-deposition, electro oxidation, electro-disinfection, electroreduction (Mickova, 2015).

2.4.6 Adsorption:

Adsorption is a mass transfer process that is a phenomenon of sorption of gases or solutes by solid or liquid surfaces. In the following sub-sections, the definition and the mechanism of adsorption and the various conventional and unconventional adsorbents that could be utilized in wastewater treatment will be briefly discussed.

I. Definition and Background

As explained in Chapter 1, adsorption is defined as "a mass transfer process which involves the accumulation of substances at the interface of two phases, such as, liquid–liquid, gas–liquid, gas–solid, or liquid–solid interface (Amosa et al., 2015, Gisi et al., 2016, Amosa et al., 2016b). Adsorption method is the deposition of adsorbate onto the surface of adsorbent. Among the unit operations in wastewater treatment, adsorption occupies an important position since it is an efficient and economically feasible process for treatment of wastewater containing dissolved organic pollutants. The most common used adsorbent in adsorption process is activated carbon,

which is widely used for the removal of heavy metal ion from wastewater (Ketsela et al., 2020). Materials used to adsorb components are called adsorbent while adsorbate is the component that being adsorbed (Grassi et al., 2012).

Adsorbent can be classified as synthetic adsorbent, natural adsorbent and semi-synthetic adsorbent. **Synthetic adsorbent** is most popular adsorbent used for research because of high adsorption capacities but, highly in cost production. Natural adsorbent such as plant, flower and leaf give very low cost production but also give low adsorption capacity. While the **semi-synthetic adsorbent** that can be define as natural material combining with chemical that possess high adsorption capacity and low cost compared to synthetic adsorbent(Sazali et al.,2020).

The adsorbents used in the adsorption process are usually in the form of spherical pellets, rods; mouldings with diameters between 0.5 and 10 mm (Ketsela et al., 2020). The metal ions that contact with the adsorbent surfaces may be attached to the surfaces of the adsorbent according to physical or chemical interaction. Then those metal ions can be adsorbed on the adsorbent by ion exchange, coordination interaction, electrostatic interaction and physical adsorption, which are considered to be the main mechanism of most adsorbents to remove metal ions (Zhang et al., 2020). Physical adsorption is enabled by the van der Waals forces between molecules and/or atoms on the adsorbent surface and adsorbate, whereas adsorbate resembles a condensed liquid form of the adsorptive (Králik, 2014).

II. Advantages

Adsorption is one of the most efficient wastewater treatment technologies and has several advantages, which are:

- Inexpensive (Chikr et al., 2020), if low cost waste products are used.
- High efficiency (Ahmaruzzaman, 2011).
- Ease of operation (Rápó and Tonk, 2021).

Simplicity of design and not generating secondary pollution (toxic sludge) (Rudi et al., 2020).

2.4.6.1 Adsorption Isotherms

Isotherm models predict the maximum adsorption capacity of a sorption system, which helps in the assessment of the feasibility of the treatment process for a specific application, the required dose of bio-sorbent and the selection of the most suitable sorbent for the given case (Kumar and Bandyopadhyay, 2006).

Isotherm models simulate the relation between the equilibrium concentration of heavy metals (Ce) and the adsorption capacity of a sorbent (q) (Ding et al., 2012). Langmuir and Freundlich models are the most commonly used isotherm models in the literature. They are used for describing the isotherm of a single solute adsorption system (Ahmaruzzaman, 2011).

I. Langmuir Isotherm

The Langmuir isotherm assumes:

(1) The adsorption process takes place as monolayer adsorption (chemical adsorption)

(2) The surface of adsorbent pellets or each adsorption site is homogeneous

(3) The adsorption heat does not vary with the coverage. In other words, in terms of the Langmuir isotherm, adsorption takes place when a free adsorbate molecule collides with an unoccupied adsorption site and each adsorbed molecule has the same percentage to desorption (Grassi et al., 2012, Sarma et al., 2015). Langmuir also assumes that there is not any interaction between the biosorbed molecules (Sarma et al., 2015).

The model can be written as:

$$q_e = \frac{q_m bc}{1 - qc} \qquad (2.1)$$

Where:

q_e is the amount of heavy metal adsorbed on a unit mass of adsorbent (mg/g)

q_m is the quantity of adsorbate adsorbed in a single monolayer (mg/g)

C is the equilibrium aqueous-phase concentration of adsorbate (mg/L)

b is the constant related to the free adsorption energy and the reciprocal of the concentration at which half of the saturation of the adsorbent is reached

II. Freundlich Isotherm

Another most widely used model is the Freundlich isotherm. Comparing with the Langmuir isotherm, the Freundlich isotherm does not have much limitation, i.e., it can deal with both homogeneous and heterogeneous surfaces, and both physical and chemical adsorption. Especially, this model frequently succeeds in depicting the adsorption behaviour of organic compounds and reactive matters (Xu et al., 2013). According to some researchers, the isotherm of adsorption from an aqueous solution is better described by Freundlich isotherm model, which presumes a heterogeneous surface energy of adsorption (Grassi et al., 2012). In other words, sorbent surfaces carrying sites of varied strength that is multi-layer adsorption (Sarma et al., 2015). Unlike Langmuir isotherm, Freundlich isotherm is an empirical model derived in 1912 (Metcalf and Eddy 2003).

$$Ln\ q_e\ =\ ln\ K_f\ +\ \left(\frac{1}{n}\right) lnC_e \qquad (2.2)$$

Where:

K_f (mg/g) (L/mg) 1/n: the Freundlich capacity factor, or the adsorption equilibrium constant. K_f is an indicator of the adsorption capacity when metal equilibrium concentration equals 1 (Zhu et al., 2008).

1/n: the Freundlich intensity parameter. According to Liu et al., (2019), it is the extent of heterogeneity of the sorption system and it can be obtained from slope of ln q_e versus ln C_e linear plot.

q_e is the amount of metal adsorbed onto the adsorbent mg/g

2.4.6.2 Factors Influencing Adsorption Capacity

Factors that impact the efficiency of adsorption are the following:

I. **Contact Time**

Contact time affects the adsorption capacity, where the time required for the adsorption process to reach equilibrium differs from one adsorbent to another, this may be due to one or more of the following reasons: (Solimana and Moustafa, 2020, Ahmaruzzaman, 2011)

(1) Changes in the chemical structure of the adsorbent

(2) Availability of surface active sites

(3) The surface area of adsorbent

(4) The ionic size of the metal ions

II. Initial Concentration of Adsorbate

The percentage of removal of heavy metal ion decreases when the initial metal ion concentration increases (Al-Senani and Al-Fawzan, 2018). The heavy metal ion initial concentration has an impact on the adsorption capacity as it acts as a driving force to overcome the resistance of the metal or the mass transfer from the liquid phase to the solid phase (Ahmaruzzaman, 2011).

III. The pH of the Solution

The percentage of metal ions adsorbed by adsorbents is greatly affected by changing the pH value of a solution, which is due to the consequent change in the distribution of the surface charge of the adsorbent (Rao et al., 2013). Each metal ion has definite pH value, at which the maximum adsorption of those metal ions occurs. This pH assigned at high pH values (i.e. in the basic region) for the cationic metals; however, it is located at low pH values (i.e. in the acidic region) for the anionic metal ions. The initial pH of the solution can control the adsorption efficiency of metal ions where it affects the chemistry of the catalyst surface and also the ionization and dissociation of the sorbent molecule (Soliman and Moustafa, 2020). In general, the adsorption capacity of heavy metal ions increases with the increasing pH (Ahmaruzzaman, 2011).

IV. Dose of the Adsorbent

The amount of adsorbent used in metal ions removal is very important because it determines the adsorption capacity of the adsorbent in batch system (Darweesh et al., 2022).For every metal ion concentration, there is a certain dose of adsorbent at which maximum adsorption will be reached. The increase in the amount of metal ions adsorbed with increasing adsorbent dose could be attributed to the increase in the number of active sites and in adsorbent surface area with increasing adsorbent dose, by other words the increased surface area of adsorbents, subsequently the increased availability of active sites and therefore increase the amount of heavy metal uptake (Solimana and Moustafa, 2020).

2.4.6.3 Batch Adsorption Process

Batch adsorption, also called static adsorption, occurs in a closed system containing a desired amount of adsorbent contacting with a certain volume of adsorbate solution (Xu et al., 2013). Batch adsorption studies give an important data and parameter on the removal of adsorbate. The small-scale experiment from the batch study can give the important information on the parameter used for adapted in industry scale by fixed bed column (Sazali et al., 2020). Batch adsorption is prefered by researchers at laboratory scale investigation as the amount of material used is small and it is less time consuming. Nevertheless, batch adsorption is convenient for small scale study but not suitable for real scale application (Sazali et al., 2020)

2.4.6.4 Fixed Bed Adsorption Process

Fixed bed adsorption, is also called dynamic adsorption, and usually occurs in an open system where adsorbate solution passes through the packed column continuously with adsorbent as represented in Figure 2.5 (Xu et al., 2013). Fixed bed adsorption is more advantageous as it is easy to operate, faster adsorption process and simplicity of scale up process (Sazali et al., 2020). Fixed-bed column process has some disadvantages which are: during the adsorption process, preferential routes can be formed, the adsorption being non-uniform; and the concentration profiles vary in time and space (Negrea et al., 2020).

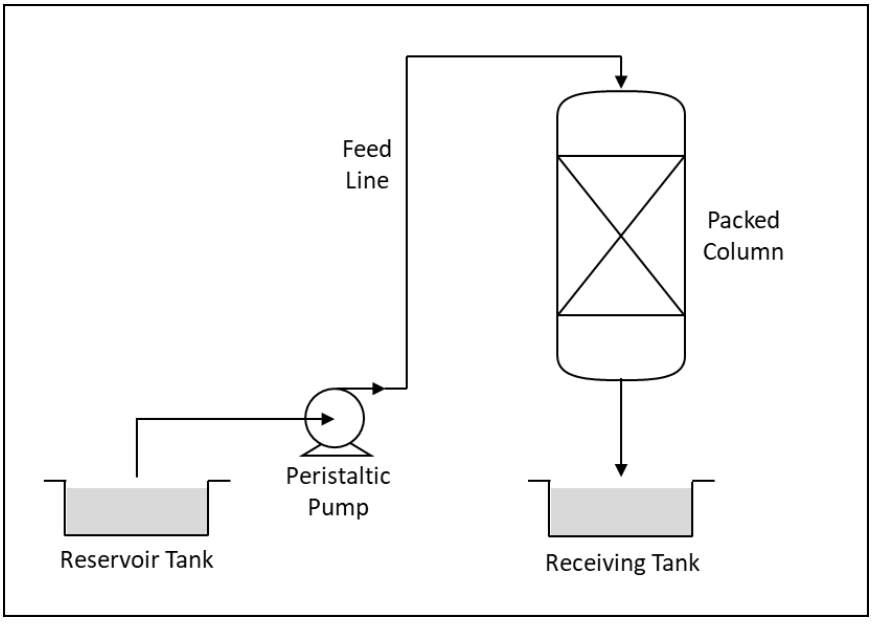


Figure 2.5 Schematic diagram of fixed bed adsorption column

The Breakthrough Curve

The performances of the adsorption process in the fixed-bed column are highlighted by the study of the breakthrough curves (Negrea et al., 2020). Breakthrough curves are the plots of the ratio C/Co (outlet adsorbate concentration/adsorbate feed concentration) versus time as shown in figure 2.6 (McCabe et al., 2001). It is one of the dynamic studies of fixed bed system. As the influent starts to enter the column, most of the mass transfer takes place near the inlet of the bed, where the fluid first contacts the sorbent. If the solid contains no adsorbate at the start, the concentration in the fluid drops exponentially to zero before the end of the bed is reached as it is shown in Figure 2.6.

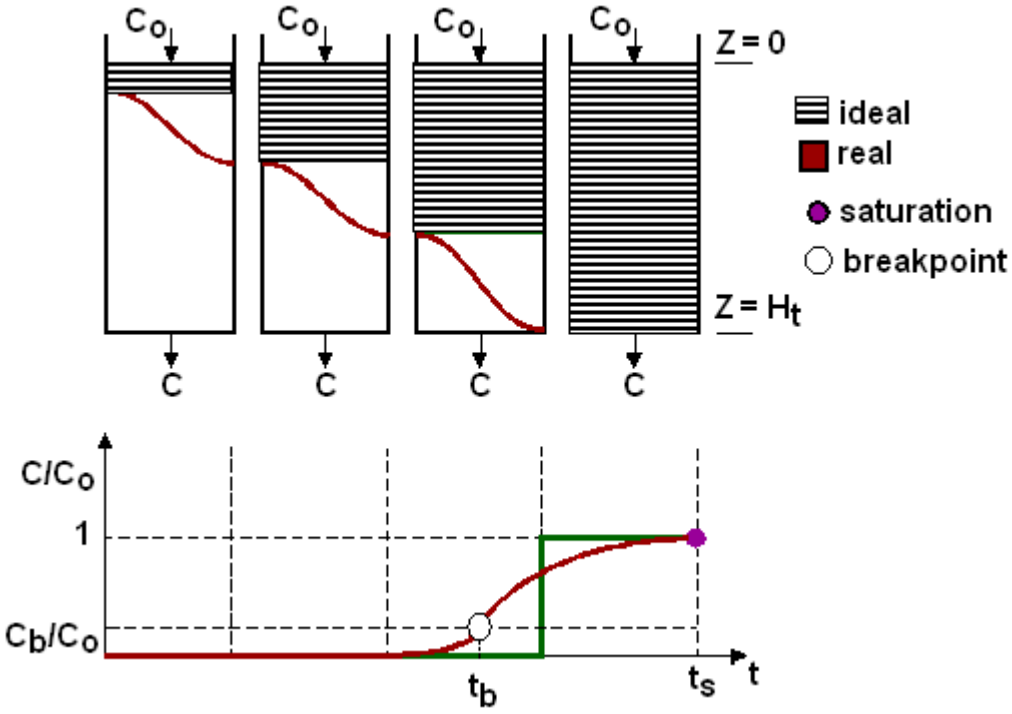


Figure 2.6 Breakthrough curve for the sorption process in fixed beds

C_o is the concentration of the inlet solution

C_b is the concentration of the breakthrough

t_b is the breakpoint time

t_s is the saturation time

As the run proceeds, the solid near the inlet is nearly saturated, and most of the mass transfer takes place further from the inlet. The concentration gradient is S shaped. The region where most of the change in concentration occurs is called the mass-transfer zone. The mass transfer zone (MTZ) is the active surface of the adsorbent where the adsorbate adsorption takes place (Negrea et al., 2020). Adsorption inside the packed bed does not occur throughout bed length during operation time. Adsorption actively occurs in a limited portion of the bed which is the mass transfer zone (MTZ), where solution composition changes and thus, mass transfer occurs.

2.5 Agriculture Wastes as Adsorbents

Adsorption using agricultural wastes is a very promising technology because of its ability of reducing the concentration of heavy metals in wastewater to minimal values and because it utilizes inexpensive abundant wastes, they are also proven to be environmentally friendly. One more advantage of using agriculture waste is regeneration and recycling of adsorbent (Kwikima et al., 2021).

Several materials have been used as adsorbents for heavy metal ions, such as activated carbon (Ademiluyi and Nze, 2016), saw dust (Ouafi et al., 2017), fly ash (Luo et al., 2011), and rice husk-based activated carbon (Nhapi et al., 2011). In the recent past, some researchers emphasized using aqua vascular weed for removal of heavy metals like water hyacinth (Sarkar et al., 2017).

2.5.1 Water Hyacinth

Certain aquatic weeds can negatively impact the livelihood of humans as well as the environment. Among these aquatic weeds, water hyacinth (*Eichhornia crassipes*) remains the most widely vicious and distributed aquatic weed (Ayanda et al., 2020). Water hyacinth is a destructive invasive alien species. It is a native of the Amazon basin of South America but has proliferated extensively globally, as seen in Figure 2.7 (Ilo et al., 2020). It is a fast growing free-floating aquatic plant presented in Figure 2.8, it is listed as one of the top 100 invaders in the world (Coetzee et al., 2014). Water hyacinth compose of 25 % cellulose, 33 % hemicellulose, and 10 % lignin (Istirokhatun et al., 2015). However, it is worth noting that this composition may vary depending on the geographical area and climatic conditions (Borbón et al., 2022)



Figure 2.7 Global spread of water hyacinth (ILO et al. 2020)



Figure 2.8 Water hyacinth whole plant (Images courtesy of J. Madsen and W. Robles (2009)

Water hyacinth can grow rapidly forming a dense mat over the surface of water as shown in Figure 2.9. The size of the mat doubles in 5 days (Zarkami et al., 2020).



Figure 2.9 Water hyacinth mat over river

2.5.1.1 Negative Impact of Water Hyacinth

Water hyacinth tolerates water level fluctuations, seasonal flow velocity variation, nutrient availability, pH, temperature and toxic substances (Dölle et al., 2021). It is characterised by high proliferation rates in nutrient-rich water bodies (Deivasigamani, 2013). This enables the plant to cover water surfaces in a short period of time forming dense mat (Yan et al., 2017). The thick mats of water hyacinth can prevent light penetration into water making difficulties for the life of aquatic animals. The dense mats of this plant can also prevent phytoplankton and submerged plants from photosynthesis activities through the lack of light penetration (Zarkami et al., 2020). Water hyacinth adjustability can cause a lot of serious problems. It can disable native species' diversity through hybridization, functioning and ecosystem modifications. It may change the aquatic habitat structure, and negatively affecting biological communities. Water hyacinth can also have a risk for human health. Its mat-like nature leads to the concentration of micro-organisms around the plant roots and shoots, it can increase the pest's population (like mosquitos) and may bring many diseases, such as filariasis, malaria and ancephalitis (Dölle et al., 2021).

2.5.1.2 Water Hyacinth in South Africa

South Africa is one of the countries that has suffered from the invasion of water hyacinth in many of its aquatic ecosystems. Water hyacinth was introduced into South Africa as an ornamental plant in 1908 (Coetzee et al. 2014).The main reason for suffering the country from this plant is that South Africa has the most eutrophic aquatic ecosystems in the world (Coetzee and Hill, 2012).

Water hyacinth is widely distributed in aquatic ecosystems throughout South Africa as illustrated in Figure 2.10 (Perez et al., 2011). Dams such as Hartbeespoort (North West province), Roodeplaat (Gauteng province) and Kleinfontein (Benoni, Gauteng) and rivers such as the Vaal (Gauteng province) are all examples of water bodies with severe water hyacinth invasion in South Africa.

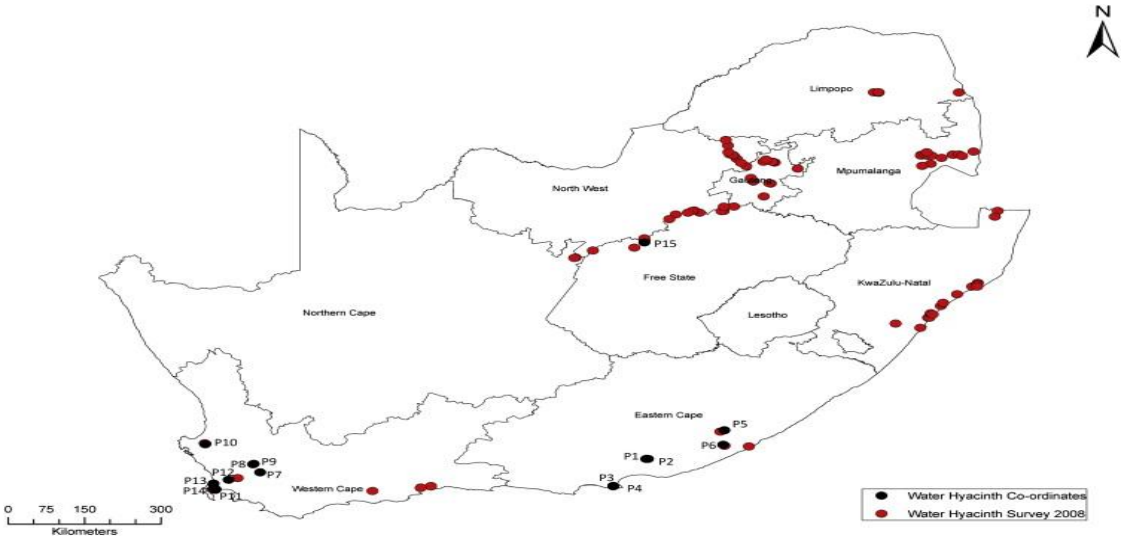


Figure 2.10 Distribution of water hyacinth in South Africa (red points), with black points indicating the water bodies that were sampled (Perez et al., 2011)

Water hyacinth remains the country's most difficult aquatic weed to control despite efforts initiated in the 1960s (Coetzee et al. 2014). The impact of water hyacinth on South Africa is both environmental and economic (Auchterlonie et al., 2021). Hartbeespoort Dam area is one of the South African areas that is blooming with the businesses of tourists and property developments because of the recreational activities. It is a major tourist attracting and it offers magnificent opportunities for water activities such as fishing, boating, rafting and tube rides. (Mokoena et al., 2017). When water hyacinth form dense mats that cause inability to access the dam, also create eye-sore, as a result a number of tourists decrease Hartbeespoort Dam and a subsequent decrease in revenue. This has also caused a decrease in the value of the surrounding properties, as water access and the view is a significant factor in the water facing property values (Auchterlonie et al., 2021)

2.6 Process Optimization

Process optimization involves the application of mathematical techniques & tools to find out the best possible solution from several available alternatives.

2.6.1 Response Surface Methodology

Heavy metals' percentage of removal due to adsorption depends on various operating variables including contact time, adsorbent dose, pH and initial metal ion concentration. Accordingly, it is of great importance to investigate the effect of different operating variables on the response or process objective function. The conventional way for investigating the effect of variables is one factor at a time (OFAT) technique. Using OFAT, only one variable is subjected to analysis while keeping all other variables at a constant value. Recently using OFAT has been considered as a time consuming and expensive technique. In the engineering context, optimization implies the improvement of a process performance through the manipulation of several variables in different combinations to get the best results.

A statistical method, known as design of experiments (DOE), is considered as a powerful tool for the process optimization. Response Surface Methodology (RSM) is one of the methodologies in DOE which includes Box–Behnken design (BBD) (Yusup and Khan, 2010), central composite design (CCD) (Cavalcante et al., 2010), Taguchi technique (Araujo and Brereton, 1996), generic algorithm coupled with artificial neural network (ANN) and other combination of fractional factorial and Doehlert experimental designs (Baş and Boyacı, 2007).

RSM is an effective statistical technique, which provides an investigative approach towards optimization. In addition, it is a collection of mathematical and statistical techniques used to determine the significance of several affecting factors in an optimum manner, even in the presence of complex interactions. The limitations posed by conventional analytical optimization methods can be eliminated by collectively optimizing all the affecting parameters using RSM (Yasin et al., 2013). RSM has important application in process design and optimization, as well as in the improvement of existing designs. Functions and data types for the coding and decoding of factor levels are providing by RSM. Convenient coding is an important element of response-surface analysis. Many software packages are available to help in designing and analysing response surface experiments, including Design-Expert (Stat-Ease, Inc., 2009), JMP (SAS Institute, Inc., 2009) and Stat graphics (Stat Point Technologies, Inc., 2009). All these help in generating Box-

Behnken design (BBD) and central-composite designs (CCD), fitting first- and second-order response surfaces and visualizing them (Bhuvaneshwari et al., 2015). The main advantages of using any of DOE methodologies are the possibility of studying the interaction effect between variables (not only the direct effect of variables as applied in OFAT) where better observations and understanding for the process, evaluating the optimum conditions for the process and to develop more efficient process (El-Tahhan et al., 2019).

Box-Behnken designs (BBD) are a class of rotatable or nearly rotatable second-order designs based on three-level incomplete factorial designs. A comparison between the BBD and other response surface designs (Doehlert matrix, central composite and three-level full factorial design) has indicated that the Doehlert matrix and BBD are slightly more efficient than the central composite design but much more efficient than the three-level full factorial design where the efficiency of one experimental design is defined as the number of coefficients in the estimated model divided by the number of experiments (Ferreira et al., 2007). One more advantage of the BBD is that it does not contain combinations for which all factors are simultaneously at their highest or lowest levels (Ferreira et al., 2007).

This optimization technique ultimately presents a regression model for a response or process objective function (Y) prediction based on the independent operating variables using a second-degree polynomial equation, referred to as the full mathematical or regression model.

Central Composite Design (CCD) is a very common method suitable for fitting second order polynomial equations, it has been frequently discussed for optimizing several research problems ranging from Fenton process to pollutant abatement to electro-forced sedimentation (Amosa and Majozi, 2016). CCD is methodically suitable for fitting a quadratic response surface, and it ultimately helps in optimizing the effective operating parameters in the experimental region, as well as analyze the behavior of the parameter interactions with minimum number of experiments (Amosa and Majozi, 2016).

2.6.2 General Algebraic Modelling System

The design of GAMS has incorporated ideas from mathematical programming and relational database theory and attempted to combine these ideas to suit the needs of strategic models. Relational database theory provides a structured frame work for developing general data

organization and transformation power. Mathematical programming provides a way of characterizing a problem and a set of methods for solving it. This has made GAMS a high-level modelling system for mathematical programming and optimization (Amosa and Majozi, 2016).

2.7 Mathematical Models of Adsorption in Packed Beds

To obtain the breakthrough curve of a given adsorption system, there are two widely used approaches: direct experimentation or mathematical modelling. The experimental method could provide a direct and incisive breakthrough curve of a given system. However, it is usually a time-consuming and economical undesirable process. The experimental method depends upon the experimental conditions, such as residence time and temprature (Xu et al., 2013).

Mathematical models predict the performance of adsorption filters under specific conditions. They can also be useful in designing and optimizing purposes in industrial scale expressed by non-linear mathematical equations. In designing we need to decide about bed specifications such as the length and cross sectional area of the bed, the type and size of the particle, the amount of particles and the operational conditions.

To model a liquid-solid column adsorption, it is necessary to some steps (Xu et al., 2013, Helfferich, 1995):

1. Liquid phase mass transfer including convective mass transfer and molecular diffusion

2. Interface diffusion between liquid phase and the exterior surface of the adsorbent (i.e., film diffusion);

3. Intrapellet mass transfer involving pore diffusion and surface diffusion

4. The adsorption isotherm equation

2.7.1 Liquid Phase Mass Transfer: Molecules or ions in the column can move in both axial and radial directions. For simplification, it is common to postulate that all cross sections are homogeneous and the radial movement could be neglected. Thus, a macroscopic mass conservation equation is acquired to represent the relationship between the corresponding variations (i.e., concentration of the adsorbed adsorbate q; concentration of the bulk solution C; distance to the inlet z; superficial velocity u; axial dispersion coefficient Dz (if the axial dispersion

is not ignored), ε is the bed porosity, t is the time, ρ_a is the adsorbent density, C_F is the initial concentration of the influent, and H is the bed height (Xu et al., 2013, Fournel et al., 2010).

$$\varepsilon \frac{\partial C}{\partial t} + U \frac{\partial C}{\partial z} + (1-\varepsilon)\rho \frac{\partial q}{\partial t} = D_z \frac{\partial^2 C}{\partial z^2} \quad (2.1)$$

$$t = 0 \rightarrow C(z,t) = 0$$

$$t = 0 \rightarrow q(z,t) = 0$$

$$t = 0 \rightarrow C(0, t = 0) = 0, C(0, t > 0) = C_f$$

$$Z = H \rightarrow \frac{\partial c}{\partial z} = 0 \quad (2.2)$$

2.7.2 Film Diffusion

The driving force of film diffusion is the concentration gradient located at the interface region between the exterior surface of adsorbent pellets and the bulk solution. As the first step of adsorption, film diffusion predominates the overall uptake rate to some extent and even becomes the rate control step in some cases. The flux film diffusion can be expressed in linear form by multiplying its driving force and the phenomenological coefficient (Xu et al., 2013, Fournel et al., 2010).

$$\frac{dq}{dt} = J_f = K_f\, a(C - C_s) \quad (2.3)$$

Where:

J_f is the mass transfer flux, a is the volumetric surface area

C_s is the adsorbate concentration at the exterior surface of adsorbent

k_f is the film diffusion coefficient

It is known that increasing the flow rate will decrease the film thickness and resistance, whereas larger film resistance can be caused by packing with smaller adsorbent pellets due to the extension of the exterior surface area (Xu et al., 2013)

2.7.3 Adsorption Isotherm

As we mentioned above, the general way to predict the breakthrough curve is to solve a set of partial differential equations which consist of a macroscopic mass conservation equation, uptake rate equation (sometimes including a set of equations), and isotherm equation. Obviously, as a prerequisite of modeling of the dynamic adsorption, the choice of the isotherm style will directly affect the effect of mathematic modeling. (Xu et al., 2013).

Here we do not intend to give a detailed discussion of various isotherms but only two models, Langmuir isotherm and Freundlich isotherm which was described above in sections (2.4.6.1, I,II), respectively.

2.8 Process Simulation

Process simulation studies offer convenient tools for determining process characteristics and their dependence on design and operating variables. Process simulations usually begin with the determination of the chemical components, and selection of suitable thermodynamic model. Subsequently, unit operations, operating conditions, input conditions and plant capacity must be specified. Most of the property data of components are available in the software library. However, if certain component property is unavailable in the simulator library, registration of the component can be made by introducing the chemical structure and the physicochemical properties of the new chemical component (Nasir et al., 2013).

Yusuf et al. (2013) simulate their model to give a solution for the dimensionless concentration of adsorbate against radial distance and obtained results are compared with previous models reported in the literature, which agree reasonably well with them. Their model studied by varying different important parameters such as particle diameter, bed porosity and fluid flowrate.

Babu and Gupta (2005) proposed generalized mathematical model that incorporates external film mass transfer resistance and pore diffusion resistance with velocity variation through column bed . Internal mass-transfer resistances due to pore diffusion mechanism are considered in the model. The proposed mathematical model for fixed-bed adsorption is solved numerically by a reduction to set of ordinary differential equations using the Explicit Finite Difference technique and compared with earlier model reported in literature. MATLAB (v.6.1) software was used to solve the model equations.

2.9 Existing Researches on Using Water Hyacinth as Adsorbent

González-Tavares et al. (2023) studied the removal of Ni (II) and Cu (II) from aqueous solution using treated Eichornia crassipes (water lily) with water (WLW) and NaOH (WLN) as an adsorbent, focusing on determining the most efficient conditions (adsorbent concentration, contact time, pretreatment, temperature). The results of the analysis of different parameters showed the conditions that give the highest metal adsorption capacity. The adsorption capacity increased as the initial concentration and contact time increased. Additionally, the percentage of removal increased as the adsorbent concentration increased, with an optimum dosage of 3 g/L. The adsorption efficiency decreased when WL was treated with NaOH compared to treatment with water for each metal ion, with decreases in the adsorption capacity of 20.1% for Ni and 31.3% for Cu. In their research the water hyacinth was treated chemically. Rosidah et al. (2023) determined the quality of activated water hyacinth as adsorbent, potentially reducing metal cadmium (Cd). Root, stem, and leaf biomass after being sifted, weighed 50 g, and put into an Erlenmeyer, then activated with 500 mL of $ZnCl_2$ 10% solution. The water hyacinth biomass solution was stirred for 10 minutes with a magnetic stirrer and allowed to stand for 24 hours. Furthermore, the biomass was filtered using Whatman filter paper No. 1, washed with demineralized water to neutral pH (pH 7±0.05) then heated in an oven at 105 °C for 1 hour, then the first biomass is ready to use. The second production of adsorbent is by heating water hyacinth roots and stems. It leaves at a temperature of 300 °C for 2.5 hours using a kiln, then cooling to room temperature. The adsorbent, which was activated by heating and chemically (T = 300 °C and $ZnCl_2$ 10%), visually looks darker with less weight than the adsorbent with chemical activation ($ZnCl_2$). Significant differences were found in activated leaves with $ZnCl_2$ and activated leaves with 300 °C and $ZnCl_2$ up to 35.55%. The best adsorbent that gives the best performance to the uptake of Cd was by using the leaves of water hyacinth dried biomass which was activated by thermal in 300 °C and chemical with $ZnCl_2$ 10%. In their research also water hyacinth was chemically treated. Mahmudah et al. (2023) modified water hyacinth to be used as adsorbent using citric acid and its functional groups (carboxyl, hydroxyl, and lactone) were analyzed using Boehm titration. Water hyacinth adsorbent was modified using various citric acid concentrations of 0.5; 1.0; 1.5; 2.0; and 2.5 M. The ratio between water hyacinth and citric acid adsorbents was 1:5. Then was stirred using a stirrer at 250 rpm for 30 minutes at room temperature and then heated at 50 °C for 24 hours. Then the temperature was raised to 120°C for 90 minutes. Then the adsorbent was washed with distilled

water until pH 7 and dried at 50°C to a constant weight. The modified adsorbent was applied to laboratory waste and the levels of copper (Cu), Chromium (Cr) and Cadmium (Cd) were analyzed using Atomic Absorption Spectrophotometry. Adsorption of chromium and cadmium metals had the highest percentage reduction at a dose of 2 g of 98% and 37.40%, while for copper metal at a dose of 1.5 g of adsorbent was 63.34%. In this research the water hyacinth was modified chemically. Hemalatha et al. (2021) studied the remediation Zn and Cr ions from electroplating industry wastewater by dried water hyacinth biomass, they divided the plant into leaves, petiole and roots and tested each part separately through batch and column experiments. They considered influential parameters including water hyacinth dosage, initial metal ions concentration, initial pH, and contact time. The water hyacinth root showed maximum Zn removal of 98.9%, and water hyacinth stem showed Cr removal of 96.4%. Thus, the results indicated that the dried WH biomass was a good and low-cost adsorbent. Huynh et al. (2021) investigated whether water hyacinth can be used to remove heavy metals, such as cadmium, arsenic, lead, zinc, and copper, from industrial wastewater. The experiments lasted 30 days and 100 g of water hyacinth was used in the pot. For planting, 30-L foam containers were used. The plants were fixed with stones. The experiment was performed using healthy, young, and acclimatized water hyacinths. Containment water with a cadmium concentration of 0.5 mg/L, arsenic concentration of 0.5 mg/L, lead concentration of 2 mg/L, zinc concentration of 5 mg/L, and copper concentration of 5 mg/L was added to five different polyethylene pots with 100 g of water hyacinth in each pot for 30 days. The efficiency of wastewater treatment for the removal of Cd, As, Pb, Zn, and Cu was assessed according to the concentrations of heavy metals in water. The elimination of contaminants from the water was quite effective when the plants were grown together. According to the results of the experiments, water hyacinth was able to reduce Cd concentration by 59.4%, as concentration by 60.8%, Pb concentration by 92.4%, Zn concentration by 60.22%, and Cu concentration by 60.74%. Liu et al. (2020) examined the Cd^{2+} sorption dynamics of an alginate encapsulated water hyacinth biochar (BAC) generated at different temperatures and modified using ferric/ferrous sulfate (MBAC). After collecting water hyacinth it was first washed several times with distilled water before it was drying in an oven at 65 °C for 24 h. The dried mass of water hyacinth was crushed to obtain an average particle size of 0.6 mm, and was then packed in a tubular vacuum furnace. In order to prevent oxidation caused by high temperatures, air was pumped out and nitrogen gas was introduced into the headspace for 10 min before pyrolyzing. Water hyacinth biochar was generated

through pyrolysis for 2 h at three different temperatures: 300 °C (BC3), 500 °C (BC5), and 700 °C (BC7). Water hyacinth biochar generated at each temperature regime was used to create three groups of magnetically modified biochar (MBC): MBC3 (300 °C), MBC5 (500 °C), and MBC7 (700 °C). The MBC was created by initially sieving the biochar to obtain a particle size of 0.25 mm and mixing 10 g of biochar from each temperature regime into 100 mL of distilled water and adding a solution composed of 3.7 g of ferric sulfate and 4 g of ferrous sulfate in 300 mL of distilled water. The biochar with ferric/ferrous sulfate solution was vigorously mixed on a magnetic stirrer for 30 min at room temperature, while drops of a 10 M NaOH solution was added until the pH was between 10 and 11. The stirring continued for another hour and the solution was allowed to settle at room temperature for 24 h. Subsequently, a 0.45 mm Millipore filter was used to separate the solids. The magnetically modified biochar samples were dried at 60 °C and sieved to <0.25 µm. Water hyacinth BC and MBC generated from each temperature group were prepared into biochar-alginate capsules(BAC)by mixing a solution of BC or MBC with water (ratio of 3:20; weight/volume (w/v)) and sodium alginate (ratio of 1:100 with water (w/v)). The solution was stirred slowly while adding 1% (w/v) $CaCl_2$. A membrane formed around the biochar instantly creating small spheres that were removed from the solution, dried in an oven for 2 h at 60 °C, and then dried again at 105 °C to obtain BAC or MBAC treatments that were 3.0 ± 0.1 mm in diameter. The maximum Cd^{2+} sorption occurred at a pH of 6 and at a solution temperature of 37 °C. Sorption equilibria for the biochar-alginate capsule (BAC) and modified biochar-alginate capsule (MBAC) treatments fit both the Langmuir (R^2 = 0.876 to 0.99) and Freundlich (R^2 = 0.849 to 0.971) equations. Langmuir isotherms had a better fit than the Freundlich isotherms, with maximum adsorption capacities ranging from 24.2 to 45.8 mg Cd^{+2} g^{-1}. Larger K_L values in Freundlich modeling suggest strong bonding of the BAC and MBAC sorbents to Cd^{2+}, with values of K_L in the MBAC treatments ranging between 31 and 178% greater than the BAC treatments. Cd^{2+} sorption followed pseudo first-order kinetics (R^2 = 0.926 to 0.991) with greater efficiency of removal using treatments with biochar generated at temperatures >500 °C.

Nyamunda et al. (2019) evaluated the effectiveness of magnetic biochar (Fe_2O_3-EC) derived from water hyacinth in the removal of Cu^{2+} and Zn^{2+} from aqueous solution. A mixture of $FeCl_2$ and $FeCl_3$ was used by chemical co-precipitation on water hyacinth biomass to prepare Fe_2O_3-EC and then it was followed by pyrolysis. Batch adsorption studies on the effects of temperature, biosorbent dosage, contact time, and initial metal ion concentration were carried out. Fe_2O_3-EC

exhibited optimum contact time, biosorbent dosage, and pH values of 65 min, 1.2 g, and 6, respectively. Fe_2O_3-EC exhibited strong magnetic separation ability and high sorption capability. These results have demonstrated that the use of Fe_2O_3-EC in metal ion removal could provide an alternative way to manage and utilize this highly problematic invasive species. However, the pre-treatment process adopted in that research is considered complicated and probably costly because it involved several chemicals; hence, a cheaper solution was needed. This research treat watet hyacinth chemically. Neris et al. (2019) conducted kinetic and isotherm investigations of Pb^{2+}, Ni^{2+}, and Zn^{2+} ions adsorption in single and tri-element aqueous systems using modified alkali-treated water hyacinth because of its higher ion adsorption capacity than acid-treated water hyacinth and water hyacinth washed with water. Analysis by FTIR confirmed that −OH and −COO− groups were the key functional groups in Zn^{2+} adsorption, while −COO− groups were a key in Pb^{2+} and Ni^{2+} adsorption. The pseudo-second order was the best kinetic model that fit the single and tri-element experimental data for all investigated ions. The selectivity order of water hyacinth in single and tri-element systems was $Pb^{2+} >> Zn^{2+} \geq Ni^{2+}$.

Yu et al. (2018) investigated the effectiveness of biochar derived from waste water hyacinth for Cr (VI) removal from aqueous solution. Biochar derived from waste water hyacinth was prepared and modified by ZnO nanoparticles. The effect of carbonization temperature (500-800 °C), ZnO content (10-50 wt %) loaded on biochar and contact time (0.17-14 h) on the Cr (VI) removal were investigated. It was found that higher than 95% removal efficiency of Cr (VI) can be achieved with the biochar loaded 30 wt% ZnO. Multiple techniques such as XRD, XPS, SEM, EDX and FT-IR were performed to investigate the possible mechanisms involved in the Cr (VI) adsorption. The results show that there is precipitation between chromium ions and Zn oxide. Furthermore, the ZnO nanoparticles acts as photo-catalyst to generate photo-generated electrons to enhance the reduction of Cr (VI) to Cr (III). The removal efficiency was 95% of Cr (VI) from a solution at neutral pH. Shen et al. (2018) tested for the first time the effectiveness of a complex of water-hyacinth derived pellets immobilized with Chlorella sp in the bioremediation of Cadmium (Cd). Results showed that the Cd (II) removal efficiency was positively related to the algal immobilization efficiency and the algal bioaccumulation capacity. Since higher surface hydrophilicity leads to higher immobilization efficiency, the water-hyacinth leaf biochar pellet (WLBp) was selected as the optimal carrier. A maximum Cd (II) removal efficiency of 92.45%

was obtained by the complex of WLBp immobilized with algal cells in stationary growth phase and illuminated with a light intensity of 119 μmol m^{-2} s^{-1}.

Sarkar et al. (2017) investigated the removal efficiency of Chromium (Cr) and Copper (Cu) on water hyacinth by filtration process. They used in their research only the shoot part of water hyacinth after converting it into powder .The shoot of the Water Hyacinth weed was segregated from rest parts and washed ten times by deionized water, cut into small pieces and dried in sunlight for 72 h. After sun drying the small spices of shoot were dried in oven at 70 ± 5 °C for 48 and grind by mortar. The shoot particles were sieved and a certain size 150 μm was used. Adsorbent capacity of water hyacinth shoot powder for Cr and Cu ion was found to be 99.98% and 99.96% for standard solution (SS) and 98.83% and 99.59% for tannery effluent (TE), respectively. The finding of this research was satisfactory but still need more economical solution as in this research the oven was used for 48 hours which will consume electricity. Mohammed et al. (2013) investigated the biosorption of some heavy metals such as Cd, Pb, Zn and Cr from the aqueous solutions by dried leaves of water hyacinth. Water hyacinth was thoroughly washed with deionized water before being left to air dry. The dried leaves were subsequently pulverized in a laboratory blender to obtain a fine powder. The variations in adsorbance of Cd, Cr, Pb and Zn on water hyacinth were recorded with establish the experimental factors and parameters (1gm dose of the biosorbent, pH 7 and one hour was the conducted time of the experiment), 58%, 46%, 30% and 26% of Pb, Cr, Cd and Zn respectively. Lead was the most adsorbed among other metals, where 58% of Pb were removed. The results showed in the pH of 5,120 min of contact time and 3 gram of adsorbent dose, the maximum removing of Pb was 91%. Biosorption by the dried leaves of water hyacinth is technique can be used for removal metal pollutants from water. Mahamadi and Nharingo (2010) used water hyacinth biomass in a batch sorption experiment to study the biosorption of Cd^{2+}, Pb^{2+}, and Zn^{2+} ions in binary and ternary systems under acidic conditions (pH = 4.84) and a temperature of 30 °C. Water hyacinth were harvested, roots separated and washed three times with running tap water and twice with deionized water. They were then sun dried for two days before being oven-dried at 65 °C for 12 h. Dried samples were crushed, ground with a mortar and pestle and sieved (size fraction of 2.5 mm). The samples were then acid-treated with 0.1 M HNO_3 for 8 h followed by washing with deionized water until a pH of 7 was attained. The biomass was then oven-dried at 65 °C for 24 h. The acid pre-treatment was done to desorb any metal ions adsorbed during plant growth and to remove any debris or soluble biomolecules that

might interact with metal ions. The biomass was stored in airtight containers and subsequently used in the adsorption experiments. The mixed action of these metals was found to be incompatible following the order Pb^{2+} Cd^{2+} Zn^{2+}, while competitive biosorption behavior was recorded for the combinations Pb–Cd and Pb–Zn as described by the Langmuir competitive model. They concluded that Pb^{2+} ions could be efficiently eliminated from aqueous solution in the occurrence of Cd^{2+} and Zn^{2+} ions, but the elimination of the Cd^{2+} and Zn^{2+} ions would be repressed in the presence of Pb^{2+}.

Zheng et al. (2009) employed water hyacinth roots as biosorbent to remove Cu (II) in aqueous media. Water hyacinth used in this work was harvested in December, 2007, from a local river in Suzhou, China. Water hyacinth roots separated from the plant were thoroughly washed 5–7 times with tap water, followed by rinsing in distilled water, and then dried at 105 °C until constant weight. The roots were then cut into segments and were reserved in a desiccator for further use. The results indicate that the sorption capacity of Cu was 22.7 mg/g at an initial pH of 5.5. Mahmood et al. (2005) used phytoremediation for removing heavy metals and other pollutants by aquatic macrophytes treatment systems (AMATS) is well established environmental protective technique. A lab scale study was conducted to test the feasibility of water hyacinth for treating textile wastewater. The water hyacinth used in research was collected from a natural pond near Jallo Park (10Km East of Lahore City, Pakistan). The plants were stocked in a little pond located in the Botanical Garden at Forman Christian College Campus, Lahore. Young plants were collected for this purpose. Water hyacinth has tremendous potential to absorb heavy metals from the textile wastewater as it resulted in 94.78% reduction of chromium, 96.88% in zinc and 94.44% reduction in copper.

References

Ademiluyi, F., Nze, J., 2016. Multiple adsorption of heavy metal ions in aqueous solution using activated carbon from Nigerian bamboo, International Journal of Research in Engineering and Technology (IJRET), 5(1): 2319–1163.

Ahmaruzzaman, M., 2011. Industrial wastes as low-cost potential adsorbents for the treatment of wastewater laden with heavy metals, Advances in Colloid and Interface Science 166 (2011): 36–59.

Alabi, M.O., Telukdarie, A., Rensburg, N.J., 2019. Industry 4.0: Innovative Solutions for the Water Industry. Proceedings of the American Society for Engineering Management 2019 International Annual Conference E. Schott, E-H. Ng, H. Keathley, and C. Krejci.

Al-Asheh, S., Aidan, A., 2020. A Comprehensive Method of Ion Exchange Resins Regeneration and Its Optimization for Water Treatment. Open access peer-reviewed chapter - ONLINE FIRST. DOI: 10.5772/intechopen.93429.

Al Moharbi, S.S., Geetha Devi, M., Sangeetha, B.M., Jahan, S., 2019. Studies on the removal of copper ions from industrial effluent by Azadirachta indica powder. Applied Water Science 10, Article number: 23 (2020).

Ali, I., Asim, M., Khan, T.A., 2012. Low cost adsorbents for the removal of organic pollutants from wastewater, Journal of Environmental Management 113 (2012): 170-183.

Al-Musharafi, S.K., 2016. Heavy Metals in Sewage Treated Effluents: Pollution and Microbial Bioremediation from Arid Regions. The open Biotechnology journal 10:352-362.

Al-Saydeha, S.A., El-Naasa, M.H., S.J., Zaidi, 2017. Copper removal from industrial wastewater: A comprehensive review. Journal of Industrial and Engineering Chemistry 56(2017) 35–44.

Al-Senani, M. G., Al-Fawzan, F.F., 2018. Adsorption study of heavy metal ions from aqueous solution by nanoparticle of wild herbs. The Egyptian Journal of Aquatic Research 44(3), 187-194.

Amosa, M., Jami, S., Alkhatib, M., Jimat, D., Muyibi, S., 2015. A two-step optimization and statistical analysis of cod reduction from bio treated pome using empty fruit bunch-based activated carbon produced from pyrolysis, Water Qual Expo Health, **7**(4): 603–616.

Amosa, M, Jami, M., Alkhatib, M., Tajari, T., Jimat, D., Owolabi, R., 2016b. Turbidity and suspended solids removal from high-strength wastewater using high surface area adsorbent: Mechanistic pathway and statistical analyses. Cogent Engineering, **3**(1): 1162384.

Amosa, M., Majozi, T., 2016. GAMS supported optimization and predictability study of a multi-objective adsorption process with conflicting regions of optimal operating conditions. Computers and Chemical Engineering, 94 (2016): 354–361.

Anastasios, Zouboulis,I., Peleka,E.N., Samaras,P., 2015 .Chapter 17 - Removal of Toxic Materials from Aqueous Streams, Mineral Scales and Deposits, Scientific and Technological Approaches, 2015, Pages 443-473.

Araujo, P., Brereton R., 1996.Experimental design II. Optimization, Trends Anal. Chem., 15(2), 63–70.

Atieh, M.A., Ji, Y., Kochkodan, V., 2017 .Metals in the Environment: Toxic Metals Removal. Bioinorganic chemistry and Application. Volume 2017 |Article ID 4309198.

Auchterlonie J., LeighEden C., Sheridan C., 2021.The phytoremediation potential of water hyacinth: A case study from Hartbeespoort Dam, South Africa. South African Journal of Chemical Engineering. (37) 31-36, 2021.

Awuchi, C., G., Twinomuhwezi, H., Gospel, C., Somtochukwu, I.V., Otuosorochi, A.I., 2020. Industrial Waste Management, Treatment, and Health Issues: Wastewater, Solid, and Electronic Wastes, Eurobean Academic Research, volume 8, 2020.

Ayanda O., Ajayi T., Asuwaju F., 2020. *Eichhornia crassipes* (Mart.) Solms: Uses, Challenges, Threats, and Prospects, The Scientific World Journal, (2020), Article ID 3452172, 1-12.

Babu, B.V, Gupta, S., 2005. Modeling and Simulation of Fixed Bed Adsorption Column: Effect of Velocity Variation .i-manager's Journal on Future Engineering and Technology, 1(1), 60-66. https://doi.org/10.26634/jfet.1.1.966.

Baş, D., Boyacı, I., 2007. Modeling and optimization I: Usability of response surface methodology. J. Food Eng., 78(3), 836–845.\][pi

Bhagawan, D., Chandan, V., Srilatha, K., Shankaraiah, G., Rani, M. Y., Himabindu V., 2018. Industrial wastewater treatment using electrochemical process. The 4th International Conference on Water Resource and Environment (WRE 2018).

Bhuvaneshwari, S., Sivasubramanian, V., Sankar, K., Aswathi, M., Harish, B., 2015. Application of response surface methodology for adsorption of Cr (VI) from wastewater streams by chitosan. Indian Journal of Chemical Technology, 22: 283–290.

Briffa, J., Sinagra, E., Blundell,R., 2020. Heavy metal pollution in the environment and their toxicological effects on humans (Review article), Heliyon 6 (2020).

Cavalcante, K., Penha, M.N.C., Mendonça,K.K.M., Louzeiro, H.C., Vasconcelos,A.C.S., Maciel, A.P., de Souza, A.G., Silva, C.F., 2010. Optimization of transesterification of castor oil with ethanol using a central composite rotatable design (CCRD) Fuel, 89(5). 1172–1176.

Chaemiso, T.D., Nefo, T., 2019. Removal Methods of Heavy Metals from Laboratory Wastewater. Journal of Natural Sciences Research, Vol.9, No.2, 2019.

Chikri R., Elhadiri N., Benchanaa M., El maguana Y., 2020. Efficiency of Sawdust as Low-Cost Adsorbent for Dyes Removal. Journal of Chemistry / 2020 / Article ID 8813420.

Choukroune, L., Nedumpara, J., J., 2021. International economic law, Text, Cases and Materials. Rights and Rights holders, 731.

Coetzee, J. A., Hill, M. P., 2012. The role of eutrophication in the biological control of water hyacinth, Eichhornia crassipes, in South Africa. BioControl, 57(2), 247–261.

Coetzee, J., Jones, R., Hill, M., 2014. Water hyacinth, Eichhornia crassipes (Pontederiaceae), reduces benthic macroinvertebrate diversity in a protected subtropical lake in South Africa. Biodivers Conserv (2014) 23:1319–1330.

Darweesh, M.A., Elgendy, M.Y., Ayad, M.I., Ahmed, A.M., Kamel, N.M., Elsayed, Hammad, E.W.A., 2022. Adsorption isotherm, kinetic, and optimization studies for copper (II) removal from aqueous solutions by banana leaves and derived activated carbon. South African Journal of Chemical Engineering, 40(2022) 10-20.

Deivasigamani, S., 2013. Influence on Certain Herbicides for the Control of Water Hyacinth (Eichhornia Crassipes) and its Impact on Fish Mortality. Journal of Biofertilizers and Biopesticides, 4(2), 2–5.

Ding, Y., Jing, D., Gong, H., Zhou, L., Yang, X., 2012. Biosorption of aquatic cadmium (II) by unmodified rice straw. Bioresource Technology 114 (2012): 20-25.

Döllen, K., Wang, Q., Tong, J., 2021. Water Hyacinths (Eichhornia crassipes) – Application for Secondary Wastewater Treatment and Biomass Production. Journal of Advances in Biology & Biotechnology, 24(1): 52-61, 2021.

Ezugbe, E.O., Rathilal, S., 2020. Membrane Technologies in Wastewater Treatment: A Review. Membranes 2020, 10, 89.

El-Tahhan, N., Majozi, T., Gadalla, M., 2019. Removal of Zn (II) and Cu (II) From Aqueous Solution Using Dried Water Hyacinth as Adsorbent: Optimization of Process Parameters Using RSM and GAM. Journal of Functional Materials and Chemical Engineering, Vol. 1, No.1.

Ferreira, S., Bruns, R., Ferreira, H., Matos, G., Davida, J.,Brand˜ao, G., Silva, E., Portugal, L., dos Reisc, P., Souza, A., dos Santos, w., 2007. Box-Behnken design: An alternative for the optimizationof analytical methods. Analytica Chimica Acta, 597 (2007) 179–186.

Fournel, L., Mocho, P., Brown, R., le Cloirec, P., 2010. Modeling breakthrough curves of volatile organic compounds on activated carbon fibers. Adsorption, 16(3):147-153.

Gautam, R.K., Sharma, A.K., Mahiya, S., Chattopadhyaya, M.C., 2015. Heavy Metals In Water: Presence, Removal and Safety, chapter 1, Contamination of Heavy Metals in Aquatic Media: Transport, Toxicity and Technologies for Remediation, Edited by Sanjay K. Sharmar. The Royal Society of Chemistry 2015Published by the Royal Society of Chemistry, www.rsc.org.

Gisi, S., Lofrano,G., Grassi, M., Notarnicola,M., 2016. Characteristics and adsorption capacities of low-cost sorbents for wastewater treatment: A review. Sustainable Materials and Technologies, (9), 10-40.

González-Tavares, C., Salazar-Hernández, M., Talavera-López, A., Salgado-Román, J.M., Hernández-Soto, R., Hernández, J.A., 2023. Removal of Ni (II) and Cu (II) in Aqueous Solutions

Using Treated Water Hyacinth (Eichhornia crassipes) as Bioadsorbent. Separations 2023, 10, 289. https://doi.org/10.3390/ separations10050289.

Grassi, M., Kaykioglu,G., Belgiorno,V.,Lofrano, G., 2012. Removal of Emerging Contaminants from Water and Wastewater by Adsorption Process. In Emerging Compounds Removal from Wastewater Natural and Solar Based Treatments, 15-37.

Hakami, M.W., Alkhudhiri, A., Al-Batty, S., Zacharof, M.P., Maddy J., Hilal,N., 2020. Ceramic Microfiltration Membranes in Wastewater Treatment: Filtration Behavior, Fouling and Prevention (Review). Membranes 2020, 10, 248.

Harding, G., Chivavava, J., Lewis, A., 2020. Challenges and shortcomings in current South African industrial wastewater quality characterisation. Water SA, 46(2) 267–277.

Helfferich, F.G., 1995. Ion Exchange, Dover Pubns.

Hemalatha, D., Narayanan, R. M., Sanchitha, S., 2021. Removal of zinc and chromium from industrial wastewater using water hyacinth (E. crassipes) petiole, leaves and root powder: equilibrium study. Materials Today: Proceedings, 43, 1834–1838. https://doi.org/10.1016/j.matpr.2020.10.725.

Huynh, A.T., Chen, Y.C., Tran, B.N.T., 2021. A Small-Scale Study on Removal of Heavy Metals from Contaminated Water Using Water Hyacinth. Processes 2021, 9, 1802. https://doi.org/10.3390/pr9101802.

Ilo, O., Simatele, M., Nkomo, S. , Mkhize, N., Prabhu, N., 2020. The Benefits of Water Hyacinth (Eichhornia crassipes) for Southern Africa: A Review. Sustainability 2020, 12, 9222.

Iloms, E., Ololade, O., Ogola, H., Selvarajan, R., 2020. Investigating Industrial Effluent Impact on Municipal Wastewater Treatment Plant in Vaal, South Africa. International Journal of Environmental Research and Public Health, 2020, 17, 1096.

Istirokhatuna, T., Rokhatib, N, Rachmawaty, R., Meriyani, M., Priyanto, S., Susanto, H., 2014. Cellulose Isolation from Tropical Water Hyacinth for Membrane Preparation. Procedia Environmental Sciences 23 (2015) 274 – 281.

Kabeer, R., Varghese, R., Jaysooryan, K., George, J., Ambily, V., Sylas, P., 2013. Removal of zinc, lead and cadmium by water hyacinth (Eichhornia Crassipes). International Journal of Current Research, 5(9): 2506–2509.

Ketsela, G., Animen, Z., Talema, A., 2020. Adsorption of Lead (II), Cobalt (II) and Iron (II) From Aqueous Solution by Activated Carbon Prepared From White Lupine (GIBITO) HSUK. Journal of Thermodynamic and Catalyst. 11: 203. doi: 10.4172/2157-7544.20.11.2.203

Králik. M., 2014. Adsorption, chemisorption, and catalysis. Chemical Papers 68 (12) 1625–1638 (2014).

Kumar, K., Roy, S., 2013. Adsorption of hexavalent chromium from aqueous solution by water hyacinth (Eichhornia Crassipes). The Ecoscan, 3(Special Issue): 205–209.

Kumar, S., Jain, S., 2013. History, Introduction, and Kinetics of Ion Exchange Materials (Review Article). Journal of Chemistry Volume 2013.

Kumar, Upendra, Bandyopadhyay, M., 2006. Sorption of cadmium from aqueous solution using pretreated rice husk. Bioresource Technology 97 (2006): 104-109.

Kwikima, M.M., Mateso, S., Chebude, Y., 2021. Potentials of agricultural wastes as the ultimate alternative adsorbent for cadmium removal from wastewater. A review. Scientific African 13 (2021) e000934.

Liu, C., Ye, J., Lin, Y., Wu, J., Price, G.W., Burton, D., Wangwat, Y., 2020. Removal of Cadmium (II) using water hyacinth (Eichhornia crassipes) biochar alginate beads in aqueous solutions. Environmental pollution 264 (2020) 114785.

Liu, Y, Ying, D, Sanguansri, L., Augustin, M.A., 2019. Comparison of the adsorption behaviour of catechin onto cellulose and pectin. Food Chemistry 271 (2019) 733–738

Luo, J., Shen, H., Markström, H., Wang, Z., Niu, O., 2011. Removal of Cu^{2+} from aqueous solution using fly ash. Journal of Minerals & Materials Characterization & Engineering, 10(6): 561–571.

Mahamadi, C., Nharingo, T., 2010. Competitive adsorption of Pb^{2+}, Cd^{2+} and Zn^{2+} ions onto Eichhornia crassipes in binary and ternary systems. Bioresource Technology, 101(3), 859–864. https://doi.org/10.1016/j.biortech.2009.08.097.

Mahmood, Q., Zheng, P., Islam, E., Hayat, Y., Hassan, M. J., Jilani, G., Jin, R. C., 2005. Lab scale studies on water hyacinth (Eichhornia crassipes Marts Solms) for biotreatment of textile wastewater. Caspian Journal of Environmental Sciences, 3(2), 83–88. http://aquaticcommons. Org/id/eprint/21677.

Mahmudah, R., Nabilah, Q., Ahdiyati,W., 2023. Water hyacinth (Eichhornia Crassipes) Modified Citric Acid as a Metal Adsorbent in Laboratory Liquid Waste. Jurnal Neutrino:Jurnal Fisika dan Aplikasinya, Vol. 15, No. 2, April 2023 (p.78-84).

McCabe, W. L., Smith, J.C., Harriot, P., 2001. Unit Operations of Chemical Engineering, McGraw-Hill International Ed., 6th ed., New York, USA, 2001.

Metcalf & Eddy. Wastewater Engineering: Treatment and Reuse. 4th ed. Edited by George Tchobanoglous, Franklin L. Burton and H. David Stensel. New York: McGraw- Hill Education, 2003.

Mickova, I., 2015.Advanced Electrochemical Technologies in Wastewater Treatment Part I: Electrocoagulation. American Scientific Research Journal for Engineering, Technology, and Sciences (ASRJETS) (2015) Volume 14, No 2, pp 233-257.

Mili´cevi´c, S., Vlahovi´c, M., Kragovi´c, M., Martinovi´c, S., Miloševi´c, V., Jovanovi´c, I., Stojmenovi´c, M., 2020. Removal of Copper from Mining Wastewater Using Natural Raw Material—Comparative Study between the Synthetic and Natural Wastewater Samples. Minerals 2020, 10, 753.

Mohammed, A.K., Ali, S.A., Najem, A.M., Ghaima, K.K., 2013. Effect of Some Factors on Biosorption of Lead by Dried Leaves of Water Hyacinth (Eichhornia Crassipes), International Journal of Pure and Applied Sciences and Technology, 17(2) (2013) 72-78.

Mokoena, M., Mokgobu, M., Mukhola, M., 2017. The economic effect of hartbeespoort dam area. Conference: global business and technology association, nineteenth annual international conferences.

Naidoo, S., Olaniran,A.O., 2014. Treated Wastewater Effluent as a Source of Microbial Pollution of Surface Water Resources. International Journal of Environmental Research Public Health 2014, 11(1), 249-270.

Nasir, N.F., Daud, W. R. W. , Kamarudin, S. K. , Yaakob, Z., 2013. Process system engineering in biodiesel production: A review, Renew. Sustain. Energy Rev., vol. 22, pp. 631–639, 2013.

Neris, J. B., Luzardo, F. H., Santos, P. F., de Almeida, O. N., & Velasco, F. G.,2019. Evaluation of single and trielement adsorption of Pb^{2+}, Ni^{2+} and Zn^{2+} ions in aqueous solution on modified water hyacinth (Eichhornia crassipes) fibers. Journal of Environmental Chemical Engineering, 7(1), 102885. https://doi.org/10.1016/j.jece. 2019.102885.

Negrea, A., Mihailescu, M., Mosoarca, G., Ciopec, M., Duteanu, N., Negrea, P., Minzatu, V., 2020. Estimation on Fixed-Bed Column Parameters of Breakthrough Behaviors for Gold Recovery by Adsorption onto Modified/Functionalized Amberlite XAD7. International Journal of Environmental Research and Public Health, 2020, 17, 6868.

Nhapi, I., Banadda, N., Murenzi, R., Sekomo, C., Wali, U., 2011. Removal of heavy metals from industrial wastewater using rice husks. The Open Environmental Engineering Journal, 4:170–180.

Nwobodo, T., Chukwu, K., 2020. COVID-19 Era and Water Supply: Challenges for Rural Communities in Eastern, Nigeria. Journal of Geoscience and Environment Protection, 8, 219-233.

Nyamunda, B.C., Chivhanga, T., Guyo, U., Chigondo, F., 2019. Removal of Zn (II) and Cu (II) Ions from Industrial Wastewaters Using Magnetic Biochar Derived from Water Hyacinth. Journal of Engineering / 2019 / Article.

Okeyo, A.N., Nontongana, N., Fadare, T.O., Okoh, A.I., 2018. Vibrio Species in Wastewater Final Effluents and Receiving Watershed in South Africa: Implications for Public Health. International Journal of Environmental Research and Public Health, 15(6), 1266.

Omarova, A., Tussupova,K., Hjorth,P., Kalishev,M., Dosmagambetova,R., 2019. Water Supply Challenges in Rural Areas: A CaseStudy from Central Kazakhstan, International Journal of Environmental Research and Public Health 2019, 16, 688.

Ouafi, R., Rais, Z., Taleb, M., Bennabou, M., 2017. Sawdust in the treatment of heavy metals-contaminated wastewater. Environmental Research Journal, 11(1): 1935–3049.

Pawliszyn, J., 2012. Comprehensive Sampling and Sample Preparation. ISBN 978-0-12-381374-9.

Péreza, E., Coetzeeb, J., Téllezc, T., Hill, M., 2011. A first report of water hyacinth (Eichhornia crassipes) soil seed banks in South Africa. South African Journal of Botany, 77 (2011) 795–800.

Pohl, A. 2020 .Removal of Heavy Metal Ions from Water and Wastewaters by Sulfur Containing Precipitation Agents. Water Air Soil Pollution (2020) 231: 503.

Rana, K., Shah, M., Limbachiya, N., 2014. Adsorption of copper Cu (II) metal ion from waste water using sulphuric acid treated sugarcane bagasse as adsorbent. International Journal of Advanced Engineering Research and Science (IJAERS), 1(1): 2349–6495.

Rao, D. G., Senthilkumar, R., Anthony Byrne,J., Feroz, S., 2013. Wastewater Treatment: Advanced Processes and Technologies. London: IWA 2013.

Rápó,E., Tonk, S., 2021. Factors Affecting Synthetic Dye Adsorption; Desorption Studies: A Review of Results from the Last Five Years (2017–2021). Molecules 2021, 26, 5419.

Rudi, N.N., Muhamad, M.S., Chuan, L.T., Alipal, J., Omar, S., Hamidon, N., Abdul Hamid, N.H. Sunar,N.M., Ali, R., Harun, H., 2020. Evolution of adsorption process for manganese removal in water via agricultural waste adsorbents. Heliyon 6(2020) e05049.

Romero-Borbón, E., Oropeza-González, A.E., González-García, Y., Córdova, J., 2022. Thermochemical and Enzymatic Saccharification of Water Hyacinth Biomass into Fermentable Sugars. Processes 2022, 10, 210. https:// doi.org/10.3390/pr10020210.

Rosidah, Sata Y., Evi, S., 2023. Removal of Cadmium (II) by Adsorption Using Water Hyacinth (Eichhornia crassipes) Dried Biomass. Journal of Ecological Engineering 2023, 24(3), 246–253.

Sazali,N., Harun, Z., Sazali, N., 2019. A review on batch and column adsorption of various adsorbent towards the removal of heavy metal. Journal of Advanced Research in Fluid Mechanics and Thermal Sciences Volume 67, Issue 2 (2020) 66-88.

Sagasta, J., Sally, L., Thebo, A. 2015. Global Wastewater and Sludge Production, Treatment and Use. Wastewater Economic Asset in an Urbanizing World by, Pay Drechsel, Manzoor Qadir Dennis Wichelns, ISBN 978-94-017-9544-9. Library of Congress Control Number: 2015931115.

Sarkar, M., Rahman, A.K.M.L., Bhoumik, N.C., 2017. Remediation of chromium and copper on water hyacinth (E. crassipes) shoot powder. Water Resources and Industry, 17, 1-6.

Sarma, P.J., Kumar, R., Pakshirajan, K., 2015. Batch and Continuous Removal of Copper and Lead from Aqueous Solution using Cheaply Available Agricultural Waste Materials. Int. J. Environ. Res. 9, no. 2 (2015): 635-648.

Sazali, N., Harun, Z., Sazali, N., 2020. A Review on Batch and Column Adsorption of Various Adsorbent towards the Removal of Heavy Metal. Journal of Advanced Research in Fluid Mechanics and Thermal Sciences 67, 2 (2020) 66-88.

Shen, Y., Zhu, W., Li, H., Ho, S. H., Chen, J., Xie, Y., Shi, X., 2018. Enhancing cadmium bioremediation by a complex of water-hyacinth derived pellets immobilized with Chlorella sp. Bioresource technology, 257, 157– 163. https://doi.org/10.1016/j.biortech.2018.02.060.

Soliman, N.K.,Moustafa, A.F., 2020. Industrial solid waste for heavy metals adsorption features and challenges; a review. Journal of Materials Research and Technology 9 (5), 10235-10253.

Tien, T.T., Linh, D.H., Vu,L.T., Hoa ,P.T.T., Phuong, N.T.T., Luu, T.L. 2017. Electrochemical Water Treatment Technology in Viet Nam: Achievement & Future Development. Science Journal of Chemistry, 5(6): 87-94.

Towler, G., Sinnott, R., 2013. Chemical Engineering Design (second edition) ISBN978-0-08-096659-5.

United Nations at a glance, 218. Sustainable Development Goal 6, Synthesis Report on Water and Sanitation. Published by the United Nations, New York, New York 10017, United States of America. Website: www.un.org/publications.

WHO/UNEP. "Water Pollution Control: A Guide to the Use of Water Quality Management Principles: Wastewater as a Resource." World Health Organization. 1997. http://www.who.int/water_sanitation_health/resourcesquality/watpolcontrol.pdf.

Wołowiec, M., Kaufman, M.K., Pruss, A., Rzepa, G., Bajda, T., 2019. Removal of Heavy Metals and Metalloids from Water Using Drinking Water Treatment Residuals as Adsorbents: A Review. Minerals 2019, 9, 487.

World Health Organization WHO (2017). Progress on Drinking Water, Sanitation and Hygiene: Update and SDG Baseline.

https://apps.who.int/iris/bitstream/handle/10665/258617/9789241512893eng.pdf;jsessionid=757602F8D9B75D5B8CADFFBF91CED5C2?sequence=1.

World Health Organization WHO (2022). World health statistics 2022: monitoring health for the SDGs, sustainable development goals. Geneva: World Health Organization; 2022. Licence: CC BY-NC-SA 3.0 IGO

Wu, Z., Zhang, L., Xia, T., Jiaa, X., Wanga, S., 2020. Heavy metal pollution and human health risk assessment at mercury smelting sites in Wanshan district of Guizhou Province, China. RSC advances, (39), 2020.

Xu, Z., Cai, J.G., Pan, B.C., 2013. Mathematically modeling fixed-bed adsorption in aqueous systems. Journal of Zhejiang University-SCIENCE A (Applied Physics & Engineering), 2013 14(3):155-176.

Yadav, M., Gupta, R., Kumar, R., Sharma, 2019. Chapter 14 - Green and Sustainable Pathways for Wastewater Purification. Advances in Water Purification Techniques, 2019, 355-383.

Yan, S. H., Song, W., Guo, J. Y., 2017. Advances in management and utilization of invasive water hyacinth (Eichhornia crassipes) in aquatic ecosystems–a review. Critical reviews in biotechnology, 37(2), 218-228.

Yasin, Y., Mohamad, M., Ahmad, F., 2013. The application of response surface methodology for lead ion removal from aqueous solution using intercalated tartrate-Mg-Al layered double hydroxides. International Journal of Chemical Engineering, 2013:1–7.

Ye, H, Zhang, L, Zhang, B., Wu, G., Du, D., 2012.Adsorptive removal of Cu (II) from aqueous solution using modified rice husk. International Journal of Engineering Research and Applications (IJERA), 2(2): 855–863.

Yu, J., Jiang, C., Guan, Q., Ning, P., Gu, J., Chen, Q., Zhang, J., Miao, R., 2018. Enhanced removal of Cr (VI) from aqueous solution by supported ZnO nanoparticles on biochar derived from waste water hyacinth. Chemosphere, 195, 632–640. https://doi.org/10.1016/j. chemosphere.2017.12.128.

Yusuff, A. S., Popoola, L. T., Omitola, O. O., Adeodu, A. O., Daniyan, I. A., 2013. Mathematical Modelling of Fixed Bed Adsorption Column for Liquid Phase Solute: Effect of Operating Variables. International Journal of Scientific & Engineering Research, 4 (8), ISSN 2229-5518.

Yusup, S., Khan, M., 2010. Base catalyzed transesterification of acid treated vegetable oil blend for biodiesel production. Biomass and Bioenergy, 34 (10), 1500-1504.

Zarkami, R., Esfandi, J., Sadeghi, R., 2020. Modelling Occurrence of Invasive Water Hyacinth (Eichhornia crassipes) in Wetlands. Wetlands (2021) 41:8.

Zhang, C., Tao, Y., Lü, T., Zhao, H., 2020. Removal of Pb (II) Ions from Wastewater by Using Polyethyleneimine-Functionalized Fe_3O_4 Magnetic Nanoparticles. Applied Science, 2020, 10, 948.

Zhang, M., Yin, Q., Ji, X., Wang, F., Gao, X., Zhao, M., 2020. Scientific Reports | (2020) 10:3285.

Zhang, X., Hao, Y., Wang, X., Chen, Z., 2017. Rapid removal of zinc (II) from aqueous solutions using a mesoporous activated carbon prepared from agricultural waste. Materials (Basel), 10(9):1002.

Zheng, J. C., Feng, H. M., Lam, M. H. W., Lam, P. K. S., Ding, Y. W., Yu, H. Q.,2009. Removal of Cu (II) in aqueous media by biosorption using water hyacinth roots as a biosorbent material. Journal of Hazardous Materials, 171(1–3), 780–785. https://doi.org/10. 1016/j.jhazmat.2009.06.078.

Zhu, B, Fan, T., Zhang, D., 2008. Adsorption of copper ions from aqueous solution by citric acid modified soybean straw. Journal of Hazardous Materials, 153 (1–2) 300-308.

Zwain, H., Vakili, M., Dahlan, I., 2014. Waste material adsorbents for zinc removal from wastewater: A Comprehensive Review. International Journal of Chemical Engineering, 2014, 13.

CHAPTER THREE

EXPERIMENTAL MATERIALS AND METHODS

3.1 Overview

All the experimental work related to the water hyacinth from South Africa was carried out in Laboratory 211 of the Richard Ward Building, Department of Chemical and Metallurgical Engineering at the University of the Witwatersrand, South Africa. The experimental work related to the water hyacinth from Egypt was carried out in the laboratory of the Department of Chemical Engineering, The Higher Technological Institute, 10^{th} of Ramadan city, Egypt.

3.2 Experimental Setup

The experimental research was divided into three core phases; Phase I, II and III, as shown in Figure 1.

In Phase I, the experiments were carried out to compare the performance of water hyacinth from the different countries, Egypt and South Africa, in the removal of copper and zinc from a water solution according to various parameters in the adsorption system, and the maximum adsorption capacity in batch reactor applications.

Phase II was carried out to investigate the optimum operating conditions using Response Surface Methodology (RSM) design and General Algebraic Modelling System (GAMS) with similar variables, model equations, and levels. The optimum parameters according to RSM and GAMS were obtained.

Phase III was the final stage of the experimental part. It was conducted using fixed-bed column tests (continuous flow). The main objectives of Phase III were to simulate the performance of the more promising water hyacinth in that specific mode of wastewater treatment and to define the impact of several of the parameters, namely the influent heavy metal concentration, bed depth, and the flowrate.

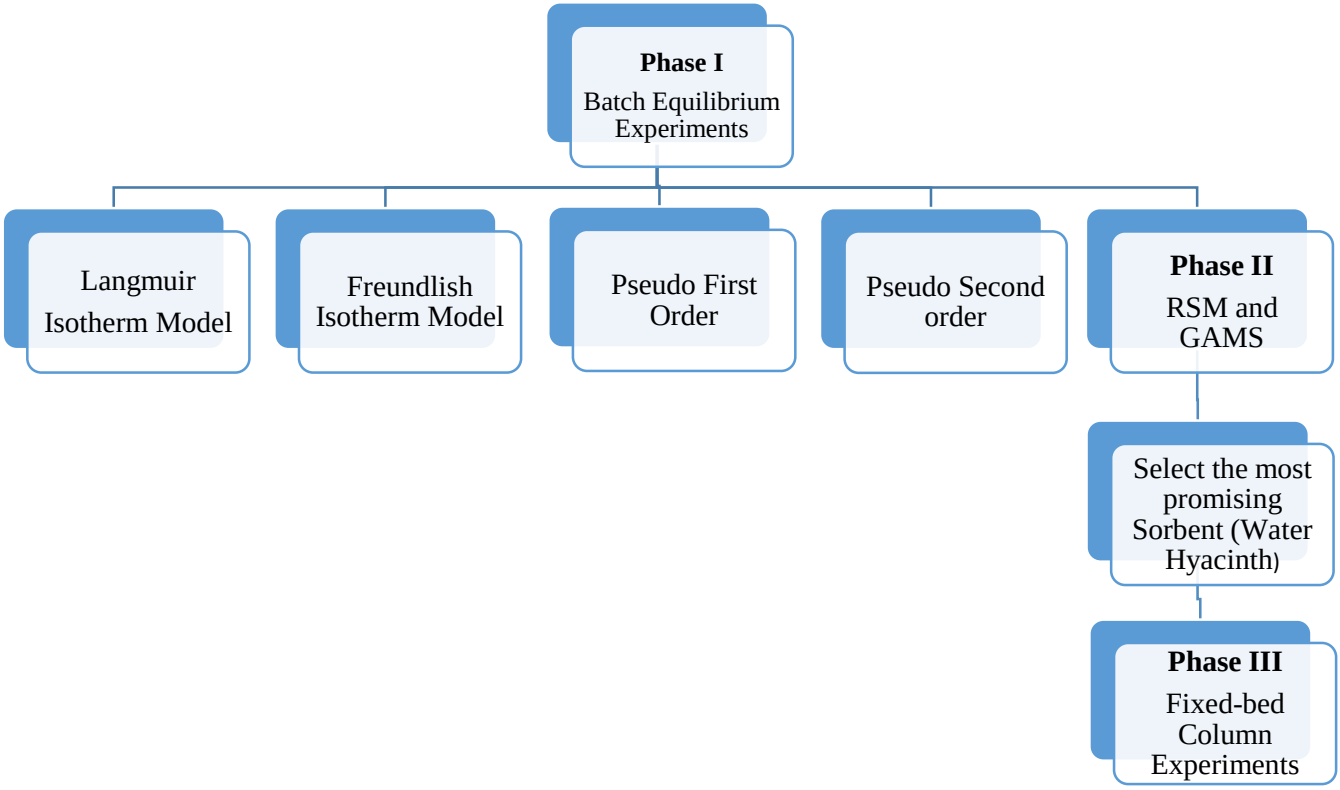


Figure 3.1: Flow chart of the experimental plan

3.3. Preparation of Water Hyacinth:

Water hyacinth was used as an adsorbent in this study and was prepared as follows:

Two samples of water hyacinth were considered in this study. The first sample of water hyacinth (Eichhornia crassipes) plants were collected from the Hartbeespoort dam in the north of Johannesburg, Gauteng province, South Africa, and the second sample was collected from Small Canal in El Sharkaya, Egypt. The growing condition for both samples was almost similar, as they grown by their own without any added materials, the temperature in Egypt and South Africa very close, so I would say that the growing conditions are very close for both samples from Egypt and South Africa. The collected plants were washed 10 times with tap water to remove adhering dirt and then washed with distilled water until the washing water became clear. The plant pieces were sun-dried on a marble sheet at a temperature of about 27 ± 2 ℃ for 10 days. The whole plant was used as adsorbent with almost 28.6% steam, 28.6% shoot and 42.8% roots. The dried plant biomass was then cut to 2–3 mm size with almost a square shape using basic cutting machine to reduce the cost. The dried water hyacinth particles were stored in pre-cleaned glass jars as shown in Figure

3.2. The removal efficiency of the contaminants under consideration of the two water hyacinth samples (from Egypt and South Africa) were compared.



Figure 3.2 Dried water hyacinth ready for use

3.4. Characterization

The functional groups within water hyacinth plants were examined using Fourier Transform Infrared Spectroscopy (FTIR). The pH measurements were done using Mettler Toledo - Five Easy FE20. All samples were analysed using Atomic Absorption Spectroscopy (AAS).

3.4.1. Fourier Transform Infrared Spectroscopy

FTIR analysis was performed using a Perkin Elmer FTIR Spectrum Two, manufactured in the USA. It was used for recording the obtained IR spectra. The spectra were recorded in a spectral range of 4000-400 cm−1, resolution of 4 cm^{-1}, and a scan speed of 2 mm/s. The FTIR analysis was carried out for the raw water hyacinth samples pre- and post- adsorption of the heavy metals to determine the main functional groups responsible for the adsorption.

FTIR is an analytical technique for defining functional groups and providing covalent bonding information (Khan et al., 2018). It depends on measuring the absorption of different infrared wavelengths by the material and producing an infrared absorption spectrum, which is commonly

designated as % transmittance versus wavenumber (cm^{-1}). Consequently, the created chemical bonds in a molecule can be identified.

3.4.2. X-Ray Fluorescence (XRF)

X-ray fluorescence (XRF) is used to analyze dried water hyacinth. It was utilized to determine the chemical composition of the water hyacinth from South Africa and Egypt. In this experiment, the X-ray fluorescence (XRF) function is used to determine the elements in the water hyacinth as a bio-adsorbent and the proportion of each ion present in both samples before adsorption.

The specimen is irradiated by photons or charged particles of sufficient energy to cause its elements to emit (fluoresce) their characteristic x-ray line spectra. The detection system allows determining energies of the emission lines and their intensities. Elements in a specimen are identified by their spectral line energies or wavelengths for qualitative analysis, and intensities are related to concentrations of elements providing opportunity for quantitative analysis (Temitope and Oyedotun, 2018).

3.5. Preparation of Stock Solution

Batch adsorption experiments involved a single element solution. Standard solutions of Cu^{2+} and Zn^{2+} were prepared. Zinc sulfate ($ZnSO_4 .7H_2O$) of Mwt 287.54 and copper sulfate ($CuSO_4 .5H_2O$) of Mwt 249.5 were used to prepare the stock solutions of metal ions in aqueous form. The stock solution was prepared by dissolving the exact quantity of metal salt in 1000 mL of distilled water to obtain the required concentration in mg/L.

3.6. Phase I- Batch Equilibrium Experiments

Batch adsorption experiments were conducted under different operating parameters, to observe the effect of untreated water hyacinth on the removal of copper and zinc. The main parameters that were studied in the batch equilibrium experiments are:

1. Contact time
2. adsorbent dose
3. pH
4. initial metal concentration

Batch equilibrium experiments were carried out at room temperature (25±2 ºC) according to the following experimental procedure:

1. A synthetic solution was prepared as described in section 3.5.
2. 50 ml of Cu^{2+} or Zn^{2+} synthetic solution was poured into a 100 mL glass bottle.
3. The pH of the samples was adjusted using 10 M NaOH and10 M HNO_3 to the specified pH value.
4. The desired dose of raw water hyacinth was weighed and added to the solution.
5. Each sample was filtered using a Whatman filter paper no. 42.
   Finally, and after the adsorption process, the samples with all the residual concentrations of Cu^{2+} and Zn^{2+} were analysed using the AAS.

3.6.1 Effect of Contact Time

The effect of contact time on the adsorption of Zn^{2+} and Cu^{2+} was investigated while keeping the biomass in contact with the metal ion solution for different periods between 0.5 to 90 minutes for Zn^{2+}, and 0.5 to 75 minutes for Cu^{2+} before they were filtered and analyzed.

The batch experiments were carried out under the following conditions:

- pH of the synthetic solution: 6 (± 0.05)
- Adsorbent dose: 1 g/50 mL
- Adsorbent particle size: 2-3 mm
- Contact time: 0.5-90 min for Zn^{2+} and 0.5- 75 min for Cu^{2+}
- Volume of Cu^{2+} or Zn^{2+} standard solution: 50 mL
- Initial Cu^{2+} or Zn^{2+} concentration: C_0 = 20 mg/L.
- Temperature: room temperature (25 ± 2 °C)

3.6.2 Effect of Adsorbent Dose

The impact of the adsorbent dose on Cu^{2+} or Zn^{2+} uptake was analyzed to determine the optimum dose of water hyacinth. The doses studied were; 0.2, 0.5, 0.75, 1, and 1.5 g /50 mL of copper ions solutions and 0.2, 0.5, 1, 1.5, 2.5, and 3 g /50 mL of zinc ions solutions. The contact time is set based on the optimum contact time defined in the preceding experiment. The conditions of the experiment are the following:

- pH of the Cu^{2+} or Zn^{2+} synthetic solution: 6 (± 0.05)
- Contact Time: 60 min
- Adsorbent particle size: 2-3 mm
- Adsorbent dose: 0.2, 0.5, 0.75, 1, and 1.5 g /50 mL for copper and 0.2, 0.5, 1, 1.5, 2.5, and 3 g /50 mL for zinc
- Volume of Cu^{2+} or Zn^{2+} standard solution: 50 mL
- Initial Cu^{2+} or Zn^{2+} concentration: C_0 = 20 mg/L
- Temperature: room temperature (25 ± 2 ℃)

3.6.3 Effect of pH

The pH of a solution has a crucial influence on heavy metals uptake as it determines the surface charge of the adsorbent, the degree of ionization and the specification of the heavy metal ions (Singh et al., 2014). The studied pH values were in a range of 2-10. The initial pH value of each sample was adjusted either with HNO_3 or NaOH using a pH meter, to monitor the change. The conditions of the experiment are the following:

- Adsorbent dose: 1 g/50 mL
- Particle size: 2-3 mm
- Contact time: 60 min.
- Volume of Cu^{2+} or Zn^{2+} standard solution: 50 mL
- pH of the synthetic solution: from 2 to 10
- Initial Cu^{2+} or Zn^{2+} concentration: C_0 = 20 mg/L
- Temperature: room temperature (25 ± 2 ℃).

3.6.4 Effect of Initial Metal Ion Concentration

The impact of the initial lead concentration on the adsorption of lead by rice straw has been studied. The conditions of the experiment are the following:

- pH of the Cu^{2+} or Zn^{2+} synthetic solution: 6
- Contact Time: 60 min
- Particle size: 2-3 mm

- Adsorbent dose: 1 g/50 mL
- Volume of Cu^{2+} or Zn^{2+} standard solution: 50 mL
- Initial Cu^{2+} or Zn^{2+} concentration: 10-400 mg/L
- Temperature: room temperature (25 ± 2 ℃)

3.6.5 Removal Efficiency

The adsorption efficiency was calculated using equation 3.1:

$$\%\, Removal = \frac{C_0 - C_e}{C_0} \times 100 \qquad (3.1)$$

Where:

C_0 is the initial metal ion concentration (mg/L)

C_e is the remaining concentration of metal ion existing in solution (mg/L).

3.6.6 Adsorption Capacity

The amount of Cu (II) and Zn (II) adsorption capacities were calculated using equation 3.2:

$$q_e = (C_0 - C_e)\frac{v}{m} \qquad (3.2)$$

Where:

q_e (mg/g) represents the adsorption capacity (amount of heavy metal ions in mg adsorbed on 1 g adsorbent)

C_0 and C_e represent Cu^{2+} or Zn^{2+} ions concentrations initially and at equilibrium, respectively.

v (L) is the volume of the solution.

m (g) is the mass of the adsorbent (Xu et al., 2021, Lui et al., 2019, Al-Senani and Al-Fawzan, 2018).

3.7. Adsorption Isotherms

Adsorption isotherms describe the equilibrium relationships between an adsorbent and adsorbate. In this study, the linearized forms of Freundlich and Langmuir were used as reported in documented studies (Langmuir, 1918 and Freundlich, 1909). The concentration range for the

isotherm study will be varied between 10 mg/l to 400 mg/L, the volume of the solution (*V)* will be 50 ml and the mass of the adsorbent *(m)* will be 1 g for both metal ions.

3.7.1 Langmuir Isotherm

Langmuir model was expressed in equation 3.3 (Wong et al., 2003a):

$$\frac{1}{q_e} = \frac{1}{q_m} + \frac{1}{q\, K_l\, c_e} \tag{3.3}$$

where,

q_e (mg/g): the amount of adsorbate per unit mass of adsorbent at equilibrium; adsorption capacity

C_e (mg/L): the equilibrium adsorbate concentration in a liquid-phase

q_m (mg/g): the maximum adsorption capacity (monolayer capacity)

K_l (L/mg): the Langmuir constant related to the theoretical maximum adsorption capacity

3.7.2 Freundlich Isotherm

The Freundlich isotherm was expressed from equation 3.4

$$Ln\, q_e = ln\, K_f + \left(\frac{1}{n}\right) lnC_e \tag{3.4}$$

K_f (mg/g) $(L/mg)^{1/n}$: the Freundlich capacity factor, or the adsorption equilibrium constant. K_f is an indicator of the adsorption capacity when the metal equilibrium concentration equals 1 (Zhu et al., 2008).

1/n: the Freundlich intensity parameter. According to Soetaredjo et al. (2013), it is the extent of the heterogeneity of the sorption system and it can be obtained from the slope of ln q_e versus ln C_e linear plot.

q_e is the amount of metal adsorbed onto the adsorbent mg/g and is calculated from equation 3.2.

3.8. Kinetic Study

One of the most important factors for an adsorption process is the prediction of the adsorption rate. The adsorption kinetics depend on the physical and chemical properties of the adsorbent that affect the adsorption mechanism.

3.8.1 Pseudo-First Order Rate Law, K_1

The equation for pseudo-first-order kinetics was initially introduced by Lagergren (1898) (Simonin, 2016). In the literature (Simonin, 2016), it is generally used in the form proposed by Ho and McKay (Ho and McKay, 1999):

$$ln\,(q_e - q_t) = ln\,q_e - K_1 t \quad (3.5)$$

Where;

q_t is the amount of solute adsorbed to the adsorbent surface at any time t (mg/g)

q_e is the amount of solute adsorbed to the adsorbent surface at equilibrium (mg/g).

t is time (min).

K_1 is the pseudo-first-order rate constant.

3.8.2 Pseudo-Second Order Rate Law, K_2

The formula for pseudo-second-order kinetics is generally employed in the form proposed by Ho and McKay (Ho and McKay, 1999) as follows;

$$\frac{t}{q_t} = \frac{t}{q_e} + \frac{1}{K_2\ q_{e2}} \quad (3.6)$$

Where;

K_2 is the pseudo-second-order kinetic rate constant

3.9 Phase II – Response Surface Methodology and General Algebraic Modelling System

This study involves the use of statistical design to optimize the process conditions for maximal adsorption of zinc and copper from aqueous solution using Box-Behnken Design (BBD) involving Response Surface Methodology (RSM). RSM design is simplified with the application of Branch-And-Reduce Optimization Navigator (BARON) solver based on General Algebraic Modelling System (GAMS) with identical factor variables, levels, and model equations.

3.9.1 Response Surface Methodology

Response Surface Methodology (RSM) is a collection of mathematical and statistical techniques for empirical model building (Nair et al., 2013). This technique is employed for modelling and analysis of problems in which a response/objective of interest is influenced by several variables (Behera et al., 2018). RSM is one of the methodologies in Design of Experiments (DOE) which includes many design packages (Riswanto et al., 2019) mentioned in section (2.6).

3.9.1.1 Box–Behnken Experimental Design

In this study, all the adsorption experiments for the removal of copper and zinc ions from waste water using raw water hyacinth (Egypt sample and South Africa sample) as adsorbent were designed according to RSM using Box–Behnken design (BBD) with the aid of Design Expert® software. The removal percentage of zinc and removal percentage of copper was selected as the objective functions for optimization. Since it is often necessary to investigate several different effects on a response of interest, contact time, adsorbent dose, pH and initial metal ion concentration were selected as process variables (Abd Malek et al., 2020, Öztürk et al., 2014).

3.9.1.2 Optimization of Adsorption Variables Using BBD Method

Each variable was represented at two levels - high and low, denoted by (+) and (-) signs, respectively. The range of variables was selected based on the batch experiments done (described in section 3.4). Box–Behnken design (BBD; Design Expert Software, Trial version11, (32-bit), Stat-Ease Inc.) of RSM was used to optimize the four independent variables, namely, contact time (X_1), adsorbent dose (X_2), pH (X_3) and initial metal ion concentration (X_4), with low (−1), medium (0), and high levels (+1) for each variable The response value is the percentage of removal of the heavy metal (Y) and the results were fit into a second-order polynomial equation. Tables 3.1 and 3.2 show the utilized experimental range and the levels of process variables for both copper and zinc respectively. This range was used for the adsorption of copper and zinc by the water hyacinths from Egypt and South Africa.

Table 3.1: Experimental Range and Levels of Process Variables for Cu^{2+}

Process variables	**Levels (Coded/actual)**		
	-1	0	+1
Contact time (X_1),	0.5	37.5	75
Adsorbent dose (X_2),	0.25	0.875	1.5
pH (X_3)	2.5	6.25	10
Initial metal ion concentration (X_4)	20	210	400

Table 3.2: Experimental Range and Levels of Process Variables for Zn^{2+}

Process variables	**Levels (coded/actual)**		
	-1	0	+1
Contact time (X_1),	0.5	47.5	90
Adsorbent dose (X_2),	0.2	1.6	3
pH (X_3)	2	6	10
Initial metal ion concentration (X_4)	10	205	400

The BBD method generates 29 experimental runs, suggested for evaluating the interactive behaviour of the control variables and finding the optimum sets of variables corresponding to each response. The experimental runs for water hyacinth from Egypt are presented in Tables 3.3 and 3.4 for the adsorbed copper and zinc, respectively, whilst the experimental runs for water hyacinth from South Africa are listed in Tables 3.5 and 3.6 for adsorbed copper and zinc, respectively.

Table 3.3: Experimental Design and Results Layout for BBD for Cu^{2+} Adsorbed by Egyptian Water Hyacinth

Run	X_1: Contact time (min)	X_2: Adsorbent Dose (g)	X_3: pH	X_4: Initial concentration (mg/L)
1	37.75	0.87	6.25	210
2	37.75	0.87	6.25	210
3	37.75	1.50	2.50	210
4	37.75	0.87	10	400
5	75	0.87	6.25	400
6	37.75	1.50	6.25	400
7	0.50	0.87	6.25	400
8	0.50	0.87	10	210
9	37.75	0.87	6.25	210
10	37.75	0.87	2.50	20
11	75	1.50	6.25	210
12	0.50	1.50	6.25	210
13	37.75	0.87	2.50	400
14	37.75	0.25	2.50	210
15	37.75	0.25	6.25	400
16	37.75	0.87	6.25	210
17	37.75	0.25	6.25	20
18	37.75	0.87	10	20
19	37.75	1.50	6.25	20
20	37.75	0.87	6.25	210
21	75	0.87	2.50	210
22	0.50	0.87	6.25	20
23	0.50	0.25	6.25	210
24	75	0.87	10	210
25	75	0.87	6.25	20
26	37.75	1.50	10	210
27	37.75	0.25	10	210
28	75	0.25	6.25	210
29	0.50	0.87	2.50	210

Table 3.4: Experimental Design and Results Layout for BBD for Zn^{2+} Adsorbed by Egyptian Water Hyacinth

Run	X_1: Contact time (min)	X_2: Adsorbent Dose (g)	X_3: pH	X_4: Initial concentration (mg/L)
1	90	1.6	6	10
2	47.5	1.6	6	205
3	47.5	1.6	6	205
4	0.5	1.6	6	400
5	90	1.6	2	205
6	47.5	1.6	10	400
7	47.5	0.2	2	205
8	47.5	0.2	10	205
9	47.5	1.6	2	400
10	0.5	1.6	6	10
11	47.5	0.2	6	400
12	47.5	0.2	6	10
13	47.5	3	10	205
14	47.5	1.6	6	205
15	90	3	6	205
16	90	1.6	6	400
17	90	0.2	6	205
18	47.5	1.6	2	10
19	47.5	1.6	10	10
20	90	1.6	10	205
21	0.5	1.6	10	205
22	47.5	3	6	400
23	0.5	0.2	6	205
24	47.5	1.6	6	205
25	47.5	1.6	6	205
26	0.5	3	6	205
27	47.5	3	6	10
28	0.5	1.6	2	205
29	47.5	3	2	205

Table 3.5: Experimental Design and Results Layout for BBD for Cu^{2+} Adsorbed by South African Water Hyacinth

Run	X_1: Contact time (min)	X_2: Adsorbent Dose (g)	X_3: pH	X_4: Initial concentration (mg/L)
1	37.75	1.50	6.25	20
2	37.75	0.87	10	400
3	37.75	0.87	10	20
4	37.75	0.87	6.25	210
5	37.75	0.87	6.25	210
6	37.75	0.87	2.50	20
7	37.75	0.25	6.25	20
8	37.75	0.87	6.25	210
9	75	0.87	6.25	400
10	37.75	1.50	10	210
11	37.75	1.50	6.25	400
12	0.50	1.50	6.25	210
13	0.50	0.87	10	210
14	37.75	0.25	2.50	210
15	75	0.87	6.25	20
16	0.50	0.87	6.25	20
17	37.75	0.87	6.25	210
18	0.50	0.87	2.50	210
19	75	1.50	6.25	210
20	37.75	0.87	6.25	210
21	0.50	0.25	6.25	210
22	37.75	1.50	2.50	210
23	75	0.25	6.25	210
24	37.75	0.87	2.50	400
25	37.75	0.25	6.25	400
26	75	0.87	10	210
27	0.50	0.87	6.25	400
28	37.75	0.25	10	210
29	75	0.87	2.50	210

Table 3.6: Experimental Design and Results Layout for BBD for Zn^{2+} Adsorbed by South African Water Hyacinth

Run	X_1: Contact time (min)	X_2: Adsorbent Dose (g)	X_3: pH	X_4: Initial concentration (mg/L)
1	0.5	0.2	2	400
2	60	3	10	10
3	0.50	0.2	2	10
4	30.25	1.6	6	205
5	30.25	1.6	6	205
6	30.25	1.6	6	205
7	30.25	1.6	6	205
8	0.50	3	10	400
9	0.50	0.2	10	10
10	0.50	3	2	400
11	60	1.6	6	205
12	30.25	3	6	205
13	30.25	1.6	6	205
14	30.25	1.6	6	400
15	60	0.2	2	400
16	60	3	2	10
17	60	0.2	10	400
18	30.25	1.6	6	205
19	0.50	0.2	10	400
20	60	3	10	400
21	0.50	3	10	10
22	60	3	2	400
23	30.25	1.6	10	205
24	30.25	1.6	2	205
25	30.25	1.6	6	205
26	60	0.2	2	10
27	60	0.2	10	10
28	0.50	3	2	10
29	30.25	1.6	6	205

3.9.1.3 Prediction and Verification of Model Equation

The model equation generated from RSM was defined to fit the experimental response results with the independent variables. The model equation should represent the response variable as a function in the independent variables. The Model order varies through each application based on the fitting adequacy of the equation for the experimental results. Linear, two factors interactions (2FI), quadratic, cubic, and modified orders are examined through the model identification. The most accurate model in fitting the experimental results should be chosen to represent the process. After selecting the model order, the model equation is defined, and the coefficients of the model equation are predicted. Generally, RSM uses a full-quadratic equation to define the model. The general second-order model is defined as shown in Equation 3.7.

$$Y = b_o + \sum_{i=1}^{n} b_i x_i + \sum_{i=1}^{n} b_{ii} x_i^2 + \sum_{i=1}^{j-1} \sum_{j=2}^{n} b_{ij}\, x_i x_j + \mathcal{E} \qquad (3.7)$$

where Y is the dependent response, b_o is the model coefficient constant, b_i, b_{ii}, b_{ij}, are coefficients for the intercept of linear, quadratic, interactive terms respectively, while x_i, x_j are independent variables where i≠j. The model adequacy was checked by the coefficient of correlation (R^2), adjusted coefficient of determination (R^2_{adj}) and the predicted coefficient of determination (R^2_{pred}).

In this study, the general quadratic equation was used to define the proposed models which represent each response function in the process variables. Statistical significance was investigated using Analysis of variance (ANOVA) by using Fisher's F-test at 95% confidence level. Statistical significance of the results was presented by p-value, where the result was considered to be significant when the p-value was less than 0.05. Several adequacies checking techniques were used to validate the proposed model including Lack-of-fit analysis and determination coefficient values.

A lack-of-fit analysis is one of the important analyses by ANOVA, which measures the failure of the regression model to represent experimental data points (Yuan et al., 2015).

3.9.2 General Algebraic Modelling System

Since the current part of this study aims to evaluate, compare and then facilitate the RSM-optimized process with the aid of General Algebraic Modelling System **(**GAMS), the second-order polynomial models generated were directly implemented in GAMS without any modification to allow for easy comparison of the optimized results. Meanwhile, the models are in non-linear form, hence, they are handled as NLP models and solved by GAMS 24.4.3 using Branch-And-Reduce Optimization Navigator (BARON). The four control variables were bounded as presented in Equation (3.8) for copper and Equation (3.9) for zinc. These ranges are used for the copper and zinc adsorbed by both water hyacinth samples from Egypt and South Africa, and it serves as the constraint necessary for the solver/researcher in searching for optimal solutions.

$$X_i^{min} \leq X_i \leq X_i^{max} \tag{3.8}$$

$$for\ i = 1, \quad i^{min} = 0.5, \quad i^{max} = 75$$

$$for\ i = 2, \quad i^{min} = 0.25, \quad i^{max} = 1.5$$

$$for\ i = 3, \quad i^{min} = 2.5, \quad i^{max} = 10$$

$$for\ i = 4, \quad i^{min} = 0.5, \quad i^{max} = 90$$

$$X_j^{min} \leq X_j \leq X_j^{max} \tag{3.9}$$

$$for\ j = 1, \quad j^{min} = 0.5, \quad j^{max} = 90$$

$$for\ j = 2, \quad j^{min} = 0.2, \quad j^{max} = 3$$

$$for\ j = 3, \quad j^{min} = 2, \quad j^{max} = 10$$

$$for\ j = 4, \quad j^{min} = 10, \quad j^{max} = 400$$

The results were compared using the percentage error. Percentage error, which is the absolute value of the difference of two values divided by the theoretical value, was applied to Cu^{2+} or Zn^{2+} in this study because the experimental result was compared with a theoretical value (model).

3.10 Phase III –Continuous Fixed-Bed Column Experiments

The second mode of application, after the batch equilibrium tests, was the fixed bed column tests. Fixed-bed column/ continuous flow system is a different application than batch experiments. Batch equilibrium studies give an insight into the efficiency of an adsorbent for the adsorption of specific heavy metals. However, they do not provide data that can be used for the scaling up required for practical industrial applications. On the other hand, column studies provide data that can be used for the scaling up required for industrial applications.

The continuous flow technique has several advantages. One of such is that a higher amount of adsorbate can be adsorbed than in the batch set-up and potentially used for industrial purposes (Patel, 2021).

Fixed-bed column tests were conducted using raw water hyacinth of particle size, 2-3 mm, and pH, 6, as deduced from the batch experiments. Water hyacinth was prepared according to the same procedure stated in Section 3.1.

3.10.1. Experimental Procedure

- The column study was performed in a cylindrical column made of glass of dimensions, 50 cm high, and internal diameter, 2 cm.
- The heavy metal solutions of the individual copper and zinc at various initial concentrations were prepared by dissolving the required amount of $CuSO_4.5H_2O$ and $ZnSO_4.7H_2O$ salts in 1L distilled water.
- Adjusting the pH of the solution to 6, optimum pH from the batch equilibrium experiments, using NaOH solution and HNO_3.
- The prepared adsorbent was first weighed with the analytical balance and then filled inside the column up to the required height.
- The flowrate of the feed solution is adjusted to the desired flow in mL/min by observing the time taken for the effluent of the column to fill a particular pre-defined volume.

- A peristaltic pump transfers the solution from the influent glass container to the adsorption column.
- At specified time intervals, the effluent samples are collected in small test tubes to be analysed via the AAS.

Figures 3.3 and 3.4 show the experimental setup of the fixed-bed column experiment and the schematic diagram of the column experimental setup respectively.

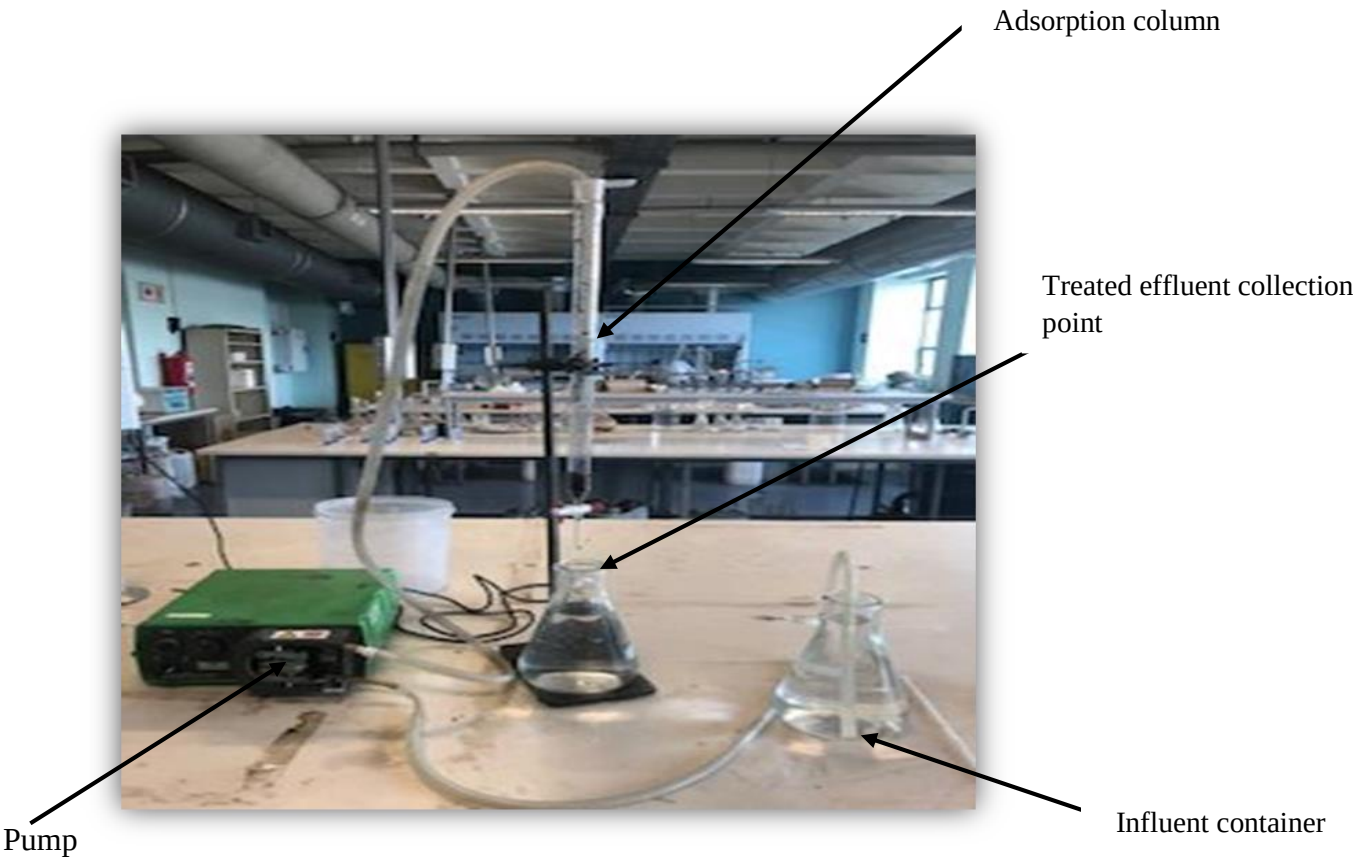


Figure 3.3. Experimental setup of a fixed-bed column experiment

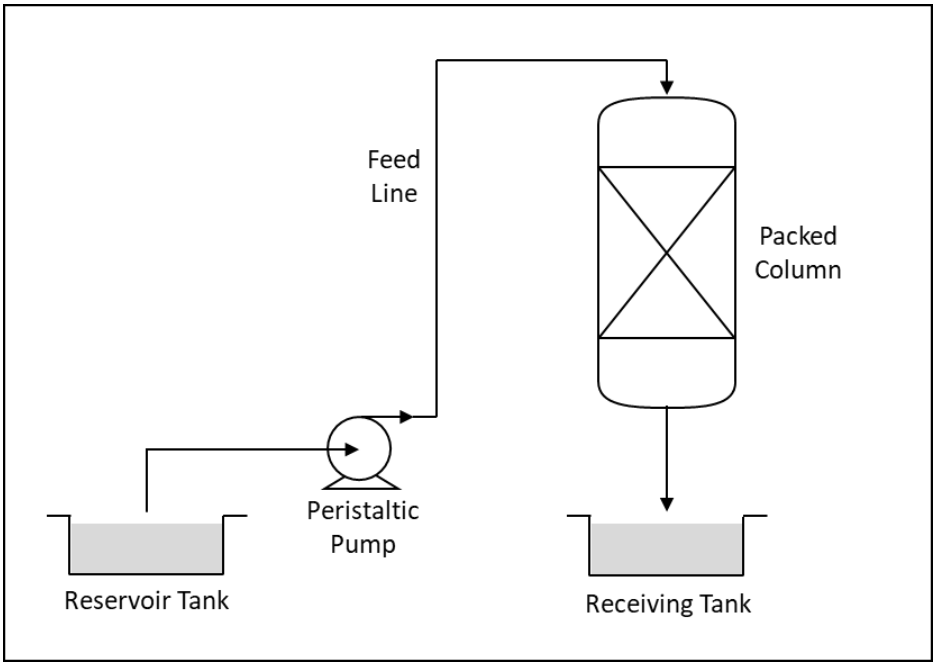


Figure 3.4. Schematic diagram of the column experimental setup

3.10.2 Effect of Initial Cu^{2+} and Zn^{2+} Concentration

Cu^{2+} and Zn^{2+} concentrations of 20 mg/L, 30 mg/L, and 50 mg/L were used to assess the impact of the initial metal ions' concentrations on the performance of the column and breakthrough curves, at pH of 6, a flowrate of 5 mL/min, and bed depth of 2 cm.

3.10.3 Effect of Bed Depth

Water hyacinth was packed in the column at bed depths of 2 cm, 4 cm, and 7 cm to evaluate the effect of the bed depth, at pH of 6, flowrate of 5 mL/min, and initial metal ions concentrations of 20 mg/L for both copper and zinc respectively.

3.10.4 Effect of Flowrate (Q)

The column was run once at a solution flow rate of 5, 7, and 10 mL/min at pH of 6, bed depth of 2 cm, and initial Cu^{2+} and Zn^{2+} concentrations of about 20 mg/L. A summary of the fixed-bed column experiments is illustrated in Table 3.7.

Table 3.7: Summary of Fixed-Bed Column Experiments Using Raw Water Hyacinth of Particle Size 2 mm – 3 mm

Initial metal ion concentration (mg/L)	Flowrate (mL/min)	Bed depth (cm)	pH
20	5	2	6
20	5	4	6
20	5	7	6
20	5	2	6
30	5	2	6
50	5	2	6
20	5	2	6
20	10	2	6
20	17	2	6

3.11 Sampling and Sample Analysis

Sample analysis was carried out for the Cu^{2+} or Zn^{2+} equilibrium concentration and the pH of the samples, as follows:

3.11.1 pH Analysis

The pH of the samples was adjusted by adding a few drops of NaOH (10 M) and/ or HNO_3 (10 M). The pH value was analysed using meter Toledo five easy pH Benchtop Meter, manufactured in the USA. Figure 3.5 shows the pH meter used in the analysis



Figure 3.5. pH meter- METTLER TOLEDO

3.11.2 Cu^{2+} and Zn^{2+} Ions Analysis

The equilibrium/ final concentration of Cu^{2+} and Zn^{2+} was analysed via an Atomic Absorption Spectrometer (A.A.S), flame type, Agilent Technologies 200 series AA systems dual-flame atomization system model, manufactured by Agilent, USA (Figure 3.6). The A.A.S used for the analysis of Cu^{2+} and Zn^{2+} provides quantitative information of the heavy metals using an analytical technique. The sample is subjected to a flame leading to thermal and chemical reactions which produce free atoms that can absorb specific wavelengths, providing Atomic Absorption Spectroscopy (EL Zayat, 2014). Samples obtained from the experimental work that exceeded the measuring range of the atomic absorption spectrometer (A.A.S), were diluted using Deuterium Depleted Water (DDW) to a ratio of 1:10 and if it still exceeded the measuring range, we dilute further to achieve the ratio, 1:20.



Figure 3.6: Atomic Absorption Spectrometer (A.A.S)

3.12 Mathematical Modelling and Simulation

Fixed-bed adsorption usually occurs in an open system where adsorbate solution continuously passes through a column packed with the adsorbent (Patel 2019, Moradi et al., 2019). The dynamic behaviour of a fixed bed column is described in terms of the effluent concentration-time profile, i.e., the breakthrough curve (Moradi et al., 2019).

The aim of modelling the mass transfer in the adsorption column is to predict the breakthrough time according to the goals of the separation process. The general way to predict the breakthrough curve is to solve a set of partial differential equations which consist of a macroscopic mass conservation equation, uptake rate equation, and isotherm equation, together with a set of initial and boundary conditions.

Finally, with a good estimate of the breakthrough curve through mathematical modelling, the adsorption process can be simulated to predict the behaviour of the system and ensure normal operation.

To implement the generic equations, the following assumptions were made:

a. The process is isothermal.

b. The packing material is made of porous particles that are spherical and uniform in size.
c. The velocity is constant along the bed.
d. The adsorption equilibrium relationship is described by Langmuir isotherm.
e. Mass transfer across the boundary layer surrounding the solid particles is characterized by the external film mass transfer coefficient, K_f.

Material Balance for Adsorption Column

Subject to the assumptions above, the following parameters can be deduced from the system:

Convective Mass Transfer across the Boundary Layer is given by: $U\frac{\partial Ci}{\partial z}$

Where; U = Superficial Velocity (m/s),

C_i = Adsorbate concentration in the mobile phase (mg/L)

Z = Axial coordinate (m)

Axial Dispersion is given by: $D_z \frac{\partial^2_C}{\partial^2_z}$

Where; D_z = Axial dispersion coefficient (m^2/s)

Materials Adsorbed by the Adsorbent is given by: $\frac{(1-\varepsilon)}{\varepsilon}\ \rho\frac{\partial q}{\partial t}$

Where; ε = Bed porosity

ρ = Density of adsorbent or particle (Kg/m^3)

q = Mass of metal ions adsorbed per unit mass of the sorbent; adsorption capacity (mg/g)

t = Time (s)

Accumulation of the Adsorbate is given by: $\frac{\partial Ci}{\partial t}$

$$\frac{\partial Ci}{\partial t} + U\ \frac{\partial Ci}{\partial z} + \frac{(1-\varepsilon)}{\varepsilon}\ \rho\frac{\partial q}{\partial t} = D_z\frac{\partial^2 C}{\partial z^2} \qquad (3.10)$$

Where initial and boundary conditions are:

t=0 c=0 for all Z

Z=0 $c=C_{feed}$

Z=L $\partial c_i / \partial z = 0$

The inter-phase mass transfer rate is expressed as follows:

$$\frac{\partial q}{\partial t} = k_f(q - q^*) \tag{3.11}$$

Isotherm Equation

$$q^* = \frac{q_m bc}{1 - qc} \tag{3.12}$$

Substituting equation (3.12) into equation (3.11)

$$\frac{\partial q}{\partial t} = k_f\left(q - \frac{q_m bc}{1 - qc}\right) \tag{3.13}$$

Substituting equation (3.13) into equation (3.10)

$$\frac{\partial c}{\partial t} + U\frac{\partial c}{\partial z} + \frac{(1-\varepsilon)}{\varepsilon}\,\rho k_f\left(q - \frac{q_m bc}{1 - qc}\right) = D_z\frac{\partial^2 C}{\partial z^2} \tag{3.14}$$

3.12.1 Calculation of Model Parameters

Model parameters were calculated using the following correlations:

Calculation of Bed Porosity:

Bed porosity is the fraction of total volume that is void.

$$Bed\ porosity = \frac{Void\ volume}{Total\ volume} \tag{3.15}$$

Calculation of Bed Density:

Bed density is calculated by dividing the mass of adsorbent filled in the entire column to the volume of the column.

$$Bed\ denisty = \frac{Mass\ of\ adsorbent}{Volume\ of\ column} \tag{3.16}$$

Calculation of axial dispersion coefficient: This was evaluated using the following equation (Rastegar and Gu, 2017)**.**

Calculation of Axial Dispersion Coefficient:

This was evaluated using the following equation (Bisht et al., 2020),

$$D_l = 0.7\, D_m + \frac{2\, R_p\, v\, \varepsilon_b}{0.18+0.008\, R_e^{0.59}} \quad (3.17)$$

For M_B<1,000, molecular diffusion (D_m) can be calculated using Wilke-Chang correlation as follows:

$$D_m = 1.173 * 10^{-16}\, (\psi\, M_B)^{\frac{1}{2}}\ \frac{T}{\mu_B\, v_A^{0.6}} \quad (3.18)$$

Where,

T = temperature

M_B = molecular weight of solvent

R_p = pellet radius (m)

ε_b = void fraction of bed (bed porosity)

V = Kinematic viscosity (m/s) = $\frac{\mu}{\rho}$ (3.19)

Ψ = association parameter for water

μ_b = viscosity of solvent ((kg/m).s)

Calculation of External Mass Transfer Coefficient:

The external mass transfer coefficient is calculated using the following correlation (Bisht et al., 2020)

$$sh = \frac{1.09}{\varepsilon}\, R_e^{0.33}\, sc^{0.33} \quad \text{For } 0.0015 < \text{Re} < 55 \quad (3.20)$$

$$\text{R}_e = \frac{v\, \rho\, d}{\mu} \quad (3.21)$$

$$sc = \frac{v}{D} \tag{3.22}$$

D = film phase diffusion coefficient

3.12.2 Simulation

Since nonlinear adsorption isotherm is considered, the preceding sets of partial differential equations (3.10) to (3.14) were solved numerically by a reduction to a set of ordinary differential equations using the Finite difference method. The finite-difference was employed due to its stability and nature of boundary conditions. However, a mathematical algorithm to solve coupled equations was developed and inserted into a computer program using MATLAB software. The parameters for the simulation of the model were calculated from the previous results of batch experiments done. This present model is studied by varying the different important parameters such as initial metal ion concentration, bed height, and flowrate.

3.12.3 Model Validation

To validate the proposed model, a set of experiments were done (shown in section 3.7) and the experimental breakthrough curves were compared with numerical results of this work.

3.13 Comparison of Model and Experimental Results

The model and experimental results were compared using the R^2, chi-squared, and mean absolute percentage error (MAPE) values

R^2 value: The closeness between model and experimental values was measured by the R^2 value

$$R^2 = 1 - \frac{Regression\ sum\ of\ square}{total\ sum\ of\ square} \tag{3.23}$$

MAPE value: The MAPE value was calculated using the following formula:

$$MAPE = \frac{100}{N} * \Sigma \left| \frac{model\ value - experimental\ value}{-model\ value} \right| \tag{3.24}$$

Chi-squared value: The chi-squared value was measured using the following formula:

$$X^2 = \Sigma \quad \frac{(model\ value - experimental\ value)^2}{experimental\ value} \tag{3.25}$$

3.14 Packed Column Design

It is not possible to design a column accurately without a test column to obtain a breakthrough curve for the liquid of interest and the adsorbent solid to be used.

3.14.1 Scale-up Procedure for the Adsorption Column

For the model building of systems using biomaterials as adsorbents in continuous systems, the residence time is an important parameter. The longer the residence time, the better the bed performance. In our system we can reach the highest residence time in two ways:

(i) Increasing the height of the bed, which allows for increasing the contact time.

(ii) Decreasing the linear flowrate through the column increases the contact time.

The linear flowrate through the bed depth was calculated according to the mini-column results. For the scale-up calculations, we increased the bed depth (H) to 400 cm. The internal diameter (D) was calculated to the new bed depth and keeping the ratio, D/H constant at a value of 0.04.

Mini Column Geometric Parameters:

- Internal diameter (cm) = 2
- Height (cm) = 50

Mini Column Operating Parameters:

- Flowrate (mL/min) = 5
- Initial concentration (mg/L) = 20
- Height of water hyacinth bed (cm) = 7
- Adsorbent weight (g) = 0.97

The data obtained from the model breakthrough curves was used to scale up the column and draw the breakthrough curve which gave the density of the adsorbent as 1970 g/mL.

Some calculations for mini column:

Filtration Rate (FR):

$$Filtration\ rate = \frac{Q}{A} \quad (3.26)$$

where,

Q = flowrate (mL/min)

A= Cross section area of the column

The volume of the packed bed:

$$The\ volume\ of\ packed\ bed = A * H \quad (3.27)$$

where,

H = height of the bed

Area of packed bed:

$$Area\ of\ Packed\ bed = \frac{Q}{FR} \quad (3.28)$$

Capacity of the bed:

$$Capacity\ of\ the\ bed = Q * C_o * t^* \quad (3.29)$$

Where,

C_o = Initial metal ion concentration (mg/L)

t^* = time when C = 0.5 C_o

Utilized capacity:

$$Utilized\ capacity = Q * C_o * t_b \quad (3.30)$$

where,

t_b = breakthrough time, defined as the time when $\frac{C}{C_o} = 0.05$

Degree of utilization:

$$Degree\ of\ utilization = \frac{Utilized}{Capacity\ of\ the\ bed} * 100 \quad (3.31)$$

Length of unused bed (LUB):

$$LUB = L\left(1 - \frac{t_b}{t^*}\right) \quad (3.32)$$

where,

L= length of the column (column height)

Length of equilibrium section (LES):

$$LES = L - LUB \quad (3.33)$$

Amount of heavy metal flown out the column:

$$Flown\ out = Q * (Area\ of\ the\ small\ triangle\ under\ the\ breakthrough\ curve)$$

$$The\ volume\ of\ flown\ out(breakthrough) = Q \times t_b$$

$$C_{avr} = \frac{flown\ out}{Volume\ of\ flown\ out}$$

$C_{avr.}$ = average concentration in the outlet solution

3.14.2. Scaling up

When the adsorption column needs to be scaled up to 400 cm.

$$\frac{H}{D} = \frac{h}{d} \quad (3.34)$$

H = height of scaled-up adsorption column

D = diameter of scaled-up adsorption column

h = height of the mini-column

d = diameter of the mini-column

Area of the scaled-up column = $\Pi\frac{d^2}{4}$

Since D is the diameter of the scaled-up adsorption column calculated from equation (3.34)

The Flowrate of the Scaled-up Column

$$\frac{Q_1}{A_1} = \frac{Q_2}{A_2} \tag{3.35}$$

where,

Q_1 = flowrate of mini column

A_1 = cross section area of mini column

Q_2 = flowrate of scaled-up column

A_2 = cross section area of scaled-up column

Since we have the value of the flowrate and the cross-section area of the mini-column and the value of the cross-section area of the scaled-up column, by cross multiplication in equation (3.35), we can calculate the flowrate of the scaled-up column.

Amount of adsorbent needed

$$Amount\ of\ adsorbent = volume\ of\ packed\ column * \rho \tag{3.36}$$

where,

ρ = density of adsorbent

To calculate the new t* = t*(of mini column)*$\frac{l_2}{l_1}$ (3.37)

L_2 = length of scaled-up column

L_1=length of mini column

To Calculate the new breakthrough time (t_b)

$$t_b = t^*_{scaled\ up\ column} - \left(t^*_{mini\ column} - t_{b\ (mini\ column)}\right) \tag{3.38}$$

Degree of utilization of the scaled-up column:

$$Degree\ of\ utilization\ of\ the\ scaled\ up\ column = \frac{t_{b\ of\ scaled\ up\ column}}{t^{*}_{of\ scaled\ up\ column}} \quad (3.39)$$

Breakthrough volume or flown out volume of the scaled-up column:

$$Q_{of\ scaled\ up\ column} \times t_{b\ of\ scaled-up\ column} \quad (3.40)$$

Amount of heavy metal flown out the column:

$$flown\ out\ of\ the\ scaled-up\ column = cross\ section\ area\ of\ the\ scaled-up\ column \times flown\ out\ the\ value\ of\ mini-column \quad (3.41)$$

$$C_{avr.} = \frac{flown\ out(of\ scaled-up\ column)}{Volume\ of\ flown\ out\ (of\ scaled-up\ column)} \quad (3.42)$$

$C_{avr.}$ = Average concentration in the outlet solution

3.15 Economic feasibility for the scaled up adsorption column

The economic feasibility analysis was conducted for the data calculated for the scaled up adsorption column for copper using water hyacinth as adsorbent.

- **Cost of manufacturing (COM)**

$$COM = 0.180\ FCI + 2.73\ C_{OL} + 1.23\ (C_{UT} + C_{WT} + C_{RM}) \quad (3.43)$$

C_{UT}: cost of utilities

C_{WT}: cost of waste treatment

C_{RM}: cost of raw material

- **Fixed capital investment (FCI)**

$$C_{TM} = F_{lag} * \sum_{i=1}^{n} C_m \quad (3.44)$$

C_{TM}: Is the capital cost (total module) of the plant (Capital cost of adsorption column)

n: is the total number of individual units

F_{lang}: Lang factor

- **Cost of operating labor (C_{OL})**

$$N_{OL} = (6.29 + 31.7\ P^2 + 0.23 N_{np})^{0.5} \quad (3.45)$$

N_{OL}: is the number of operators per shift

P: is number of processing steps

N_{np}: number of non-particulate processing steps = Σ Equipment

- **Cost of utilities (C_{UT})**

Power needed for the pump to lift ≈ 4 m^3 to the adsorption column per day

Pump power (w) = height of column * flowrate * g* density of water* p (pa) (3.46)

- **Cost of raw material (water hyacinth) (C_{RM})**

  Costs of controlling and harvesting water hyacinth was calculated according to a research done by Wang et al., in 2019.

References

Abd Malek, N.N., Yousef, E., Jawad, A.H., 2020. Optimization of Adsorption Parameters for Reactive Red 4 (RR4) Removal by Cross-linked Chitosan-Epichlorohydrin using Box-Behnken Design. Science Letters, 14(1).

Al-Senani, M., Al-Fawzan, G., 2018. Adsorption study of heavy metal ions from aqueous solution by nanoparticle of wild herbs. The Egyptian Journal of Aquatic Research, 44(3), 187-194.

Beheraa,S., Meenaa, H., Chakrabortya,S., Meikap, B.C., 2018. Application of response surface methodology (RSM) for optimization of leaching parameters for ash reduction from low-grade coal. International Journal of Mining Science and Technology 28(4), 621-629.

Bisht, R., Agarwal, M., Singh, K., Gupta, R., Dohare, R., 2020. Continuous Fixed-Bed Adsorption of Heavy Metals Using Biodegradable Adsorbent: Modelling and Experimental Study. J. Environ. Eng., 2020, 146(2): 04019110.

EL Zayat, M.A., 2014. Adsorption of Heavy Metals Cations in Wastewater Using Cement Kiln Dust. PhD diss. The American University in Cairo, 2014.

Ho, Y., McKay, G., 1999, 'Pseudo-second order model for sorption processes', *Process Biochem,* 1999 (34): 451–465.

Khan, S.A., Khan, S.B., Khan, L.U., Farooq, A., Akhtar, K., Asiri, A.M., 2018. Fourier Transform infrared spectroscopy: Fundamentals and Application in Functional Groups and Nanomaterials Characterization. Springer International Publishing AG, part of Springer Nature 2018, Handbook of Materials Characterization.

Liu, L, Luo, X-B, Ding, L, Luo, S-L. 2019. Application of nanotechnology in the removal of heavy metal from water. In: Luo X, Deng F, eds. Nanomaterials for the Removal of Pollutants and Resource Reutilization. Elsevier; 2019:83-147.

Mortadi, S., Elham, M., Ramin, K., 2019. Stability Determination of the Modified Activated Carbon to Adsorb Thiophenic Compounds from Model Diesel Fuel. Iran. J. Chem. Chem. Eng., 38(4).

Nair, A., Makwana, A., Ahammed, M., 2014. The use of response surface methodology for modelling and analysis of water and wastewater treatment processes: a review. Water Science & Technology 69(3):464-478.

Öztürk, D., Şahan, T., Dişli, E., Aktaş, N., 2014. Optimization with response surface methodology (RSM) of adsorption conditions of Cd (II) ions from aqueous solutions by pumice. Hacettepe J. Biol. & Chem., 2014, 42 (2), 183-192.

Patel, H., 2019. Fixed-bed column adsorption study: a comprehensive review. Applied Water Science (2019).

Patel H., 2021. Comparison of batch and fixed bed column adsorption: a critical review. International Journal of Environmental Science and Technology. DOI: 10.1007/s13762-021-03492-y.

Rastegar, S., Gu, T., 2017. Empirical correlations for axial dispersion coefficient and Peclet number in fixed-bed columns. Journal of Chromatography A 1490. DOI: 10.1016/j.chroma.2017.02.026.

Riswanto, F.D.O., Rohman, A., Pramono, S., Martono,S., 2019. Application of response surface methodology as mathematical and statistical tools in natural product research. Journal of Applied Pharmaceutical Science, 9(10), 125-133.

Singh, J., Ali, A., Prakash, V., 2014. Removal of lead (II) from synthetic and batteries wastewater using agricultural residues in batch/column mode. Int. J. Environ. Sci. Technol. 11 (2014): 1759-1770.

Simonin, J., 2016. On the comparison of pseudo-first order and pseudo-second order rate laws in the modeling of adsorption kinetics. Chemical Engineering Journal. 300 (2016): 254-263.

Soetaredjo, Edi, F., Kurniawan, A., Lu Ki, O., Ismadji, S., 2013. Incorporation of selectivity factor in modelling binary component adsorption isotherms for heavy metals- biomass system. Chemical Engineering Journal 219 (2013): 137-148.

Temitope, D., Oyedotun, T., 2018. X-ray fluorescence (XRF) in the investigation of the composition of earth materials: a review and an overview, Geology, Ecology, and Landscapes, 2:2, 148-154, DOI: 10.1080/24749508.2018.1452459.

Turton, R., Bailie, R.C., Whiting, W.B., Shaeiwitz, J.A., Bhattacharyya, D., Analysis, Synthesis, and Design of Chemical Processes Fourth Edition. ISBN-13: 978-0-13-261812-0, ISBN-10: 0-13-261812-5.

Wong, K.K., Lee, C.K., Low, K.S., Haron, M.J., 2003. Removal of Cu and Pb by tartaric acid modified rice husk from aqueous solutions. Chemosphere 50 (2003 a): 23- 28

Wang, Z., Zheng, F., Xue, S., 2019. The Economic Feasibility of the Valorization of WaterHyacinth for Bioethanol Production. Sustainability 2019, 11, 905.

Xu, L., Liu,Y., Wang, J., Tang ,Y., Zhang, Z., 2021. Selective adsorption of Pb^{2+} and Cu^{2+} on amino-modified attapulgite: Kinetic, thermal dynamic and DFT studies. Journal of Hazardous Materials, 404(A), 124140.

Yuan J., 2015. Multiple responses optimization of ultrasonic-assisted extraction by response surface methodology (RSM) for rapid analysis of bioactive compounds in the flower head of Chrysanthemum morifolium Ramat.," Ind. Crops Prod., vol. 74, pp. 192–199, 2015.

Zhu, B., Fan, T., Zhang, D., 2008. Adsorption of copper ions from aqueous solution by citric acid modified soybean straw." Journal of Hazardous Materials (ELSEVIER) 153 (2008): 300-308.

CHAPTER FOUR

RESULTS AND DISCUSSION

Introduction

This chapter describes and discusses the results of what had been done in this research. The first section shows results of the characterisation of untreated water hyacinth collected from the different countries (Egypt and South Africa) by XRF (X-Ray Fluorescence) and FTIR (Fourier Transform Infrared) .The second section describes the adsorption experiments, firstly the batch experiments, Optimisation of parameters by two techniques are then described using RSM (Response Service Methodology) and GAMS (General Algebraic Modelling System). Fixed bed column experiments results, modelling and simulation results are explained extensively. Validation of the mathematical model and its comparison between the experimental data is also discussed. Finally the result of the design of industrial scaled adsorption column and the economic estimation of process is showed.

4.1 Characterisation of Water Hyacinth

Two analysis were done for the characterization of water hyacinth, X-Ray fluorescence (XRF) and Fourier Transform Infrared Spectroscopy (FTIR). XRF was done to detect the elements in the adsorbent and to show the chemical composition of water hyacinth from each country. FTIR was done to determine the main functional groups responsible for the adsorption of heavy metal ions on the water hyacinth.

4.1.1 X-Ray Fluorescence (XRF)

XRF was employed for quantitative chemical analysis to assess the water hyacinth from South Africa and Egypt as raw adsorbents before adsorption of either copper or zinc. Table 4.1 shows the elements detected in both samples of water hyacinth in mg/L, while Table 4.2 shows the metal oxides in (%wt) that are found in both water hyacinth samples from both countries. It was observed that most of the heavy metal ions detected were found in both water hyacinth samples, however, with different concentrations. Sc, Co, Br, Sr, Zr, Mo, Cd, Sn, Cs, Ba, Ce, Sm, Hf, W and Th were found to occur in higher concentration in the sample from Egypt than in the sample from South Africa. Ce and Sm were not detected in the South Africa sample while Cr, Sb and Ta were not

detected in the sample from Egypt. The total sum of heavy metal ions detected in Egyptian and South African water hyacinth samples was 492.5 mg/L and 434 mg/L, respectively. Table 4.2 shows the chemical composition of both water hyacinth samples, it is observed that the South African water hyacinth sample contains metal oxides with higher percentage than Egyptian water hyacinth sample. Al_2O_3, MgO, CaO, Na_2O, K_2O, P_2O_5 and SO_3 were found in South African water hyacinth sample in higher percentage than that in Egyptian sample. Fe_2O_3 was found in Egyptian water hyacinth sample in higher percent than that in South African sample. According to researches done by Szymoniak et al., 2022, Primo et al., 2020 and Hassan et al., 2017, metal oxides can be used in its form or in Nano particle size form to remove heavy metal ions from wastewater, that makes South African water hyacinth a better adsorbent as it contains a higher percentage of metal oxides.

Table 4.1: Percentage of Elements (%, wt) that Found in of Raw Water Hyacinth Samples from South Africa and Egypt before Adsorption

Main Constituents	South Africa (mg/L)	Egypt (mg/L)
Sc	0.7	2.2
Cr	4.2	----
Mn	218.1	189.3
Co	0.2	1.0
Ni	7.1	0.6
Cu	7.1	6.6
Zn	52.1	36.0
Ga	6.7	5.5
As	7.2	2.2
Br	17.5	49.0
Rb	14.2	6.1
Sr	35.6	113.3
Zr	3.6	6.0
Nb	2.4	0.9
Mo	0.6	3.4
Ag	0.8	0.5
Cd	1.2	1.5
Sn	5.6	6.4
Sb	0.8	----
Te	3.4	2.7
Cs	2.7	3.1
Ba	3.6	7.1
La	1.4	1.2
Ce	-----	6.4
Sm	------	4.9
Hf	7.5	8.7
Ta	2.1	---
Pb	6.2	5.4
W	1.2	4.3
Th	9.7	10
U	1.8	1.6

Table 4.2: Chemical Composition (%, wt.) of Raw Water Hyacinth Samples from South Africa and Egypt before Adsorption

Main Constituents (wt%)	South Africa	Egypt	% Difference
SiO_2	0.28	0.28	0
Al_2O_3	0.04	0.03	25%
$Fe_2O_3^{tot.}$	0.04	0.07	75%
MgO	0.4	0.15	62.5%
CaO	1.91	1.46	23.6%
Na_2O	0.28	0.04	85.7%
K_2O	3.36	2.66	20.8%
P_2O_5	1.4	0.59	57.9%
SO_3	0.73	0.28	61.6%

4.1.2. Fourier Transform Infrared Spectroscopy (FTIR)

FTIR analysis was carried out for raw water hyacinth from Egypt and South Africa pre and post adsorption of copper in order to determine the main functional groups responsible for the adsorption. The FTIR spectra, shown in Figure 4.1 and Figure 4.2, were analysed and the wave numbers of the peaks and their corresponding functional groups are presented in Table 4.3 and Table 4.4, for Egyptian water hyacinth.

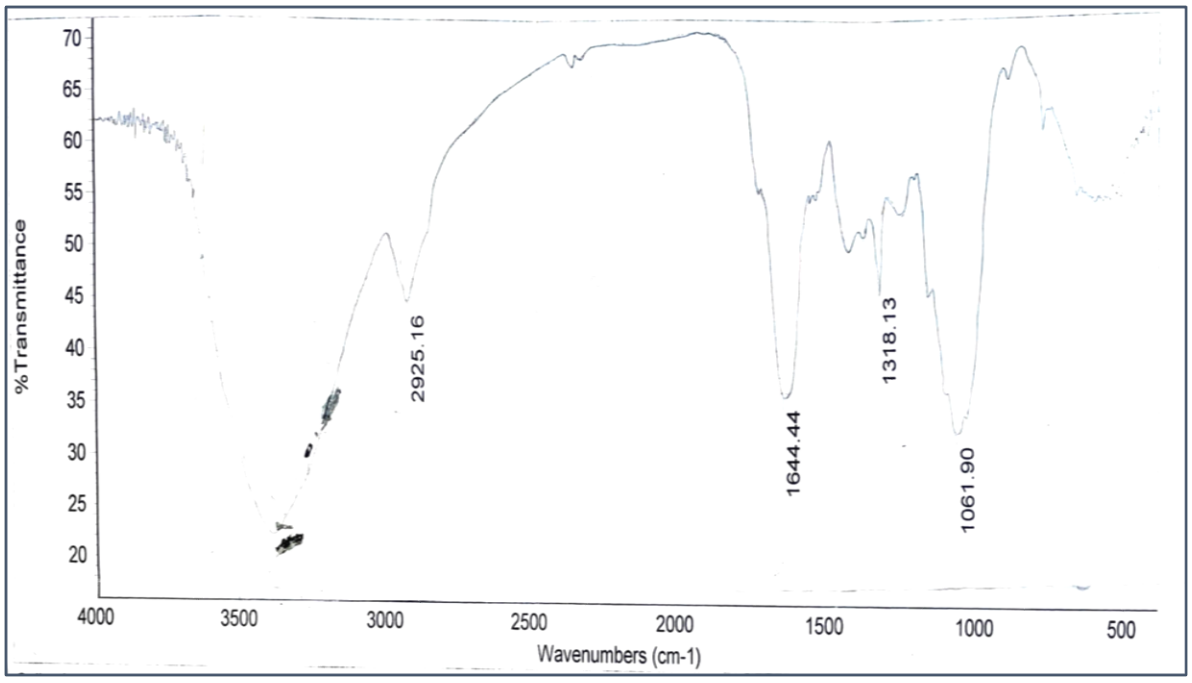


Figure 4.1: FTIR spectrum of Egyptian water hyacinth before adsorption of Cu^{2+}

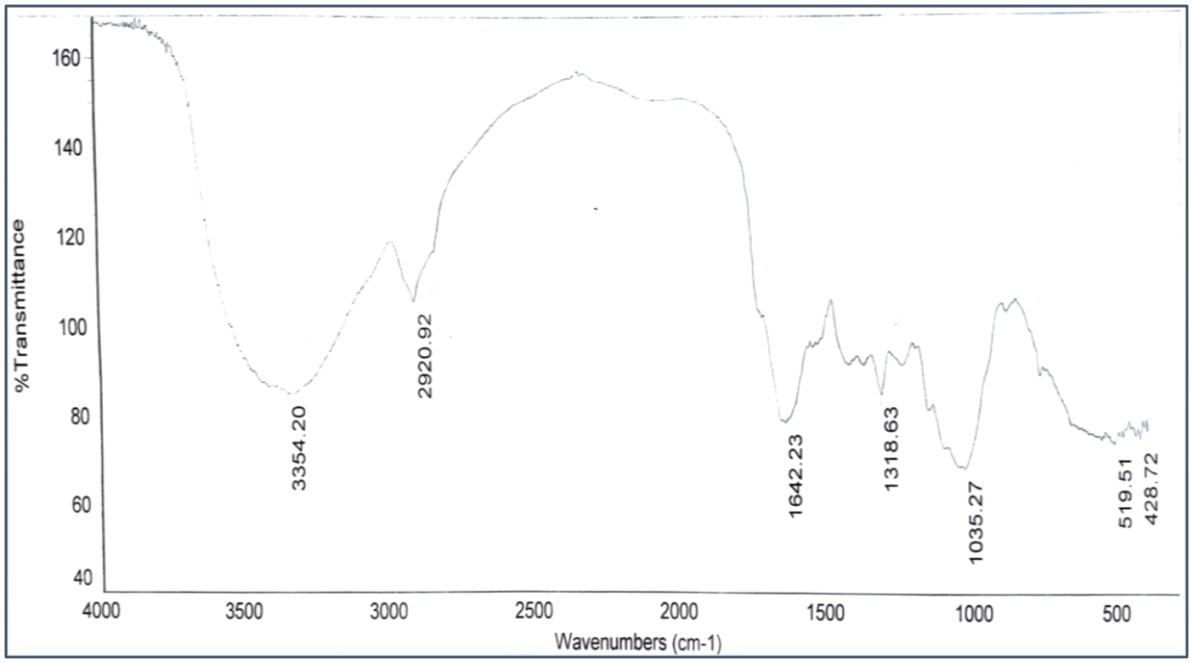


Figure 4.2: FTIR spectrum of Egyptian water hyacinth after adsorption of Cu^{2+}

Table 4.3: FTIR of Egyptian Water Hyacinth Sample before Adsorption of Cu^{2+}

Wave number	Functional group
3400	O-H
2925.16	C-H
1644.44	C=O
1318.13	C-O
1061.90	SiO_2 or MgO

Table 4.4: FTIR of Egyptian Water Hyacinth Sample after Adsorption of Cu^{2+}

Wave number	Functional group
3354.2	O-H
2920.92	C-H
1642.23	C=O
1318.63	C-O
1035.25	SiO_2 or MgO

FTIR analysis was carried out for raw water hyacinth from Egypt samples pre and post adsorption of Cu^{2+} in order to determine the main functional groups responsible for the adsorption. The FTIR spectra, shown in Figures 4.1 and 4.2, were analyzed and the wave numbers of the peaks and their corresponding functional groups are presented in Table 4.3 and Table 4.4. According to the illustration of (Singh et al., 2014) of the functional groups corresponding to a range of wave numbers, the largest peak of wave number 3400 cm^{-1} shown in Figure 4.1, corresponds to either free or H-bonded O-H groups that could be present in carboxylic acids on the surface of water hyacinth. The peak at 1644.44 cm^{-1} wave number corresponds to the C=O that could exist in the carboxylic acids. As for peaks of wave numbers in the range of 1318.13 to 1061.90 cm^{-1}, are an indication of C-O bond, and bands of wave number 2925.16 cm^{-1} are an indication of C-H bond. C-O bond may be due to carboxylic acids, or fiber carbonaceous that are present in the structure of water hyacinth that is composed of lignin and cellulose, this finding was similar as in

(Soetaredjo et al., 2013) research. Those groups probably act as proton donors that once get deprotonated, the hydroxyl group or the carboxyl group adsorbs the heavy metal ions (Singh et al., 2014)

As illustrated in Figures 4.1 and 4.2, the peak representing the O-H bond was shifted from 3400 cm-1 to 3354 cm^{-1}, which is a significant change that indicated surface -OH group was one of the functional group responsible for adsorption (Munene et al., 2020). Whereas, the peak of the C=O bond was shifted from 1644.44 to 1642.23 cm^{-1}, and the peak of the C-O bond was shifted from 1318.13 to 1318.63 cm^{-1}, this minor shift indicated that these groups were not involved in the adsorption process (Munene et al., 2020).

Those shifts can be attributed to the surface complexation created between Cu^{2+} and the carboxylic acids functional groups; hence, it is an indication that chemical complexation between Cu^{2+} and the carboxyl groups could be one of the mechanisms partially responsible for the adsorption of Cu^{2+} via water hyacinth.

The FTIR spectra analysis of raw and Cu^{2+} loaded adsorbents indicated the complex formation of Cu^{2+} ion with different functional groups that are present in the bio-adsorbent. Mainly surface hydroxyl group, and silicon oxide were responsible for Cu^{2+} adsorption. Table 4.5 summarizes the change in spectral structure when copper was adsorbed on water hyacinth from Egypt.

Table 4.5: Changes in Spectral Structure When Copper was Adsorbed on Egyptian Water Hyacinth Sample

Wave number (cm^{-1})		**Functional groups identified in the raw water hyacinth**	**Intensity**	
Before	After		Before	After
3404.02	3354.20	O-H carboxylic acid, alcohol, water, phenol	23.753	84.677
1644.44	1642.23	C=O acid, esters	35.622	78.217
2925.16	2920.92	C-H bending (alkanes) or C-O stretch and O-H deformation (acids	44.805	105.318
1318.13	1318.63	C-O Alcohols, Acids, Esters, Ether	46.563	84.478

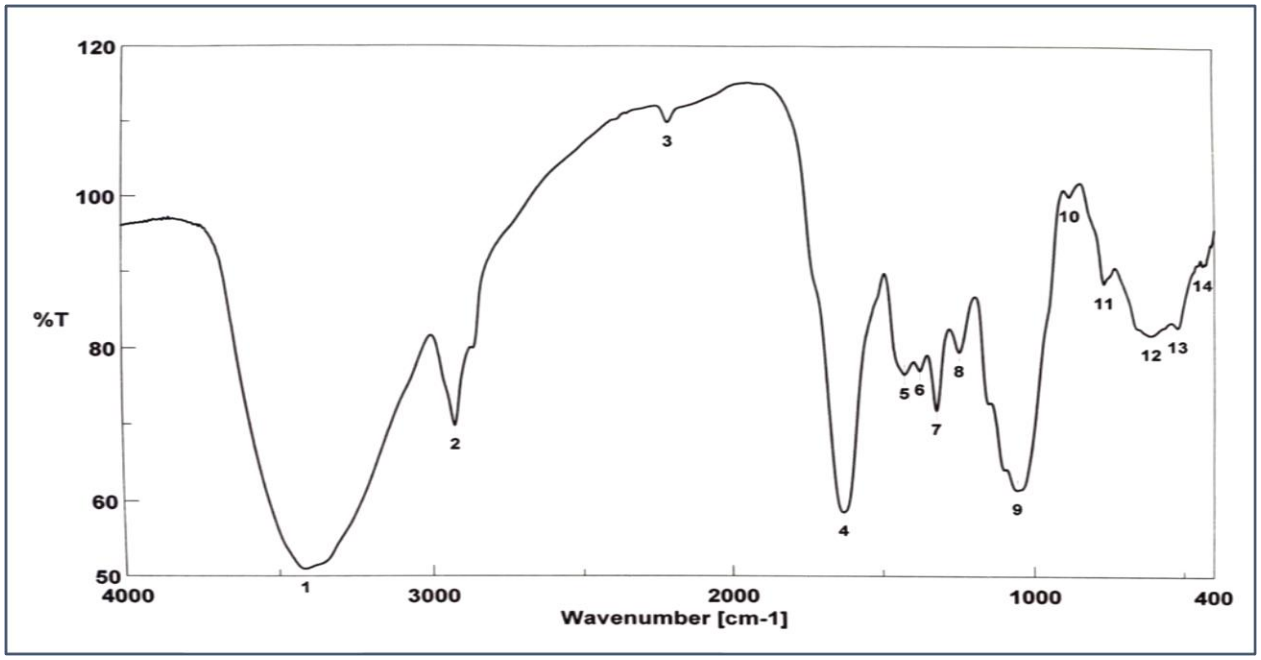


Figure 4.3: FTIR spectrum of South African water hyacinth before adsorption of Cu^{2+}

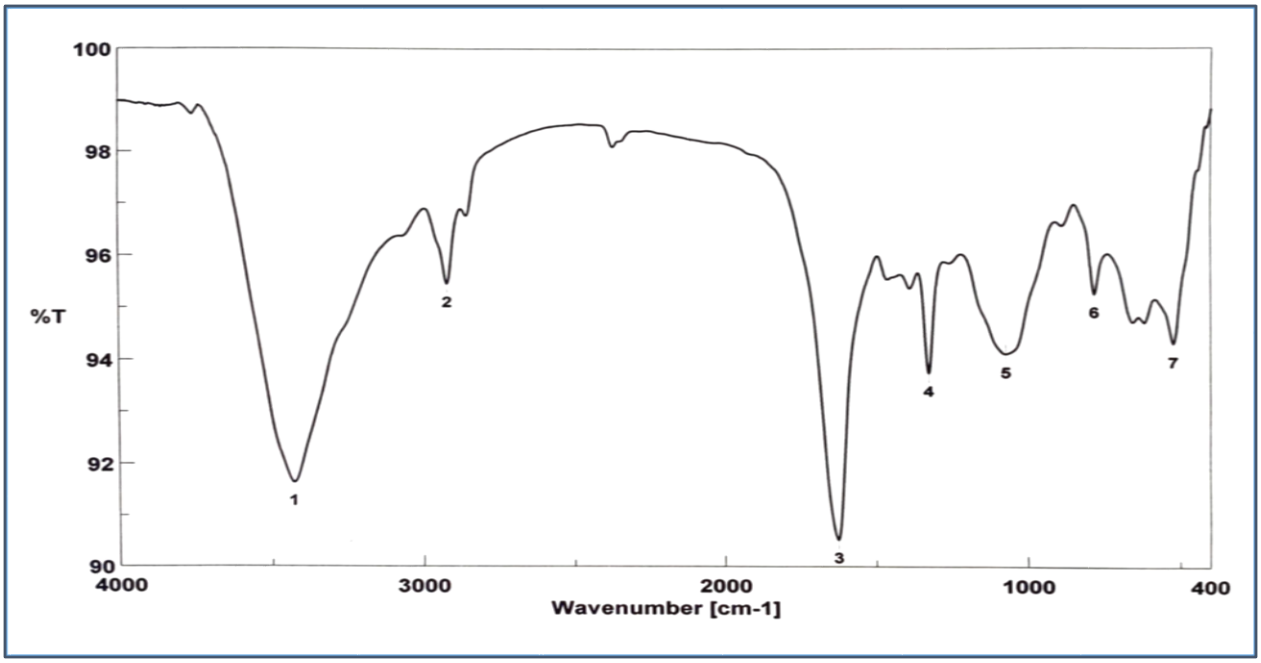


Figure 4.4: FTIR spectrum of South African water hyacinth after adsorption of Cu^{2+}

Table 4.6: FTIR of SA- Water Hyacinth Sample before Adsorption of Cu^{2+}

Wave number	Functional group
3417.24	O-H
2923.56	C-H
1629.55	C=O
1321.96	C-O
1056.8	SiO_2 or MgO

Table 4.7: FTIR of SA-Water Hyacinth Sample after Adsorption of Cu^{2+}

Wave number	Functional group
3430.74	O-H
2923.56	C-H
1624.73	C=O
1318.11	C-O
1068.37	SiO_2 or MgO

Tables 4.6, 4.29 and Figures 4.3, 4.4, show the FTIR analysis for raw water hyacinth from South African samples pre and post adsorption of Cu^{2+}. The O-H band in the region of 3300-3200 cm^{-1} is reduced in intensity after adsorption of Cu^{2+} ions, Figure 4.3. The reduction in intensity could be attributed to copper ions being attached to the functional groups in the region 3300-3200 cm^{-1} which reduced the peak height hence the absorption band stretching to a lesser degree (Munene et al.,2020). The adsorption of Cu^{2+} ions caused C=O to shift from 1629.55 to 1624.73 cm^{-1} while the band at 1321.96 cm^{-1} shifted to 1318.11cm^{-1}. The shifting of bands showed that Cu^{2+} ions were adsorbed by the relevant functional groups. The adsorption of copper ions caused the C-O band to reduce in intensity (Munene et al.,2020). The use of FTIR spectroscopy has shown that during adsorption of heavy metal ions by water hyacinth adsorption bands either disappeared or reduced in intensity. The observations are summarized in Table 4.8.

It is observed that during the heavy metal adsorption on the water hyacinth , there was a reduction in the intensity, disappearance or a shift in the functional groups confirming that the functional groups are responsible for the metal ion adsorption (Munene et al.,2020).

Table 4.8: Changes in Spectral Structure when Copper was adsorbed on the SA-Water Hyacinth

Wave number(cm^{-1})		**Functional groups identified in the raw water hyacinth**	**Intensity**	
Before	After		Before	After
3417.24	3430.74	O-H carboxylic acid, alcohol, water, phenol	51.0145	91.6386
1629.55	1624.73	C=O acid, esters	58.6904	90.533
2923.56	2923.56	C-H bending (alkanes) or C-O stretch and O-H deformation (acids	70.1331	95.4712
1321.96	1318.11	C-O Alcohols, Acids, Esters, Ether	72.217	93.7708

4.2 Phase I- Batch Equilibrium Experiments

A comparative analysis using preliminary equilibrium batch tests was carried out for two different sources of water hyacinth (one from Egypt and one from South Africa) without chemical or thermal treatment, in order to assess their percent uptake of Cu^{2+} and Zn^{2+} in an aqueous solution. The conditions of the experiment were:

- Adsorbent dose: 1 g /50 mL
- Volume of Cu^{2+} or Zn^{2+} standard solution: 50 mL
- pH: 6
- Initial Cu^{2+} or Zn^{2+} concentration = 20 mg/L.
- Temperature: room temperature (25 ± 2 °C).

Batch equilibrium experiments were conducted in order to depict the impact of four essential factors on the percentage removal of Cu^{2+} and Zn^{2+} in water hyacinth.

The studied factors are the following:

1) Contact time
2) Sorbent dose
3) pH of the solution
4) Initial Cu^{2+} and Zn^{2+} concentration

The percentage of removal of Cu^{2+} or Zn^{2+} ions adsorbed in the water hyacinth was calculated as described in equation 3.1.

4.2.1 Effect of Contact Time

This experiment was carried out in order to determine the time needed for the adsorption process between water hyacinth and copper or zinc to reach equilibrium. Time intervals studied were 0.5, 1, 5, 10, 20, 30, 45, 60, 45 and 75 min. respectively. The batch experiments were carried out under the following conditions:

- Adsorbent dose: 1 g
- Adsorbent particle size: 2-3 mm
- Volume of Cu^{2+} or Zn^{2+} standard solution: 50 mL
- pH of the synthetic solutions: 6
- Initial Cu^{2+} or Zn^{2+} concentration = 20 mg/L
- Temperature: room temperature ($25 \pm 2^{o}C$)

As shown in Figure 4.5. The adsorption kinetics of copper and zinc via water hyacinth was rapid. Initially ion uptake was rapid for both zinc and copper, this behavior was for both samples the one from Egypt and the one from South Africa. This is due to sufficient and readily available sites for adsorption to occur (Nyamunda et al., 2019). Subsequently, adsorption increased in the second phase but with a much slower rate due to ions diffusing into the interior observed surface (Nyamunda et al., 2019) until an equilibrium was reached. For Cu^{2+}, increasing the contact time also increased the adsorption percentage until there was no change after 60 minutes for both samples from Egypt and South Africa. This indicates that the equilibrium concentration was obtained in one hour as there was no significant change in equilibrium after that time. The maximum removal was

noted at 60 minutes, and the percentage of removal of copper by water hyacinth from Egypt and from South Africa observed was 85.5 % and 99.2 % respectively. This indicates that the adsorption capacity of the dried water hyacinth from South Africa is much more efficient. The reason for this was the canal that water hyacinth collected from Egypt is close to some industrial sites so the plant is already adsorbed by heavy metals and that was observed when XRF (X-Ray Fluorescence) analysis was done, so the active site is not totally free, also according to XRF analysis it was found that the water hyacinth from South Africa has more oxides than that from Egypt, this oxides enhance the adsorption process, so that is the reason that the water hyacinth from south Africa has higher percentage of removal than that from Egypt.

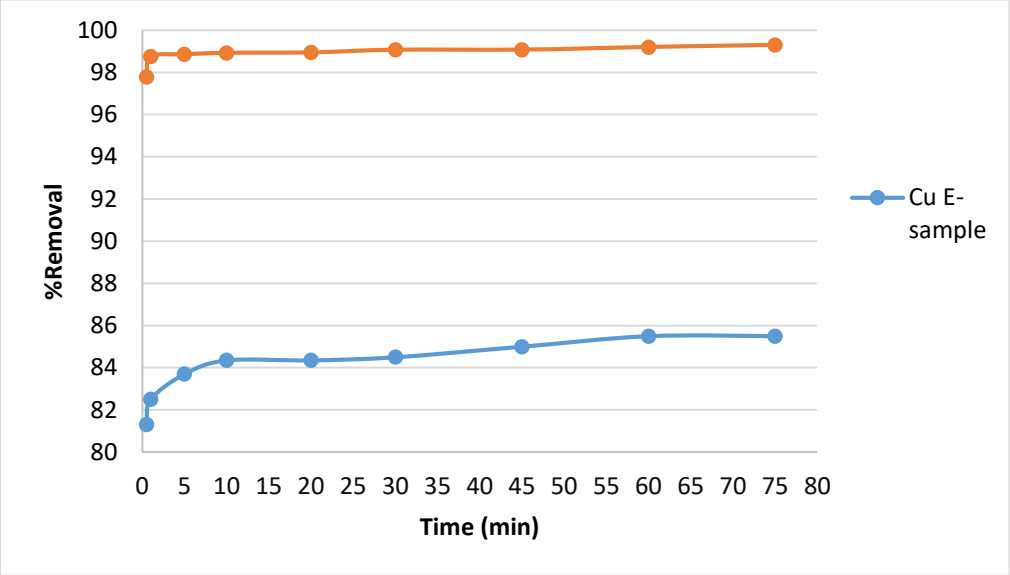


Figure 4.5: Impact of contact time on % removal of Cu^{2+} with initial concentration of 20 mg/L by water hyacinth from Egypt and South Africa (1 g) at pH 6

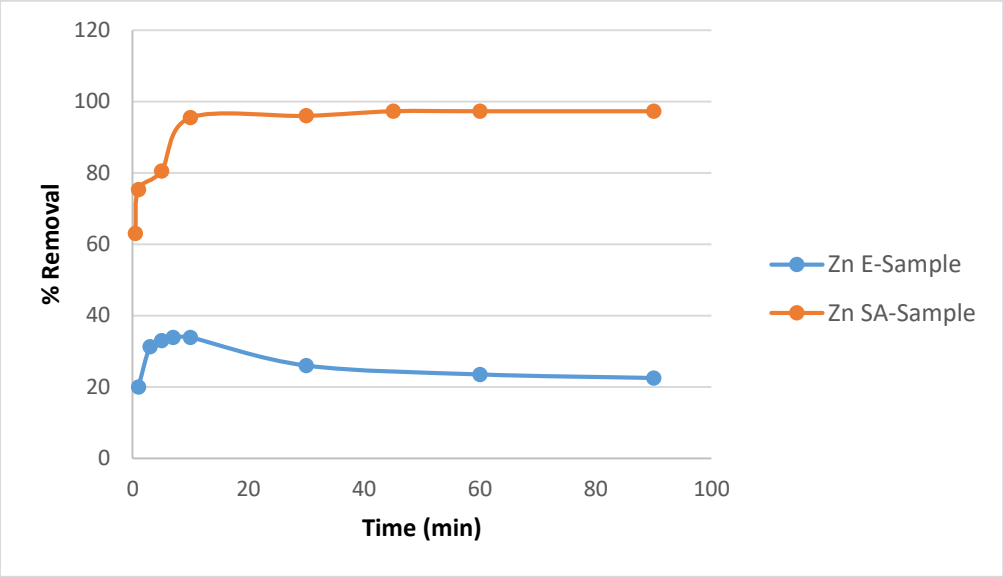


Figure 4.6: Impact of contact time on % removal of Zn^{2+} with initial concentration of 20 mg/L by water hyacinth from Egypt and South Africa (1 g) at pH 6

In the case of Zn^{2+}, increasing the contact time from 0.5 to 10 minutes led to a rapid uptake of the heavy metal until the percentage removal reached 33.9%. Beyond this point, it was observed that the adsorbed solute tends to desorb back into solution, this behavior existed only in case of water hyacinth from Egypt, desorption happens when a molecule gains energy to overcome the activation barrier of the bonding energy that keeps it in the surface, this energy usually gained when temperature increase .These results agree with previous studies (Obi, 2015, Rani et al., 2016). For the adsorption of zinc by the water hyacinth from South Africa it was observed that during the first few minutes the rate was very fast; 95.5% removal was achieved in the first 10 min, afterwards the rate of slowed down until it reached equilibrium This performance could be due to the fact that rapid mass transfer on the outer surface of the adsorbent has taken place first, afterwards a slower internal diffusion process has started to occur (Wong et al., 2003a). The % removal was found to slightly increase up to 97.3% after 60 minutes; however, the difference is considered insignificant, this was shown in Figure 4.6.

4.2.2 Effect of Adsorbent Dose

A batch study was conducted for a range of doses of water hyacinth of particle size 2-3 mm, in order to assess the impact of the adsorbent dose on copper and zinc uptake. The doses studied for copper were; 0.25, 0.5, 0.75, 1 and 1.5 g/50 mL solution, and for zinc were; 0.25, 0.5, 0.75, 1, 1.5 and 3 g/ 50 mL solution. The conditions of the experiment were the following:

- Optimum Contact Time: 75 min for copper and 90 min zinc for both water hyacinth samples
- pH of the Cu^{2+} or Zn^{2+} synthetic solution: 6
- Adsorbent particle size: 2-3 mm
- Volume of lead standard solution: 50 mL
- Initial $Cu^{2+}$and Zn^{2+} concentration = 20 mg/L
- Temperature: room temperature (25 ± 2 ^{o}C)

The percentage of removal of both zinc and copper increased with increasing dose of adsorbent (Cherono et al., 2021). The rate of adsorption depends on the driving forces per unit area and in this case, since the initial concentration was constant, increasing the adsorbent dosage led to an increase in the surface area of the adsorbent available and thus increased uptake of the heavy metal was observed. This explanation agrees with previous studies on many other adsorbents (Ahmed et al., 2016, Al Saadi et al., 2016, Jami et al., 2016, Murithi et al., 2014, Sivakumar, 2015, Vandenbruwane et al., 2007).

The percentage of Cu^{2+} removed by water hyacinth from Egypt and South Africa reached 85.5% and 99.3% respectively at optimum dose 1.5 g/50 mL solutions. For a 1 g/50 mL and 1.5 g/ 50 mL there was no significant change in the % removal of Cu^{2+} using water hyacinth from South Africa 99.2%, while the percentage of Cu^{2+} removed by water hyacinth from Egypt was the same 85.5% this could be due to a state of equilibrium between the bio-sorbent and the heavy metal preventing the bio-sorbent from further bio-sorption (Kardam et al., 2014), as shown in Figure 4.7. Since the difference in the percent removal compared to the 1.5 g/50 mL is insignificant, it is preferred to achieve the best results using the least quantity of bio-sorbent in order to reduce the quantity of water hyacinth needed; consequently, reduce the cost of transportation and preparation of the material.

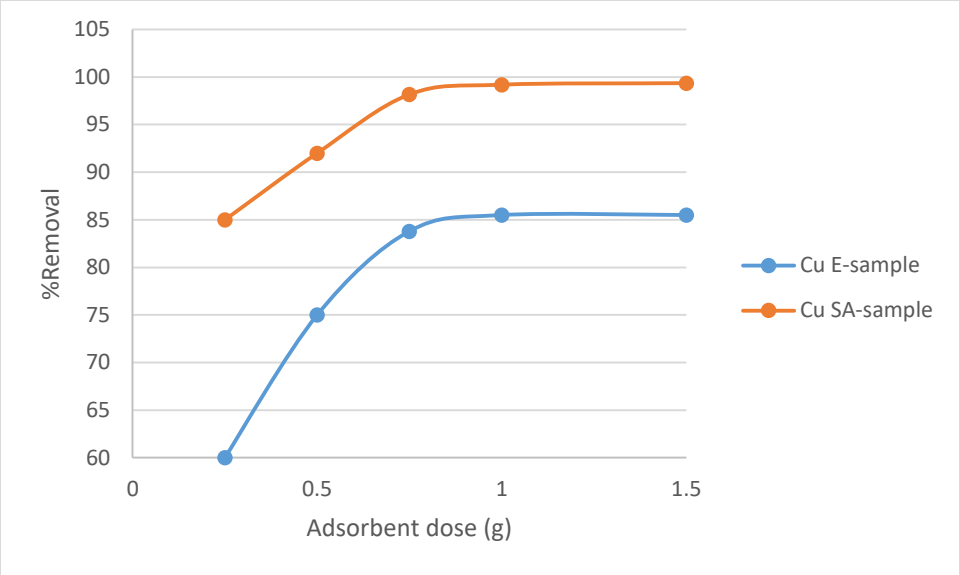


Figure 4.7: Impact of water hyacinth dose on the uptake of Cu^{2+}

Figure 4.8 shows the uptake of Zn^{2+} using water hyacinth from Egypt and from South Africa. The percentage of Zn^{2+} removed by water hyacinth from Egypt and South Africa reached 45% and 99.5% respectively dose at optimum dose 3g/50 mL solutions, respectively. This confirm that the South African water hyacinth is much more efficient than the one from Egypt for the same reason discussed in section 4.2.1.

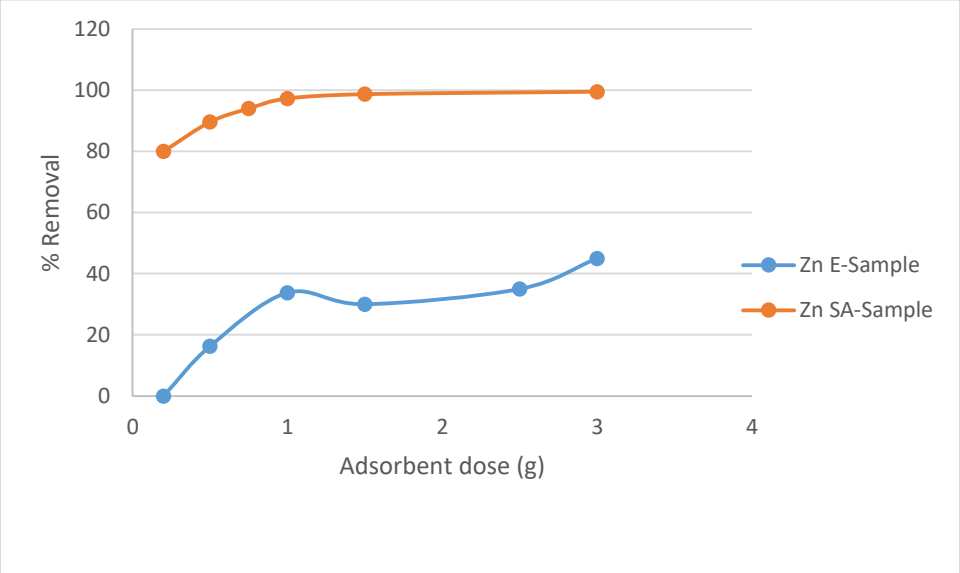


Figure 4.8: Impact of water hyacinth dose on the uptake of Zn^{2+}

4.2.3 Effect of pH on the Removal of Cu^{2+} and Zn^{2+}

Batch equilibrium experiments were carried out in order to assess the optimum pH of the solution. The conditions of the experiment were the following:

- Adsorbent dose: 1 g/L
- Adsorbent particle size: 2-3 mm
- Contact time: 60 min.
- Volume of Cu^{2+} or Zn^{2+} standard solutions: 50 mL
- pH of the synthetic solution: 2.5, 3, 5.5, 6.5 and 10
- Initial Cu^{2+} or Zn^{2+} concentrations = 20 mg/L.
- Temperature: room temperature (25 ± 2 ^{o}C)

The amount of metal uptake by adsorbents was found to be highly affected by varying the pH of a solution due to the consequent change in the distribution of the surface charge of the adsorbent (Ouyang et al., 2019, Rao et al., 2013), as well as its degree of ionization and its functional groups (Rao et al., 2013). The conducted studied show that, the lower the pH, the more H^{+} ions present competing with the metal ions for adsorption sites, thus reducing their adsorption. On the other hand, the higher the pH, the less the H^{+} ions competing with metal ions for adsorption sites (Pham et al., 2021). It was observed in Figures 4.9 and 4.10 that the percentage of removal of both copper and zinc was low as pH decrease and it starts to increase gradually as pH increase followed by a gradual decrease in percentage of removal. This decrease at higher pH values can be attributed to a significant reduction in the concentration of positive charges on the surface of the adsorbent by the deprotonation of acid groups and the competitiveness between heavy metal ions and OH^{-} ions for sites on the adsorbent.

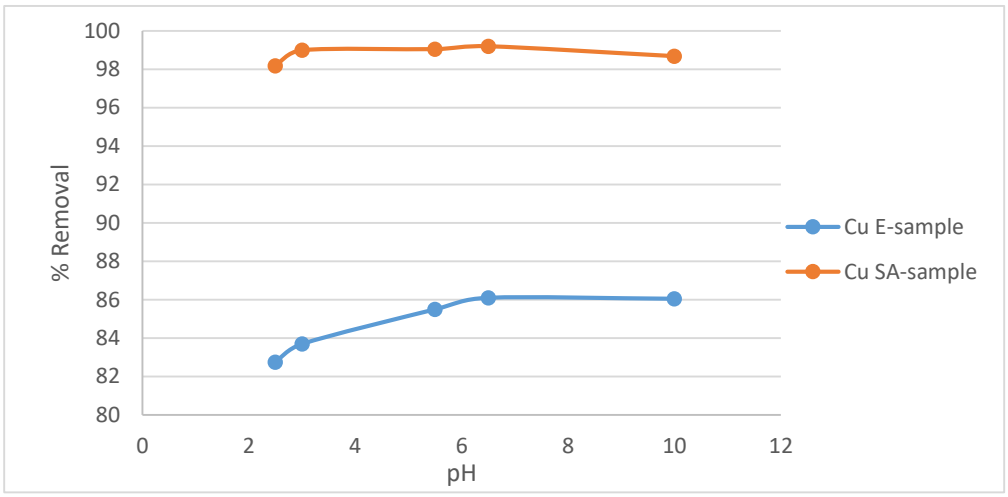


Figure 4.9: Impact of pH on the percentage of removal of water hyacinth for the removal of Cu^{2+}

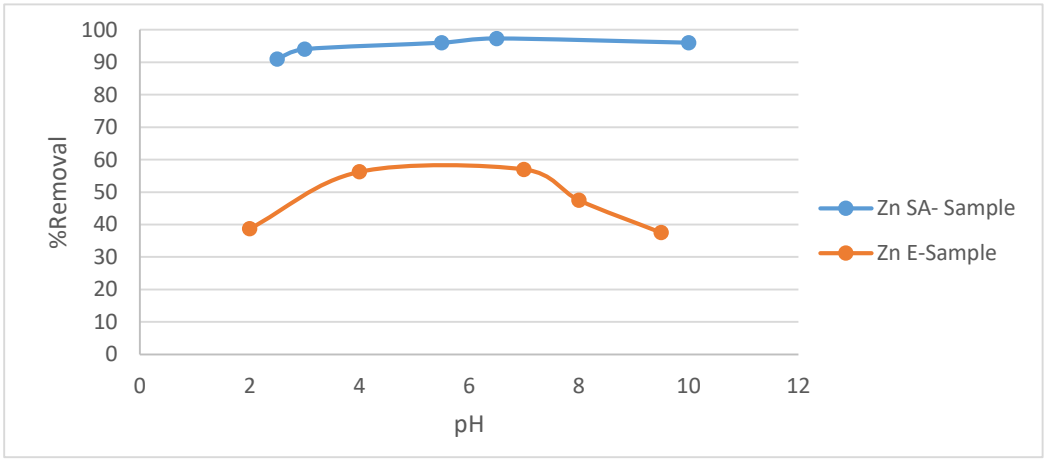


Figure 4.10: Impact of pH on the percentage of removal of water hyacinth for the removal of Zn^{2+}

4.2.4 Effect of Initial Cu^{2+} and Zn^{2+} Concentrations

The impact of the initial metal ions concentration on the adsorption of copper and zinc by water hyacinth has been studied. The experiments were all conducted at pH of 6 since the highest % removal was observed at this pH. The conditions of the experiment were the following:

- pH of the Cu^{2+} and Zn^{2+} synthetic solution: 6 (this was the optimum pH obtained from the pH experiments)
- Bio-sorbent dose: 1 g/L
- Adsorbent particle size: 2-3 mm

- Contact time: 60 min.
- Volume of Cu^{2+} and Zn^{2+} standard solutions: 50 mL
- Temperature: room temperature (25 ± 2 ^{o}C)
- Initial Cu^{2+} concentration 20, 30, 50, 100, 150, 250 and 400 mg/l, and 10, 20, 30, 40, 50, 100, 150, 250 and 400 mg/L for Zn^{2+}.

It is obvious from Figures 4.11 and 4.12 that the % removal relatively decreased with the continuously increasing Cu^{2+} or Zn^{2+} concentrations. To illustrate, at a high concentration of copper or zinc, such as 400 mg/L the metal uptake was low compared to lower concentrations of both heavy metal ions. This is attributed to the competition between the increasing metal ions on the available active sites on the surface area of the adsorbent. Upon the increase of metal ions, while the dose of adsorbent is kept constant, the available active sites get rapidly saturated (Rashed et al., 2020, Aly et al., 2014). Increasing the initial Copper metal ion concentration from 20 mg/L to 400 mg/L results in a decrease in the removal ratio of 29.2% in case of Egypt sample while decrease in removal ratio of 27.7% in case of South Africa sample. For Zinc the decrease in removal ratio was 71.8% and 36.3% for Egypt and South Africa samples, respectively.

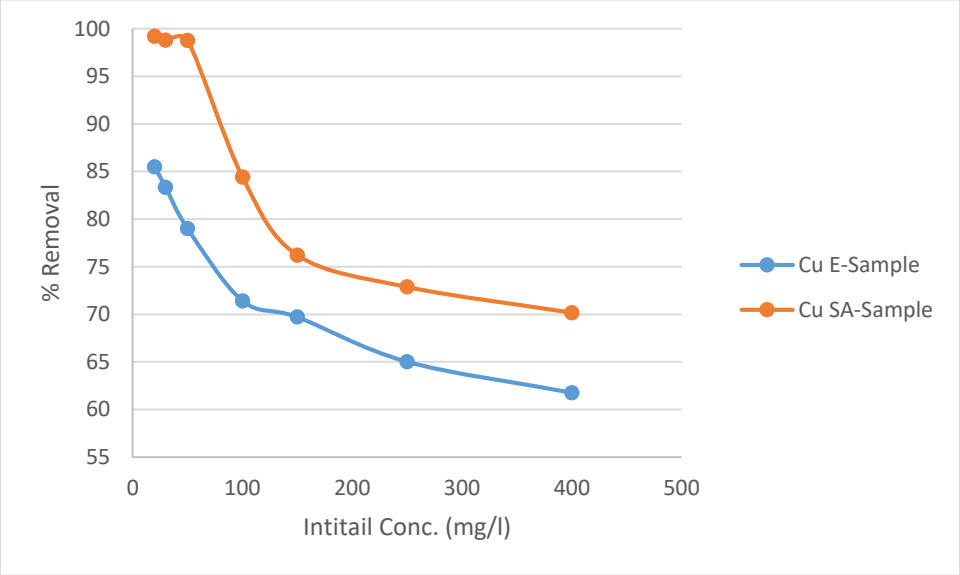


Figure 4.11: Impact of initial Cu^{2+} concentration on % removal of Cu^{2+} by water hyacinth

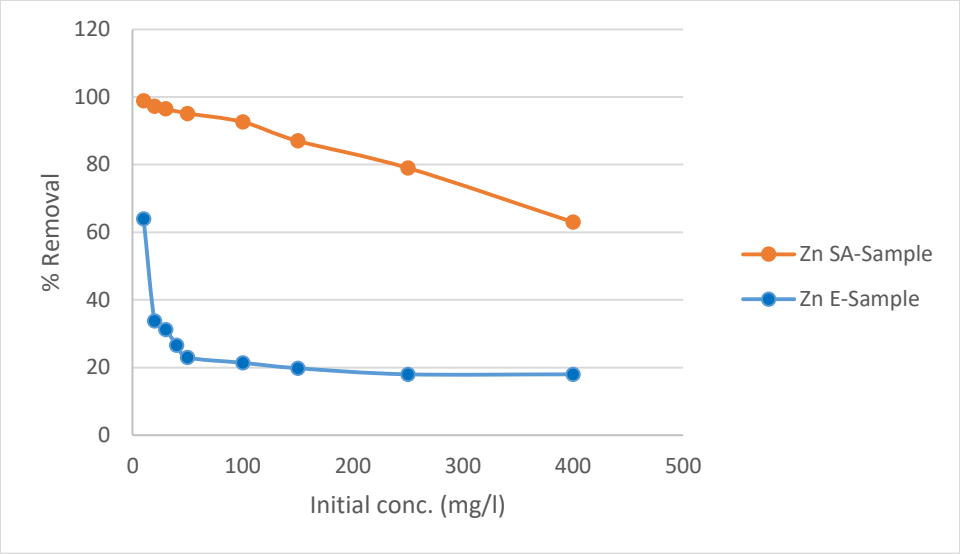


Figure 4.12: Impact of initial Zn^{2+} concentration on % removal of Zn^{2+} by water hyacinth

4.3 Adsorption Isotherm Models

The batch equilibrium experimental data of water hyacinth were fitted and analysed via the most two widely used models in the literature in the following sub-sections. The batch equilibrium data analysed by Langmuir isotherm and Freundlich isotherm was acquired using the water hyacinth dose; 1g/50 mL of a particle size 2-3 mm, over a wide range of initial Cu^{2+} and Zn^{2+} concentrations; 10-400 mg/L.

4.3.1 Langmuir Isotherm Model

Langmuir isotherm model assumes monolayer sorption via physical forces (Sarma et al., 2015). The Langmuir equation was presented by the equation in section 3.7.1.

The parameters of Langmuir isotherm are presented in Tables 4.9 and 4.10 for water hyacinth Egypt sample and South Africa sample respectively. Based on Langmuir isotherm, the maximum predicted adsorption capacities of Cu^{2+} and Zn^{2+} using raw water hyacinth Egypt sample are 17.7 and 11.88 mg/g respectively, while when the South African raw water hyacinth was used the adsorption capacities of Cu^{2+} and Zn^{2+} are 20.24 and 13.3 respectively. As shown in Figures 4.13, 4.14, 4.15 and 4.16, the batch equilibrium data has been perfectly fitted in the Langmuir model. The correlation coefficient (R^2) of Cu^{2+} and Zn^{2+} adsorbed by Egypt water hyacinth was found to be 0.8484 and 0.8203, respectively as listed in Table 4.9. The linearity of the plot suggests the

creation of a homogenous monolayer of metal ions on the outer surface of the sorbent (Kardam et al., 2014).

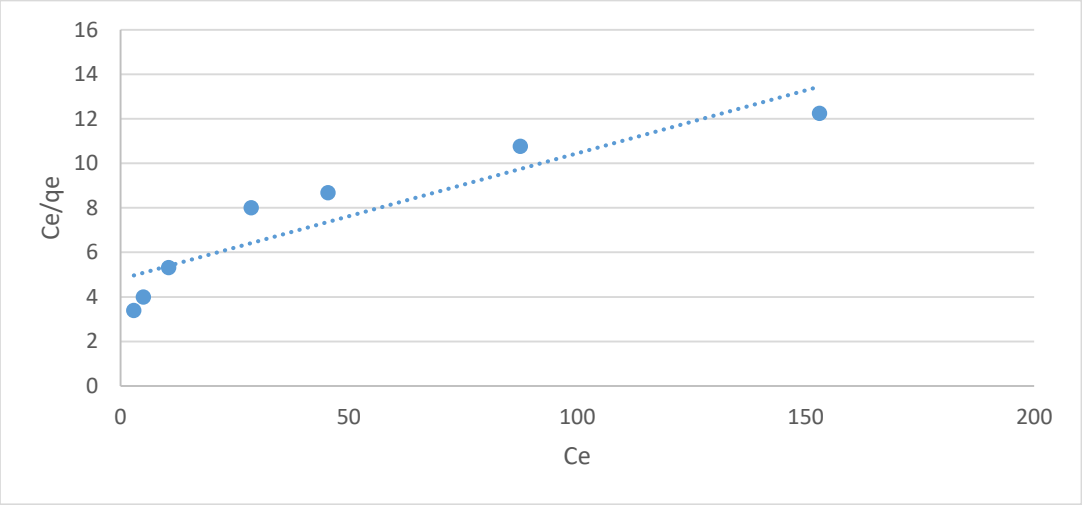


Figure 4.13: Langmuir isotherm for adsorption of Cu^{2+} using Egyptian water hyacinth sample

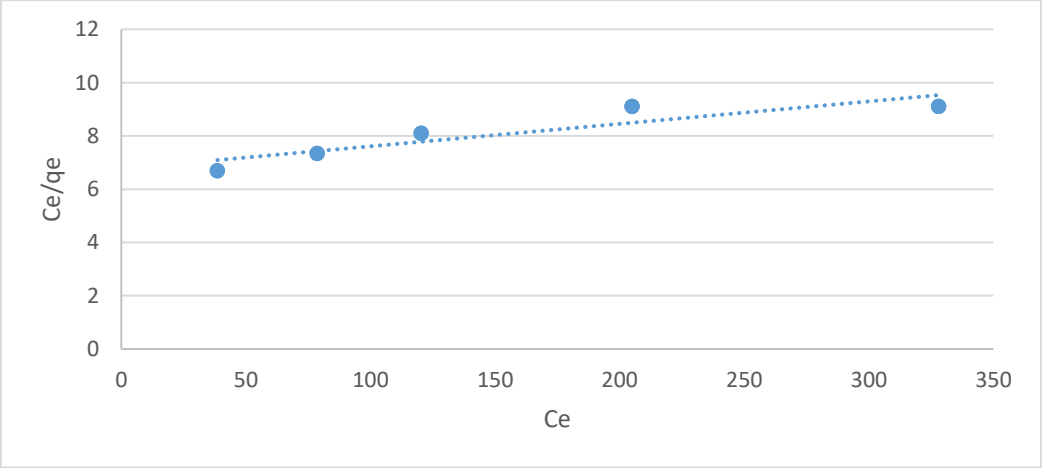


Figure 4.14: Langmuir isotherm for adsorption of Zn^{2+} using Egyptian water hyacinth sample

Table 4.9: Parameters of Langmuir Isotherm for Adsorption of Copper and Zinc using Egyptian Water Hyacinth

Heavy metal	**q_{max} (mg/g)**	**b (l/g)**	**R^2**
Cu^{2+}	17.669	0.0118	0.8484
Zn^{2+}	11.876	0.0124	0.8203

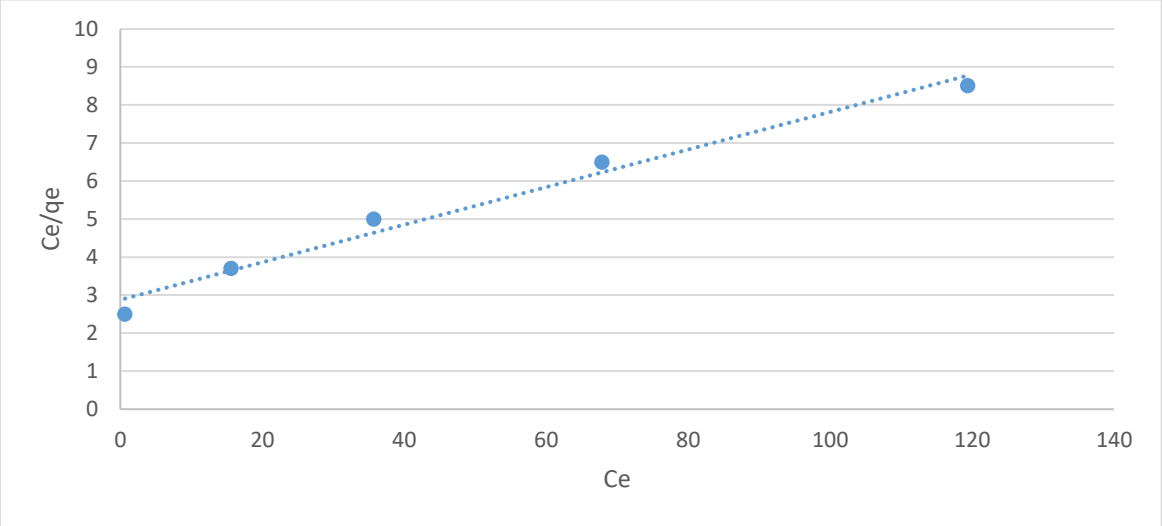


Figure 4.15: Langmuir isotherm for adsorption of Cu^{2+} using water hyacinth SA-sample

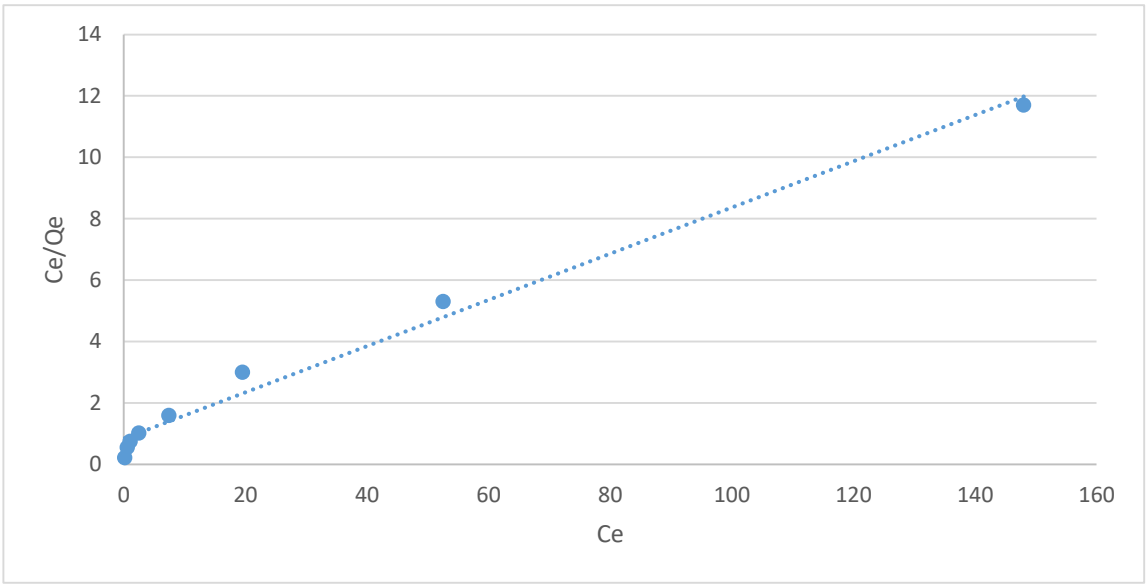


Figure 4.16: Langmuir isotherm for adsorption of Zn^{2+} using water hyacinth SA-sample

Table 4.10: Parameters of Langmuir Isotherm for Adsorption of Copper and Zinc using SA- Water Hyacinth Sample

Heavy metal	**q_{max} (mg/g)**	**b (l/g)**	**R^2**
Cu^{+2}	20.24	0.017	0.9801
Zn^{+2}	13.3	0.09	0.9869

Table 4.11 presents the q_{max} achieved in several research studies using water hyacinth. The maximum adsorption capacity achieved by raw water hyacinth in the current research is considerably higher than some treated water hyacinth the results reported in the literature.

Table 4.11: Maximum Adsorption Capacity of Water Hyacinth for Cu^{2+} and Zn^{2+} in Various Studies

Bio-sorbent	Heavy metal	q(mg/g)	Reference
Raw water hyacinth (Egypt sample)	Cu^{2+} Zn^{2+}	17.669 11.876	Current study
Raw water hyacinth (South Africa sample)	Cu^{2+} Zn^{2+}	20.24 13.3	Current study
Magnetic Biochar Derived from Water Hyacinth	Cu^{2+}	3.53	(Nyamunda B., et al. 2019)
	Zn^{2+}	9.42	
Modified water hyacinth (*Eichhornia crassipes*) fibers	Zn^{2+}	18.9	(Neris et al. 2019)
Water hyacinth roots (dried in 70°C oven) ,0.25mm	Pb^{2+}	49.7	(Jahangiri , et al. 2021)

4.3.2 Freundlich Isotherm Model

The basic assumption of Freundlich model is the heterogeneous surface energy of adsorption (Grassi et al., 2012). The non-linear form of the model were described before in section 3.7.2.

The constants in Freundlich isotherm can be calculated from the plot of log q_e versus log C_e. (Metcalf & Eddy 2003). Figures 4.17 and 4.18 show Freundlich isotherm plot for C^{2+} and Zn^{2+} adsorption by water hyacinth from Egypt. The isotherm parameters of the model are presented in

Table 4.12. The Freundlich isotherm model is fitted best with experimental data of the adsorption studies as it poses high correlation coefficient (R^2) of 0.98 and 0.99 for Zn^{2+} and Cu^{2+}, respectively.

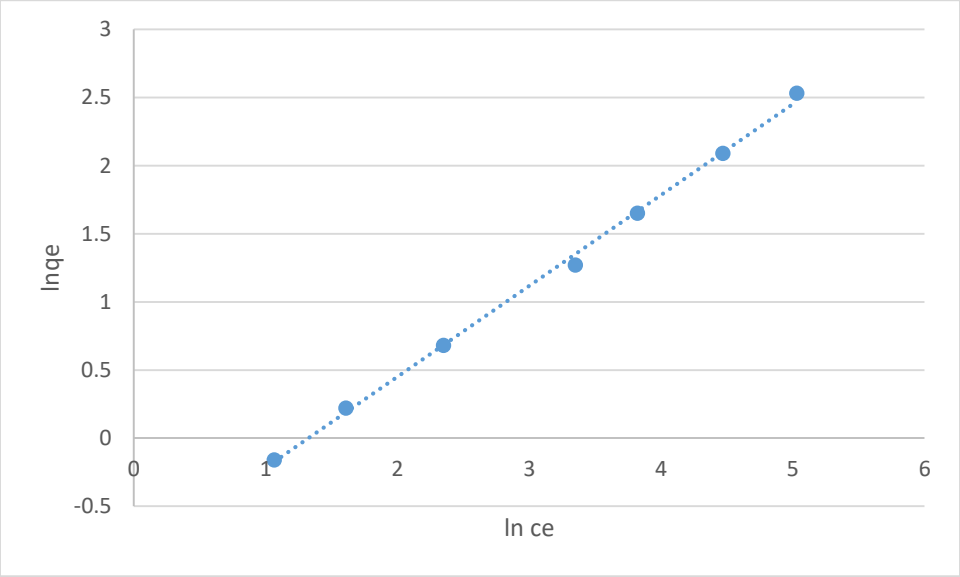


Figure 4.17: Freundlich isotherm for adsorption of Cu^{2+} using Egyptian water hyacinth sample

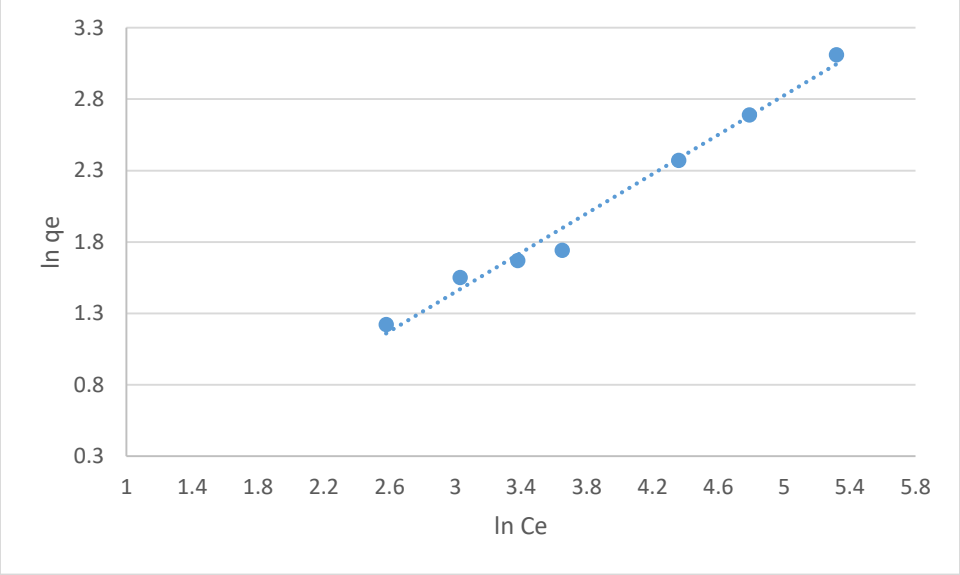


Figure 4.18: Freundlich isotherm for adsorption of Zn^{2+} using Egyptian water hyacinth sample

Table 4.12: Parameters of Freundlich Isotherm for Adsorption of Copper and Zinc using Egyptian Water Hyacinth Sample

Heavy metal	K_f (mg/g)	n	R^2
Cu^{2+}	2.42	1.5	0.99
Zn^{2+}	2.13	1.37	0.98

Figures 4.19 and 4.20 show Freundlich isotherm plot for C^{2+} and Zn^{2+} adsorbed by water hyacinth from South Africa, respectively. The isotherm parameters of the model are presented in Table 4.13. The Freundlich isotherm model is fitted well with experimental data of the adsorption studies as it poses high correlation coefficient (R^2) of 0.98 and 0.94 for Zn^{2+} and Cu^{2+}, respectively.

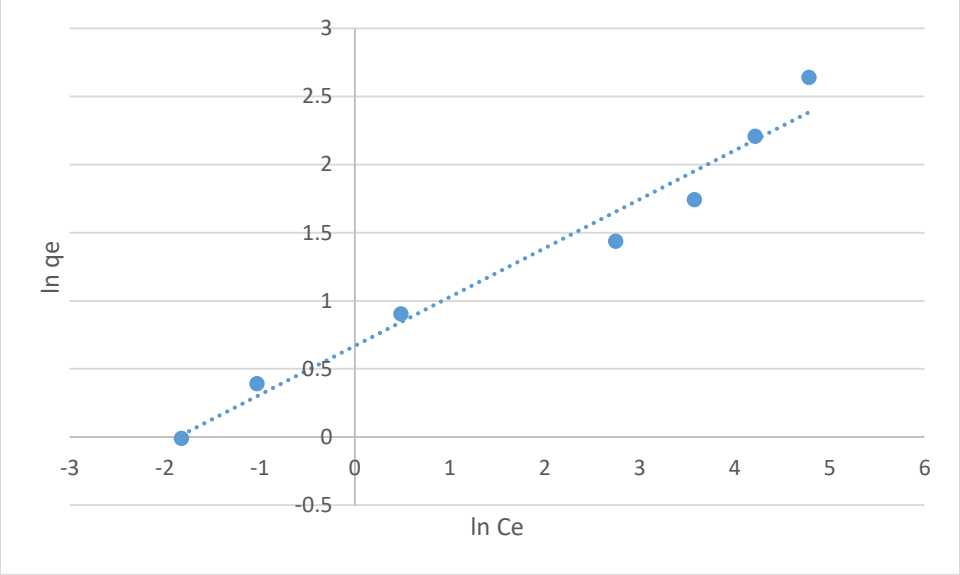


Figure 4.19: Freundlich isotherm for adsorption of Cu^{2+} using water hyacinth SA-sample

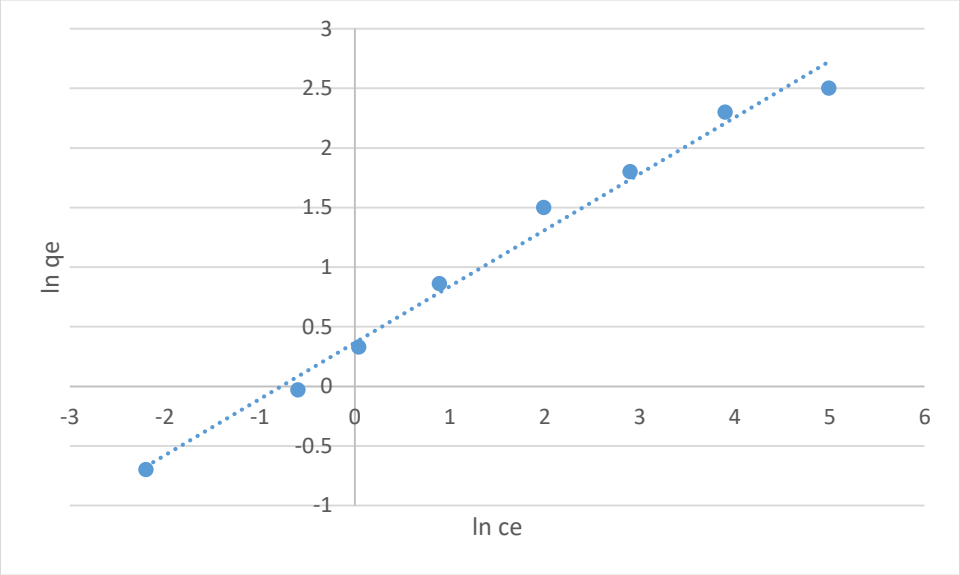


Figure 4.20: Freundlich isotherm for adsorption of Zn^{2+} using water hyacinth SA-sample

Table 4.13: Parameters of Freundlich Isotherm for Adsorption of Copper and Zinc using SA-Water Hyacinth Sample

Heavy metal	K_f (mg/g)	n	R^2
Cu^{2+}	2.11	2.86	0.94
Zn^{2+}	1.44	2.12	0.98

4.4 Kinetic Model

The plotting of log (q_e-q_t) versus time deviated considerably from the theoretical data after short a period as shown in Figures 4.21, 4.23, 4.25 and 4.26. The plots and intercepts of curves were used to determine the first order constant K_{pf}, capacity q_e and the corresponding coefficients for the determination of (R^2_1) values.

The pseudo-second-order kinetic model suggests that the values of K_{ps} and the corresponding coefficients for the determination of (R^2_2) values were determined from the slopes of the plots Figures 4.22, 4.24, 4.27 and 4.28. Both pseudo-first-order and pseudo-second-order kinetic models were applied over variable time periods of 0.5 to 60 min of adsorption. A solution temperature of (25±2◦C) and a pH value of 6 were used with an adsorbent dose of water hyacinth of 1 g for both Cu^{2+} and Zn^{2+}.

Nevertheless, extremely high R^2 values (close to unity) were observed for the pseudo-second-order model for both Cu^{2+} and Zn^{2+} adsorbed by both water hyacinths from Egypt and South Africa, results are summarized in Tables 4.14 and 4.15 for water hyacinth from Egypt and South Africa respectively . A similar phenomenon was observed in heavy metal ions onto different adsorbents (Jeyaseelan and Gupta, 2016, Farooq et al., 2010). Therefore it was concluded that the kinetics of adsorption follows a second order kinetic mechanism.

The pseudo-second-order kinetic model is based on solid-phase adsorption of divalent metals, and the good fit of this model supports the assumption that chemisorption corresponds to the rate-controlling step for the adsorption of Cu^{2+} and Zn^{2+} on both sources of the water hyacinth (Amin et al., 2017).

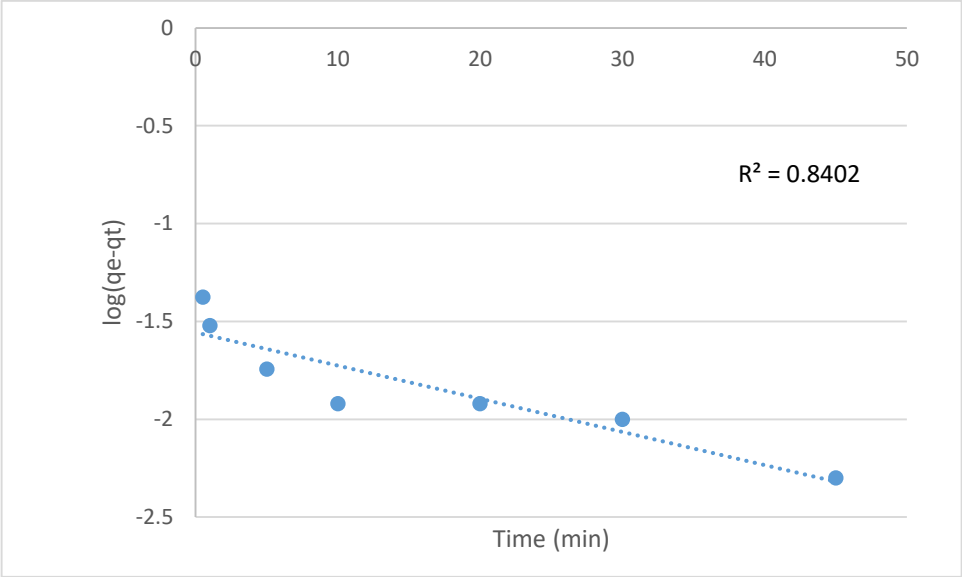


Figure 4.21: Pseudo first order adsorption kinetics of Cu^{2+} adsorbed on Egyptian water hyacinth, initial concentration 20 mg/L, wt. of adsorbent 1g, T=25±2°C

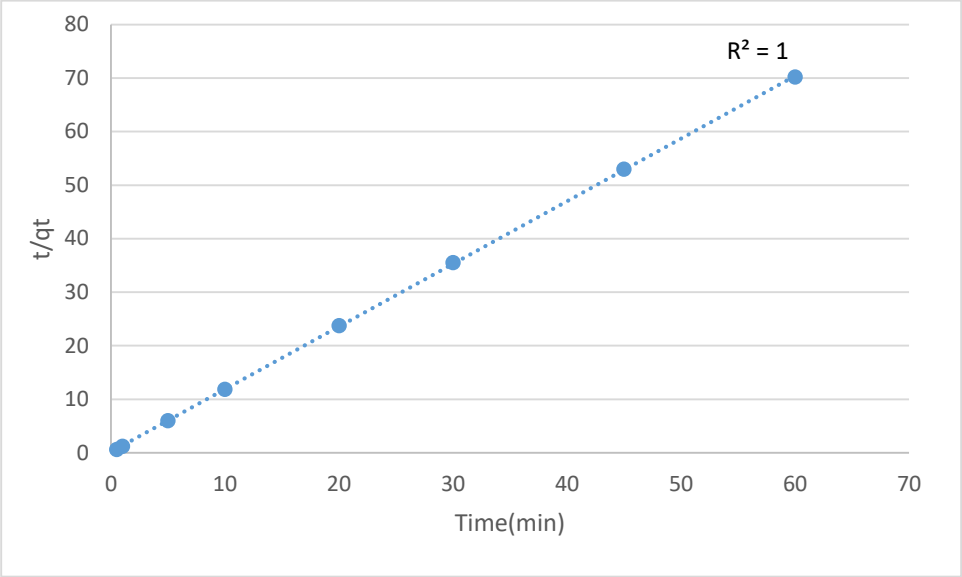


Figure 4.22: Pseudo second order adsorption kinetics Cu^{2+} adsorbed on Egyptian water hyacinth, initial concentration 20 mg/L, wt. of adsorbent 1g, T= 25±2°C

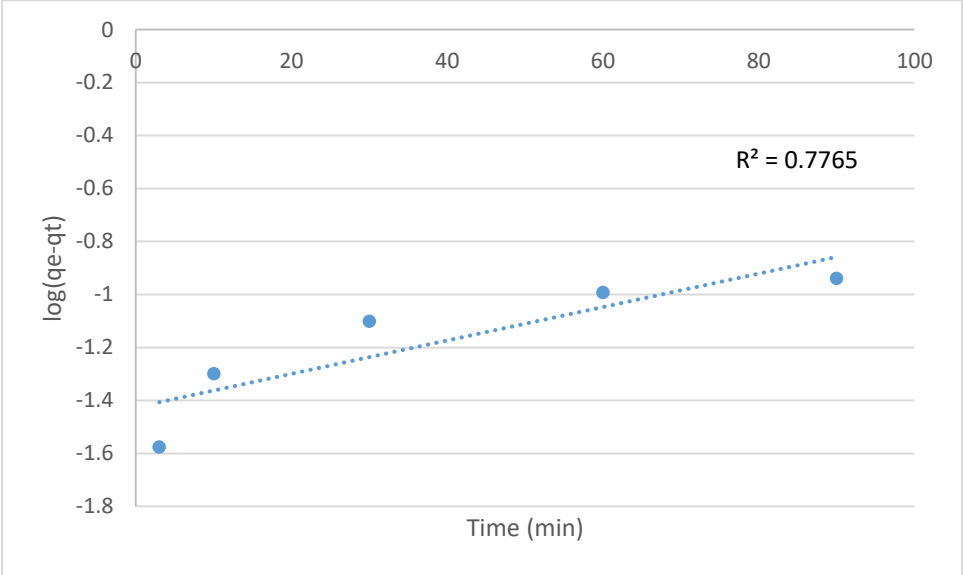


Figure 4.23: Pseudo first order adsorption kinetics of Zn^{2+} adsorbed on Egyptian water hyacinth, initial concentration 20 mg/L, wt. of adsorbent 1g, T=25±2°C

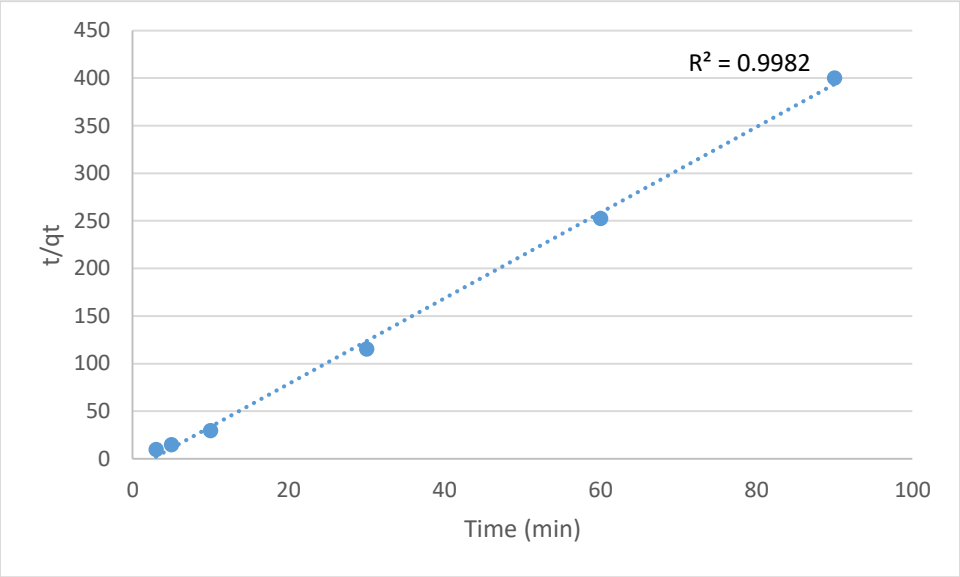


Figure 4.24: Pseudo second order adsorption kinetics of Zn^{2+} adsorbed on Egyptian water hyacinth, initial concentration 20 mg/L, wt. of adsorbent 1g, T=25±2°C

Table 4.14: Adsorption Kinetics Parameters of Zn^{2+} and Cu^{2+} Ions on Egyptian Water Hyacinth Sample

Metal Ions	**Pseudo first order kinetic model**			**Pseudo second order kinetic model**		
	$K_{pf.}$ (g/mg)	**q_e**	**R_1^2**	**K_{ps} (g/mg)**	**q_e(g/mg.min)**	**R_2^2**
Zn^{2+}	-0.014	0.037	0.78	1.76	0.22	0.99
Cu^{2+}	0.033	0.23	0.84	9.34	0.85	1

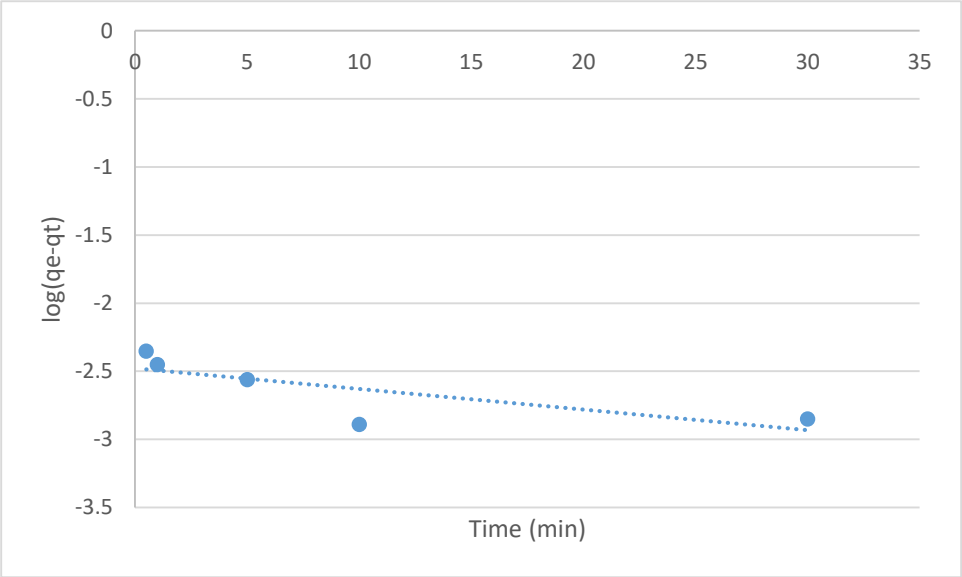


Figure 4.25: Pseudo first order adsorption kinetics of Cu^{2+} adsorbed on SA-water hyacinth, initial concentration 20 mg/L, wt. of adsorbent 1g, T=25±2°C

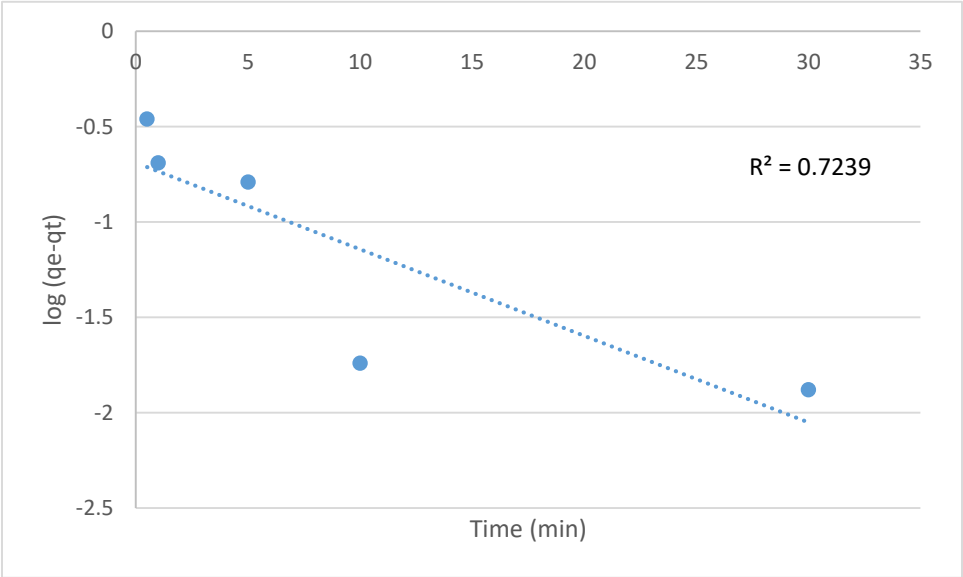


Figure 4.26: Pseudo first order adsorption kinetics of Zn^{2+} adsorbed on SA-water hyacinth, initial concentration 20 mg/L, wt. of adsorbent 1g, T=25±2°C

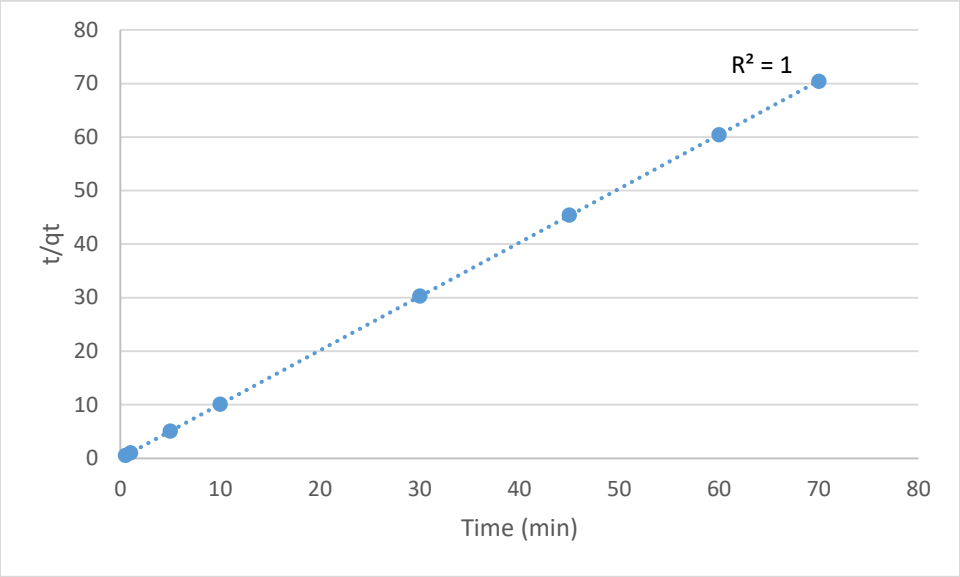


Figure 4.27: Pseudo second order adsorption kinetics of Cu $^{2+}$ adsorbed on SA-water hyacinth, initial concentration 20 mg/L, wt. of adsorbent 1g, T=25±2°C

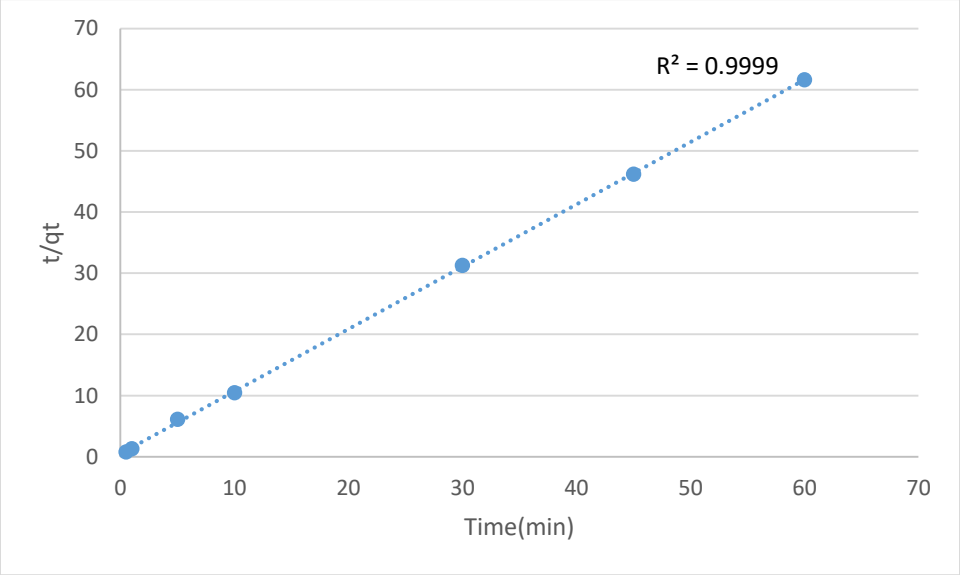


Figure 4.28: Pseudo second order adsorption kinetics of Zn^{2+} adsorbed on SA-water hyacinth, initial concentration 20 mg/L, wt. of adsorbent 1g, T=25±2°C

Table 4.15: Adsorption Kinetics Parameters of Zn^{2+} and Cu^{2+} Ions on Dried Water Hyacinth SA-Sample

Metal Ions	Pseudo first order kinetic model			Pseudo second order kinetic model		
	$K_{pf.}$ (g/mg)	q_e	R_1^2	K_{ps} (g/mg)	q_e(g/mg.min)	R_2^2
Zn^{2+}	0.1	0.2	0.72	2.18	0.98	0.99
Cu^{2+}	0.03	0.003	0.58	27.5	0.99	1

4.5 Phase II- Design of Experimental Combinations

Using the BBD has required performing relatively few combinations of variables while covering wide range of their levels. It also has a great influence in determining and optimising the response function. In this study, adsorption process was carried out for the removal of zinc and copper from aqueous solution using water hyacinth as an adsorbent. All adsorption experiments for the heavy metal ions removal were designed according to RSM using BBD with the aid of a Design Expert® software and the percentage removal of zinc and percentage removal of copper were selected as the objective functions for optimization. Since it is often necessary to investigate several different variables effects on the response of interest, contact time, adsorbent dose, pH and initial metal ion concentration were selected as process variables.

Experimental design and results layout for BBD for the statistical combination of independent variables with the experimental responses are presented in Tables 4.16 and 4.17 for copper and zinc adsorbed by water hyacinth from Egypt respectively, and Tables 4.18 and 4.19 for copper and zinc adsorbed by water hyacinth from South Africa, respectively.

Table 4.16: Experimental Design and Results Layout for Box–Behnken Design Cu^{2+} Adsorbed by Egyptian Water Hyacinth

Run	X_1 : Contact time (min)	X_2 : Adsorbent Dose (g)	X_3: pH	X_4: Initial concentration (mg/L)	Y_1:% of removal of Cu
1	37.75	0.87	6.25	210	67.3
2	37.75	0.87	6.25	210	67.3
3	37.75	1.50	2.50	210	73
4	37.75	0.87	10	400	60
5	75	0.87	6.25	400	60.5
6	37.75	1.50	6.25	400	65
7	0.50	0.87	6.25	400	49
8	0.50	0.87	10	210	63
9	37.75	0.87	6.25	210	67.3
10	37.75	0.87	2.50	20	83.7
11	75	1.50	6.25	210	74
12	0.50	1.50	6.25	210	64
13	37.75	0.87	2.5	400	57
14	37.75	0.25	2.5	210	9
15	37.75	0.25	6.25	400	3
16	37.75	0.87	6.25	210	67.3
17	37.75	0.25	6.25	20	59
18	37.75	0.87	10	20	84.5
19	37.75	1.50	6.25	20	85.2
20	37.75	0.87	6.25	210	67.3
21	75	0.87	2.50	210	58
22	0.50	0.87	6.25	20	81
23	0.50	0.25	6.25	210	30
24	75	0.87	10	210	67
25	75	0.87	6.25	20	85.5
26	37.75	1.50	10	210	69
27	37.75	0.25	10	210	13
28	75	0.25	6.25	210	14
29	0.50	0.87	2.50	210	44

Table 4.17: Experimental Design and Results Layout for Box–Behnken Design Zn^{2+} Adsorbed by Egyptian Water Hyacinth

Run	X_1 : Contact time (min)	X_2 : Adsorbent Dose (g)	X_3: pH	X_4: Initial concentration (mg/L)	Y_1: % of removal of Zn
1	90	1.6	6	10	46
2	47.5	1.6	6	205	22
3	47.5	1.6	6	205	22
4	0.5	1.6	6	400	12
5	90	1.6	2	205	26
6	47.5	1.6	10	400	18
7	47.5	0.2	2	205	2
8	47.5	0.2	10	205	2
9	47.5	1.6	2	400	17
10	0.5	1.6	6	10	23
11	47.5	0.2	6	400	1
12	47.5	0.2	6	10	3
13	47.5	3	10	205	28
14	47.5	1.6	6	205	22
15	90	3	6	205	27
16	90	1.6	6	400	17.5
17	90	0.2	6	205	2
18	47.5	1.6	2	10	58
19	47.5	1.6	10	10	58
20	90	1.6	10	205	26
21	0.5	1.6	10	205	19
22	47.5	3	6	400	24
23	0.5	0.2	6	205	2
24	47.5	1.6	6	205	22
25	47.5	1.6	6	205	22
26	0.5	3	6	205	31
27	47.5	3	6	10	61
28	0.5	1.6	2	205	22
29	47.5	3	2	205	30

Table 4.18: Experimental Design and Results Layout for Box–Behnken Design Cu^{2+} Adsorbed by SA- Water Hyacinth

Run	X_1 : Contact time (min)	X_2: Adsorbent Dose (g)	X_3: pH	X_4: Initial concentration (mg/L)	Y_1:% of removal of Cu
1	37.75	1.50	6.25	20	99.1
2	37.75	0.87	10	400	68
3	37.75	0.87	10	20	98
4	37.75	0.87	6.25	210	73
5	37.75	0.87	6.25	210	73
6	37.75	0.87	2.5	20	97.8
7	37.75	0.25	6.25	20	97.7
8	37.75	0.87	6.25	210	73
9	75	0.87	6.25	400	69.5
10	37.75	1.50	10	210	72.5
11	37.75	1.50	6.25	400	70
12	0.50	1.50	6.25	210	71
13	0.50	0.87	10	210	69
14	37.75	0.25	2.50	210	67
15	75	0.87	6.25	20	98.5
16	0.50	0.87	6.25	20	97.5
17	37.75	0.87	6.25	210	73
18	0.5	0.87	2.5	210	69
19	75	1.50	6.25	210	67
20	37.75	0.87	6.25	210	73
21	0.50	0.25	6.25	210	65
22	37.75	1.5	2.5	210	71
23	75	0.25	6.25	210	68
24	37.75	0.87	2.5	400	66
25	37.75	0.25	6.25	400	59
26	75	0.87	10	210	71.5
27	0.50	0.87	6.25	400	62
28	37.75	0.25	10	210	68.5
29	75	0.87	2.5	210	72.51

Table 4.19: Experimental Design and Results Layout for Box–Behnken Design Zn^{2+} Adsorbed by SA- Water Hyacinth

Run	X_1 : Contact time (min)	X_2: Adsorbent Dose (g)	X_3: pH	X_4: Initial concentration (mg/L)	Y_1 : % of removal of Zn
1	0.5	0.2	2	400	2
2	60	3	10	10	99
3	0.5	0.2	2	10	45
4	30.25	1.6	6	205	79
5	30.25	1.6	6	205	79
6	30.25	1.6	6	205	79
7	30.25	1.6	6	205	79
8	0.50	3	10	400	34
9	0.50	0.2	10	10	52
10	0.50	3	2	400	20
11	60	1.6	6	205	82
12	30.25	3	6	205	91.5
13	30.25	1.6	6	205	79
14	30.25	1.6	6	400	40
15	60	0.2	2	400	3
16	60	3	2	10	94
17	60	0.2	10	400	8
18	30.25	1.6	6	205	79
19	0.5	0.2	10	400	4
20	60	3	10	400	67
21	0.5	3	10	10	89
22	60	3	2	400	62
23	30.25	1.6	10	205	77
24	30.25	1.6	2	205	73
25	30.25	1.6	6	205	79
26	60	0.2	2	10	56
27	60	0.2	10	10	59
28	0.5	3	2	10	86
29	30.25	1.6	6	205	79

4.6 Heavy Metals Response

The model results for the adsorption process are presented in this section, as well as model equations that characterize the essential parameters of an adsorption process. The restricted cases of the objectives were analysed, and the general parameters that could influence individual objective components were identified. The generated second-order polynomial models were directly implemented in GAMS without any modification, to allow easy comparison of the optimized results

4.6.1 Model Fitting and Adequacy Checking

Design Expert software generated regression equations representing an empirical relationship between the response variable and the reaction parameters. The generic quadratic equation shown in Equation 3.7 which is presented again in Equation 4.2, has been used to obtain a polynomial regression model by fitting the experimental results.

$$Y = \beta_o + \beta_1 X_1 + \beta_2 X_2 + \beta_3 X_3 + \beta_4 X_4 + \beta_5 X_5 + \beta_{12} X_1X_2 + \beta_{13} X_1X_3 + \beta_{14} X_1X_4 + \beta_{15} X_1X_5 + \beta_{23} X_2X_3 + \beta_{24} X_2X_4 + \beta_{25} X_2X_5 + \beta_{34} X_3X_4 + \beta_{35} X_3X_5 + \beta_{45} X_4X_5 + \beta_{11} X_1^2 + \beta_{22} X_2^2 + \beta_{33} X_3^2 + \beta_{44} X_4^2 + \beta_{55} X_5^2 \quad (4.2)$$

Where,

Y is the dependent response

β_o is the model coefficient constant

β_1, β_{11}, β_{12}, are coefficients for intercept of linear, quadratic, interactive terms respectively

X_1, X_2, X_3, X_4 and X_5 represent the independent variables

ANOVA (Analysis of variance) generated the regression equations for the optimization of medium constitutes for copper and zinc adsorbed by water hyacinth Egypt sample, regression equations are represented in Equations 4.3 and 4.4:

The percentage removal of Copper (Y_1) is a function of contact time (X_1), adsorbent dose (X_2), pH (X_3) and initial metal ion concentration (X_4).

$$Y_1 = 10.88214 + 0.080054X_1 + 109.68103\ X_2 + 6.24092X_3 - 0.239127X_4 + 0.279195\ X_1 X_2 - 0.017897\ X_1 X_3 + 0.000247\ X_1 X_4 - 0.85333\ X_2 X_3 + 0.075368\ X_2 X_4 + 0.000772\ X_3 X_4 - 0.002673\ X_1^2 - 51.66933\ X_2^2 - 0.341926\ X_3^2 + 0.000186\ X_4^2 \quad (4.3)$$

The regression equation for the optimization of medium constitutes: % removal of Zinc (Y_2) is a function of contact time (X_1), adsorbent dose (X_2), pH (X_3) and initial metal ion concentration (X_4)

$$Y_2 = 23.29651 - 0.253351\ X_1 + 37.89735\ X_2 - 2.69092\ X_3 - 0.171095X_4 - 0.016807X_1\ X_2 + 0.008824X_1X_3 + 0.000377\ X_1X_4 - 0.089286X_2\ X_3 - 0.033883\ X_2\ X_4 + 0.000321\ X_3X_4 + 0.001176\ X_1^2 - 5.5168\ X_2^2 + 0.183594\ X_3^2 + 0.000306X_4^2 \quad (4.4)$$

The regression equation for the optimization of medium constitutes for copper and zinc adsorbed by water hyacinth South Africa sample are represented in equations 4.5 and 4.6 respectively:

$$Y_1 = 93.30192 + 0.171394\ X_1 + 13.87071\ X_2 + 0.720856\ X_3 - 0.240597\ X_4 - 0.075168\ X_1X_2 - 0.001790\ X_1\ X_3 + 0.000230\ X_1\ X_4 - 1.94837 * 10^{-15}\ X_2\ X_3 + 0.020211\ X_2\ X_4 + 0.000632\ X_3\ X_4 - 0.001489\ X_1^2 - 6.79467\ X_2^2 - 0.055407\ X_3^2 + 0.000298X_4^2 \quad (4.5)$$

$$Y_2 = 40.47149 + 0.276165\ X_1 + 22.07824\ X_2 + 3.36600\ X_3 + 0.017948\ X_4 + 0.105042\ X_1X_2 - 0.004202\ X_1X_3 + 0.000474\ X_1X_4 + 0.111607\ X_2X_3 + 0.002289\ X_2X_4 + 0.000641\ X_3\ X_4 - 0.004510\ X_1^2 - 3.75867\ X_2^2 - 0.240184\ X_3^2 - 0.000394\ X_4^2 \quad (4.6)$$

The model results for the adsorption process are presented. Model Equations 4.3 – 4.6 characterize the essential parameters of an adsorption process. The restricted cases of the objectives were analysed, and the general parameters that could influence individual objective components were identified. Analysis of variance (ANOVA) with respect to each pollutant was carried out and it was observed that all the models were highly significant (p-value < 0.05), thus, indicating that the models provided good fits to the experimental data, the coefficient of determination (R^2), adjusted

R^2 and predicted R^2. This illustrates the close agreement between the experimental and model values. Moreover, most of the control variables had significant effects on the objectives or responses of the adsorption process except for contact time and pH for Cu^{2+} and Zn^{2+} in the cases they are adsorbed by water hyacinth from Egypt and pH for Cu^{+2} adsorbed by water hyacinth from South Africa. It is therefore deemed unnecessary to eliminate any of the variables from the models, the summary is presented in Tables 4.18-4.19.

4.6.1.1 RSM Prediction for Removal of Copper

A maximum percentage of removal of 85.5% was attained at control variables of 75 min. contact time, 0.875 g adsorbent dose, 6.25 pH and 20 mg/L initial metal ion concentration. When these control variables were fitted into the model in Equation 4.3, the resulting percentage of removal was 86.26%, which has a percentage error of 0.88%. Furthermore, when South African water hyacinth was used a maximum percentage of removal of 96.3 % at 37.7 min. contact time, 1.5 g adsorbent dose, pH 6.25 and 20 mg/L initial metal ion concentration with an error percent amounts to 2.8% when applied in the model in Equation 4.5.

4.6.1.2 RSM Predication for Removal of Zinc

The model value presented in Equation 4.4 gave 64.48% percentage of removal at 47.5 min., 3g dose of hyacinth, pH 6 and 10 mg/L using Egypt's water hyacinth, while the model presented in Equation 4.6 which was applied on the removal of zinc using South African water hyacinth as adsorbent gave 98.7% percentage of removal at 60 min, 2.5 g, pH 10 and 10 mg/L.

Analysis of variance (ANOVA) has been applied to examine the significance of the model parameters at 95% confidence level. The significance of each parameter has been determined by F-test and p-value. The higher the value of F-test and the smaller the p-value is the significance of the corresponding parameter. ANOVA has been used to validate the RSM model coefficient using F-test and p-value, these values are 29.97 and <0.0001 for copper, respectively and 18.76 and <0.0001 for Zn, respectively, which proved that the developed quadratic model is statistically significant with 95% confidence level. F-test and P-value for tests done using South African water hyacinth are 145.24 and <0.0001 for copper respectively and 70.28 and <0.0001 for zinc respectively.

The determination of coefficient values, R^2 and R^2_{adj}, which measure the reliability of the model fitting, have been calculated for both heavy metals and both adsorbents from Egypt and South Africa and are presented in Table 4.20.

These values indicate that the variance has been attributed to the variables which insures the high significance of the predicted model. Moreover, these results conclude that only 0.03 and 0.06 for Cu^{2+} and Zn^{2+} adsorbed by Egyptian water hyacinth, respectively, of the total variation is not well defined by the developed model. For South African water hyacinth only 0.01 and 0.02 for Cu^{2+} and Zn^{2+}, respectively, of the total variation is not well defined by the developed model. This result ensure the model fitting to the experimental data. The standard deviations (SD) have recoded low values as presented in Table 4.20, which indicates significant and precise predicted model.

Table 4.20: ANOVA for Quadratic Models Egypt –Water Hyacinth, SA-Water Hyacinth

Indices	**Objectives/Response (E-WH)**		**Objectives/Response (SA-WH)**	
	% Removal of Cu Y_1	**% Removal of Zn y_2**	**% Removal of Cu Y_1**	**% Removal of Zn y_2**
R^2	0.97	0.94	0.99	0.98
Adjusted R^2	0.93	0.89	0.99	0.97
Predicted R^2	0.81	0.71	0.96	0.87
Model p-value	<0.0001	<0.0001	<0.0001	<0.0001
SD	5.9	5.79	1.45	4.9

4.6.2 Statistical Analysis

According to the ANOVA results shown in Table 4.21, it is clear that in the case of using water hyacinth from Egypt, the amount of adsorbent and the initial metal ion concentration have a more significant effect on the response of the adsorption process than the contact time and the pH. The amount of adsorbent has the highest significant effect in the case of both copper and zinc recording p-value and F-value of 0.0001 and 218.95, respectively for copper and 0.0001 and 100.3, respectively in case of zinc.

In the case of using South African water hyacinth as adsorbent, it was observed that the initial metal ion concentration had the highest significant effect on the response for copper with recording p-value and F-value 0.0001 and 1501.5, respectively. For zinc, the amount of adsorbent and initial metal ion concentration have significant effect on the response. The initial metal ion concentration has the highest significant effect recording p-value and F-value of 0.0001 and 263.24, respectively. Table 4.22 summarize those results.

Table 4.21: Quadratic Regression Model of ANOVA for Removal of Cu^{2+} and Zn^{2+} using Egyptian Water Hyacinth

Indices	**Objectives/Response**			
	Y_1		**Y_2**	
	P-value	**F-value**	**P-value**	**F-value**
Model p-value	<0.0001	29.97	<0.0001	18.76
X_1 p-value	0.1920	1.88	0.3477	0.94
X_2 p-value	<0.0001	218.95	<0.0001	100.3
X_3 p-value	0.1418	2.42	0.7324	0.12
X_4 p-value	<0.0001	81.52	<0.0001	87.2

Table 4.22: Quadratic Regression Model of ANOVA for Removal of Cu^{2+} and Zn^{2+} Using SA-Water Hyacinth

Indices	**Objectives/Response**			
	Y_1		**Y_2**	
	p-value	**F-value**	**p-value**	**F-value**
Model p-value	<0.0001	145.24	<0.0001	70.3
X_1 p-value	0.0174	7.26	0.4658	0.5622
X_2 p-value	0.0002	25.71	<0.0001	261.95
X_3 p-value	0.4158	0.7	0.0895	3.33
X_4 p-value	<0.0001	1501.5	<0.0001	263.24

4.7 General Algebraic Modelling System (GAMS)

The second order polynomial models generated from RSM (Equations 4.3, 4.4, 4.5 and 4.6) for both heavy metals and both sources of water hyacinth were applied directly in GAMS without any modification, to allow easy comparison of the optimized results.

4.7.1 GAMS Prediction for Removal of Copper

For the copper removal using Egypt's water hyacinth, GAMS application suggested 56.674 min. contact time, 1.178 g adsorbent dose, 6.196 pH and 20 mg/l initial metal ion concentration as the optimal solution with optimized percentage of removal of 93.449%. This represents a percentage of error of 7.4% when compared with the experimental results. GAMS application suggested 33.6 min. contact time, 0.86 g adsorbent dose, 6.07 pH and 20 mg/L initial metal ion concentration as the optimal solution with optimized percentage of removal of 99.6% when copper was removed using South African water hyacinth. This represents a percentage error of 0.8 % when compared with the experimental results.

4.7.2 GAMS Predication for Removal of Zinc

When the GAMS approach was applied for the percentage of removal of zinc using water hyacinth from Egypt, the optimal solution of control variables obtained was 5 min. contact time, 3 g adsorbent dose, pH of 2 and 10 mg/L initial metal ion concentration with a maximum percentage of removal of 78.08%. This represents a percent error of 11.63% when compared with the experimental results. GAMS application suggested 100% percentage of removal at 38.426 min. contact time, 2.5 g adsorbent dose, pH 8.025 and 42.92 mg /L when using South African water hyacinth for the removal of zinc and this represents a percent of error 0.012%. According to this results, although GAMS gives higher percentage of removal but it is not realistic as the percentage of error is high, while RSM gives low error percent between the model and the experimental result.

The conflicting region of control variables is summarized in Tables 4.23 and 4.24.

Table 4.23: The Conflicting Region of Control Variables Egyptian Water Hyacinth

Objective functions	Optimized results and control variables across each platform			
	Experiment	RSM prediction	GAMS prediction	% Error
% Removal of Cu	85.5% at 75 min. 0.875g 6.25pH 20 mg/L	86.261% at 75 min. 0.875g 6.25 pH 20 mg/L	93.449% at 56.674 min. 1.178g 6.196pH 20 mg/L	0.88 % for RSM 7.4% for GAMS
% Removal of Zn	61% 47.5 min. 3g 6pH 10 mg/L	64.48% 47.5 min. 3g 6pH 10 mg/L	78.081% 5min. 3g 2pH 10 mg/L	5.4% for RSM 11.6% for GAMS

Table 4.24: The Conflicting Region of Control Variables SA-water Hyacinth

Objective functions	Optimized results and control variables across each platform			
	Experiment	RSM prediction	GAMS prediction	% Error
% Removal of Cu	99.1% at 37.7 min. 1.5 g, pH 6.25 and 20 mg/L	96.3 % at 37.7 min., 1.5 g, pH 6.25 and 20 mg/L	99.6% at 33.6 min. 0.86 g , pH 6.07 and 20 mg/L	2.8 % for RSM 0.8 % for GAMS
% Removal of Zn	98.5% at 60 min. 2.5 g, pH 10 and 10 mg/L	98.7% at 60 min 2.5 g, pH 10 and 10 mg/L	100% at 38.4 min. 2.5 g, pH 8 and 42.9 mg/L	0.008% for RSM 0.012% for GAMS

4.8 Phase III- Fixed Bed Column Experiments

The third phase of the experimental plan, after the batch equilibrium tests of water hyacinth from Egypt and South Africa, and the optimization of process parameters using RSM and GAMS, is the fixed bed column tests. The comparison study of the water hyacinth from Egypt and the one from South Africa showed that water hyacinth from South Africa gave better adsorption results and therefore is here used in the fixed bed adsorption column experiments.

The results of the column tests are presented as breakthrough curves, which are the plots of either the ratio of the effluent Cu^{2+} or Zn^{2+} concentration to the influent Cu^{2+} or Zn^{2+} concentration (C/C_0) versus service time (t).

Breakthrough time (t_b) is the time when the effluent concentration reaches a critical point which is defined based on the specific application (Singh et al., 2020, Farooq et al., 2013). Breakthrough time was set in several researches as the time when the effluent concentration (C) reaches a certain percentage of the influent concentration of Cu^{2+} or Zn^{2+} (C_0), usually in the range of 5%-10% (Singh et al., 2020, Sarma et al., 2015, Chatterjee and Schiewer, 2014, Farooq et al., 2013). Other important parameters are the exhaustion time (t_e) and exhaustion concentration (C_e) where the packed column reaches full saturation.

The time at which the breakthrough occurs and the shape of the breakthrough curve, normally S shape, are very vital for determining the operation conditions and dynamic of adsorption column (Singh et al., 2020, Farooq et al., 2013). The shape of a breakthrough curve is a function of the sorbent geometry, and operating conditions (Farooq et al., 2013). The area above the S curve is the amount of adsorbed Cu^{2+} or Zn^{2+} while the area under the curve is the amount of un-adsorbed Cu^{2+} or Zn^{2+}.

The total amount of Cu^{2+} or Zn^{2+} sent to the packed water hyacinth column was calculated as shown in the equation below:

$$m_{total} = \frac{C_o \, Q \, t_{total}}{1000} \tag{4.7}$$

Where:

C_0 = is the initial copper concentration (mg/L)

Q = Flowrate (mL/min)

t_{total} = exhaustion time (min)

Several important parameters have been calculated in order to analyze the performance of the column tests, such as uptake capacity (mg/g), which is the mass of Cu^{+2} or Zn^{+2} adsorbed per unit mass of sorbent, at exhaustion (q_e), as shown in the equations below (Chatterjee and Schiewer, 2014).

$$q_{total} = \frac{Q}{1000} \int_{t=0}^{t=total} C_{ad} \, dt \tag{4.8}$$

$$q_e = \frac{q_{total}}{m} \tag{4.9}$$

Where;

$q_{total=}$ Maximum column capacity (mg/g)

Q= Flowrate (mL/min)

C_{ad}= Adsorbed concentration (mg/L)

q_e: uptake capacity of the column at exhaustion, nearly full saturation, of the water hyacinth column (mg/g)

M: mass of water hyacinth in the column (g)

Mass transfer zone (MTZ) is the zone where the sorbent is actively adsorbing the metal ions and did not reach saturation, the MTZ moves through the column in the direction of the flow until it reaches the end of the column, then breakthrough takes place (Chatterjee and Schiewer 2014, Metcalf & Eddy 2003). According to Chatterjee and Schiewer (2014), MTZ is calculated as per the equation below:

$$MTZ = \left(1 - \frac{t_b}{t_e}\right) * L \qquad (4.10)$$

Where;

MTZ: length of the mass transfer zone (cm)

t_b: time when breakthrough occurs (h); C/C_o= 5%

t_e: time when exhaustion occurs (h)

L: length of the adsorption column (cm)

The parameters studied in the continuous flow tests are:

1) Initial Cu^{2+} or Zn^{2+} Concentration
2) Bed depth
3) Flowrate of the Cu^{2+} or Zn^{2+} solution feeding the packed column

4.8.1 Effect of Initial Metal Ion Concentration

A glass column with length of 50 cm and internal diameter of 2 cm was used. Dry water hyacinth was packed into the column; the bed depth was 2 cm, weighing around 0.5 g. The performance of the column was analysed at Cu^{2+} and Zn^{2+} concentrations of 20 mg/L, 30 mg/L, and 50 mg/L, at a flowrate 5 mL/min and pH 6. Using Equations 4.7 to 4.10, the calculated parameters are shown in Tables 4.25 and 4.26 for copper and zinc, respectively.

Table 4.25: Parameters of Fixed- Bed Column Tests at Various Cu^{2+} Concentrations (bed depth 2 cm; Q 5 ml/min; pH 6)

Cu^{2+} concentration (mg/L)	**Time (h)**		**m_{tot} (mg)**	**q_{tot}**	**q_e (mg/g)**	**MTZ (cm)**
	t_b	**t_e**				
20	0.9	23.3	139.8	42	84	1.9
30	0.45	16	144	43	86	1.94
50	0.42	14.8	222	82	165	1.95

Table 4.26: Parameters of Fixed- Bed Column Tests at Various Zn^{2+} Concentrations (bed depth 2 cm; Q 5 ml/min; pH 6)

Zn^{2+} concentration (mg/L)	**Time (h)**		**m_{tot} (mg)**	**q_{tot}**	**q_e (mg/g)**	**MTZ (cm)**
	t_b	**t_e**				
20	2.5	25	150	48	96	1.8
30	1.3	20.5	184.5	58.5	117	1.87
50	0.6	18.1	271.5	75	150	1.93

Figures 4.29 and 4.30 illustrate that both breakthrough and exhaustion for Cu^{2+} and Zn^{2+} occurred faster and the slope of the curves got steeper as the initial concentration of Cu^{2+} or Zn^{2+} (C_0) was increased. In other words, the service time or the life span of the adsorption column gets shorter with increasing the influent copper or zinc concentrations. Similar trends were reported by Saravanan, et al., (2018) in the removal of zinc from aqueous solution using dual surface-modified biomass and Chen et al., (2012) in the removal of hexavalent chromium using modified corn stalk.

To illustrate, at 20 mg/L influent concentration for copper the time needed for water hyacinth to reach breakthrough and full saturation was 0.9 h(54 min) and 23.3 h (1398 min), respectively, as shown in Table 4.25 and Figure 4.29. Upon increasing the Cu^{2+} concentration to 50 mg/L, the service time to breakthrough (t_b) dropped to 0.42h (25.2 min) and the service time to exhaustion (t_e) dropped to 14.8 (888min) h.

In case of zinc at 20 mg/L influent concentration the time needed for water hyacinth to reach breakthrough and full saturation was the maximum; 2.5 h and 25 h, respectively, compared to the higher Zn^{2+} concentrations, as shown in Table 4.26 and Figure 4.30. Upon increasing the Zn^{2+} concentration to 50 mg/L, the service time to breakthrough (t_b) dropped to 0.6 h (36 min) and the service time to exhaustion (t_e) dropped to 18.1 h (1086 min).

The length of the MTZ in case of both Cu^{2+} and Zn^{2+}, slightly increased with the increase in the initial Cu^{2+} or Zn^{2+} concentration.

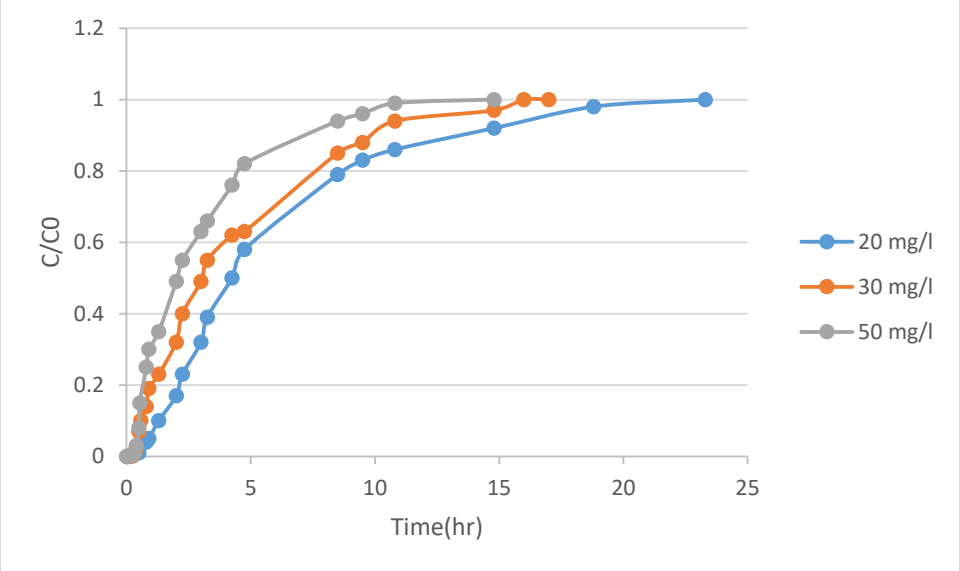


Figure 4.29: Breakthrough curves of Cu^{2+} adsorption by water hyacinth at various initial Cu^{2+} concentrations (bed depth 2cm; flowrate 5mL/min; pH 6)

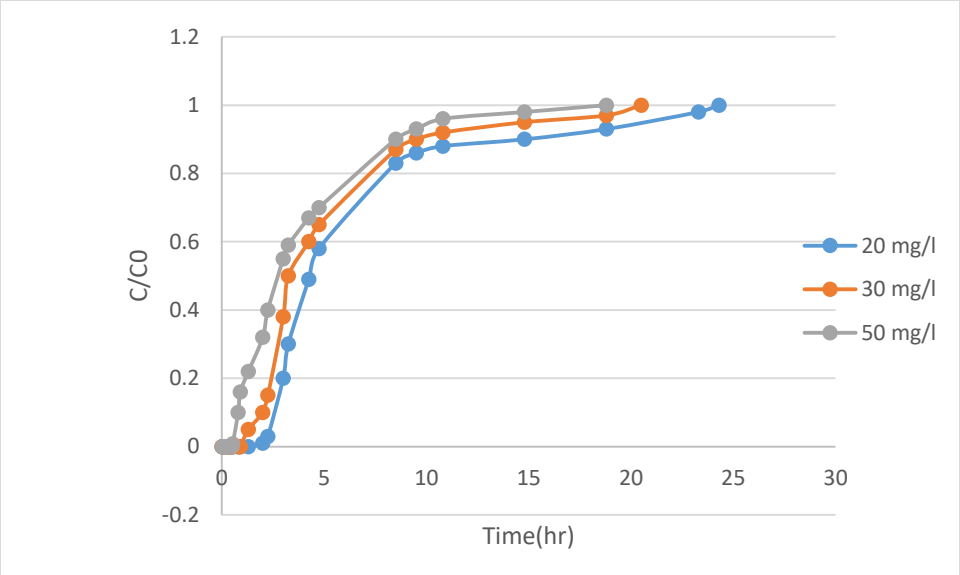


Figure 4.30: Breakthrough curves of Zn^{2+} adsorption by water hyacinth at various initial Zn^{2+} concentrations (bed depth 2cm; flowrate 5mL/min; pH 6)

4.8.2 Effect of Bed Depth

The impact of the bed depth on the breakthrough curves was analysed. Column tests were run at a flowrate of 5 mL/min and 2 cm, 4 cm and 7 cm bed depths, corresponding to 0.5 g, 1.1g and 1.7 g, respectively dry weight of water hyacinth was packed in the column. A glass column with diameter of 2 cm and length of 50 cm was used. The Cu^{2+} or Zn^{2+} concentrations in the three cases were 20 mg/L and the pH of the synthetic solution was adjusted to 6. The significant parameters for copper and zinc were calculated and are presented in Table 4.27 and 4.28 respectively, and the breakthrough curves for both heavy metals are shown in Figure 4.31 and Figure 4.32.

Table 4.27: Parameters of Fixed- Bed Column Tests for Cu $^{2+}$ at Various Bed Depths (C_o= 20 mg/L; flowrate 5 mL/min; pH 6)

Bed depth (cm)	Time (h)		m_{tot} (mg)	q_{tot}	q_e (mg/g)	MTZ (cm)
	t_b	t_e				
2	0.9	23.3	139.8	42	84	1.9
4	3	26	156	63	57.3	3.5
7	5.3	30	180	96	56.5	5.8

Table 4.28: Parameters of Fixed- Bed Column Tests for Zn^{2+} at Various Bed Depths (C_o= 20 mg/L; flowrate 5 mL/min; pH 6)

Bed depth (cm)	Time (h)		m_{tot} (mg)	q_{tot}	q_e (mg/g)	MTZ (cm)
	t_b	t_e				
2	2.5	25	150	48	96	1.8
4	2.8	26	156	51	46.3	3.6
7	5	28	168	75	44.1	5.7

The increase in the bed depth led an increase in the service time to breakthrough and exhaustion of the adsorption columns, as shown in Figures 4.31 and 4.32. The same trend was reported by several researchers (Saravanan et al., 2018, Sarma et al., 2015, Farooq et al., 2013). Upon the increase in the bed depth from 2 cm to 7 cm, the service time at breakthrough and at exhaustion increased from 0.9 h and 23.3 h, respectively up to 5.3 h and 30 h, respectively for copper. The analysis for zinc showed that both the service time at breakthrough and exhaustion increased from 2.5 h and25h, respectively up to 5h and 28 h respectively. This could be explained by the fact that, as the amount of water hyacinth increases in the column and the bed depth is longer, the surface area, and consequently the active sites on the surface of water hyacinth that are available for the adsorption process increase as well (Sarma et al., 2015). Therefore, it takes a longer time to get them all saturated by metal ions. The same trend is observed for the adsorbed mass of both copper and zinc on the surface of water hyacinth at breakthrough and exhaustion, see Tables 4.27 and 4.28.

Figures 4.31 and 4.32 demonstrate the impact of the bed depth increase on the increase in the residence time of wastewater. This is attributed to the concept that for short bed depths, the residence time of the solution in the column is short; hence, preventing the metal ions to completely diffuse into all the available adsorbent packed in the column; however, when the column is longer the residence time increases giving a chance for the metal ions to get adsorbed on all the available binding sites on the surface of the adsorbent (Fauzia et al., 2021). Moreover, the length of the mass transfer zone (MTZ) increased with the increase in the bed depth, which is logical because the

MTZ is a function of the bed depth. Normally, a steep slope of a breakthrough curve is an indication of a smaller MTZ (Chen et al., 2012).

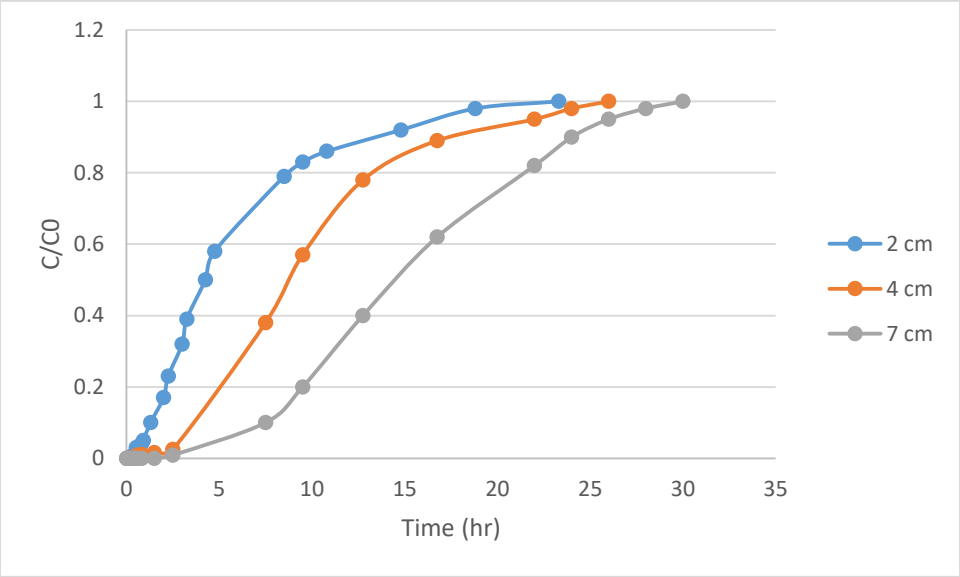


Figure 4.31: Breakthrough curves of Cu^{2+} adsorption by water hyacinth at various bed depths (C_0= 20mg/L; flowrate 5 mL/min; pH 6)

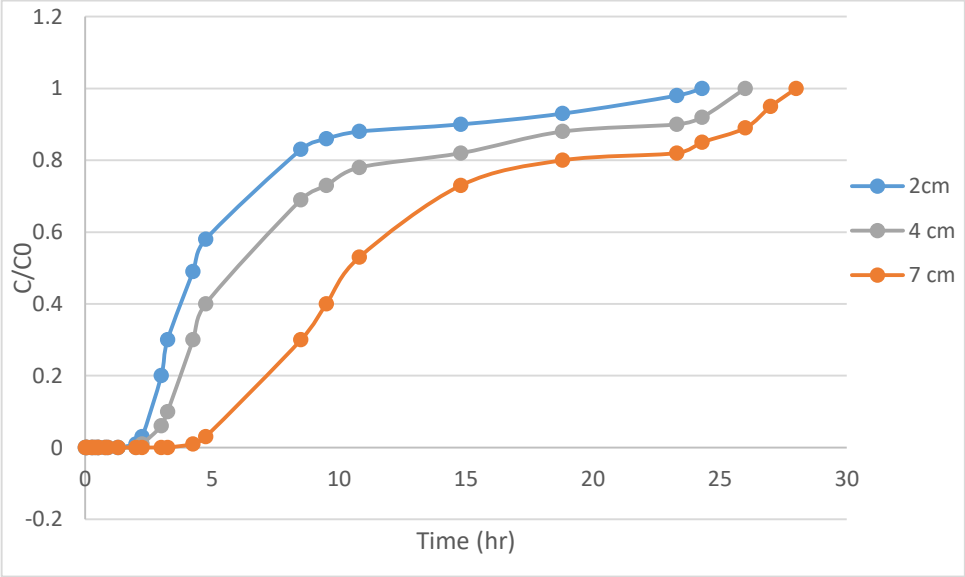


Figure 4.32: Breakthrough curves of Zn^{2+} adsorption by water hyacinth at various bed depths (C_0= 20 mg/L; flowrate 5 mL/min; pH 6)

4.8.3 Effect of Flowrate (Q)

The impact of the solution flowrate on the shape and the parameters of the breakthrough curves were analysed in this sub-section. The tests were run at 5 mL/min, 10 mL/min and 17 mL/min flowrates and the breakthrough curves were compared. The bed depth was 2 cm, corresponding to an average of 0.5 g dry water hyacinth, pH 6, and Cu^{2+} and Zn^{2+} initial concentrations were around 20 mg/L each. The main parameters were calculated and are presented in Tables 4.29 and 4.30.

Table 4.29: Parameters of Fixed- Bed Column Tests for Cu^{2+} at Various Feed Solution Flowrates (C_0= 20 mg/L; bed depth=2 cm; pH 6)

Q (mL/min)	Time (h)		m_{tot} (mg)	q_{tot}	q_e (mg/g)	MTZ (cm)
	t_b	t_e				
5	0.9	23.3	139.8	42	84	1.9
10	0.46	17	204	40	80	1.95
17	0.3	16.7	340.68	40.8	81.6	2

Table 4.30: Parameters of Fixed- Bed Column Tests for Zn^{2+} at Various Feed Solution Flowrates (C_0= 20 mg/L; bed depth=2 cm; pH 6)

Q (mL/min)	Time (h)		m_{tot} (mg)	q_{tot}	q_e (mg/g)	MTZ (cm)
	t_b	t_e				
5	2.5	25	150	48	96	1.8
10	1.3	18.8	225.6	48	96	1.86
17	0.83	14.8	301.9	47.6	95.2	1.9

It could be observed that breakthrough time (t_b) and exhaustion time (t_e) became shorter as the flowrate increased for both metal ions. The longer breakthrough time, the longer adsorbent can be used before it became saturated and has to be replaced or regenerated. As shown in Figure 4.33, the service time of the adsorption column at breakthrough (t_b) for copper increased from 0.3 h at a flowrate of 17 mL/min to 0.9 h at a flowrate of 5 mL/min. Similarly, the exhaustion time increased from 16.7h at Q= 17 mL/min to 23.3 h at Q= 5 mL/min. The same trend was observed for Zn^{2+},

which increased from 0.83 at Q= 17 mL/min to 2.5 at Q= 5 mL/min, and from 14.8h h at Q= 17 mL/min to 25h at Q= 35 mL/min at breakthrough and exhaustion, respectively, as presented in Figure 4.34 and Table 4.30 When the flowrate of the contaminated water is doubled from 5mL/min to 10mL/min the breakthrough time is reduced by 48% percent and the time it takes to reach exhaustion becomes shorter by 24.8%.

A high flowrate results to in poor distribution of Cu^{2+} or Zn^{2+} ions in the adsorption bed resulting in insufficient resident time for the diffusion of Cu^{2+} or Zn^{2+} ions within the adsorbent bed. As a result, the solution leaves before equilibrium occurs, resulting in a low uptake capacity and removal efficiency (Yahya et al., 2020). Moreover, the higher flowrate decreased the external of mass transfer resistance leading the saturation of adsorbent (Fauzia et al., 2021). Therefore, the lower flowrate (5 mL/min) was chosen for further use.

The slope of the breakthrough curve at 17 mL/min is much steeper than at 5 mL/min flowrate with significantly reduced breakthrough and exhaustion times in the case of both copper and zinc (Chittoo and Sutherland, 2020).

Moreover, the adsorption capacity (q) of Cu^{2+} and Zn^{2+} ions exhibited the same decreasing trend with increasing the flowrate of the feed solution. At the breakthrough, the adsorption capacity at 17 mL/min decreased to 81.6 mg/g compared to 84 mg/g at 5 mL/min flowrate for copper, and to 95.2 mg/g at 17 mL/min to 96 mg/g at 5 mL/min for zinc. The same trend was reported by several researchers (Futalan and Wan, 2022, Al Mesfer et al., 2020, Lo´pez-Cervantes et al., 2017, Tsai et al., 2016).

The MTZ changes with the variation in the flowrate because dispersion, diffusion and channelling of the metal ions in a granular medium are mainly affected by the flowrate of the solution (Metcalf & Eddy 2003). The length of the mass transfer zone, MTZ is observed to increase from 1.9 cm to 2 cm for copper with flowrate increase from 5 mL/min to 17 mL/min and increase from 1.8 cm to 1.9 cm for zinc with flowrate increase from 5 mL/min to 17 mL/min. A broader mass transfer zone causes the breakthrough and exhaustion to occur earlier, this result is in agreement with (Verduzco-Navarro et al., 2020, Tsai et al., 2016, Futalan et al., 2011).

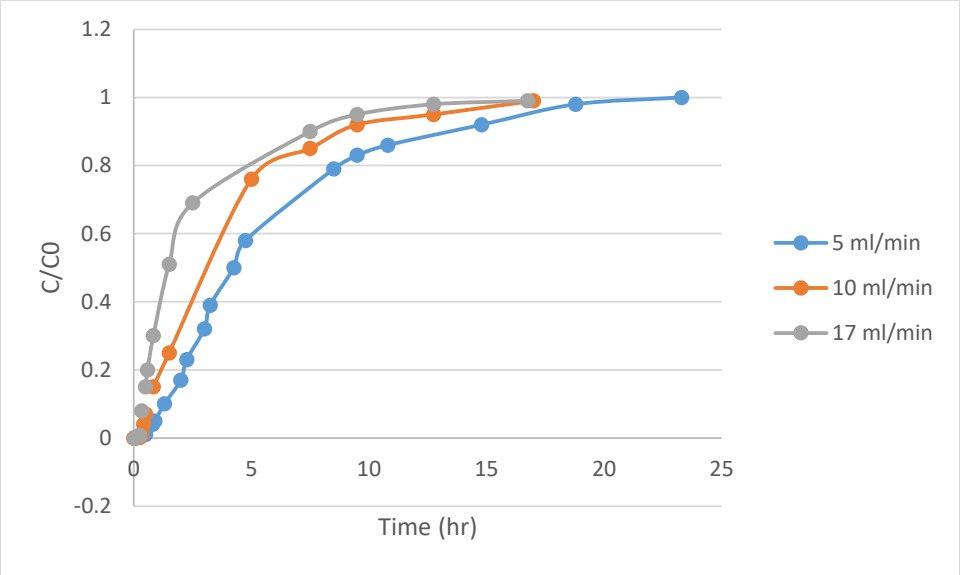


Figure 4.33: Breakthrough curves of the adsorption of Cu^{2+} by raw water hyacinth at various flowrates (C_o= 20 mg/L; bed depth=2 cm; pH 6)

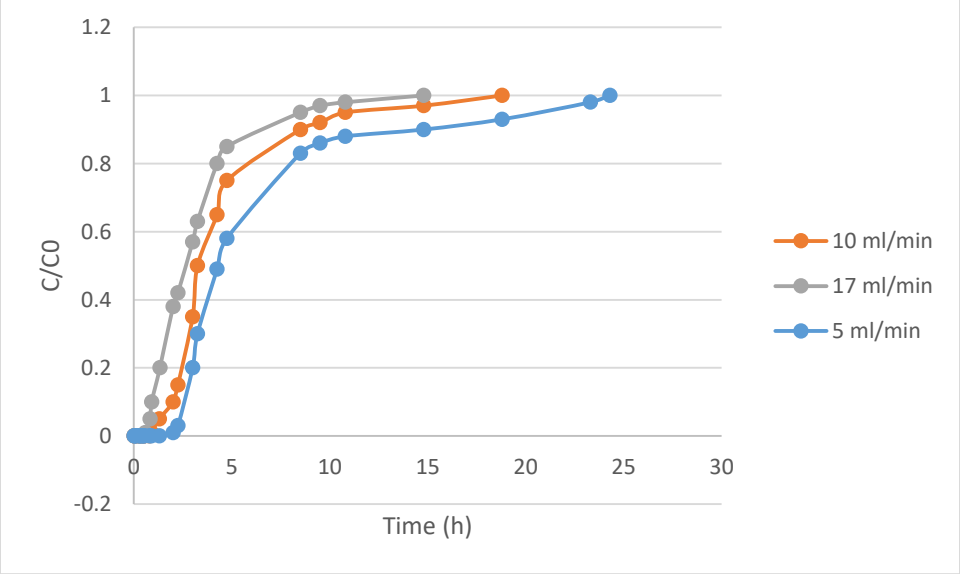


Figure 4.34: Breakthrough curves of the adsorption of Zn^{2+} by raw water hyacinth at various flowrates (C_o= 20 mg/L; bed depth=2 cm; pH 6)

4.9 Mathematical Modelling and Simulation

The proposed mathematical model for the fixed bed column is simulated and validated using the calculated parametric values shown in Table 4.28. The present model is also compared with the experimental data done and showed in section 4.8.

4.9.1 Model Development

The model proposed here is implemented with MATLAB. To validate the model, input parameters corresponding to experimental conditions are used in this model, for experiments consisting of tests of copper and tests of zinc adsorption in water hyacinth packed bed filters. The breakthrough curves for different levels of inlet concentrations (20 mg/L, 30 mg/L, and 50 mg/L), different levels of bed height (2 cm, 4 cm, 7 cm) and different flowrate (5 mL/min, 10 mL/min, 17 mL/min) for both copper and zinc are then plotted to be compared with the experimental data.

4.9.2 Model Validation

The comparison of experimental results and the model predictions for Cu^{2+} and Zn^{2+} adsorption using water hyacinth are shown in Figures 4.35 to 4.52. Model parameter values for simulation in the present study are listed in Table 4.31.

Table 4.31: Model Parameters Value for Simulation

Parameter	Value
Bed Porosity (ε)	0.47
Bed diameter (m)	0.02
Bed height (m)	0.02, 0.04, 0.07
Bed density(ρ_b)(Kg/m^3)	107
Particle density (Kg/m^3)(assumed)	1970
Particle radius (m)	0.003
Axial dispersion coefficient (D_L)(m^2/sec)	$1.85*10^{-5}$
Flowrate (mL/min)	5, 10, 17
Initial concentration (mg/L)	20, 30, 50
Particle porosity (ε_p)(assumed)	0.43

The shape of the breakthrough curves obtained using the proposed generic model were found to be almost similar for Cu^{2+} and Zn^{2+} removal. This indicates the suitability of the generic models for copper and zinc removal using water hyacinth.

4.9.2.1 Model Breakthrough Curve Vs Experimental Breakthrough Curve Results

- **Effect of Initial Metal Ion Concentration**

  Changes in the initial Cu^{2+} and Zn^{2+} concentrations have significant influences on the characteristics of the breakthrough curves for both copper and zinc. The adsorption performance of water hyacinth was tested by varying the inlet concentration of copper and zinc from 20 to 50 mg/L. The breakthrough curves for water hyacinth obtained at different initial concentrations of copper and zinc were described in section 4.8.1.

  It is observed that the adsorbent becomes saturated faster at higher concentration of adsorbate due to the higher availability of Cu^{2+} or Zn^{2+} ions. For a low initial Cu^{2+} or Zn^{2+} concentration, breakthrough occurs very late and surface of the water hyacinth is saturated with Cu^{2+} or Zn^{2+} at a relatively longer time. This fact is probably associated with the availability of adsorption sites around or inside the adsorbent particles that are able to capture the heavy metal ions at lesser retention time this (Gupta and Bhattacharyya, 2011). It can be observed from Figures 4.35 and 4.38 that describe the experimental data for Cu^{2+} and Zn^{2+} adsorption at initial concentration of 20 mg/l for each metal separately using water hyacinth, fit well with the models during the latter part of adsorption, but not so in the initial time period of adsorption as reflected in the respective breakthrough curves.

  When the initial concentration increase from 20 mg/L to 30 mg/L as shown in Figure 4.36 for copper and 4.39 for zinc, it was observed that the experimental data fit better with the model regarding the breakthrough and saturation time while there was a small deviation in the intermediate points. When the initial concentration increased to 50 mg/L the experimental data fit the model the most for both copper and zinc, although the breakthrough and saturation times aren't so close as the case of 30 mg/L however, the overall breakthrough curves for copper and zinc fit the experimental data the most as shown in Figure 4.37 for copper and 4.40 for zinc, see Table 4.32.

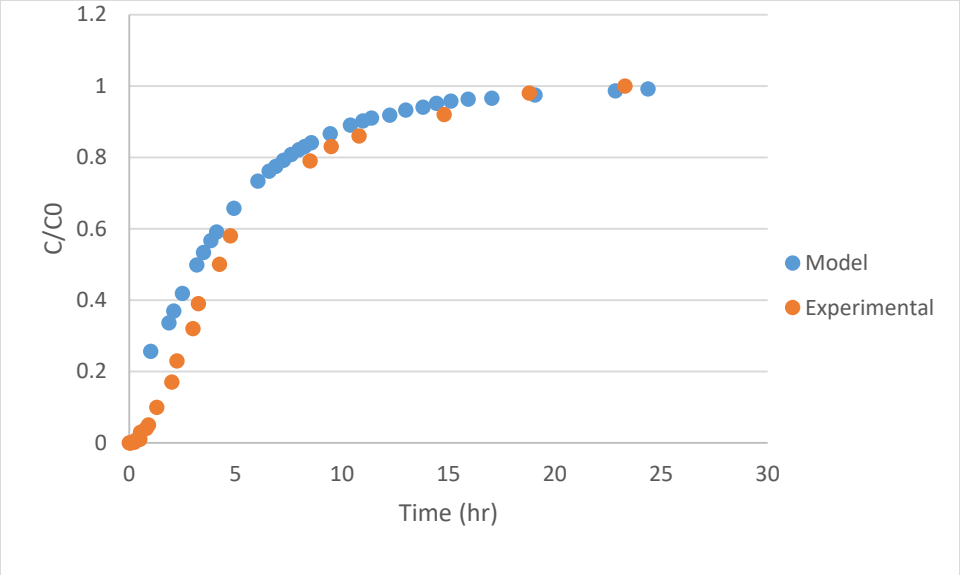


Figure 4.35: Comparison between theoretical and experimental results obtained using proposed mathematical model for the adsorption of Cu^{2+} at various initial concentrations (C_{b0} = 20 mg/l, Q = 5 mL /min and bed height = 2 cm)

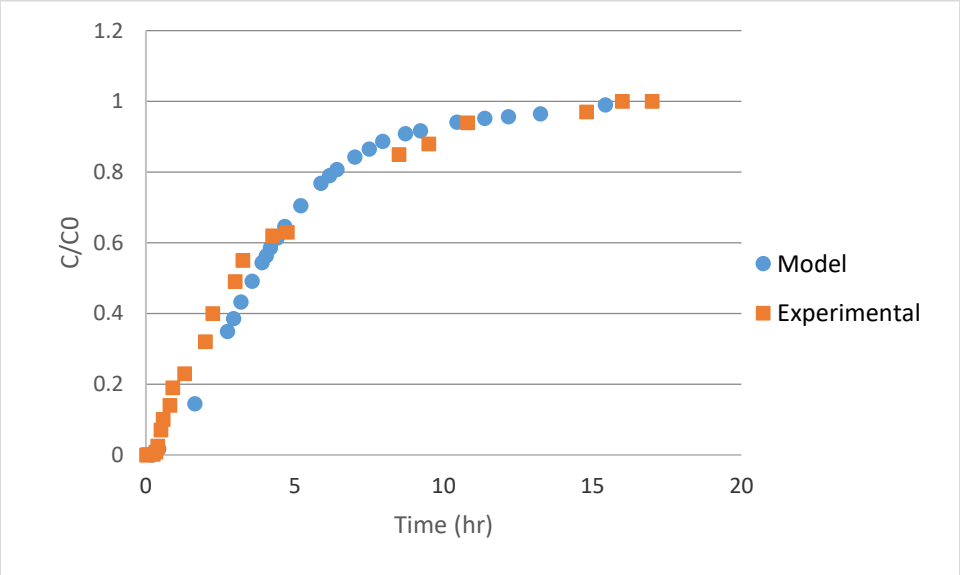


Figure 4.36: Comparison between theoretical and experimental results obtained using proposed mathematical model for the adsorption of Cu^{2+} at various initial concentrations (C_{b0} = 30 mg/L, Q = 5 mL /min and bed height = 2 cm)

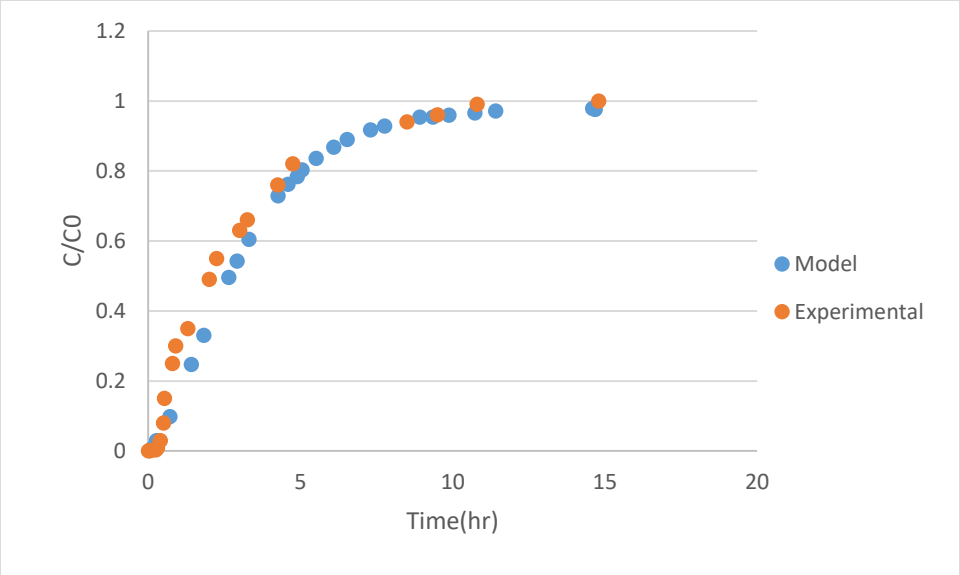


Figure 4.37: Comparison between theoretical and experimental results obtained using proposed mathematical model for the adsorption of Cu^{2+} at various initial concentrations (C_{b0} = 50 mg/L, Q = 5 mL /min and bed height = 2 cm)

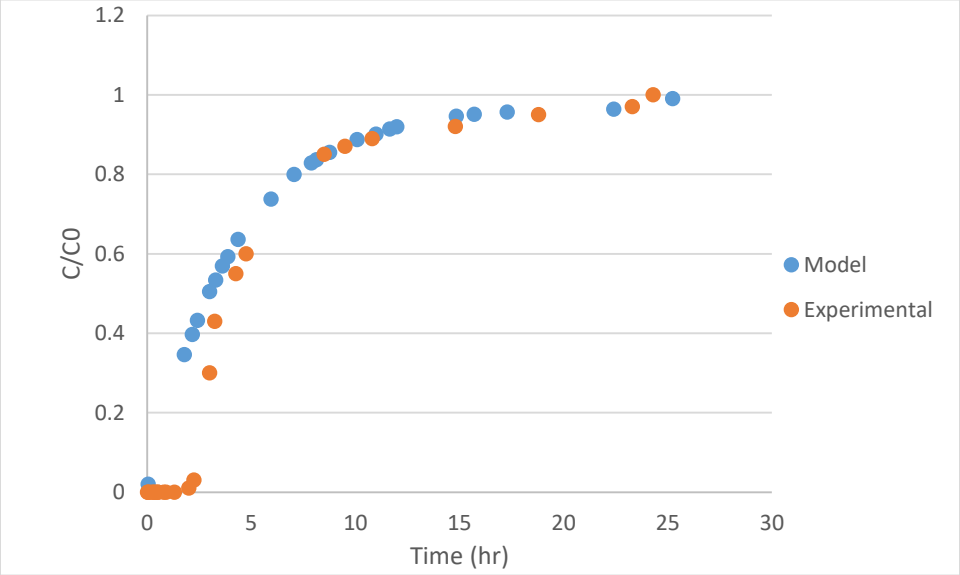


Figure 4.38: Comparison between theoretical and experimental results obtained using proposed mathematical model for the adsorption of Zn^{2+} at various initial concentrations (C_{b0} = 20 mg/L, Q = 5 mL /min and bed height = 2 cm)

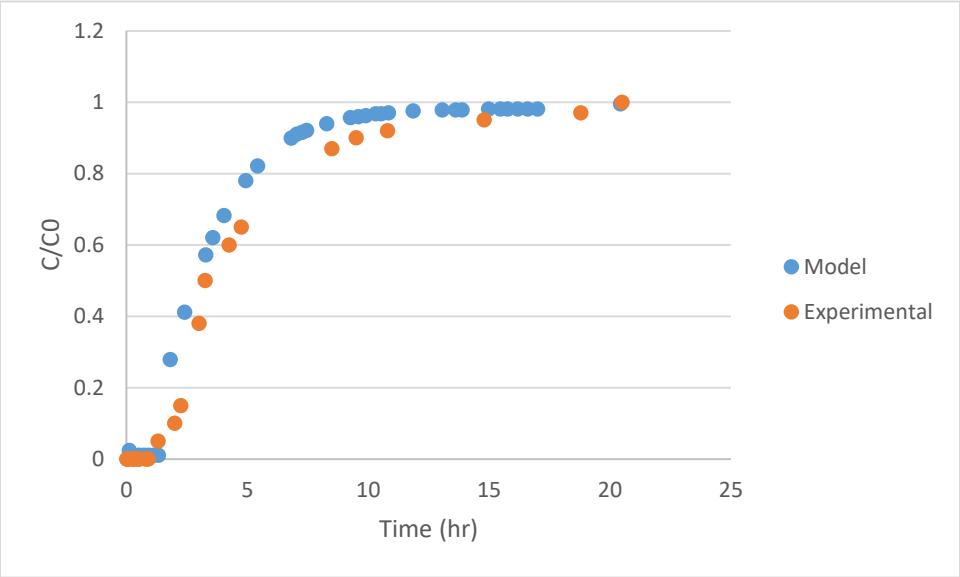


Figure 4.39: Comparison between theoretical and experimental results obtained using proposed mathematical model for the adsorption of Zn^{2+} at various initial concentrations (C_{b0} = 30 mg/L, Q = 5 mL /min and bed height = 2 cm)

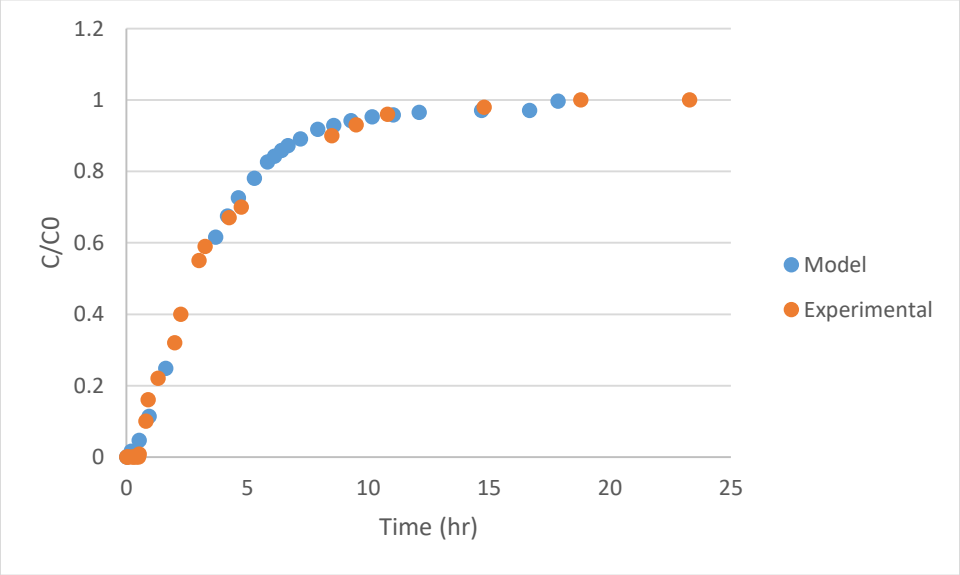


Figure 4.40 Comparison between theoretical and experimental results obtained using proposed mathematical model for the adsorption of Zn^{2+} at various initial concentrations (C_{b0} = 50 mg/L, Q = 5 mL /min and bed height = 2 cm)

Table 4.32: Model and Experimental Breakthrough Curves Parameters at Various Cu^{2+} and Zn^{2+} Concentrations (bed depth 2 cm, Q 5 mL/min, pH 6)

Initial conc. (mg/L)	Breakthrough time(hr) (t_b)				Saturation time (hr) (t_e)			
	Cu		Zn		Cu		Zn	
	Experimental	Model	Experimental	Model	Experimental	Model	Experimental	Model
20 (mg/L)	0.9	0.7	2.5	1.3	23.3	24.3	25	25
30 (mg/L)	0.45	0.48	1.3	1.4	16	15.5	20.5	20.4
50 (mg/L)	0.42	0.29	0.6	0.52	14.8	15	18.1	17.8

- **Effect of Flowrate**

Figures 4.41-4.46 describe the behavior of breakthrough curves at varying flowrates on the effluent concentration, two other parameters (bed height, inlet copper and zinc concentrations) were fixed. Adsorption time was found to be decreasing with rise in flowrate. Higher flowrates correspond to enhanced external mass transfer coefficients which in turn leads to greater adsorption rates, eventually resulted in decreasing the breakthrough times (Gupta, 2020). It can be observed from Figures 4.41 and 4.44 that the experimental data for Cu^{2+} and Zn^{2+} adsorption at flowrate of 5mL/min for each metal separately using water hyacinth, fit well with the models during the latter part of adsorption as reflected in the respective breakthrough curves.

When the flowrate increases from 5 mL/min to 10 mL/min as shown in Figure 4.42 for copper and figure 4.45 for zinc, it was observed that the experimental data fit the most with the model in case of both copper and zinc. Especially for zinc as the whole breakthrough curve including the breakthrough time and exhaustion time. In case of copper the model breakthrough time and exhaustion time weren't that close to that of the experimental data. As flowrate increased to 17 mL/min the model and experimental breakthrough times and exhaustion times are close in case of copper. In case of zinc the model data fit the experimental data better than the 5 mL/min but less than the 10 mL/min as shown in figure 4.43 for copper and 4.46 for zinc, See Table 4.33

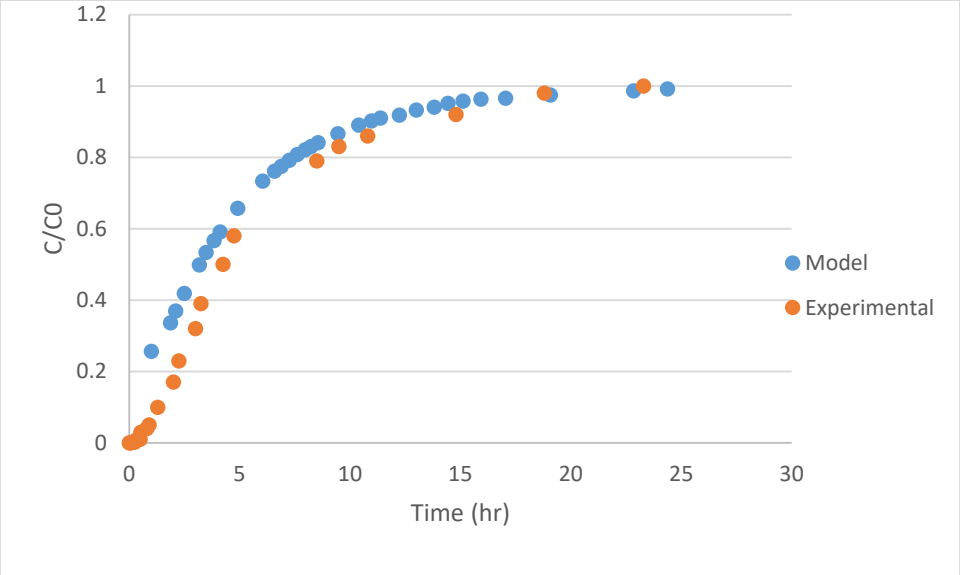


Figure 4.41: Comparison between theoretical and experimental results obtained using proposed mathematical model for the adsorption of Cu^{2+} at various flowrates (C_{b0} = 20 mg/L, Q = 5 mL /min and bed height = 2 cm)

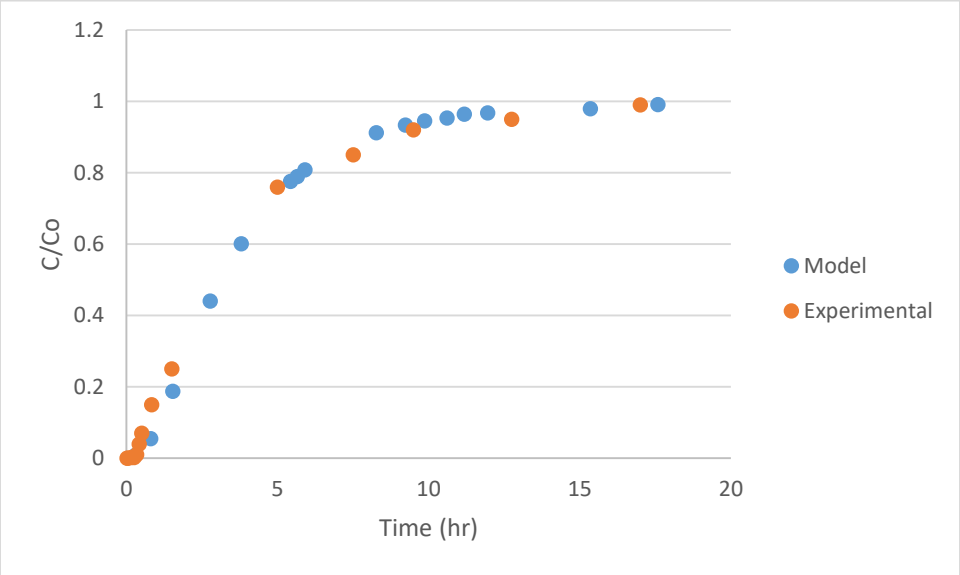


Figure 4.42: Comparison between theoretical and experimental results obtained using proposed mathematical model for the adsorption of Cu^{2+} at various flowrates (C_{b0} = 20 mg/L, Q = 10 mL /min and bed height = 2 cm)

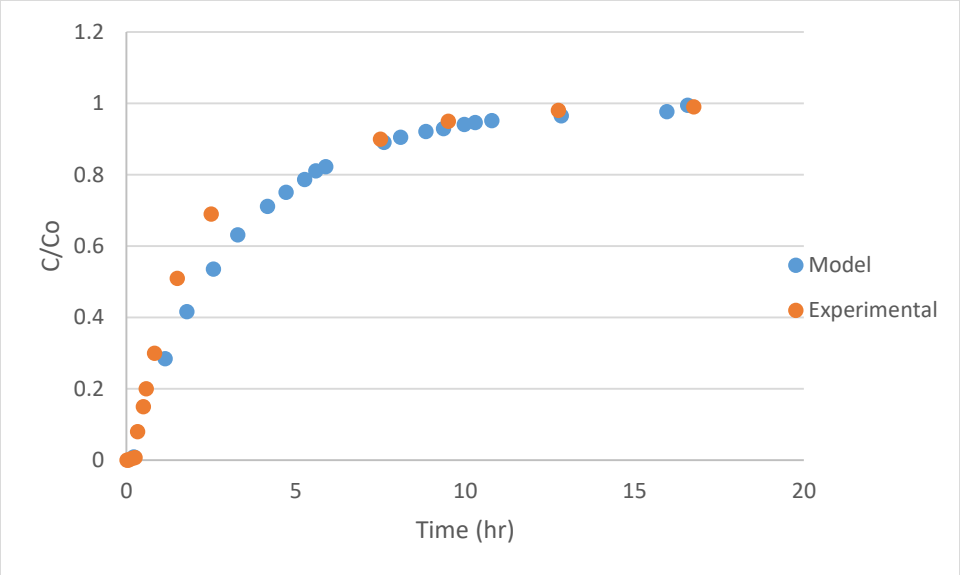


Figure 4.43: Comparison between theoretical and experimental results obtained using proposed mathematical model for the adsorption of Cu^{2+} at various flowrates (C_{b0} = 20 mg/L, Q = 17 mL /min and bed height = 2 cm)

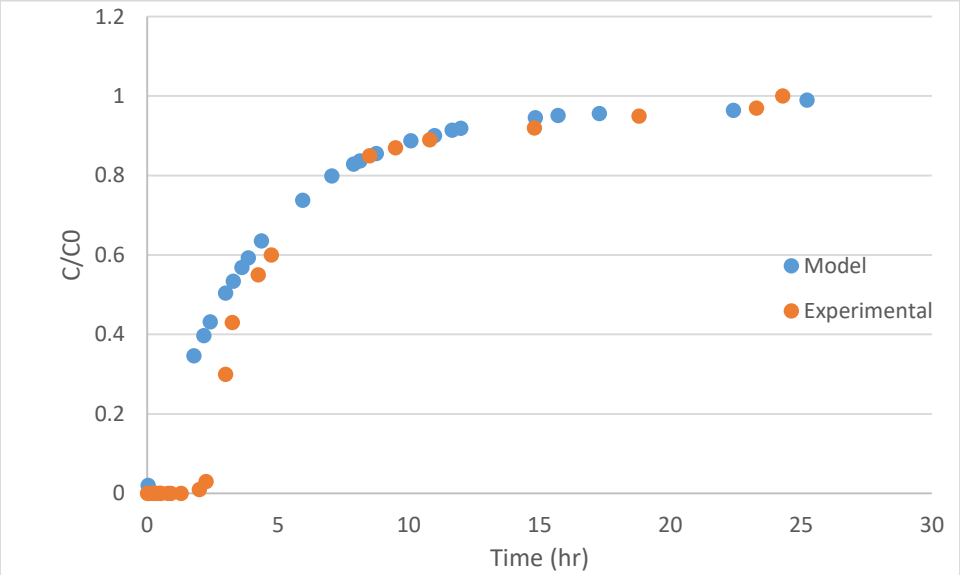


Figure 4.44: Comparison between theoretical and experimental results obtained using proposed mathematical model for the adsorption of Zn^{2+} at various flowrates (C_{b0} = 20 mg/L, Q = 5 mL /min and bed height = 2 cm)

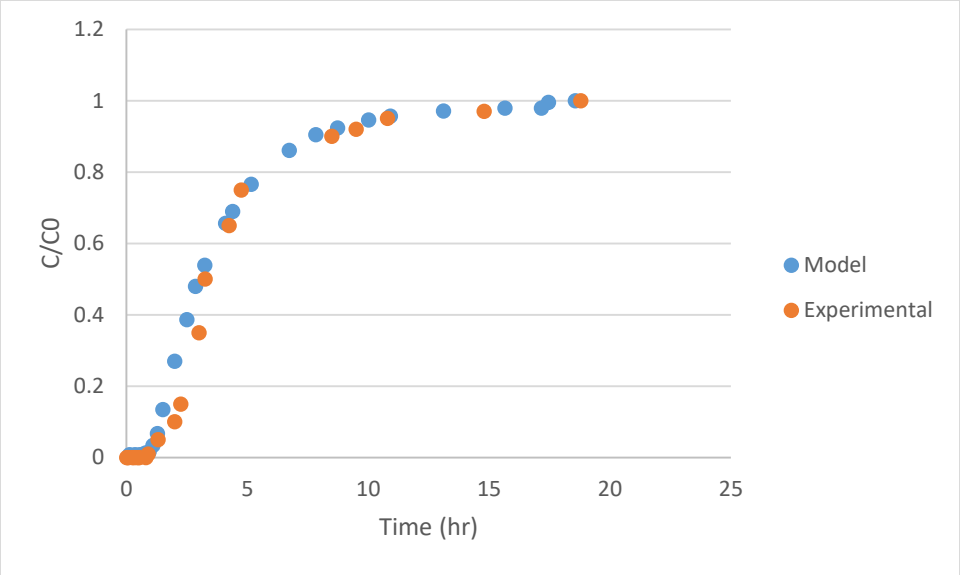


Figure 4.45: Comparison between theoretical and experimental results obtained using proposed mathematical model for the adsorption of Zn^{2+} at various flowrates (C_{b0} = 20 mg/L, Q = 10 mL /min and bed height = 2 cm)

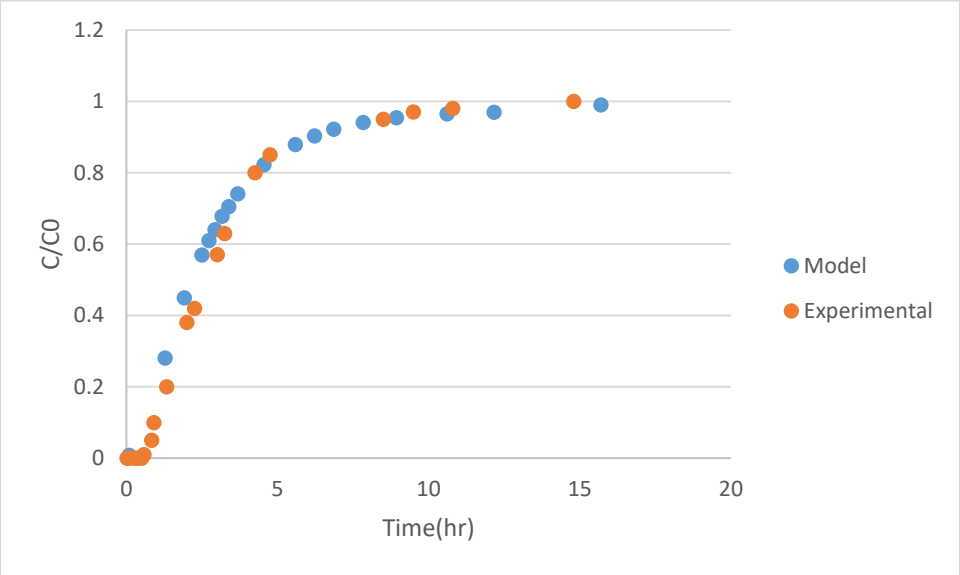


Figure 4.46: Comparison between theoretical and experimental results obtained using proposed mathematical model for the adsorption of Zn^{2+} at various flowrates (C_{b0} = 20 mg/L, Q = 17 mL /min and bed height = 2 cm)

Table 4.33: Model and Experimental Breakthrough Curves Parameters at Various Cu^{2+} and Zn^{2+} Flowrates (bed depth 2 cm; initial conc. 20 mg/L; pH 6)

Flowrate (mL/min)	Breakthrough time(hr) (t_b)				Saturation time (hr) (t_e)			
	Cu		Zn		Cu		Zn	
	Experimental	Model	Experimental	Model	Experimental	Model	Experimental	Model
5	0.9	0.7	2.5	1.3	23.3	24.3	25	25
10	0.46	0.6	1.3	1.27	17	17.5	18.8	18.5
17	0.3	0.5	0.83	0.55	16.7	16.5	14.8	15.7

- **Effect of Bed Height**

The result of varying bed height is plotted in Figures 4.47-4.49 for copper and 4.50-4.52 for zinc. To investigate the effect of varying bed height on the effluent concentration, fixed flowrate and inlet concentration were set to 5 mL/min and 20 mg/L, respectively.

It was observed that the breakthrough times decreased with decreasing bed height of adsorption column of both Cu^{2+} and Zn^{2+} as presented in Table 4.34. The higher copper and zinc uptake was achieved at higher bed height due to increase in the mount of the water hyacinth which provides more binding sites for the metal ions (Renu et al., 2020). The increase in bed height would create a longer distance for the mass transfer zone to reach the exit resulting in an extended breakthrough time (Murithi et al., 2016).

It was observed from Figures 4.47- 4.52 that the model fit well with the experimental date for the three bed heights that were tested for both Cu^{2+} and Zn^{2+}. The best fit regarding the breakthrough point and saturation point for copper was at bed height 7 cm and for zinc was at bed height 4 cm, but according to the overall breakthrough curve we can say that at bed height 4 cm for both copper and zinc the model fit the experimental data the most.

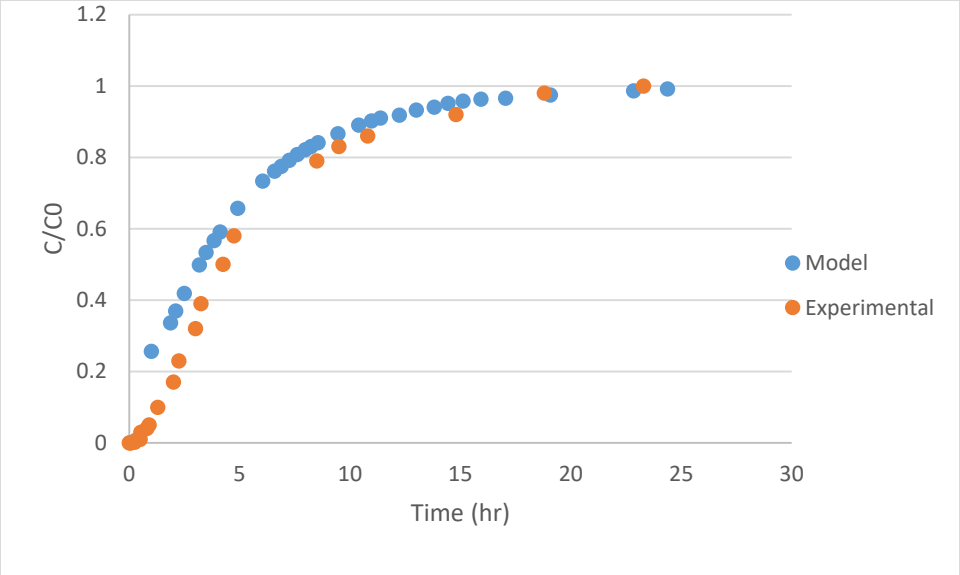


Figure 4.47: Comparison between theoretical and experimental results obtained using proposed mathematical model for the adsorption of Cu^{2+} at various bed height (C_{b0} = 20 mg/L, Q = 5 mL /min and bed height = 2 cm)

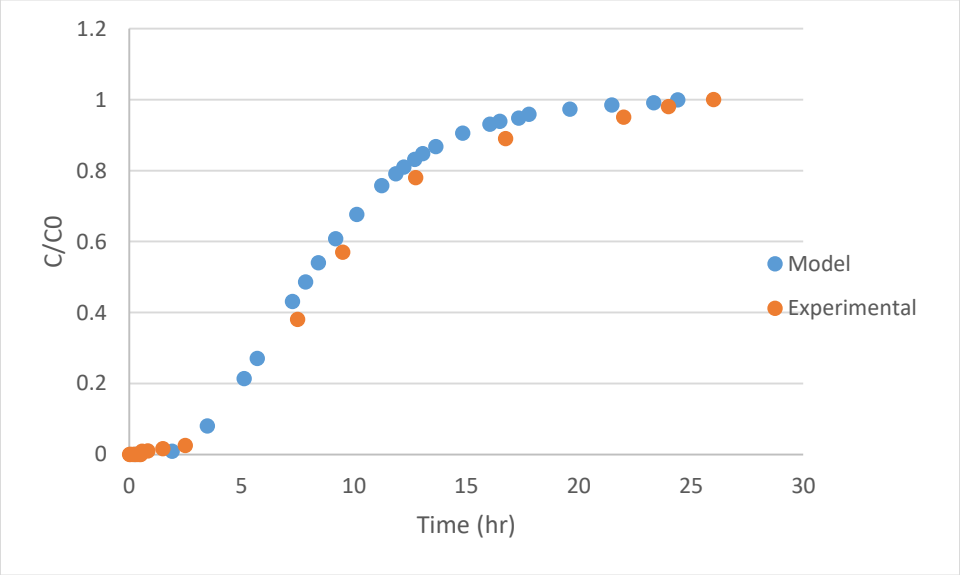


Figure 4.48: Comparison between theoretical and experimental results obtained using proposed mathematical model for the adsorption of Cu^{2+} at various bed height (C_{b0} = 20 mg/L, Q = 5 mL /min and bed height = 4 cm)

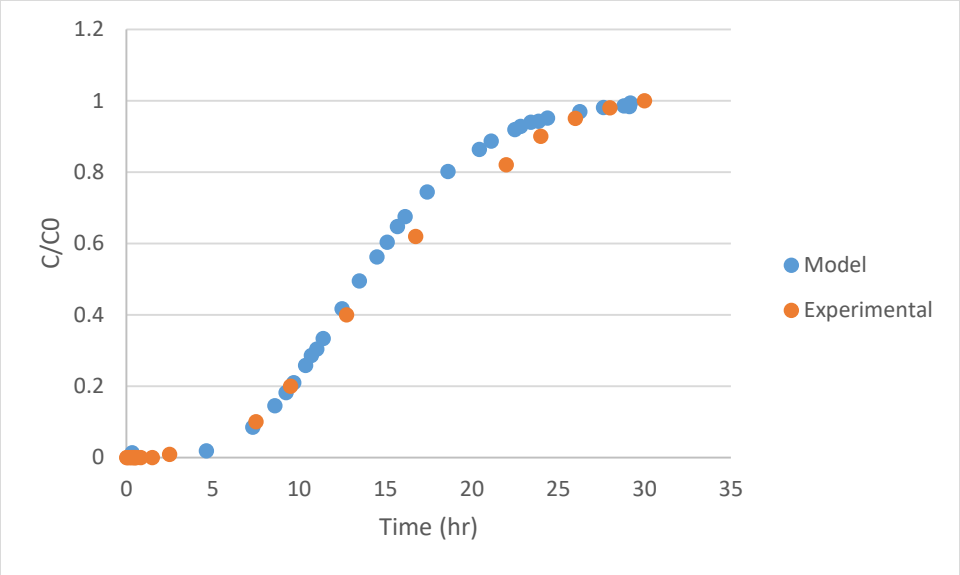


Figure 4.49: Comparison between theoretical and experimental results obtained using proposed mathematical model for the adsorption of Cu^{2+} at various bed height (C_{b0} = 20 mg/L, Q = 5 mL /min and bed height = 7 cm)

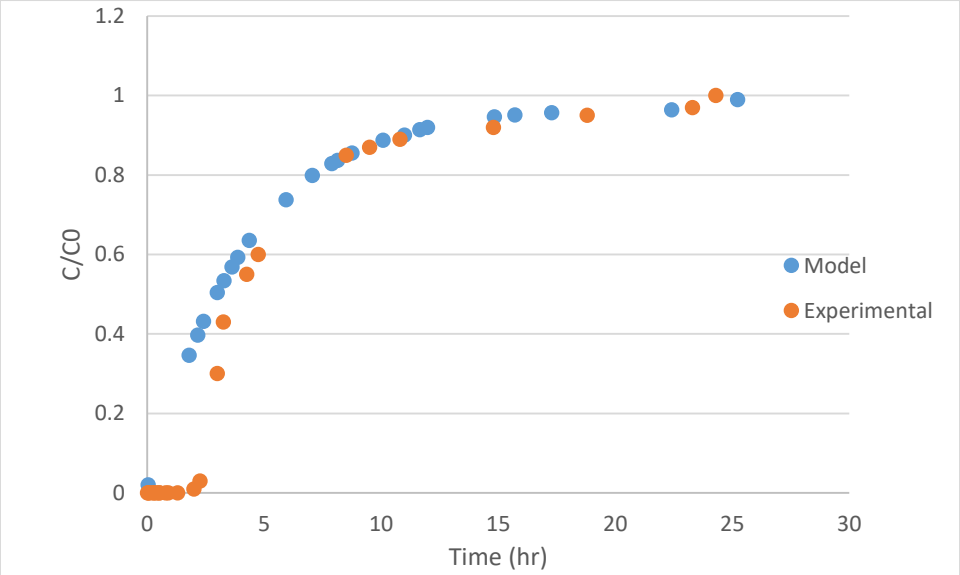


Figure 4.50: Comparison between theoretical and experimental results obtained using proposed mathematical model for the adsorption of Zn^{2+} at various bed height (C_{b0} = 20 mg/L, Q = 5 mL /min and bed height = 2 cm)

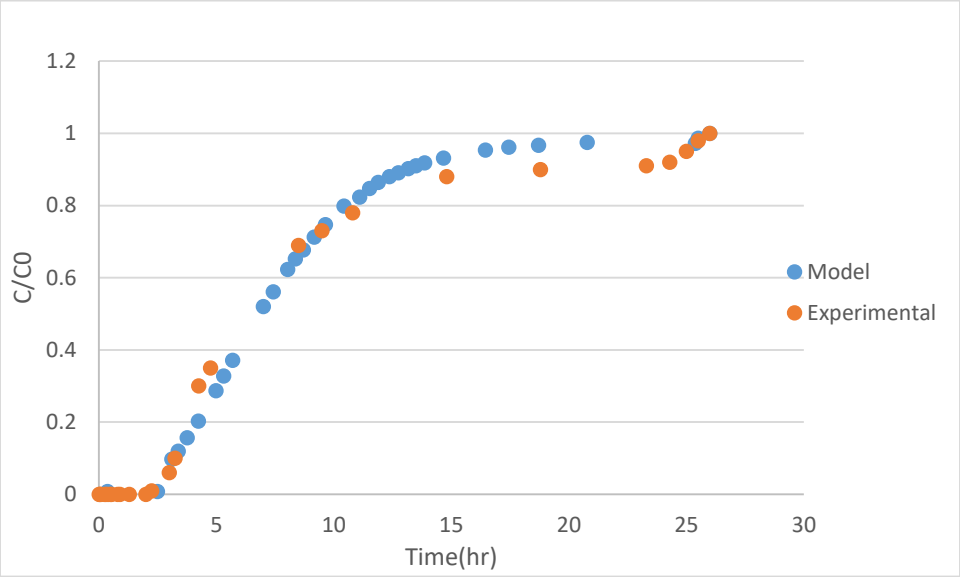


Figure 4.51: Comparison between theoretical and experimental results obtained using proposed mathematical model for the adsorption of Zn^{2+} at various bed height (C_{b0} = 20 mg/L, Q = 5 mL /min and bed height = 4 cm)

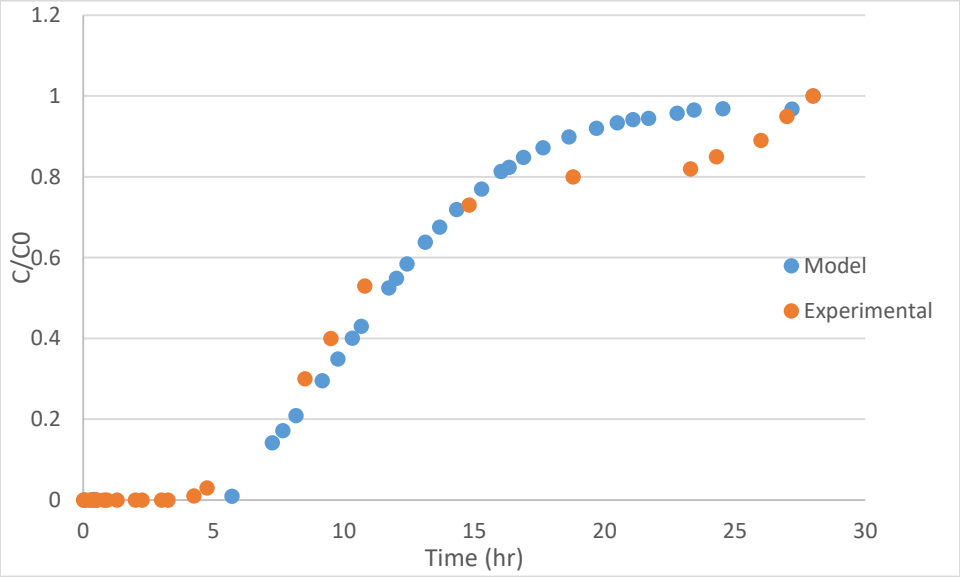


Figure 4.52: Comparison between theoretical and experimental results obtained using proposed mathematical model for the adsorption of Zn^{2+} at various bed height (C_{b0} = 20 mg/L, Q = 5 mL /min and bed height = 7 cm)

Table 4.34: Model and Experimental Breakthrough Curves Parameters for Cu^{2+} and Zn^{2+} at Various Bed Height (flowrate 5 mL/min, initial conc. 20 mg/L, pH 6)

Bed height (cm)	Breakthrough time(hr) (t_b)				Saturation time (hr) (t_e)			
	Cu		Zn		Cu		Zn	
	Experimental	Model	Experimental	Model	Experimental	Model	Experimental	Model
2	0.9	0.7	2.5	1.3	23.3	24.3	25	25
4	3	3.2	2.8	2.8	26	25	26	26
7	5.3	5.5	5	6	30	29.5	28	28

4.10 Model Validation (Comparison of Model and Experimental Results)

Model and experimental results were compared using the R^2, chi-squared, and mean absolute percentage error (MAPE) values. The higher R^2 and lower chi-squared and MAPE values indicate closeness between model and experimental data. The breakthrough curves obtained from the experimental data and model data are shown in Figures 4.35-4.52. In Figures 4.35-4.40 the R^2 value is 0.95, 0.98 and 0.98 for copper, 0.92, 0.97 and 0.99 for zinc respectively for 20, 30, and 50 mg/L. The chi-squared value is 0.79, 0.09 and 0.13 for copper, 0.18, 0.2 and 0.017 for zinc respectively for initial concentrations of 20, 30, and 50 mg/L. The MAPE value is 23.9%, 18.3% and 7.4 % for copper, 3.2%, 11.32% and 3.5% for zinc respectively for initial concentrations 20, 30 and 50 mg/L. It was obvious from the results of comparing the model and experimental data according to R^2, chi-squared, and mean absolute percentage error (MAPE) values for the initial concentration of copper and zinc, that the model fits the experimental data most in the case of initial concentration 50 mg/L for copper and also for 50 mg/L in case of zinc, where the R^2 is very high while chi-square and MAPE have low values.

In Figures 4.41-4.46, the R^2 value is 0.95, 0.98 and 0.97 for copper, 0.92, 0.98 and 0.99 for zinc respectively for flowrates of 5, 10, and 17 mL/min. The chi-squared value is 0.79, 0.08 and 0.058 for copper, 0.18, 1.09 and 0.06 for zinc respectively for flowrates of 5, 10, and 17 mL/min. The MAPE value is 23.9%, 14.3 % and 6.7% for copper, 3.2%, 2.9% and 12.2% for zinc respectively for flowrates of 5, 10, and 17 mL/min. From the model and experimental data comparison in the

case of flowrate, the model fits the data most in the case of 17 mL/min according to R^2, chi-squared, and mean absolute percentage error (MAPE) values for copper, while in case of zinc the model fit the experimental data most according to the R^2 value and chi-square value at flowrate 17 mL/min, and according to MAPE at flowrate 10 mL/min.

In Figures 4.36-4.42, the R^2 value is 0.95, 0.99 and 0.99 for copper, 0.92, 0.98 and 0.96 for zinc respectively for bed heights 2, 4 and 7 cm. The chi-squared value is 0.79, 0.05 and 0.04 for copper, 0.18, 0.08 and 0.104 for zinc respectively for bed heights 2, 4 and 7 cm. The MAPE value is 23.9% 5.8 % and 3.6 % for copper, 3.2 %, 16 % and 14.3 % for zinc respectively for bed heights 2, 4 and 7 cm. It is obvious that the model data fit the experimental data the most at bed height 7 cm for copper and 4 cm bed height for zinc.

Table 4.35 shows the results of model and experimental data comparison according to R^2, chi-squared, and mean absolute percentage error (MAPE) values. The results indicates that the model and experimental data are close. The high R^2 values and low chi-squared and MAPE values for all parameters demonstrates that the proposed model can predict column behavior with acceptable accuracy.

Table 4.35 Results of Model and Experimental Comparison

Variables		**Cu^{2+}**			**Zn^{2+}**		
		R^2	**Chi - square**	**MAPE**	**R^2**	**Chi-square**	**MAPE**
Initial Concentration	20 mg/L	0.95	0.79	23.9%	0.92	0.18	3.2%
	30 mg/L	0.98	0.09	18.3%	0.97	0.2	11.32%
	50 mg/L	0.98	0.13	7.4%	0.99	0.017	3.5%
Bed Height	2 cm	0.95	0.79	23.9%	0.92	0.18	3.2%
	4 cm	0.99	0.05	5.8%	0.98	0.08	16%
	7 cm	0.99	0.04	3.6%	0.96	0.104	14.3%
Flowrate	5 mL/min	0.95	0.79	23.9%	0.92	0.18	3.2%
	10 mL/min	0.98	0.08	14.3%	0.98	1.09	2.9%
	17 mL/min	0.97	0.058	6.7%	0.99	0.06	12.2%

4.11 Scale up Procedure for Packed Bed Adsorption Column

For the model building of systems using biomaterials as adsorbents in continuous systems, residence time is an important parameter as described in section 3.14.1. The linear flowrate through the bed depth was chosen according to the best conditions of mini-column results (5 mL/min).

For scale-up study, the bed depth (H) was increased from 50 cm to 400 cm (Amanuel, 2019) and thus the internal diameter (D) will increase, while keeping constant the ratio D/H (Inglezakis and Poulopoulos, 2006) at a value of 0.04. This value corresponds to the 50 cm high mini-column of 2cm in internal diameter and the linear flowrate through the column was maintained constant at 5 mL/min. Comparison of geometric and operating parameters used with mini and scaled up column are indexed in Table 4.36 for Cu^{2+} and 4.37 for Zn^{2+}.

The breakthrough time (t_b), exhaustion time (t_e) and t^* (time when C =0.5 C_o), calculated from mini-column experiments were used to predict the parameters of the scaled up column. The experimental and model results about the breakthrough curves of the adsorption of Cu^{2+} and Zn^{2+} obtained by measuring the outlet heavy metal ion concentrations are shown in Figures 4.35-4.52 for both Cu^{2+} and Zn^{2+}, which presents the C_t /C_0 f (t) function.

In the scale-up approach using the Length of Unused Bed (LUB) model, the unused bed length for both the small column and scaled up column had to be maintained constant to obtain similar mass transfer characteristic, and thus the length of unused bed in scaled up column for Cu^{2+} was taken as 33.4 cm like the small column, while the Length of Equilibrium Section (LES) increased from 16.6 cm to 366.6 cm, the internal diameter of the column will increase from 2 cm in the case of the small column to 16 cm in the scaled up column.

Results of the scaling up adsorption column for the removal of Cu^{2+} using water hyacinth as adsorbent show that the breakthrough time (t_b) increased from 318 min. in small column to 7038 min in scaled up column resulting in greater uptake capacity and by consequence decreasing the concentration of Cu^{2+} ions in the outlet from 0.03 mg/L in the small column to 0.004 mg/L in the scaled up column. Thus, the degree of utilization increase from 33.1% in the small column to 91.6% in the scaled up column.

Assuming 80% efficiency the scale up column can run for one day, will needs 19.44 hr to treat 3.6864 m^3 of contaminated water using 22 kg of water hyacinth as adsorbent.

Table 4.36: Data of Parameters of Mini Adsorption Column for Cu^{2+} Vs Scaled up Column

Variables	Small Column	Scaled up column
Column diameter (Cm)	2	16
Column height (Cm)	50	400
Cross section area of column (Cm^2)	3.14	200.96
t^* (min.)	960	7680
t_b (min.)	318	7038
$C_{avr.}$ (mg/L)	0.03	0.004
Degree of utilization	33.1%	91.6%
Volume (m^3)	0.000157	0.08
Maximum volume of water treatment	0.009	4.608
Flowrate (mL/min)	5	320

Comparison of parameters used with small and scaled up columns for the removal of Zn^{2+} from wastewater using water hyacinth as adsorbent was shown in Table 4.36.

The Length of Unused Bed (LUB) in scaled up column for Zn^{2+} was taken as 40 cm like the small column, while the Length of Equilibrium Section (LES) increased from 10 cm to 360 cm, the internal diameter of the column will increase from 2 cm in the case of the small column to 16 cm in the scaled up column.

The breakthrough time (t_b) increased from 300 min. in small column to 5550 min in scaled up column resulting in greater uptake capacity and by consequence decreasing the concentration of Zn^{2+} ions in the outlet from 0.006 mg/L in the small column to 0.001 mg/L in the scaled up column. Thus, the degree of utilization increases from 40% in the small column to 92.5% in the scaled up column.

Assuming 80% efficiency will need 19.44 hr to treat 3.440 m^3 of contaminated water using 22 kg of water hyacinth as adsorbent for the scaled up column to run for one day.

Table 4.37: Data of Parameters of Mini Adsorption Column for Zn^{2+} Vs Scaled up Column

Variables	Small Column	Scaled up column
Column diameter (Cm)	2	16
Column height (Cm)	50	400
Cross section area of column (Cm^2)	3.14	200.96
t^* (min.)	750	6000
t_b (min.)	300	5550
$C_{avr.}$ (mg/L)	0.006	0.001
Degree of utilization	40%	92.5%
Volume (m^3)	0.000157	0.08
Maximum volume of water treatment (m^3)	0.0084	4.300
Flowrate (mL/min)	5	320

4.12 Economic Feasibility for the Scaled up Adsorption Column

The economic feasibility analysis was conducted for the data calculated for the scaled up adsorption column for copper using water hyacinth as adsorbent. One run for almost 1 day will treat 3.686 m^3 contaminated water using 22 kg water hyacinth, therefore this column can treat 1345.39 m^3 / year using 8.0665 tons of water hyacinth/year.

4.12.1 Cost Estimation

(1) Costs of Controlling and Harvesting Water Hyacinth (Wang et al., 2019)

- Cost of water hyacinth control per ton = US$ 3.3, since the adsorption column needs almost 8 tons of water hyacinth per year, therefore cost of controlling 8 tons of water hyacinth per year =US$ 26.6 (Wang did his research in china, I assumed the same process of controlling and harvesting of water hyacinth)

- Cost of worker's wage needed in the controlling and collecting process = US$ 32.3 for 8 tons water hyacinth per year (Cost of one South African labour per day was assumed to be R 250).
- Cost of harvesting machines according to the research by Wang et al. in 2019 is US$ 3840/set (assumed to be the same in South Africa as china) that is working for 8 hours to harvest 100 tons/day, that is equal to US$ 480 / set/ hr .

This type of machine can harvest 100 tons/day (Wang et al., 2019), therefore it can harvest 12.5 tons/hr, therefore cost of renting machine for one hour to harvest 12.5 tons of water hyacinth = US$ 480.

Therefore, the total cost of controlling and harvesting water hyacinth = Total cost of controlling water hyacinth + Cost of worker's wage + cost of harvesting water hyacinth

The total cost of controlling and harvesting water hyacinth = US$ 26.6+ US$ 32.3 +US$ 480 = US$ 538.9

(2) Capital Cost of Adsorption Column

- Cost of equipment= $C_p^\circ * F_p * F_M$ (4.11)
  - $C_p^\circ = purchased\ cost\ for\ base\ conditions\ (purchase\ cost\ of\ vessel)$
  - $F_p = Pressure\ factor$
  - $F_M = Material\ factor$

$$C_p^\circ = \frac{US\$\ 6000}{volume}$$

Since volume of the scaled up adsorption column= 0.08 m^3, therefore

$$C_p^\circ = \frac{US\$\ 6000}{volume} * 0.08 = US\$\ 480$$

$$C_m = C_p^\circ * F_M = C_p^\circ (B_1 + B_2 * F_M * F_p) \quad (4.12)$$

C_m: Bare module equipment cost

B_1: Constants for Bare Module Factor

B_2: Constants for Bare Module Factor

$C_m = 480\ (2.25 + (1.82 * 3 * 1))$

C_m = US$ 3700.8

Equipment description, vertical (including tower) stainless steel, identification number = 20, F_M= 3 (Calculated according to cost of equipment equation from book Analysis, Synthesis and Design of Chemical Processes)

- **Fixed Capital Investment (FCI)**

$$C_{TM} = F_{lang} * \sum_{i=1}^{n} C_m \qquad (4.13)$$

C_{TM}: Is the capital cost (total module) of the plant (Capital cost of adsorption column)

n: is the total number of individual units

F_{lang}: Lang factor

$$C_{TM} = 3.63 * 3700.8 = US\$\ 13{,}432.1$$

Column lifetime is assumed to be 10 years to full depreciation.

$$C_{TM} = US\$\ 13{,}432.1 \div 10\ years = US\$\ 1{,}343/year$$

- **Cost of Operating Labor (C_{OL})**

$N_{OL} = (6.29 + 31.7\ P^2 + 0.23 N_{np})^{0.5}$

N_{OL}: is the number of operators per shift

P: is number of processing steps

N_{np}: number of non-particulate processing steps = Σ Equipment

$N_{OL} = (6.29 + 31.7(1)^2 + 0.23(1))^{0.5}$

$N_{OL} = 6.18 \approx labor$

Operating labor= (4.5)*(6.18) = 27.81 ≈ 28 labor/year

Cost of Operating Labor (C_{OL}) = 28 *65,000R= 182000 R/year= US$ 12,093 /year (Calculated according to cost of labor equations chapter 8 , Analysis, Synthesis and Design of Chemical Processes, the cost of one labor was estimated to be 250 R/day).

- **Cost of Utilities**

  Power needed for the pump to lift ≈ 4 m^3 to the adsorption column per day

  Pump power (w) = height of column * flowrate * g* density of water* p (pa)

  Power of pump = 4* 0.32*9.8*1000*1

  Power needed by pump = 0.209 KW

  Cost of electricity for business consumption in South Africa =1.0209 R KWh= US$ 0.079

  (According to global petrolprices.com)

  Therefore, cost of electricity = 2213.48 R/year= US$ 147.08 /year

- **Cost of Waste Treatment**

  According to the research done by Nahman in 2011, the cost of landfilling of waste products was almost 16 US$ per ton (almost 256 R/ton). As our column will need 8.0665 tons per year, therefor the cost of waste treatment per year will be: 16*8.0665=129.064 US$/year.

Therefor,

- **Cost of Manufacturing (COM)**

$$\boldsymbol{COM = 0.180\,FCI + 2.73\,C_{OL} + 1.23\,(C_{ut} + C_{wt} + C_{Rm})} \qquad (\mathbf{4.14})$$

C_{ut}: cost of utilities

C_{wt}: cost of waste treatment

C_{Rm}: cost of raw material

COM = (0.180*13,432.1) + (2.73*12,093) + 1.23 (147.08 +129.064+538.9)

COM = US$ 36,434.1

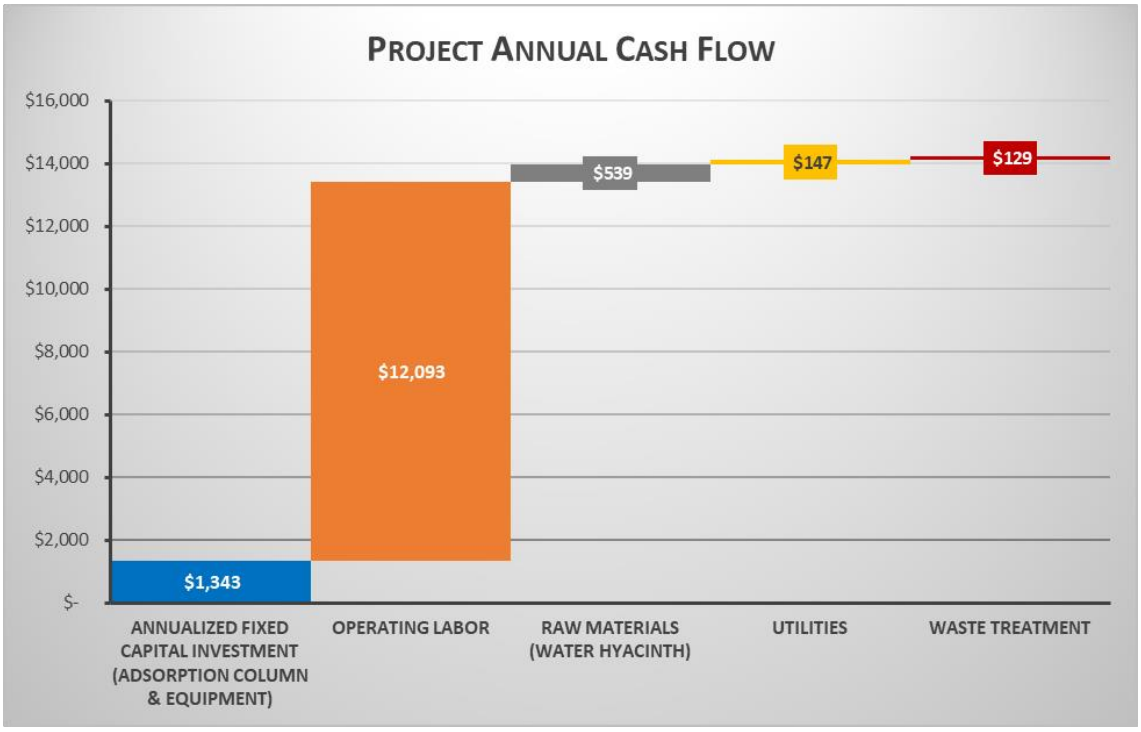
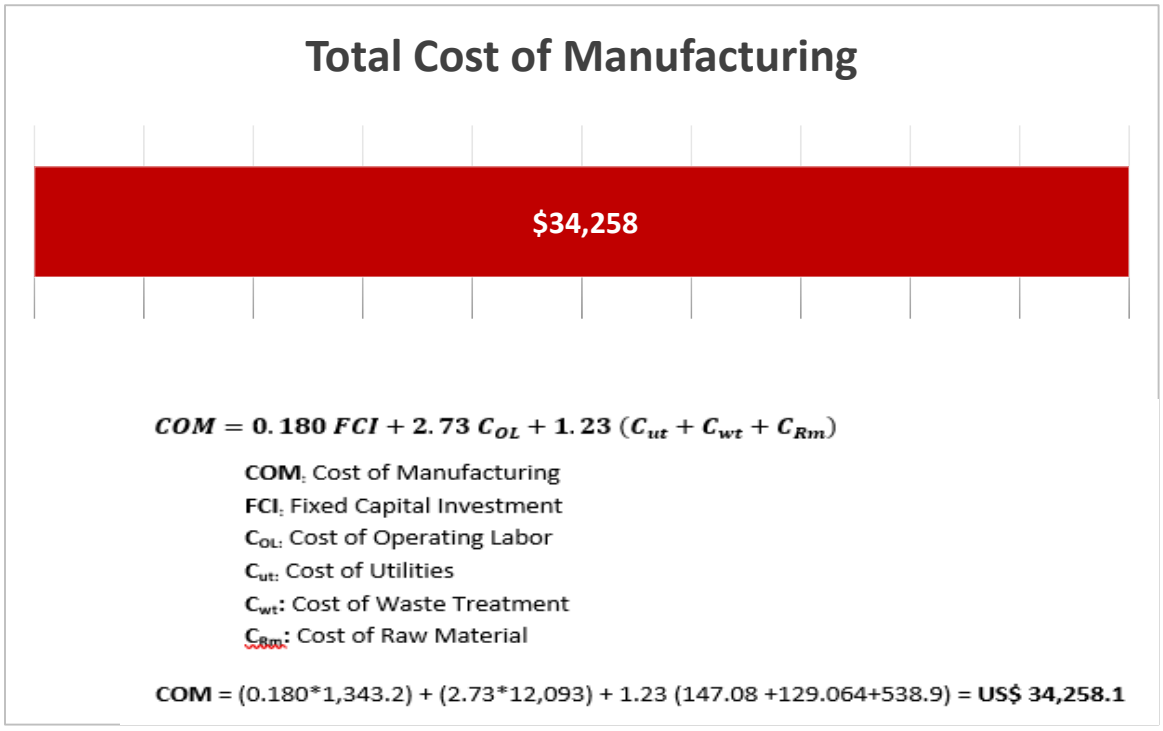


Figure 4.53: Project annual cash flow



Figur 4.54: Total cost of manufacturing

References

Ahmed, Y.M., Al-Mamun, A., Jameel, A.T., AlKhatib, M.F.R., Amosa, M.K., AlSaadi, M.A., 2016. Synthesis and Characterization of Carbon Nanofibers Grown on Powdered Activated Carbon. Journal of Nanotechnology, **2016**, 10.

Al Mesfer, M., Danish, M., Khan, M.I., Ali, H.I., Hasan, M., El Jery, 2020. Continuous Fixed Bed CO_2 Adsorption: Breakthrough, Column Efficiency, Mass Transfer Zone. Processes 2020, 8, 1233; doi: 10.3390/pr8101233.

Al Saadi, M.A., Al Mamun, A., Alam, M.Z., Amosa, M.K., Atieh, M.A., 2016. Removal of Cadmium from Water by CNT-PAC Composite: Effect of Functionalization. Nano, 11(1), 7.

Aly, Z., Graulet, A., Scales, N., Hanley, T., 2014. Removal of aluminium from aqueous solutions using PAN-based adsorbents: characterisation, kinetics, equilibrium and thermodynamic studies. Environmental Science and Pollution Research, 21(5), 3972-3986.

Amanuel, L., 2019. Wastewater Treatment Plant and its Design for Textile Industry. Current Trends in Fashion Technology & Textile Engineering, Volume 5 (3).

Amin, M.T., Alazba, A.A., Shafiq, M., 2017. Removal of Copper and Lead using Banana Biochar in Batch Adsorption Systems: Isotherms and Kinetic Studies. Arab J Sci Eng, 2017.

Chittoo, B.S., Sutherland, C., 2020. Column breakthrough studies for the removal and recovery of phosphate by lime-iron sludge: Modelling and optimization using artificial neural network and adaptive neuro-fuzzy inference system. Chinese Journal of Chemical Engineering, (28) 7, 1847-1859.

Chatterjee, Abhijit, Schiewer, S., 2014. Effect of Competing Cations (Pb, Cd, Zn, and Ca) in Fixed-Bed Column Biosorption and Desorption from Citrus Peels. Water Air Soil Pollution 1854 (2014): 225-238.

Chen, S., Yue, Q., Gao, B., Li, Q., Xu, X., Fu, K., 2012. Adsorption of hexavalent chromium from aqueous solution by modified corn stalk: A fixed bed column study. Bioresource Technology 113 (2012): 114–120.

Cherono, F., Mburu, N., Kakoi, B., 2021. Adsorption of lead, copper and zinc in a multi-metal aqueous solution by waste rubber tires for the design of single batch adsorber. Heliyon 7 (2021) e08254.

El-Gendy, N.S.,El-Gharabawy, A.A.S.A.,Abu Amr, S.S., Ashour, F.H.,2015. Response surface optimization of an alkaline transesterification of waste cooking oil, Int. J. ChemTech Res., vol. 8, no. 8, pp. 385–398, 2015.

Futalan, C.M., Wan, M.W., 2022. Fixed-Bed Adsorption of Lead from Aqueous Solution Using Chitosan-Coated Bentonite. International Journal of Environmental Research and Public Health. 2022, 19, 2597. https://doi.org/10.3390/ ijerph19052597.

Farooq, U., Khan, M.A., Athar, M., Kozinski, J.A., 2013. Biosorption of Pb (II) and Cr (III) from aqueous solutions: breakthrough curves and modeling studies. Environ Monit Assess 185 (2013): 845–854.

Farooq, U., Kozinski, J.A., Khan, M.A., Athar, M., 2010. Biosorption of heavy metal ions using wheat based biosorbents–A review of the recent literature. *Bioresource technology*, **101**(14), 5043-5053.

Fauzia, S., Aziz, H., Dahlan, D., Zein, R., 2021. Modelling for removal of Cr (VI) and Pb (II) using sago bark (Metroxylon sagu) by fixed-bed column method. Egyptian Journal of Chemistry, Vol. 64, No. 8 pp. 3981 - 3989.

Futalan, C.M., Kan, C.C., Dalida, M.L., Pascua, C., Wan, M.W., 2011. Fixed-bed column studies on the removal of copper using chitosan immobilized on bentonite. Carbohydr. Polym. 2011, 83, 697–704.

Grassi, M., Gul, K., Vincenzo, B., Giusy, L., 2012. Removal of Emerging Contaminants from Water and Wastewater by Adsorption Process. In Emerging Compounds Removal from Wastewater Natural and Solar Based Treatments, 15-37. Salerno: Springer, 2012.

Gupta, N.K., 2020. Modelling, simulation, and experimental validation for toluene removal from gas phase in a fixed bed adsorption column. INDIAN CHEMICAL ENGINEER, VOL. 62, NO. 2, 150–169.

Gupta, S.S., Bhattacharyya, K.G., 2011. Kinetics of adsorption of metal ions on inorganic materials: A review. Advances in Colloid and Interface Science 162 (2011) 39–58.

Hassan, K., Jarullah, A.A., Saadi, S.K., 2017. Synthesis of Copper Oxide Nanoparticle as an Adsorbent for Removal of Cd (II) and Ni (II) Ions from Binary System. International Journal of Applied Environmental Sciences, 12 (11) 2017, 1841-1861.

Inglezakis, V.J., Poulopoulos,S.G., 2006. Adsorption, Ion Exchange and CatalysisDesign of Operations and Environmental Applications, Book • 2006, chapter 2, Pages 31-56.

Jahangiri, M.F., Moutushi, T. H., Moniruzzaman, M., Hoque, S., 2021. Removal of lead from aqueous solutions and wastewaters using water hyacinth (Eichhornia crassipes) roots. Water Practice & Technology Vol 00 No 0, 16(1–3).

Jami, M.S., Rosli, N.-S., Amosa, M.K., 2016. Optimization of Manganese Reduction in Biotreated POME onto 3A Molecular Sieve and Clinoptilolite Zeolites. Water Environment Research, 88(6), 566-576.

Kardam, A., Raj, K.R., Srivastava, S., Srivastava, M.M., 2014. Nanocellulose fibers for biosorption of cadmium, nickel, and lead ions from aqueous solution." Clean Techn Environ Policy 16 (2014): 385–393

Jeyaseelan, C., Gupta, A., 2016. Green Tea Leaves as a Natural Adsorbent for the Removal of Cr (VI) From Aqueous Solutions. Air, Soil and Water Research, **9**, ASWR. S35227.

Lo´pez-Cervantes, J., Sa´nchez-Machado, D.I., Sa´nchez-Duarte, R.G., Correa-Murrieta, M.A., 2017. Study of a fixed-bed column in the adsorption of an azo dye from an aqueous medium using a chitosan– glutaraldehyde biosorbent. Adsorption Science & Technology 2018, Vol. 36(1–2) 215–232.

Metcalf & Eddy. Wastewater Engineering: Treatment and Reuse. 4th ed. Edited by George Tchobanoglous, Franklin L. Burton and H. David Stensel. New York: McGraw- Hill Education, 2003.

Munene, J.M, Onyatta, J.O. Yusuf, A.O., 2020. Characterization of Water Hyacinth Powder Using FTIR Spectroscopy and the Adsorption Behaviour of Pb^{2+}, Cd^{2+}, Zn^{2+}, Ni^{2+} and Cr^{2+} in Aqueous Solution. Asian Journal of Applied Chemistry Research. 6(1): 47-55, 2020; Article no.AJACR.57606.

Murithi, G., wa-Thiong'o, K., Warui, S.K., Muthengia, W., 2016. Fixed Column Study for the Removal of Zinc (II) Ions from Waste Water by Bone Char Rice Husks Ash and Water Hyacinth Composite-Mixture.International Journal of Science and Research (IJSR), 5(2).

Murithi, G., Onindo, C.O., Wambu, E.W., Muthakia, G.K., 2014. Removal of cadmium (II) Ions from water by adsorption using water hyacinth (Eichhornia crassipes) biomass. BioResources, 9(2), 3613-3631.

Singh, N., Das, S.K., 2011. FTIR Study for the Cr(VI) Removal from Aqueous Solution Using Rice Waste Tarun Kumar, Department of Petroleum Engineering, Indian School of Mines, Dhanbad – 826004, India and Department of Chemical Engineering, University of Calcutta, 92, A. P. C. Road, Kolkata - 700 009, India.

Nahman, A., 2011. Pricing landfill externalities: Emissions and disamenity costs in Cape Town, South Africa. Waste Management 31(9-10):2046-56.

Neris, J.B, Luzardo, F.H.M., Almeida, O.N., Santos, P.F., Garcia, f., 2019. Evaluation of single and tri-element adsorption of Pb^{2+}, Ni^{2+} and Zn^{2+} ions in aqueous solution on modified water hyacinth (Eichhornia crassipes) fibers. Journal of Environmental Chemical Engineering 7(1):102885.

Nyamunda, B., Chivhanga, T., Guyo, U., Chigondo, F., 2019. Removal of Zn (II) and Cu (II) Ions from Industrial Wastewaters Using Magnetic Biochar Derived from Water Hyacinth. Volume 2019 |Article ID 5656983.

OBI, C., 2015. Sorption characteristics of water hyacinth leaf biomass on the removal of Cu (II) ion from aqueous solution', International Journal of Innovative Environmental Studies Research, 3(3): 36–43.

Ouyang, D., Zhuo, Y., Hu, L., Zeng, Q., Hu, Y., He, Z., 2019. Research on the Adsorption Behavior of Heavy Metal Ions by Porous Material Prepared with Silicate Tailings. Minerals 2019, 9, 291.

Pham, B.N., Kang, J.-K., Lee, C.-G., Park, S.J., 2021. Removal of Heavy Metals (Cd^{2+}, Cu^{2+}, Ni^{2+}, Pb^{2+}) from Aqueous Solution Using Hizikia fusiformis as an Algae-Based Bioadsorbent Applied Science. 2021, 11, 8604.

Primo, J., Bittencourt, C., Acosta, S., Sierra-Castillo, A., Colomer, J.F., Jaerger, S., Verônica, C., Fauze, T., Anaissi, J., 2020. Synthesis of Zinc Oxide Nanoparticles by Ecofriendly Routes: Adsorbent for Copper Removal from Wastewater. Green and sustainable chemistry, original research article, Front. Chem., https://doi.org/10.3389/fchem.2020.571790

Rani, N., Singh, B., Shimrah, T., 2016. Chromium (VI) removal from aqueous solutions using eichhornia as an adsorbent. Journal of Water Reuse and Desalination, 7(4): 461–467.

Rao, D. G., R. Senthilkumar, J., Byrne, A., Feroz, S., 2013. Wastewater Treatment: Advanced Processes and Technologies. London: IWA.

Rashed, M. N., Arfien, A.A., El-Dowy, F.A., 2020. Adsorption of Heavy Metals on Chemically Modified Muscovite. Aswan University Journal of Environmental Studies (AUJES), 1(2), 183-203.

Renu, A. M., Singh, K., Gupta, R., Doharek. R., 2020. Continuous Fixed-Bed Adsorption of Heavy Metals Using Biodegradable Adsorbent: Modelling and Experimental Study. J. Environ. Eng., 2020, 146(2): 04019110.

Saravanan, A., Senthil, Kumar, P., Yaswanthraj, M., 2018. Modeling and analysis of a packed bed column for the effective removal of zinc from aqueous solution using dual surface-modified biomass. PARTICULATE SCIENCE AND TECHNOLOGY 2018, VOL. 36, NO. 8, 934–944.

Sarma, P.J., Kumar, R., Pakshirajan, K., 2015. Batch and Continuous Removal of Copper and Lead from Aqueous Solution using Cheaply Available Agricultural Waste Materials. Int. J. Environ. Res. 9, no. 2 (2015): 635-648.

Singh, J., Ali, A., Prakash, V., 2014. Removal of lead (II) from synthetic and batteries wastewater using agricultural residues in batch/column mode. Int. J. Environ. Sci. Technol. 11 (2014): 1759-1770.

Singh, S., Srivastava, C.V., Goyal, A., Mall, I.D., 2020. Breakthrough modeling of furfural sorption behavior in a bagasse fly ash packed bed. Environmental Engineering Research 25(1) 104-113.

Sivakumar, D., 2015. Hexavalent chromium removal in a tannery industry wastewater using rice husk silica. Global Journal of Environmental Science and Management, 1(1), 27-40.

Soetaredjo, Edi, F., Kurniawan, A., Lu Ki, O., Ismadji, S., 2013. Incorporation of selectivity factor in modelling binary component adsorption isotherms for heavy metals- biomass system. Chemical Engineering Journal 219 (2013): 137-148.

Szymoniak, L., Claveau-Mallet, D., Haddad, M., Barbeau, B., 2022. Application of Magnesium Oxide Media for Remineralization and Removal of Divalent Metals in Drinking Water Treatment: Drinking Water Quality and Human Health, Water 2022, 14(4), 633.

Tsai, W.C., de Luna, M.D., Bermillo-Arriesgado, H.L., Futalan, C.M., Colades, J.I., Wan, M.W., 2016. Competitive Fixed-Bed Adsorption of Pb (II), Cu (II), and Ni (II) from Aqueous Solution Using Chitosan-Coated Bentonite. International Journal of Polymer Science Volume 2016, Article ID 1608939, 11 pages.

Turton, R., Bailie, R.C., Whiting, W.B., Shaeiwitz, J.A., Bhattacharyya, D., Analysis, Synthesis, and Design of Chemical Processes Fourth Edition. ISBN-13: 978-0-13-261812-0, ISBN-10: 0-13-261812-5.

Vandenbruwane, J., De Neve, S., Qualls, R.G., Sleutel, S., Hofman G., 2007. Comparison of different isotherm models for dissolved organic carbon (DOC) and nitrogen (DON) sorption to mineral soil. Geoderma, 139(1-2), 144-153.

Verduzco-Navarro, I.P., Rios-Donato, N., Jasso-Gastinel, C.F., Martínez-Gómez, A.J., Mendizábal, E., 2020. Removal of Cu (II) by Fixed-Bed Columns Using Alg-Ch and Alg-ChS Hydrogel Beads: Effect of Operating Conditions on the Mass Transfer Zone. Polymers 2020, 12, 2345.

Wang, Z., Zheng, F., Xue, S., 2019. The Economic Feasibility of the Valorization of WaterHyacinth for Bioethanol Production. Sustainability 2019, 11, 905.

Wong, K.K., Lee, C.K., Low, K.S., Haron, M.J., 2003. Removal of Cu and Pb by tartaric acid modified rice husk from aqueous solutions. Chemosphere 50 (2003 a): 23-28.

Yahya, M.D., Muhammed, I.B., Obayomi, K.B, Olugbenga, A.G., Abdullahi, U.B., 2020.Optimization of fixed bed column process for removal of Fe (II) and Pb (II) ions from thermal power plant effluent using NaoH-rice husk ash and Spirogyra. Scientific African 10(2020).

CHAPTER FIVE

CONCLUSIONS AND RECOMMENDATIONS

In light of the aforementioned reasons, the aim of the current research is to study the feasibility and the efficiency of water hyacinth as low-cost waste adsorbent (without any chemical nor thermal treatment) in the removal of copper and zinc from synthetic wastewater in batch and continuous processes. Water hyacinth from different locations (South Africa and Egypt) was investigated to explore the effect of the location of water hyacinth on its adsorption capacity for the removal of Cu^{2+} and Zn^{2+}. After that, the RSM and GAMS were used to optimize process conditions for maximal biosorption of Cu^{2+} and Zn^{2+} from aqueous solutions. Moreover this research was done to determine the generic equations that best describes the adsorption mechanism of the hyacinth to remove Cu^{2+} and Zn^{2+} from wastewater and validate the proposed generic model against experimental data. The breakthrough curves provide us with the information needed for design of adsorption column.

5.1 Conclusions

The main concluded points from this research are summarized below:

- The results showed that the location and environment from which the hyacinth is harvested prescribes its ability to adsorb heavy metals. Regarding the removal efficiency of copper and zinc from wastewater, batch equilibrium experiments have proved that water hyacinth from South Africa yields the highest removal of 99.1% for copper at 37.7 minutes of contact time when 1.5 g of adsorbent is used to purify a solution at a pH of 6.25 ~~of~~ and 20 mg/L initial Cu^{2+} concentration. Hyacinth from South Africa also yields 98.5% removal of zinc after 60 minutes of contact time, with 2.5 g adsorbent dose, at a pH of 10 and 10 mg/L Zn^{2+} ion concentration. Water hyacinth from Egypt gave 85.5% for copper removal at 75 minutes contact time, 0.875 g adsorbent dose, 6.25 pH and 20 mg/L Cu^{+2} ion concentration, and 61% for zinc removal at 47.5 minutes contact time, 3 g adsorbent dose, 6 pH and 10 mg/L Zn^{2+} ion concentration. The hyacinth from South Africa exhibited a higher percentage of removal for both copper and zinc than that from the Egyptian sample, which is attributed to a higher total sum of heavy metal ions detected in

Egyptian water hyacinth than the South African sample. The total sum of heavy metal ions detected in Egyptian and South African water hyacinth samples was 492.5 mg/L and 434 mg/L respectively. A higher total sum of loaded heavy metals means that less active sites are available for adsorption. In addition, it was observed from XRF analysis that the chemical composition of the South African water hyacinth sample contained a higher percentage of metal oxides than the Egyptian water hyacinth sample. Al_2O_3, MgO, CaO, Na_2O, K_2O, P_2O_5 and SO_3 were found in the South African water hyacinth sample in higher percentage than that in the Egyptian sample. According to some researches in the literature, metal oxides can be used in their original form or in nanoparticle size form to remove heavy metal ions from wastewater which makes the South African water hyacinth a better adsorbent. Results produced from FTIR spectra analysis of raw and metal loaded adsorbents indicated the complex formation of metal ion with different functional groups that are present in the adsorbent. Mainly surface hydroxyl group, and silicon oxide were responsible for metal adsorption.

- The batch equilibrium data for South African water hyacinth was perfectly described by Langmuir model. The linearity of the plot suggested the creation of a homogenous monolayer of metal ions on the outer surface of the sorbent.
- The maximum adsorption capacity (q_{max}) derived from Langmuir model for the adsorption of Cu^{2+} and Zn^{2+} via water hyacinth from Egypt is 17.669 mg of Cu^{2+}/g of water hyacinth and 11.876 mg of Zn^{2+}/g of water hyacinth. For the water hyacinth from South Africa the maximum adsorption capacity (q_{max}) derived from Langmuir model for the adsorption of Cu^{2+} and Zn^{2+} via raw water hyacinth is 20.24 mg of Cu^{2+}/g of and 13.3 mg of Zn^{2+}/g of water hyacinth, respectively. This value is higher than some values reported in the literature for pre-treated water hyacinth, especially in the case of removal of copper. This result is important as it confirms that utilizing raw water hyacinth is more feasible than pre-treated water hyacinth since it is a very promising biosorbent that is economically viable and can be easily prepared.
- The kinetics of the adsorption process fitted well with the pseudo-second order kinetic equation.
- Bio-sorption of Cu^{2+} and Zn^{2+} via water hyacinth is basically due to many reasons, which are:

(i) Surface complexation with carboxylic functional groups on the surface of raw water hyacinth, as illustrated by the FTIR analysis.

(ii) Metal oxides, as illustrated by XRF results

(iii) Physical forces of attraction, as manifested by Langmuir isotherm

In the current study, the RSM and GAMS were used to optimize process conditions for maximal biosorption of Cu^{2+} and Zn^{2+} from aqueous solutions.

- RSM prediction using water hyacinth from South Africa gave higher removal of 93% for copper with an error of, 2.8%, whilst the RSM resulted in 98.7% for zinc removal with an error margin of 0.008%. RSM prediction using water hyacinth from Egypt gave a percentage of removal of 86.26% for copper with an error percent, 0.88%, while it gave 64.48% for zinc removal with an error percent of 5.4.
- GAMS prediction using water hyacinth from South Africa gave a percentage removal of 99.6% for copper with an error percent of 0.8, whilst zinc removal was 100% with an error percent 0.012. GAMS prediction using water hyacinth from Egypt gave a percentage of removal of 93.445~~%~~ with an error percent 7.4 ~~%~~, while it gave 78.08% for zinc removal with error percent 11.6. From this result, although GAMS predication gave higher percentage of removal the error percent is higher than that of RSM, so the RSM prediction is more applicable because the error between the model result and the experiment result is low.
- In fixed-bed column tests, the service time of the column and the volume of wastewater treated up to breakthrough and exhaustion are directly proportional to the bed depth; on the other hand, they are inversely proportional to the initial Cu^{2+} and Zn^{2+} concentrations and the flowrate of the feed solution.
- Untreated water hyacinth managed to treat a significant number of bed volumes to breakthrough and exhaustion at lower flowrates. Water hyacinth sorption column of small bed depth (2cm) was not efficient in treating high concentrations of Cu^{2+} and Zn^{2+}; 50mg/l; therefore, for high concentrations larger depths are required.
- The shape of the breakthrough curves obtained using the proposed generic model were found to be almost similar for Cu^{2+} and Zn^{2+} breakthrough curves obtained experimentally. This indicates the suitability of the generic models for copper and zinc removal using water hyacinth.

- Assuming 80% efficiency, the large scale-up adsorption column for the removal of copper will need 19.44 hours to treat 3.6864m^3 of contaminated water using 22kg of water hyacinth as adsorbent. Meanwhile for zinc the scale up column will need 19.44 hours to treat 3.440m^3 of contaminated water using 22kg of water hyacinth as adsorbent, so the same amount of adsorbent at the same time can remove a copper water contaminant by 6.7% more than zinc water contaminant.
- Cost of the adsorption column US$3,700.8
- The cost of manufacturing (COM) of the adsorption column is US$36,275.

5.2 Recommendations for Future Work

There are various uncertainties associated with the development of a mathematical model that can characterize the water hyacinth in South Africa, future work could address these uncertainties. More extensive research on the efficiency of the South African water hyacinth without treatment and of different particle sizes is recommended considering the good results yielded by this research. The further study could also be extended to the removal efficiency of the South African water hyacinth for other heavy metals, such as cadmium, chromium and mercury due to their adverse health impacts as explained in Chapter 1.

Also investigating the selectivity of the South African water hyacinth in case more than one heavy metal existed in the wastewater, as well as investigating the applicability of the research outcomes on real industrial wastewater.

Finally, applying RSM and GAMS for the optimization of multiple contaminants and validating the generic model using different heavy metal ions, could add value to the future study.